AGARD-LS-55

AGARD

ADVISORY GROUP FOR AEROSPACE RESEARCH & DEVELOPMENT

7 RUE ANCELLE 92 NEUILLY SUR SEINE FRANCE

AGARD LECTURE SERIES No. 55

on

Composite Materials

NORTH ATLANTIC TREATY ORGANIZATION

NORTH ATLANTIC TREATY ORGANIZATION

ADVISORY GROUP FOR AEROSPACE RESEARCH AND DEVELOPMENT

(ORGANISATION DU TRAITE DE L'ATLANTIQUE NORD)

AGARD Lecture Series No.55

COMPOSITE MATERIALS

B.Walter Rosen

Lecture Series Director

The material in this book has been assembled to support a Lecture Series under the sponsorship of the Structures and Materials Panel and the Consultant and Exchange Program of AGARD.

THE MISSION OF AGARD

The mission of AGARD is to bring together the leading personalities of the NATO nations in the fields of science and technology relating to aerospace for the following purposes:

- Exchanging of scientific and technical information;
- Continuously stimulating advances in the aerospace sciences relevant to strengthening the common defence posture;
- Improving the co-operation among member nations in aerospace research and development;
- Providing scientific and technical advice and assistance to the North Atlantic Military Committee in the field of aerospace research and development;
- Rendering scientific and technical assistance, as requested, to other NATO bodies and to member nations in connection with research and development problems in the aerospace field.
- Providing assistance to member nations for the purpose of increasing their scientific and technical potential;
- Recommending effective ways for the member nations to use their research and development capabilities for the common benefit of the NATO community.

The highest authority within AGARD is the National Delegates Board consisting of officially appointed senior representatives from each Member Nation. The mission of AGARD is carried out through the Panels which are composed for experts appointed by the National Delegates, the Consultant and Exchange Program and the Aerospace Applications Studies Program. The results of AGARD work are reported to the Member Nations and the NATO Authorities through the AGARD series of publications of which this is one.

Participation in AGARD activities is by invitation only and is normally limited to citizens of the NATO nations.

Published May 1972

678.046

Printed by Technical Editing and Reproduction Ltd
Harford House, 7–9 Charlotte St, London. W1P 1HD

PREFACE

This Lecture Series is sponsored by the Structures and Materials Panel and the Consultant and Exchange Program.

The objective of the Lecture Series is to present an up-to-date review of the procedures for utilization of advanced composite structural materials.

After a review of materials (fibres, reinforced plastics, metal matrix composites), their physical properties and strength, the fabrication methods for the materials is presented.

One complete session is devoted to the presentation of experimental methods, analytical methods, automated design, and future trends.

General considerations of the application of advanced composites and airframe application of composites terminate the formal lecture.

A Round Table discussion with the participation of all the speakers concludes the Lecture Series presented in Oslo (Norway) on 1 and 2 June, Copenhagen (Denmark) on 5 and 6 June, and Lisbon (Portugal) on 8 and 9 June 1972.

B.Walter Rosen
Lecture Series Director

LIST OF SPEAKERS

Lecture Series Director

Dr B.Walter Rosen
President
Materials Sciences Corporation
P.O. Box 254
Fort Washington, Pa. 19034
U.S.A.

Professor R.J.Diefendorf
Rensselaer Polytechnic Institute
Materials Division
Troy, New York 12181
U.S.A.

Dr B.E.Read
Division of Materials Applications
National Physical Laboratory
Teddington, Middlesex
England

Dr I.C.Taig
British Aircraft Corporation Ltd
Military Aircraft Division
Warton Aerodrome
Preston PR4 1AX
England

Mr Max E.Waddoups
Project Structures Engineer
General Dynamics Corporation
P.O. Box 748
Fort Worth, Texas 76101
U.S.A.

CONTENTS

DESIGN OF COMPOSITE MATERIALS

by

B. Walter Rosen
President
Materials Sciences Corporation
Blue Bell Office Campus
1777 Walton Road
Blue Bell, Pa. 19422

SUMMARY

Studies of the relationships between the effective properties of fiber composite materials and the mechanical and geometric properties of their constituents are reviewed. The aims of such studies are, first, to provide the ability to analyze the performance of structures utilizing these heterogeneous materials, and second, to provide guidelines for the development of improved materials.

First, the rationale for designing a material to suit the application is described. The feasibility of accomplishing this aim through the use of high stiffness and high strength filamentary materials is discussed. It is emphasized that the design cycle with composites involves many more steps than the equivalent metallic structural design process.

The second section of the paper develops the relationships governing the thermomechanical properties of composites. The importance of heterogeneity and anisotropy are treated. Theoretical results are presented for composite elastic moduli, thermal expansion coefficients, thermal conductivities, and specific heats. Results are presented in a form easily usable for parametric study of candidate materials during the preliminary design phase.

The final section of the paper explores the status of the understanding of the tensile, compressive and shear strengths of unidirectional composites. The definition of the mode of failure is emphasized.

PART I - THE MODERN COMPOSITES CONCEPT

INTRODUCTION

The concept of designing a material to yield a desired set of properties has received impetus from the growing acceptance of composite materials. This utilization of the diversity of contemporary high strength and high stiffness fibers in various structural applications has motivated a new interest in the study of relationships between the mechanical and physical properties of composites and those of their constituents. The aims of such studies are, first, to provide the ability to analyze the performance of structures utilizing these heterogeneous materials, and second, to provide guidelines for the development of improved materials.

Inclusion in the structural design process of the material design phase has had a significant impact upon the entire design process; particularly upon the preliminary design phase. In this preliminary design, the number of materials which may be considered for a design generally will include many for which experimental materials properties data are not available. Thus, preliminary material selection may be based on analytically predicted properties. These analytical methods are the result of studies of the relationship between effective properties of composites and the properties of their constituents (studies which are frequently described by the misnomer "micromechanics"). The understanding of the relationships between the overall or average response of a composite and the properties of its constituents permits the representation of the inhomogeneous composite by an effective homogeneous (and generally, anisotropic) material. The properties of this homogeneous material are the effective properties of the composite; that is, they are the properties which relate the average values of the state variables in the composite. When the effective properties of a unidirectional composite have been determined, the material may be viewed as a homogeneous anisotropic material for many aspects of the design process.

The last decade has witnessed a significant increase in the understanding and utilization of fibrous composite materials. That decade has also witnessed a much larger increase in the amount of published literature in this field. The present paper provides a brief review of the available capability for composite material design and analysis. The aim is to provide guidance for one who seeks to become familiar with the tools required for designing fiber composite materials. The paper attempts to identify the key concepts associated with the use of these unique materials, and to indicate source publications for detailed explanation. In addition to the publications discussed herein, there is a valuable portion of the composites literature represented by the published collections of papers presented at conferences devoted solely to composite materials. Additionally there have appeared several books which contain chapters by different authors on various aspects of composite materials behavior. These publications are identified on the bibliography list. They are of particular value for locating the widely scattered

experimental data available for composites.

The Lecture Series on Composite Materials is organized to provide a review of the design cycle from a description of constituent properties to the test of an actual composite structure. Thus, the program contains a review of requirements, and existing and potential properties of fiber and matrix materials. Fabrication methods for commercially available fibers and processing characteristics of available matrix materials are described along with the resulting properties and materials cost. Material design capabilities are defined by describing existing relationships between macro and micro properties of composites. Requirements and potential for the material mechanical and physical properties required for preliminary design are discussed. Composite fabrication procedures for polymer and metal matrix composites are treated. Experimental methods for determining properties of the resulting materials are described. The structural design process is then defined with emphasis upon the impact of materials upon design. The role of the computer in composite design is emphasized. Trends in both design methods and structural configuration are described. Consideration of the special factors which must be treated in the application of composites to practical structures is presented. This is illustrated by description of specific airframe composites applications. Prospects for fiber utilization are discussed.

This composites design concept has shown its greatest advances in aerospace applications. However, it is well to note that, although the development of the so-called "advanced" composites has taken place primarily within the aerospace industry, even the most expensive of these new composite materials have found usage in the commercial market place. Continued reduction in fiber material costs, coupled with continued attention to sound design practices will undoubtedly lead to a substantial multiplication of the number of applications of these composites.

EFFECTIVE MATERIAL PROPERTIES

Certain definitions are of importance in the discussion of composites, particularly in the treatment of anisotropy and heterogeneity. Materials whose properties at a point vary in different directions are anisotropic; those with properties which vary from point to point are heterogeneous. On a small enough scale even the commonly considered homogeneous materials are inhomogeneous. That is, the common structural metals, on a small scale, consist of crystals. Each of these crystals is anisotropic. Its properties in different directions are different and a group of polycrystals randomly oriented represents a heterogeneous material since the properties in a given direction vary from point to point. Thus, there are two concepts, heterogeneity and anisotropy, which are pertinent to the study of composite materials. A composite can be one or both or neither of these depending upon the constituents and the scale of interest. For example, consider a fiber composite material; that is, a mixture of fibers contained in a matrix material which binds the fibers together. The two phases may individually be isotropic or anisotropic materials. When the fibers are oriented within the matrix - for example, a set of filaments, all parallel to a given line, embedded in an otherwise isotropic and homogeneous matrix - the composite material is heterogeneous but isotropic. That is, the properties at any point are the same in all directions but from point to point the properties differ. This is on a small scale; however, for contemporary filaments whose cross-sectional dimensions are extremely small, practical interest focusses on the average of stresses and strains over a dimension which is large compared to this cross-sectional dimension. For that purpose it is possible to consider the materials response in an average way to be anisotropic but homogeneous; that is, one may consider a material which has the same average properties as a given fiber composite material. This new average or "effective", material will have properties in the fiber direction which differ substantially from those in a direction transverse to the filaments. This makes it an anisotropic material. Since one is not concerned with the local perturbations associated with the individual filaments, this may be considered to be a homogeneous material. This replacement of actual by effective material provides the transition from icromechanics to macromechanics. On a microscopic scale, the composite is a heterogeneous isotropic material; whereas on a macroscopic scale, it is an anisotropic but homogeneous material. In general the problem can be compounded by recognition that the individual phases by themselves may be anisotropic, and secondly, that the geometry of the phases may be such as to produce a great variety of macroscopic anisotropies.

DESIGN APPROACH

An essential factor in a discussion of design with composites is the recognition that there are many more steps involved in a composite structural design than there are in the equivalent metallic structural design process. This design cycle for composite structures is illustrated in figure 1. The important factor in this composite design cycle is the recognition that materials design must be performed simultaneously with structures design. Thus the structural design engineer starts with a selection of constituents and a choice of the volume fractions of these two constituents. These selections define a unidirectional composite, which is the basic element of a composite structure. This unidirectional composite is characterized by certain effective properties which relate the average values of the state variables in much the same way that physical properties of homogeneous materials relate the local values of these state variables.

When contemporary high strength, high stiffness fibers are utilized to reinforce plastics, they yield composites which are very strong and stiff in the fiber direction and generally have very poor properties in the transverse directions. Thus, for the

practical structural design where a multiplicity of loading directions and conditions must be considered, the elementary structure of this material is obtained by forming a laminated composite wherein layers of the unidirectional material are oriented in various directions. At this point effective properties of the laminate can be determined. These define the properties of the basic material with which to perform structural design. It is at this stage, that the composite design cycle first reaches the starting point for structural design with isotropic metals. From this stage, the designer proceeds to the determination of the configuration of each of the structural elements and to the overall structural design configuration. In the case of composites, the availability of these many different materials enhances the opportunity to close the design loop by performing a structural efficiency analysis of the resulting structure and determining the design improvements or changes in constituent properties which can generate improved performance for the composite structure. The following sections will discuss these various aspects of the composite design cycle.

UNIDIRECTIONAL FIBER COMPOSITE MATERIALS

The first phase in the design cycle requires relations between the effective properties of unidirectional composites and the properties of their constituents. For this purpose, one may consider the basic material schematically illustrated in figure 2. The fundamental material consists of a parallel set of fibers randomly placed within an otherwise homogeneous matrix material. From this three dimensional composite one may visualize that two dimensional layers may be formed which can then be assembled in specified sequence in order to obtain the basic laminate configuration. The unidirectional material has effective overall physical properties which relate average values of the state variables. These properties can be determined by studying the material subjected to simple loading conditions. This is best illustrated by considering the basic mechanical properties relating average stress to average strain.

Elastic Constants

The unidirectional composite material behaves as an effective anisotropic material. In the most general case, it may be an orthotropic material having nine independent elastic constants. For a random distribution of fibers over a given cross section, the transverse plane may be considered to be an isotropic plane and the composite itself is then a transversely isotropic composite having five independent elastic constants. The same situation exists when the composite has fibers arranged in a regular hexagonal array. For the transversely isotropic material the five independent elastic constants can be evaluated by considering the loading conditions shown in figure 2. Thus a simple unidirectional applied stress in the fiber direction is sufficient to define an axial Young's modulus, E_a^*, and the associated axial Poisson's ratio, ν_a^*. For pure shear in the axial plane, the axial shear modulus, G_a^*, is defined. When a two dimensionally isotropic state of stress is applied in the transverse plane under conditions of plane strain, the effective plane strain transverse bulk modulus, k_t^*, is defined. For pure shear in this transverse plane, the fifth constant, the transverse shear modulus, G_t^*, can be determined. When these five constants are known, it is possible from them to determine any other desired elastic constants; for example, the transverse Young's modulus of the material.

With the desired loading conditions defined, it is possible to determine the properties analytically or experimentally, that is, one could fabricate the desired material and measure its properties. The development of analytical methods to study this problem has been motivated by the recognition that in the material design process, it is desirable to retain the freedom to consider a wide range of potential materials, rather than to limit the preliminary design to properties of composite materials which have already been evaluated experimentally. An extensive review by Hashin (ref.3) of the properties of unidirectional fibrous composites has recently been presented. Only limited aspects of this theory will be discussed herein.

Two methods which are based on sound theoretical grounds exist for evaluation of elastic constants. One of these utilizes computerized numerical methods to solve the boundary value problem of a regular array of parallel fibers in a matrix material. Initial studies of this type were presented by Pickett (ref. 4). Studies utilizing other numerical methods and different regular geometries were treated in refs. 5,6, and 7. For a discussion of these numerical methods, see ref. 3. The results of these methods are a set of elastic constants which are appropriate for the particular geometric array being studied. The shortcomings of this method of approach are: first, the requirement that solutions can be costly; second, that the regular array being analyzed is not necessarily representative of materials currently being fabricated. The second method of analysis is that of the composite cylinder assemblage model (ref. 8). This model contains some of the random characteristics desired to represent the composite. The shortcoming of the method is that the model contains fibers of varying sizes and hence, although this introduces randomness of structure, it does not accurately represent the geometry of actual composite materials. The advantage of this second approach is that the results are simple, closed-form, analytical expressions for the desired elastic constants. For four of the five independent constants, (it should be noted that Hill, ref. 9, has shown that three of the five constants are interrelated) these results are exact for the model geometry considered. For the fifth, the transverse shear modulus, the results obtained are in the form of upper and lower bounds on this modulus. The upper bound has been found to provide reasonable agreement with experimental data and hence is recommended for use by the structural designer. A simple analytical expression is also available for this property.

The existence of a set of simple and reliable expressions relating the effective elastic properties of a composite to the geometry and properties of the constituents is an extremely useful result for the evaluation of various potential materials in the preliminary design phase. However, the availability of these results is a far greater value because of the existence of a remarkable series of interactions among the various physical properties of a fibrous composite. When a fiber having known physical properties, is used in a unidirectional composite material, to form a two phase oriented material, the potential user of such a material may be interested in a wide variety of physical properties. Not only the elastic constants discussed above but various thermal and electrical properties. The evaluation of any of these physical properties as a function of the constituent properties may be a difficult problem, however, certain results are available in the literature by which many of the composite physical properties can be related to other physical properties. Three major aspects of the relationship among the different physical properties are illustrated schematically in figure 3. These relate to the problems of thermoelasticity, viscoelasticity and conduction, all of which may be of importance to the structural designer; particularly for consideration of structures performing at elevated temperatures.

Thermal Expansion Coefficients

One set of physical properties which benefits from relations of the type described above are the effective thermal expansion coefficients. Levin (ref. 10) has obtained a set of simple relations between the effective expansion coefficients and the effective elastic moduli of two-phase materials. It has been shown (ref. 11) that relations can be obtained for general anisotropic composites of generally anisotropic phases. For the unidirectional fibrous composite of two isotropic phases, as considered above, there are two different thermal expansion coefficients, the axial α_a^*, and the transverse α_t^*. When effective elastic constants are known, by whatever means they are determined, then these thermal expansion coefficients can be found directly, as long as the individual phase properties are known.

Viscoelastic Moduli

The second group of physical properties which can be related to previously obtained properties are the effective viscoelastic moduli of fibrous composite. In the cases where the individual phases exhibit viscoelastic behavior, and their creep compliances or relaxation moduli are known, they can be used to determine equivalent effective properties for the composite as a whole. The ability to do this stems from a correspondence principle for quasi-static time dependent deformation of a fibrous composite (see refs. 12 and 3). The effective viscoelastic properties can be obtained by substitution into the expressions for effective elastic properties. Extensive discussion of this subject is presented in ref. 3. The availability of these viscoelastic moduli enable an assessment of the damping characteristics of a fibrous composite. These properties can be of significance in studying vibration characteristics of a fibrous composite structure. Influence of temperature upon viscoelastic response has been considered in ref. 13. Application to composite structures has been treated in refs. 14 and 15.

Conductivities

The third set of properties indicated in figure 3 which can be obtained when elastic properties are known are the conductivities of a material. By analogy between the governing field equations for the thermal, electrical and magnetic conductivity problems and the axial shear problem for a fibrous composite these effective conductivities can be determined by a direct replacement of phase conductivity for phase shear moduli in the analytical results for the latter property.

The analysis described up to this stage has presented the definition of an integrated theory which evaluates many of the required physical properties of unidirectional fibrous composites. However there still remains the question of material strength which must be used to perform structural design.

Strength

The understanding of the influence of constituent properties upon composite strength is not as definitive as are the results obtained in the literature for the other physical properties. The primary reason for this is the influence of material heterogeneity, as indicated schematically on figure 4. Here, the simple problem of assessing the tensile strength of unidirectional fiber composites under a unidirectional load parallel to the fiber axes is considered. A range of complexities results. First, since the fibers are generally brittle materials, their strength varies from point to point and fiber strength can only be defined by statistical measures. As a result of this, when load is applied to the composite, some fractures of fibers will occur, at relatively low load levels, at weak points of the fibers. In the vicinity of these fractures there will be perturbations of the stress field. The resulting stress concentrations can cause a multiplicity of other failure modes. Thus we may have interface separation, matrix yielding, or matrix cracking, or the stress concentration may cause crack propagation. It is to be expected in the general case, that a combination of these possible failure modes will occur. Thus, under increasing load there will be a continual increase in the number of damaged regions and in the size of these damaged regions. This growth of internal damage will continue until either a crack propagation becomes unstable causing failure, or until the interaction of the large number of damaged regions causes overall failure of the material.

Studies have been made of the statistical relationship between unidirectional tensile strength of the composite and the properties of the constituents, (see refs. 16 to 19, and the review in ref. 3). These studies provide insight into the influence of the variability of filament strength upon composite behavior. They also provide some of the information necessary to quantatively compare filaments at different statistical populations, and to define specifications for desirable filaments. Alternate approaches to evaluation of composite tensile strength have utilized the parameters of classical fracture mechanics (see refs. 20 - 22). Questions relating to interpretation of tensile strength behavior on this basis are discussed by Zweben (ref. 23).

Analysis of composite strength as a function of constituent properties for other types of loading has met with very limited success. Results have been obtained for compression in the fiber direction, (refs. 24 and 25), and for axial and transverse shear and extension by limit analysis methods (see refs. 26-30). In general, it seems fair to conclude that, although an improved understanding of failure mechanisms has been obtained, composite strength values under various loads cannot be predicted from constituent properties with the reliability of the analyses for the other physical properties.

Failure Criteria

Approaches to the definition of failure criteria for design purposes have utilized both the evaluation of micro-stresses in the material and also the view that the unidirectional fibrous composite can be treated as a homogeneous anisotropic material. Emphasis has been placed upon the latter approach. Such a material will have different strength values for loads in different directions and also for tensile and compressive loads. It must be recalled that when the composite material is used in a laminate the unidirections layers will experience combined loads even when the loads applied to the laminate as a whole, are unidirectional loads. This results from the interaction between the layers. It is therefore of importance to describe the strength characteristics of unidirectional fibrous composites under combined loads. The approach to this problem is to consider that when the unidirectional material is subjected to unidirectional loading conditions that the strength values are known. The principle values of interest are: the axial strength (tensile and compressive strength for loads in the fiber direction); the transverse strength, both in tension and compression; and the axial shear strength. In some cases there will also be interest in the transverse shear strength; that is, the strength under pure shear stress in a plane perpendicular to the fibers. It would be desirable to know these unidirectional strengths from an analytical study of the constituent properties. This would provide the same freedom to the preliminary design studies that are available by virtue of the understanding of the other physical properties. However it is most reasonable to view these unidirectional strength properties as quantities which will be obtained by simple experimental measurements. The question to be resolved then is whether the interaction curve or surface can be defined in terms of these simple unidirectional properties. To date, the approaches to this problem fall largely within the category which one may describe as curve fitting. Thus the literature contains various proposed interaction curves which are postulated in a form suitable to fit experimental data.

If the unidirectional fibrous composite behaves in the fashion of a homogeneous anisotropic material, we can state that the failure surface for the material must be a function only of the following four stresses; the stress in the fiber direction, $\bar{\sigma}_a$; the maximum axial shear stress on a plane parallel to the fiber direction $\bar{\tau}_a$; and the isotropic $\bar{\sigma}_t$ and deviatoric $\bar{\tau}_t$ components of the principle stresses in the transverse plane. Thus it is convenient to postulate a failure criterion in the following form.

$$F\ (\bar{\sigma}_a,\ \bar{\tau}_a,\ \bar{\sigma}_t,\ \bar{\tau}_t) = 1$$

Two requirements are of importance if this failure criterion is to be of value. First, the quantities which must be utilized in this expression should be quantities which can be obtained from simple experimental tests. Second, the failure criterion must reflect the fact that for unidirectional extensional load there are unequal strengths in extension and compression for these materials. It is necessary to note also that unlike a homogeneous material there is little justification for postulating that material failure will not occur under a hydrostatic state of tress, since in a composite material, such a state of stress does not give rise to an isotropic state of strain. Utilizing the form used to express the shape of the anisotropic yield surface [31], Tsai [32], postulated a quadratic failure surface for the composite material. In terms of the variables used above, the general quadratic failure surface is of the following form:

$$A_{11}\,\bar{\sigma}_a^{\,2} + A_{12}\,\bar{\sigma}_a\,\bar{\sigma}_t + A_{22}\,\bar{\sigma}_t^{\,2} + B_1\,\bar{\sigma}_a + B_2\,\bar{\sigma}_t + C_{11}\,\bar{\tau}_a^{\,2} + C_{22}\,\bar{\tau}_t^{\,2} = 1 \qquad (1)$$

Various types of interaction curves have been postulated in the literature. See for example refs. 33, and 34. In general the major uncertainty is associated with the interaction term. When the interaction term is retained in the failure surface, then the coefficient can only be evaluated by running a combined stress test. This greatly complicates the experimental data necessary for the construction of a failure surface. Indeed it then creates the problem that for uniaxial strengths which differ for tension and compression it should be expected that the coefficient of the cross term (for example A_{12} in eq. 1) will be dependent upon the signs of the coefficients. For this case, four values of this coefficient will be required, to reflect the different combination of signs for the axial stress and transverse stress (see the discussion in ref. 35). Any

increase in information of this type which is to be properly reflected in the failure criteria increases the number and types of tests which must be conducted for any given material. The validity of any failure criterion is reflected in the way it represents actual experimental data for combined loads. Unfortunately, as changes are made in a failure criterion, in order to improve agreement with experiment, the results become more complex. When it becomes necessary to obtain a large number of data points to define the curve, the analytical expression for the curve is no longer of great importance.

The requirement for the structural design for those cases where experimental data are not available, is to have a capability to assess the composite strength that can be expected from given combinations of materials. It seems logical to expect that this capability will require consideration of the details of the failure mechanism as influenced by the heterogeneity of the composite material, since for stresses in different directions on the composite the associated failure modes have very different characteristics. On this basis, consideration has been given to the details of the internal stress field (e. g. ref. 36). These approaches have generally been based upon a regular array of fibers. Hence the uncertainty of local values of the stress field due to the uncertainties of geometric details raises questions about the reliability of such failure predictions.

Discussion

The status of the understanding of unidirectional composites may be briefly summarized by saying that there exists an extensive theory for evaluating effective physical properties of fibrous composites as functions of their constituents properties. An important aspect of this theory is the strong interrelationship of various effective physical properties. Further, it should also be stated that the literature represents an existing difference of opinion on suitable methods for evaluation of effective elastic constants. No single method is available which completely fulfills all the required characteristics: of being based on sound fundamental principles; of providing consistently good agreement with theory; of being practical for use in design procedures; and of adequately reflecting the nature of the internal geometry of fibrous composite. The author recommends the results of reference 8, as summarized in equations 1 - 5, as the current, most suitable method for structural analysis. Understanding of the strengths of fibrous composites is still a subject which requires further extensive research. Such research must recognize both the heterogeneity of the composite geometry and the variability of constituents.

LAMINATE STRUCTURAL ANALYSIS

When the effective physical properties of a unidirectional composite are know, the material may be viewed as a homogeneous anisotropic (transversely isotropic or orthotropic material. This representation is valid strictly only for homogeneous states of average stress and average strain. However it appears reasonable to use the effective properties whenever the average stresses and average strains vary slowly over a dimension which is large compared to a fiber cross-section dimension. Thus, when a laminate is formed from layers of unidirectional glass fiber reinforced plastics, it is reasonable to treat each layer as an anisotropic continuum and study the laminate using layered plate theory. On the other hand, a similar procedure for boron fiber reinforced plastics might be viewed with some uncertainty, inasmuch as the layer thickness for this case is only slightly greater than the fiber diameter. Nevertheless, this anisotropic layered plate theory is in widespread use for all types of composites and represents a suitable starting point for this discussion. The structural analysis of a laminated material seeks to define for the basic laminate element, the relationship between the stress resultants and the moment resultants, on the one hand, and the middle surface strains and curvatures on the other hand. For the elastic portion of the design problem, a general linear relationship between these quantities can be postulated. The constants in this relationship can be evaluated by utilizing the stress-strain relations for the individual layers and the Kirchoff-Love assumptions of plate theory. Basically, this involves a transformation, of the stress-strain relations of each layer, from the layer principal axes to the laminate principal axes. This is followed by integration through the thickness to define the force and moment resultants in terms of the displacements and curvatures. This theory was described in detail in ref. 37. (portions of which are more readily available in ref. 38) Early treatment of the problem was also presented in refs. 39 and 40. More recent comprehensive treatments are presented in refs. 41 and 42.

The results of this laminate analysis can be represented by a 6 x 6 matrix array of coefficients in the generalized force displacement relations. In general, the laminate does not have the symmetries of a homogeneous material, and as a result of this, all of the elastic coefficients in the matrix may be non-zero indicating coupling effects in the laminate. These effects are the generalization of the phenomenon found in a bi-metallic strip which exhibits a change of curvature, as well as a strain, when subjected to an in-plane force.

$$\begin{Bmatrix} N_i \\ M_i \end{Bmatrix} = \begin{bmatrix} a_{ij} & b_{ij} \\ b_{ij} & d_{ij} \end{bmatrix} \times \begin{Bmatrix} \varepsilon_j^o \\ \kappa_j^o \end{Bmatrix}$$

where N_i are the three stress resultants

M_i are the three moment resultants

ε_j^o are the three reference surface strain components

κ_j^o are the three change of curvature components

and a_{ij}, b_{ij}, and d_{ij} are the laminate properties.

In these relations the b_{ij} vanish for a homogeneous isotropic material or an orthotropic material with principal elastic axes, x_L and x_T. Thus in these cases, there is no coupling between bending and extension. However some forms of coupling do exist for even simple laminates. For example, for a laminate composed of an even number of identical orthotropic layers whose principal axes are alternately oriented at $+\theta$ and $-\theta$ to the x_L axis, there is coupling between the twisting curvature and the extensional forces; between the bending curvatures and the shear force; between the shear strain and the bending moments; and between the extensional strains and the twisting moment.

When the same layers are alternated symmetrically about the middle surface there is coupling between twisting curvature and bending moments, and between bending curvatures and twisting moments only. This is generally the minimum type of coupling found for laminates having orthotropic laminae oriented at other than 0° or 90°, although even this can be eliminated by certain special laminate configurations.

In both of the last two cases the coupling terms become relatively smaller as the number of layers increases. The coupling effects introduce significant complications into the analysis of laminated plates. However, methods of solution utilizing plate and shell theories modified to incorporate these effects are available.

PLATE AND SHELL ANALYSIS

The laminate analysis described previously, defined the effective elastic properties which relate the force and moment variables to the displacement and curvature variables. With these properties known, the composite laminate generally may be treated as a homogeneous anisotropic material and existing analyses for such materials may be utilized. For the basic theory for such materials reference should be made to references 40 and 43 - 45. A listing of reference material for the stress, stability and vibration analyses of anisotropic plates and shells may be found in ref. 46.

Although the approach outlined to this point defines a method for analysis of most composite structures, several problems do remain. First, much of the literature on analysis of homogeneous anisotropic structures applies to orthotropic materials. Thus the coupling effects discussed above are not considered. Second, the existence of layers creates a possible problem due to interlaminar stresses. Additionally the low shear stiffness of unidirectional composites results in an increase in the effects of transverse shear upon plate and shell behavior. These problems are the subject of current research.

PART II - DESIGN FOR PHYSICAL PROPERTIES

The design of a fibrous composite material to yield the properties desired for a particular application requires analytical relationships between the effective properties of the composite and the mechanical and geometrical properties of its constituents. A two phase unidirectional fibrous composite is considered first. This is defined as a material containing a parallel set of strong and stiff fibers embedded in a homogeneous matrix material. For this case, simple and reliable theoretical results are available for the evaluation of composite elastic moduli, thermal expansion coefficients thermal conductivities and specific heats. These results are presented herein as a summary. Additionally, the status of recent studies of the tensile strength in the fiber direction is examined. Here the results in the literature are less definitive than those for moduli, etc. However it is possible to demonstrate that the influence upon composite strength of the statistical nature of the strength of contemporary advanced filaments can be analyzed.

The contents of this section reproduce portions of the discussion presented by this author in ref. 47.

Effective Properties

The concept of effective properties is based upon treatment of average values of the state variables. When a multiphase material, in which the characteristic dimension of a typical inhomogeneity (or phase region) is small compared to the specimen dimension, is used as a structural material, we may be interested in the response to loads on both a microscopic and a macroscopic level. The former, detailed stress analysis is perhaps of interest for development of failure analyses; while the latter, overall response, is of interest for structural performance. This is analogous to the comparable views of a so-called isotropic polycrystalline metal in which average stress, strain and displacement fields are adequate for most structural design properties, while microscopic details of the stress field may contribute to an understanding of failure mechanics.

It can be shown that for a multiphase material the volume averages of the stress components can be expressed as functions only of the boundary tractions (and the body forces, if they are non-vanishing). Similarly, the volume averages of the strain components can be expressed as functions of the surface displacements only. Also the

average temperature is surface temperature, when the latter is constant. All of these relations are independent of phase geometry and phase properties. The insensitivity of these macroscopic state variables to internal details, and the direct relationship between these variables and the boundary conditions, are strong recommendations for the validity of their use to characterize the state of the composite. The composite properties which relate these average state variables are defined as the effective material properties. Thus, the ratio of a given average stress to the corresponding average strain defines an effective elastic stiffness of the composite. The ratio of the average free thermal strain to the average temperature rise defines the effective thermal expansion coefficient of the composite. When all of the effective composite properties are known, one may view the inhomogeneous composite as if it were a homogeneous and generally anisotropic material.

The study of the relationship between the effective properties and the constituent properties has the two-fold aim of providing the information necessary to determine the macroscopic state variables for a composite subjected to specified boundary conditions, and of defining desirable changes in constituent properties to yield improved performance in a given environment.

Elastic Moduli

Relations among the average stresses and average strains in the unidirectional fibrous composite have been studied for simple boundary conditions on either the displacements, or the tractions. In particular the boundary conditions considered are those which, when applied to homogeneous materials, give rise to uniform strains, ε_{ij}^{o}, (for displacement boundary conditions) and to uniform stresses, σ_{ij}^{o}, (for traction boundary conditions) throughout the material. In the composite material, it can be shown that, although local stresses and strains are generally far from uniform, the average strains $\bar{\varepsilon}_{ij}$, for the displacement boundary conditions described above are given rigorously by:

$$\bar{\varepsilon}_{ij} = \varepsilon_{ij}^{o} \tag{2}$$

and the average stresses , $\bar{\sigma}_{ij}$, for the traction boundary conditions described, are given by:

$$\bar{\sigma}_{ij} = \sigma_{ij}^{o} \tag{3}$$

Furthermore, it follows from the fact that the field equations are linear, that for either case (2) or (3) above, the average stresses and average strains are linearly related. Thus the effective stress-strain relations may be written

$$\bar{\sigma}_{ij} = C^{*}_{ijkl}\,\bar{\varepsilon}_{kl}$$

where the constants, C^{*}_{ijkl}, are the effective elastic moduli.

Specifically, for the unidirectional composite, the material is transversely isotropic and has five independent moduli. Evaluation of these effective moduli requires some consideration of the matrix geometry. Several possible types of cross-sectional (normal to the fiber direction) geometry are presented in Fig. 5 . The hexagonal array is typical of the regular arrays which have been studied with the aid of computers, by numerical methods, (e.g. Chen and Cheng, ref. 7). The geometry labeled "real" indicates that the actual material is generally characterized by an irregular or random cross-sectional geometry. Material models which reflect aspects of this non-uniform phase geometry include the arbitrary phase geometry and the composite cylinder assemblage geometry shown in the lower portion of the figure. For the former, rigorous bounds can be obtained (see Hill ref. 9 and Hashin ref. 48) for each of the independent moduli. These bounds will generally be far apart when the phase moduli are, as they apply to any phase geometry including the cases of a continuous phase geometry of either the stiffer or the less stiff material.

The composite cylinder assemblage is a model proposed by Hashin and Rosen (ref. 8). This model incorporates randomness of structure and permits the derivation of simple closed form expressions for the effective elastic moduli. The five independent moduli are conveniently selected to be the axial Young's modulus, E_a^{*}, the associated Poisson ratio for uniaxial stress in the fiber direction, ν_a^{*}, the transverse plane-strain bulk modulus, k_t^{*}, the axial shear modulus, G_a^{*}, and the transverse shear modulus, G_t^{*}. The results for these composite moduli in terms of the matrix and fiber elastic properties are given by:

$$E_a^{*} = \bar{E} + \frac{4v_f v_m (\nu_f - \nu_m)^2}{\frac{v_m}{k_f} + \frac{v_f}{k_m} + \frac{1}{G_m}} \tag{4}$$

$$\nu_a^{*} = \bar{\nu} + \frac{v_f v_m (\nu_f - \nu_m)\left(\frac{1}{k_m} - \frac{1}{k_f}\right)}{\frac{v_m}{k_f} + \frac{v_f}{k_m} + \frac{1}{G_m}} \tag{5}$$

$$k_t^{*} = \frac{k_m k_f + \bar{k} G_m}{v_m k_f + v_f k_m + G_m} \tag{6}$$

$$G_a^* = G_m \frac{v_m G_m + (1 + v_f) G_f}{(1 + v_f) G_m + v_m G_f} \tag{7}$$

where:
E Young's modulus
G Shear modulus
k Plane strain bulk modulus
K Bulk modulus (used subsequently)
ν Poisson's ratio
v Phase volume fraction
f Subscript to denote fiber
m Subscript to denote matrix
a Subscript to denote axial
t Subscript to denote transverse
Overbar denotes volume-weighted average of phase properties

$$G_t^* = G_m \frac{(\alpha + \beta_m v_f)(1 + \rho v_f^3) - 3 v_f v_m^2 \beta_m^2}{(\alpha - v_f)(1 + \rho v_f^3) - 3 v_f v_m^2 \beta_m^2} \tag{8}$$

where:

$$\alpha = \frac{\gamma + \beta_m}{\gamma - 1} \qquad \beta = \frac{1}{3 - 4\nu}$$

$$\rho = \frac{\beta_m - \gamma \beta_f}{1 + \gamma \beta_f} \qquad \gamma = \frac{G_f}{G_m}$$

The results (4) to (7) are exact for the model treated. The expression (8) for G_t^* is equivalent to the upper bound for this assemblage as found by Hashin and Rosen (ref. 8).

With the moduli (4) - (8) available, other important constants can be evaluated. Thus for example, the transverse Young's modulus, E_t^*, and the Poisson's ratio in the transverse plane, ν_t^*, are given by:

$$E_t^* = \frac{4 k_t^* G_t^*}{k_t^* + G_t^* \left(\frac{1 + \frac{4 k_t^* \nu_a^{*2}}{E_a^*}}{}\right)} \tag{9}$$

$$\nu_t^* = \frac{1}{2} \left(\frac{E_t^*}{G_t^*} \right) - 1 \tag{10}$$

The transverse Young's modulus given by equation (9) is compared with experimental data of Whitney and Riley (ref. 49) in Figure 6 for Boron fibers in an epoxy matrix. Similarly the results of equation (9) are compared with the experimental data of Adams and Doner (ref. 5) for glass/epoxy composites in Fig. 7. Also shown are the numerical results by the same authors for a square array. The comparisons of Figures 6 and 7 indicate the nature of the support for the conclusion that the composite cylinder assemblage results provided good agreement with experimental data and with elaborate numerical results. The simple expressions (4) - (8) for the five independent moduli are therefore recommended for use.

It should also be noted that the composite cylinder assemblage analysis yields local stress distributions. There appears to be little reason to believe that these stresses are any less reliable than those obtained by numerical methods, in view of the uncertainty of the actual geometry. The results presented above can be used in a laminated plate analysis to evaluate the elastic properties of plates with planar arrays of fibers. Also, these results can be used with the correspondence principle to obtain effective viscoelastic properties (see Hashin ref. 12).

Thermal Expansion Coefficients

Evaluation of the response of composite materials to temperature changes is important, not only for high and low temperature applications, but also for fabrication considerations such as the choice of the cure temperature for fiber reinforced plastics. For the elastic composite, the stress-strain relations (3) are modified to include thermal expansion coefficients. Thus, with the strains as the dependent variables, the thermoelastic stress-strain relations are:

$$\bar{\varepsilon}_{ij} = S^*_{ijkl} \bar{\sigma}_{kl} + \alpha^*_{ij} \bar{\theta} \tag{11}$$

Here the effective elastic compliances, S^*_{ijkl}, are obtained from (3) by inversion. The effective thermal expansion coefficients, α^*_{ij}, relate the average strains, $\bar{\varepsilon}_{ij}$, to the average temperature rise, $\bar{\theta}$, for traction free surfaces (i.e. for zero average stresses).

Levin (ref. 10) has obtained simple relationships between the effective expansion coefficients and the effective elastic moduli of two phase materials. For the unidirectional fibrous composite of two isotropic phases, considered above, there are two

different expansion coefficients (the axial, α_a^*, and the transverse, α_t^*) given by:

$$\alpha_a^* = \bar{\alpha} + \left(\frac{\alpha_1-\alpha_2}{\frac{1}{\bar{K}_1}-\frac{1}{\bar{K}_2}}\right)\left[\frac{3(1-2\nu_a^*)}{E_a^*} - \left(\frac{\bar{1}}{\bar{K}}\right)\right] \tag{12}$$

$$\alpha_t^* = \bar{\alpha} + \left(\frac{\alpha_1-\alpha_2}{\frac{1}{\bar{K}_1}-\frac{1}{\bar{K}_2}}\right)\left[\frac{3}{2k_t^*} - \frac{3\nu_a^*(1-2\nu_a^*)}{E_a^*} - \left(\frac{\bar{1}}{\bar{K}}\right)\right] \tag{13}$$

When the moduli of equations (4) - (8) are used in equations (12) and (13), effective expansion coefficients can be evaluated directly from phase properties. Typical results are presented in Fig. 8 for phases having high modulus fibers in an epoxy matrix. The dominant influence of the fiber expansion coefficient, α_f, upon the axial composite expansion coefficients, α_a^*, is evident. In this case, for low fiber volume fractions, the transverse expansion coefficient, α_t^*, is larger than that of the binder or matrix material, α_m.

For the evaluation of expansion coefficients of composites having more than two phases, it is necessary to treat the strain energy. For the material without temperature changes which was discussed earlier, the strain energy could be written simply in terms of average stresses and strain and effective elastic moduli. The form of these expressions being the same as for the homogeneous material. In the thermoelastic case, it can be shown that in order to write the energy functions only in terms of average values of the state variables (stress, strain and temperature) and effective composite properties, it is necessary to include the effective specific heat as well as the effective elastic moduli and effective thermal expansion coefficients, (see Rosen ref. 50). These energy expressions can then be used to bound all the effective properties. Also they can be used to yield results for composite heats.

Thermal Properties

The effective specific heat of a composite at either constant pressure or constant volume, is not the volume-weighted average of the appropriate phase specific heats. The reason for this is that a temperature change at constant volume of the composite generally takes place with volume changes in each phase. A similar observation can be made for the constant pressure case.

The effective specific heat at constant pressure, c_p^*, can be found for the two phase fibrous composite to be (see Rosen and Hashin ref. 11):

$$\frac{c_p^* - \bar{c}_p}{T_o} = \frac{v(\alpha_f-\alpha_m)^2}{\left(\frac{1}{\bar{K}_f}-\frac{1}{\bar{K}_m}\right)^2}\left[\left(\frac{\bar{1}}{\bar{K}}\right) - S^*_{iijj}\right] \tag{14}$$

T_o is the reference temperature. The sum of the effective compliances, S^*_{iijj}, for an effectively isotropic composite is the inverse of the bulk modulus. For the unidirectional fibrous composite it is given by:

$$S^*_{iijj} = \frac{(1-2\nu_a^*)^2}{E_a^*} + \frac{1}{k_t^*} \tag{15}$$

Although the specific heat theoretically differs from the "rule of mixtures" value, it should be noted that

$$\bar{c}_v \geq c_p^* \geq \bar{c}_p \tag{16}$$

Since there is a very small difference between the outermost terms of inequality (16), for solids, the rule of mixtures does provide a useful numerical result.

The effective thermal conductivities of the unidirectional fibrous composite can also be expressed in terms of the phase properties, (see Hashin ref. 51). The composite axial conductivity, μ_a^*, is given simply by:

$$\mu_a^* = \bar{\mu} = v_f\mu_f + v_m\mu_m \tag{17}$$

μ_f and μ_m are the phase conductivities.

The transverse conductivity can be defined rigorously for the composite cylinder assemblage and is given by:

$$\mu_t^* = \mu_m \frac{v_m\mu_m + (1+v_f)\mu_f}{(1+v_f)\mu_m + v_m\mu_f} \tag{18}$$

Thus the effective properties required for thermoelastic analysis of a fibrous composite are available. Each one of the elastic moduli, the thermal expansion coefficients

and the thermal conductivities along with the specific heat is given by a simple formula. Further, the strain energy expression and the associated thermoelastic variational principles are formulated so that an energy approach can be utilized for the solution of thermoelastic properties.

PART III - DESIGN FOR STRENGTH

The high tensile strength of contemporary uniaxial fibrous composites is well recognized and widely utilized. In contrast, the present understanding of the tensile failure mechanism and the influence thereon of constituent properties is extremely limited. There are, however, several existing analyses which provide the initial elements of a rational theory for the tensile failure of fibrous composites. Analyses and tests of uniaxial composites have indicated that their strength in compression is also attractively high. The mechanics of composite compressive failure are also reviewed herein. Other studies of composites have demonstrated that weaknesses in the direction transverse to the fibers are to be expected and will limit the efficiency of composites used in thin plate and shell structures. This leads to the utilization of composites in the form of multi-directional laminates. Treatment of design criteria for laminates is discussed in the section of this Lecture Series prepared by Waddoups.

Tensile Strength

Two important factors must be treated in the study of strength of fiber composite materials. These are the non-uniformity of fiber strength and the heterogeneity of the composite. Non-uniform strength is characteristic of most current high-strength filaments. This is illustrated in fig. 9 , which shows typical strength distributions for a group of single filaments of two different types of commercial glass fibers. This statistical distribution is generally attributed to a distribution of imperfections along the length of these brittle fibers.

Two important consequences of the wide distribution of fiber strengths should be noted. First, the fiber strength will generally be length dependent. The longer the fiber, the greater the likelihood of encountering a weak spot. Thus, average values of the strength of the brittle fibers are of little meaning if they are not related to the test gauge length. The second effect is that in a composite, one can always expect some fiber breaks at relatively low stresses. Understanding tensile strength requires solution of the problem of determining effects subsequent to these initial internal breaks. It is because this requires knowledge of local values of the stresses, that the strength problem is complex.

At each local fiber break, several possible effects may occur. In the vicinity of the fiber break the local stresses are highly non-uniform. As indicated in fig. 4 , this may result in a crack propagating along the fiber interface or across the composite. In the former case, the fibers separate from the composite after breaking and the material behaves as a dry bundle of fibers. In the second case, the composite fails due to the normal crack and the strength is governed by that of the weak fiber. This latter mode may be considered to be a "weakest link" failure. If the matrix and interface properties are of sufficient strength and toughness to prevent these failures, then continued load increase will produce new fiber failures at other locations in the material. This statistical accumulation of internal damage is indicated schematically in the last sketch of fig. 4 . In actuality, it is to be expected that all three effects will generally occur prior to material failure. That is, fractures will propagate along and normal to the fibers and these fractures will occur at various points within the composite. This is represented schematically in fig. 10 .

Fibers are generally much stiffer than matrix materials, and therefore they carry the bulk of the axial load, unless the fiber volume fraction, v_f, is very small. Therefore the study of the tensile strength of composite materials centers on the behavior of the fibers and what happens when they break at various locations as a composite is loaded. Composite strength can be expressed directly in terms of the average fiber stress at composite failure for resin-matrix composites. In the case of metal matrix composites, it is necessary to superpose a contribution of the matrix to axial load-carrying capacity. Previous treatments of tensile failure modes have recently been reviewed in ref. 52. Portions of that review are repeated in the following discussion.

Weakest Link Failure

When a unidirectional composite is loaded in axial tension, scattered fiber breaks occur through the material at various stress levels. It is possible that one of these fiber breaks may cause the fracture of one or more adjacent fibers, followed by a continued propagation leading to overall failure. This produces a catastropic mode of failure associated with the occurrence of one, or a small number of, isolated fiber breaks. This is referred to as the "weakest link" mode of failure. The lowest stress at which this type of failure can occur is the stress at which the first fiber will break. The expressions for the expected value of the weakest element in a statistical population (see e. g. Ref. 16) have been applied to determine the expected stress at which the first fiber will break by Zweben (Ref. 53). Assuming that the fiber strength is characterized by a Weibull distribution of the form

$$F(\sigma) = 1 - \exp(-\alpha L \sigma^{\beta}) \tag{19}$$

the expected first fiber break will occur at a stress

$$\sigma_w = \left(\frac{\beta-1}{NL\alpha\beta}\right)^{1/\beta} \quad (20)$$

where α and β are parameters of the Weibull distribution, L is the length of the fiber and N is the number of fibers in the material. Thus, eq. 20 provides an estimate of the failure stress associated with the weakest link mode.

It should be pointed out that the occurrence of the first fiber break is a necessary, but not a sufficient condition for failure. That is, the occurrence of a single fiber break need not precipitate catastrophic failure. Indeed, in most materials it does not. This is fortunate because, as shown by eq. 20 the weakest link failure stress decreases with increasing material size (length and number of fibers). For practical materials in realistic structures, σ_w is quite low. Other conditions that must be satisfied if the weakest link mode of failure is to occur, are discussed in ref. 52.

Cumulative Weakening Failure

If the weakest link failure mode does not occur it is possible to continue loading the composite and, with increasing stress, fibers will continue to break randomly throughout the material. When a fiber breaks there is a redistribution of stress in the vicinity of the fracture site. This stress perturbation is the origin of important mechanisms involved in composite failure. The interface shear stress acting on the broken fiber localizes the axial fiber dimension over which the stress in the broken fiber is greatly reduced. Were it not for some form of interfacial shear stress, a broken fiber would be unable to carry any load and the composite would be, in effect, a bundle of fibers from the standpoint of resisting axial tensile loading.

An important function of the matrix is to localize the reduction of fiber stress when one breaks. The axial dimension over which the axial fiber stress is significantly reduced, which will be referred to as the ineffective length, δ, is a significant length parameter involved in the failure of fiber composite materials. The magnitude of δ depends on the stress distribution in the region of the fiber break This distribution is quite complex and is influenced by fiber and matrix elastic properties as well as any inelastic phenomena, such as debonding, matrix fracture or yield, etc., that may occur. The definition of δ is somewhat arbitrary since the stress in the broken fiber is a continuously varying quantity.

The concept of representing this variable stress field in a fiber composite material having distributed fractures, by an assemblage of elements of length, δ, was introduced by Rosen (ref. 18). In this model as shown in fig. 11 the composite is considered to be a chain of layers of dimension equal to the ineffective length. Any fiber which fractures within this layer will be unable to transmit a load across the layer. The applied load at that cross-section is then assumed to be uniformly distributed among the unbroken fibers in each layer. The effective load concentrations, which would introduce a nonuniform redistribution of these loads, are not considered initially. A segment of a fiber within one of these layers may be considered as a link in the chain which constitutes an individual fiber. Each layer of the composite is then a bundle of such links and the composite itself a series of such bundles as shown in fig. 11 . Treatment of a fiber as a chain of links is appropriate to the hypothesis that fracture is due to local imperfections. The links may be considered to have a statistical strength distribution which is equivalent to the statistical flaw distribution along the fibers. The realism of such a model is demonstrated by the length dependence of fiber strength.

For this model it is necessary to define the link dimension, δ; the probability of failure of fiber elements of that length; and then the statistical strength distribution of the assemblage. This analysis leads to the "cumulative weakening" mode of failure. The definition of ineffective length is discussed further below. The determination of the link strength distribution is treated in Ref. 18. When these are known, the relationship of the strength of the assemblage to the strength of the elements, or links, can be treated by the methods of Ref. 16. The result, for fibers having a strength distribution of the form (1.1) is given in Ref. 18 as:

$$\sigma^* = (\alpha\delta\beta e)^{-1/\beta} \quad (21)$$

where σ^* is the statistical mode of the composite tensile strength based on fiber area.

As pointed out above, the cumulative weakening model represents the varying stress near a fiber break by a step function in stress. The model also neglects the possibility of failures involving parts of more than one layer. More importantly, the overstress in unbroken fibers adjacent to the broken fibers has not been considered. This stress concentration increases the probability of failure for these adjacent elements, and creates the probability of propagation of fiber breaks. This combination of variable fiber strength and variable fiber stress can be expected to lead to a growth both in the number of damaged regions and in the size of a given damaged region. This is represented schematically in fig. 10, wherein the cross hatched regions at the ends of cracks represents the ineffective length of the broken group.

In this situation described above, there exists the possibility that one damaged group may propagate causing failure, or that the cumulative effect of many smaller damaged groups will weaken a cross-section causing failure. The latter possibility is considered in ref. 52. The former possibility, which was proposed by Zweben (ref. 53), is reviewed briefly below. First a discussion of the stresses in the vicinity of a broken fiber is

in order.

Internal Stresses

The stress field around a broken fiber has been studied by many authors. Among the early studies are those of Refs. 54 and 55. These, or similar stress distributions were used in Refs. 18 and 56 to define ineffective lengths. More recently the studies of Refs. 57-60 have utilized shear lag analyses to define load distributions in two and three-dimensional unidirectional fiber composites. These results can be used to determine the load concentrations in unbroken fibers required to assess the probability of propagation. The results of these investigations showed the elastic load concentrations in two-dimensional (planar) arrays of parallel fibers in axial tension are large and increase with the number of broken filaments. Elastic load concentrations for three-dimensional arrays of parallel fibers are lower. The effects of fiber debonding, or matrix cracking, and matrix plasticity for the case of one broken fiber was studied in Refs. 57 and 58. It was found that non-elastic effects such as debonding and plasticity can significantly reduce load concentration factors. This would serve to reduce the likelihood of fiber break propagation.

The effects of an elastic-perfectly-plastic matrix and interfacial failure on the perturbed region adjacent to a single broken fiber were studied by Hedgepeth and Van Dyke (refs 57 and 58). They found that, after debonding of a smooth, frictionless interface, broken fibers will debond completely when the load is increased only slightly above the fiber fracture load. Experience with real materials indicates that complete debonding is rarely observed and thus the assumption of no post-failure shear transfer appears to be unrealistic. The results for the elastic-plastic matrix material predict a more gradual extension of the perturbed region with increasing stress. For real materials the post-failure shear transfer probably lies somewhere in between the extremes of zero stress transfer and perfect plasticity (constant shear stress).

Fiber Break Propagation Failure

The effects of stress perturbations on fibers adjacent to broken ones are of significance. When a fiber breaks, the average stress in the remaining fibers must increase. Because of the matrix, the stress redistribution is highly non-uniform. The shear stress that arises in the matrix when a fiber breaks results in localized increases of average stress in the fibers surrounding the break. In order to differentiate this increase in the average stress over a fiber cross-section from the increase at a point, the term "load concentration" is used for the former and the conventional term "stress concentration" for the latter.

The load concentrations increase the probability of fiber failure, and introduce the propagation of fiber breaks as a mechanism of failure. The probability of occurrence of this mode of failure increases with the average fiber stress because of the increasing number of scattered fiber breaks and the increasing stress level in overstressed fibers.

The fiber break propagation mode of failure was studied by Zweben, (Ref. 53) who proposed that the occurrence of the first fracture of an overstressed fiber could be used as a measure of the tendency for the fiber breaks to propagate and hence as a failure criterion for this mode. (at least for small volumes of material) The effects of load concentrations upon fiber break propagation in 3D unidirectional composites, as well as upon cumulative weakening failures, was treated in Ref. 61. In Ref. 62, Zweben presented experimental evidence for a variety of fiber-matrix systems to support the contnetion that the first multiple break is a lower bound to strength. Although the first multiple break criterion may provide good correlation with experimental data for small specimens and may be a lower bound on the stress associated with fiber break propagation it gives very low stresses for large volumes of materials, which appear to conflict with practical experience with composites. However, there does not appear to be a sufficient body of reliable data available to assess the influence of material size on strength.

Discussion

Results of the statistical cumulative weakening tensile failure analysis of ref. 18 are presented in Fig. 12 in non-dimensional fashion. The ratio of the strength of a large composite to the mean strength of a set of individual fibers of length, L, is plotted as a function of the coefficient of variation (standard deviation divided by mean value) of the single fiber population. Curves are presented for various values of the ratio of fiber test length, L, to the ineffective length, δ . For reference fibers of length, δ , the composite strength is less than the average fiber strength and decreases for increasing variation of fiber strength. (This is illustrated by the solid curve of Fig.12). However for the more commonly used reference fiber test length, L/ is much larger than unity and the individual fiber strength is more sensitive than the composite strength to the fiber coefficient of variation. This yeilds ratios of composite strength to mean fiber strength which are greater than unity. (Indicated by the dashed curves of Fig.12). These curves indicate that the composite strength is expected to be a high fraction of the average strength of very short length fibers. Thus, the composite may well be of higher strength than a set of individual fibers of moderate length. Fiber length is considered short when it is on the order of the ineffective length, (which is characteristically on the order of ten to one hundred fiber diameters). By this criterion, a one inch length of present commercial glass or carbon fiber is a long fiber.

Several analyses of the failure mechanics for this case have been presented and they will be reviewed briefly in this section. It was suggested in ref. 66, that the mechanism of failure was a micro-instability of the fibers in a fashion analogour to the buckling of a column on an elastic foundation. It has been demonstrated that this will occur even for a brittle material, such as glass. For example, fig. 16 from ref. 24 shows single E-glass filaments embedded in blocks of epoxy which have been cooled to produce a compressive strain. The three separate specimens contain fibers of 0.0050 in., 0.0035 in. and 0.0004 in. The photoelastic stress pattern emphasizes the repetitive nature of the deformation pattern for each fiber and supports the contention that the deformations result from an elastic instability.

Analyses of this instability were performed independently in refs. 24 and 25. The analyses treat a layered two-dimensional medium wherein the fibers are assumed to buckle sinusoidally. When adjacent fibers buckle 180° out of phase with each other, the major matrix strains are extensional; when they buckle in phase, the major strains are shear strains. These two modes are denoted the extensional and shear modes respectively.

The resulting compressive strength for the shear mode is given by:

$$\sigma_c = \frac{G_b}{1 - v_f} \tag{22}$$

The associated strain is

$$G_c = \frac{1}{v_f(1 - v_f)} \left(\frac{G_b}{E_f}\right) \tag{23}$$

The equivalent results for the extension mode are given by:

$$\sigma_c = v_f \left[\frac{2E_f E_b v_f}{3(1-v_f)}\right]^{1/2} \tag{24}$$

and

$$G_c = \left[\frac{2v_f}{3(1-v_f)}\right]^{1/2} \left(\frac{E_b}{E_f}\right)^{1/2} \tag{25}$$

The stresses of eqs. (22) and (24) are plotted in fig. 17 for glass reinforced plastics as a function of fiber volume fraction. The figure shows that, except for small fiber volume fractions, the shear mode governs composite strength. The failure strain defined by eqs. (23) and (25) are plotted in fig. 18 which shows that for many composites, the computed failure strain levels exceed the proportional limit strain for the matrix. In an effort to assess the significance of this result the matrix was treated as an elastic perfectly plastic material and the secant modulus was used to define matrix stiffness. For the generally dominant shear mode, this led to the following result, in place of eq. (22):

$$\sigma_c = \left[\frac{v_f E_f \sigma_y}{3(1-v_f)}\right]^{1/2} \tag{26}$$

where σ_y is the matrix yield stress level.

The stresses of eq. (26) are labelled "inelastic" on fig. 17.

The results of the present analysis indicate that composite compressive strength is independent of fiber diameter. Observed departures from this prediction may possibly be associated with the improved collimation attainable with a larger diameter filament.

The internal instability of a layered medium was initially treated in ref. 66. Since the fiber composite instability was studied in refs. 24 and 25 by a two-dimensional approximation of the material geometry, the result of ref. 66 is directly comparable. When the fiber to binder modulus ratio is large the exact result of ref. 66 reduces to eq. (22).

Concluding Remarks

The results of these studies, indicate that for the elastic case, the binder Young's modulus, is the dominant parameter. However, for the inelastic case, there are strength limitations which depend both upon the fiber modulus and upon the binder strength. The nature of changes made in matrix properties to improve the compressive strength of composites of a given fiber depends upon the base of reference. In some cases performance is limited by a binder yield stress at a given fiber modulus, whereas for other cases a gain in compressive strength could be achieved by improving the binder modulus. The analytical results provide guidance for determination of reasonable changes in matrix properties to yield improved composite compressive strength.

SHEAR STRENGTH

The two principal directions of applied shear stress are: (1) in a plane which contains the filaments, and (2) in a plane normal to the filaments. In the first case, as the following failure analysis will show, the filaments provide essentially no reinforcement to the composite and the shear strength depends upon the shear strength of the matrix material. In the second case, some reinforcement may occur and , at high volume fractions of filaments, it may be substantial. Because the analysis shows that reinforcement does not take place in the planes of the filaments, these planes may be considered planes of shear weakness.

Planes of shear weakness do indeed exist in filamentary composites. Unfortunately failures involving these planes have acquired the designation "interlaminar shear failures", the implication being that they occurred because of shear stresses induced between laminae. In point of fact, it is just as reasonable to define these failures as

The effect of load concentration alone is best illustrated by treatment of a composite containing finite length fibers of uniform strength. The load in such fibers varies along the length of any given fiber. It is zero at the fiber end, and it is a maximum at the point opposite an adjacent fiber end. If many of the fibers are adjacent to a fiber end, the composite will fail when the load at the overstressed point is equal to the uniform fiber strength. Thus the strength of the composite will be less than that of the fibers.

As indicated earlier, the influence of both the statistical nature of the fiber strength and the non-uniformity of stress in the vicinity of a fiber end should be taken into account in a composite tensile failure model. One approach to this problem by Zweben (ref. 53) involves the determination of the expected number of multiple breaks in the material. When this method is applied to a tensile test specimen, results similar to those shown in Fig. 13 are obtained. In this figure, taken from ref. 61, the expected number of breaks, E_1, due to the basic strength distribution of the fibers is plotted as a function of average fiber stress. As a result of these breaks and the resulting load concentrations in adjacent fibers (as evaluated, for example by Hedgepeth (ref. 60) for the two-dimensional case, and Hedgepeth and VanDyke (ref. 57) for the three-dimensional case) there will be some multiple breaks in the composite. The expected number of groups of n adjacent broekn fibers, E_n, is plotted for n equal to two, three and four. These curves are plotted for boron fibers in an aluminum matrix. Experimental data for such composites, obtained by Kreider and Leverant (ref. 63) yielded strength in the range indicated. The curves for multiple breaks rise sharply in this range.

This statistical measure of size and distribution of internal cracks suggests the possibility of using a fracture mechanics type failure criterion. This is indicated schematically in fig. 14 (from ref. 61) wherein it is suggested that the methods used to obtain the curves of expected numbers of multiple breaks, as shown in fig. 13, can be used to yield plots of crack size versus nominal stress for fixed values of probability. If a curve of applied stress necessary to cause failure in a composite having a maximum crack of a given size could be obtained, then the intersections of the curves shown would define probability of failure at given stress values.

An approach which may be used to obtain the upper curve of fig. 14 is that of Cooper and Kelly (ref.64) in which a deterministic analysis is performed on a material with non-uniform, but known geometry. Bounds on the expected value of composite strength were generated in ref. 61. The cumulative weakening model, neglecting load concentrations was used to provide an upper bound to the strength. The stress, σ_2, at which the expected value of multiple breaks is unity measures the beginning of a crack propagation was used to represent a lower bound to the strength. These bounds on the expected value of tensile strength are shown in fig. 15 along with individual experimental data points from ref. 63. The curve for the weakest link theory (stress, σ_1, at which the expected value of number of broken fibers is unity) is also shown. The curves for σ_1 and σ_2 are based on fiber strength data measured on fibers extracted from composites. For comparison the curve labelled σ_1^* is based on virgin fiber data. Using this information, only a small number of fiber fractures would be expected prior to failure. This is not in accord with experimental results. The agreement indicated by fig. 15 provides encouragement for continued studies utilizing the statistical failure models. However for large volume specimens, the lower bounds can be expected to become unrealistically low. In ref. 52, load concentration effects were incorporated into a statistical model. The model for this failure mode was formulated to reflect the following three effects, which are deemed to be of importance in the tensile failure of high strength fibrous composites:

1. The variability of fiber strength will result in distributed fiber fractures at stress levels well below the composite strength.
2. Load concentrations in fibers adjacent to broken fibers will influence the growth in size of the crack regions to include additional fibers.
3. High shear stresses will cause matrix shear failure or interfacial debonding which will serve to arrest the propagating crack.

In this model, the sequence of events leading to failure is as follows: first distributed fiber breaks occur at relatively low stress levels; these breaks grow in size due to load concentrations; additional new damage regions are introduced and grow in size; shear stresses at the large groups of broken fibers cause debonding or longitudinal matrix cracking; the debond or non-elastic region grows in size with increasing load and the maximum fiber load concentration factors are decreased; failure occurs due to this cumulative weakening of the composite.

Concluding Remarks

Analyses of tensile strength, which relate the composite strength to the statistical strength properties of the fibers have been developed. These analyses are imperfect and not suitable for quantitative prediction of composite strength. They have, however, contributed to the understanding and definition of the desirable characteristics of the matrix and the interface. These studies have established the importance of the statistical characteristics of fiber strength and the importance of material heterogeneity. Although these developments are incomplete, they have demonstrated that the "rule of mixtures" need no longer be a substitute for an understanding of material behavior.

COMPRESSIVE STRENGTH

Uniaxial fiber composite materials have well collimated fibers have yielded extremely high compressive strengths under loads parallel to the filaments. (e.g. ref. 65)

"intra-laminar shear failures". In any event, it is important to recognize that filaments provide little resistance to shearing in any planes containing them.

The confusion surrounding the shear stresses in a laminate seems to stem from the failure to recognize that interlaminar shear stresses occur only in regions where there is a change in curvature, or a change in the external load, or at an edge; while the intralaminar shear stresses are in general non-zero throughout the laminate. The interlaminar shear stresses act in an arbitrary direction with respect to the principal elastic axes of any particular lamina. Thus, they have components in planes both parallel to and normal to the fiber direction. Specifically, if a local tangent plane to the laminate middle surface is defined as the L-T plane, and the local normal is the N direction, then the interlaminar shear stresses are the stress components τ_{NL} and τ_{NT}. In consideration of any particular lamina having principal elastic axes x_1, x_2, and x_3, where the 1 direction is the fiber direction, the 2 direction is the transverse direction in the lamina plane, and the 3 direction is the direction normal to the lamina (same as the N direction), the interlaminar shear stress components, τ_{NL} and τ_{NT}, may be resolved into local components, τ_{31} and τ_{32}. The component τ_{31} acts in a plane parallel to the fibers. For a transversely isotropic composite this stress has the same effect as the intralaminar shear stress τ_{21}. The stress component τ_{32} is in a plane normal to the filaments and is a through-the-thickness type shear stress. Thus consideration of interlaminar shear requires an understanding of the composite shear strength in two principal planes. These strengths have been explored in ref. 27 by use of limit analysis methods. The approach is reviewed below.

Limiting Strengths

The approach to the shear failure analysis is to consider that a uniaxial fibrous composite is comprised of strong and stiff fibers embedded in a matrix which is characterized by its initial elastic modulus and by a maximum stress leve. Accordingly, the matrix is idealized so that its stress-strain relation is that of an elastic, perfectly-plastic material. For homogeneous materials the existence of this plastic region generally signifies the possibility of unbounded structural deformations beyond some limiting load.

For the composite, the theorems of limit analysis of plasticity (e. g. refs. 67 and 68), may be utilized to obtain upper and lower bounds of a composite limit load, (ref. 27). This is defined as the load at which the matrix yield stress permits composite deformation to increase with no increase in load. This limit load has been defined as composite failure and may be considered as an approximation to the strength of a composite having a ductile matrix. The assumptions are made that the filaments are elastic-brittle and that the matrix is elastic-perfectly plastic and obeys the Von Mises yield criterion.

The lamina analyzed is comprised of a matrix containing a uniaxial set of filaments. The reinforcements are assumed in the "random" array configuration described in ref. 8 so that all filaments are considered surrounded by circular cylindrical surfaces such that the ratios of filaments radius to surrounding circular binder radius are the same for all cylinders. One of these cylinders, consisting of a filament and associated concentric binder shell, will be referred to as a composite cylinder.

The procedure is to select "admissible" stress and velocity fields for construction of the lower and upper bounds respectively. (Details are presented in ref. 27). An admissible stress field must satisfy the equilibrium equations everywhere and the traction boundary conditions where specified. In the approach utilized, a uniform stress field was used as the admissible stress field in all cases. A kinematically admissible velocity field is a continuous (with certain permissible exceptions) field which satisfies the displacement and velocity boundary conditions. For the present approach, the elastic displacement fields of ref. 8 were used as admissible velocity fields to obtain the upper bounds for the two shear strengths described above. The results obtained from this bounding procedure for axial shear are presented in fig. 19. The upper bound is plotted as a function of v_f as shown by the solid curve, coinciding with the lower bound at $v_f = 0$ and approaching the value $\frac{4}{\pi}$ as $v_f \to 1$. From Fig. 19, it appears that the maximum possible increase in in-plane shear strength due to the filamentary reinforcements is approximately 27%. For transverse shear, the bounds are plotted in fig. 20, as a function of v_f. In this case the upper bound approaches infinity (because of the assumption of rigid filaments) as $v_f \to 1$. The implication here is that reinforcement against transverse shear may in fact take place.

CONCLUDING REMARKS

This lecture has attempted to support the claim that rational methods for analysis of composite materials and structures do exist. The author intends that this lecture will serve to guide new workers in the field of composites to appropriate sources in the literature. Many basic problems remain unsolved. However, there is a continually decreasing need to resort to analyses based on the sometimes crude and approximate assumptions made in the early portions of the last decade.

I have tried to indicate that the understanding of the relationship between physical properties of laminated fibrous composites and those of their constituents rests on a sound base. On the other hand, much remains to be done; particularly in such areas as: failure criteria, reliability assessment, non-destructive evaluation, damage tolerance, fatigue, creed, and joints and attachment problems.

It appeats that composite materials have not yet had the anticipated impact on structural design which would lead to creative, new structural configurations. One need not be disappointed in this fact, for we are only at the beginning of the new materials engineer-

ing era. Time to come will undoubtedly see changes in structural design methods that will lead to widespread utilization of composites. The improvements in properties; the existence of unique combinations of properties; and the fabrication simplications which can result from the use of fibrous composites will lead to their utilization as the prominent materials of construction in all engineering disciplines.

References

1. Drucker, P.F. Age of Discontinuity, Harper and Row, New York.
2. Peterson, G. P.,"Development and Performance of Advanced Composite Structure", 1971 AIAA Structures Design Lecture, Part II.
3. Hashin, Z.. "Theory of Fiber Reinforced Materials", Final Report, Contract NAS1-8818, Univ. of Pennsylvania, 1971.
4. Pickett, G., "Elastic Moduli of Fiber Reinforced Plastic Composites" in Fundamental Aspects of Fiber Reinforced Plastic Composites, R.T. Schwartz and H.S. Schwartz, Eds. Chap. 2, Interscience, 1968.
5. Adams, D.F.,Doner,D.R.,Thomas,R. L.,"Mechanical Behavior of Fiber-Reinforced Composite Materials", AFML-TR 67-96, 1967.
6. Pickett, G., Johnson, M.W., "Analytical Procedures for Predicting the Mechanical Properties of Fiber Reinforced Composites", AFML-TR-65-220, 1965.
7. Chen, C.H., Cheng, S., "Mechanical Properties of Fiber Reinforced Composites", J. Comp. Mats., 1, 30, 1967.
8. Hashin, Z., Rosen, B. W., "The Elastic Moduli of Fiber Reinforced Materials", J. Appl. Mech., 31, 223, 1964.
9. Hill, R., "Theory of Mechanical Properties of Fibre-Strengthened Materials-I. Elastic Behavior", J. Mech. Phys. Solida, 12, 199, 1964.
10. Levin, V. M., "On the Coefficients of Thermal Expansion of Heterogeneous Materials", (in Russian) Mekhanika Tverdogo Tela, 88, 1969.
11. Rosen, B. W., Z. Hashin, "Effective Thermal Expansion Coefficients and Specific Heats of Composite Materials", Int. J. Engng. Sci., 8, 157, 1970.
12. Hashin, Z., "Viscoelastic Fiber Reinforced Materials", AIAA J., 1411, 1966.
13. Schapery, R. A., "Stress Analysis of Viscoelastic Composite Materials", J. Comp. Mats., 1, 228, 1967.
14. Roscoe, R., "Bounds for the Real and Imaginary Parts of the Dynamic Moduli of Composite Viscoelastic Systems", J. Mech. Phys. Solids., 17, 17, 1969.
15. Hashin, Z., Brull, M. A., Chu, T. Y., Zudans, Z., "Static and Dynamic Viscoelastic Behavior of Fiber Reinforced Materials and Structures", USAAVLABS TR 68-70, Oct. 1968.
16. Gucer, D. E., Gurland, J., "Comparison of the Statistics of Two Fracture Modes", J. Mech. Phys. Solids, 10, 365, 1962.
17. Parratt, N. J., "Defects in Glass Fibers and their Effect on the Strength of Plastic Mouldings", Rubber and Plastics Age, 263, March 1960.
18. Rosen, B. W., "Tensile Failure of Fibrous Composites", AIAA J., 2, 1985, 1964.
19. Zweben, C., Rosen, B. W., "A Statistical Theory of Materials Strength with Application to Fiber Composites", J. Mech. Phys. Solids, 18, 189, 1970.
20. Cooper, G. A., Kelly, A., "Tensile Properties of Fibre-Reinforced Metals: Fracture Mechanics", J. Mech. Phys. Solids, 15, 279, 1967
21. Kelly, A., Davies, G. J., "The Principles of the Fiber Reinforcement of Metals", Metallurgical Reviews, Vol. 10. 1965.
22. Kelly, A., Tyson, W. R., " Fiber Strengthened Materials", in High Strength Materials, V. F. Zackay, Ed., J. Wiley, New York, 1965.
23. Zweben, C., "On the Strength of Notched Composites", AIAA Preprint 71-369, 1971.
24. Rosen, B. W., "Mechanics of Composite Strengthening" , in Fiber Composite Materials. Am. Soc. for Metals, Metals Park, Ohio, 1965.
25. Schuerch, H., "Prediction of Compressive Strength in Uniaxial Boron Fiber-Metal Matrix Composite Materials", AIAA Journal, Vol. 4, Jan. 1966.
26. Hashin, Z., "Transverse Strength" in N. F. Dow and B. W. Rosen - "Evaluations of Filament-Reinforced Composites for Aerospace Structural Applications", NASA CR-207, 1965.
27. Shu, L. S., Rosen, B. W., "Strength of Fiber Reinforced Composites by Limit Analysis Method", J. Comp. Mats., 1, 366, 1967.
28. Shu, L. S., "The Evaluation of the Strength of Fiber-Reinforced Composites" in Mechanics of Composite Materials, F. W. Wendt, H. Liebowitz and N. Peronne, Eds., 723, Pergamon Press, 1970.
29. Hill, R., "Theory of Mechanical Properties of Fibre-Strengthened Materials:II. Inelastic Behavior", J. Mech. Phys. Solids, 12, 213, 1964.
30. McLaughlin, P. V., Batterman, S. C.,"Limit Behavior of Fibrous Materials", Int. J. Solids & Structures, 6, 1357, 1970.
31. Hill, R.,"A Theory of the Yielding and Flow of Anisotropic Metals", Proc. Roy. Soc. (London), A193, 281, 1948.
32. Azzi, V. D., Tsai, S. W., "Anisotropic Strength of Composites", Exp. Mech., 5, 283, 1965.
33. Hoffmann, O., "The Brittle Strength of Orthotropic Materials", J. Comp. Mats.,1, 200 1967.
34. Gol'denblat, I. I. and Kopnov, V. A., "Strength Criteria for Anisotropic Materials, Izv. AN SSSR Mekh., No. 6, 1965.
35. Tsai, S. W., Wu, E. M., "A General Theory of Strength for Anisotropic Materials" J. of Comp. Mats., 5, 58, Jan. 1971.
36. Foye, R. L., Baker, D. J., "Design/Analysis Methods for Advanced Composite Structures", AFML-TR-70-299, Vol. I, Feb. 1971.
37. Dong, S. B., Matthiesen, R. B., Pister, K. S., Raylor, R. L., "Analysis of Structural Laminates", ARL 76, Office of Aerospace Research, USAF, Wright-Patterson AFB, Sept. 1961.
38. Dong, S. B., Pister, K. S., Taylor, R. L., "On the Theory of Laminated Anisotropic Shells and Plates", J. of Aerospace Science, Vol. 29, No. 8 pp. 969-975, 1962.

39. Reissner, E., Stavsky, Y., "Bending and Stretching of Certain Types of Heterogeneous Aeolotropic Elastic Plates", J. of Applied Mechanics, Vol. 28, pp. 402-408, 1961.
40. Leknitskii, S. G., Theory of Elasticity of an Anisotropic Elastic Body, translated by P. Fern, Holden-Day Publishing, 1963.
41. Stavsky, Y., in Composites Engineering Laminates edited by Dietz, A. G. H., MIT Press, Mass. 1969.
42. Calcote, Lee R., The Analysis of Laminated Composite Structures, Van Nostrand-Reinhold, 1969.
43. Hearmon, R. F. S., An Introduction to Applied Anisotropic Elasticity, Oxford Univer-Press, London, 1961.
44. Ledhnitsky, S. G., Anisotropic Plates English Translation, Am. Iron Steel Inst., 1965.
45. Ambartsumyan, S. A., "Theory of Anisotropic Shells", NSDS TTF-118, 1964.
46. Anon, "Structural Design Guide for Advanced Composite Applications", AFML, Adv. Composites Division, January 1971.
47. Rosen, B. W., "Thermomechanical Properties of Fibrous Composites",Proc. Roy. Soc. (London) 319 79-94, 1970.
48. Hashin, Z., "On Elastic Behavior of Fiber Reinforced Materials of Arbitrary Transverse Geometry," J. Mech. Phys. Solids, Vol. 13, pp. 119-134, 1965.
49. J. M. Whitney, and Riley, M. B., "Elastic Properties of Fiber Reinforced Composite Materials", AIAA Journal, 4, 1537, 1966.
50. Rosen, B. W.,"Thermoelastic Energy Functions and Minimum Energy Principles for Composite Materials", Int. J. Enging. Sci. Vol. 8 pp. 5-18, Pergamon Press, 1970.
51. Hashin, Z., "Theory of Composite Materials", in Mechanics of Composite Materials, New York, Pergamon Press, 1968.
52. Rosen, B. W., and Zweben, C. H., "Tensile Failure Criteria for Fiber Composite Materials", Final Report, NASA Contract NAS1-10134, August 1971.
53. Zweben, C. H., "Tensile Failure Analysis of Fibrous Composites," AIAA Journal, Vol. 6, No. 12, December 1968.
54. Cox, H. L."The Elasticity and Strength of Paper and Other Fibrous Materials", British J. of Appl. Phys., Aug. 1951.
55. Dow, N. F., "Study of Stresses Near a Discontinuity in a Filament-Reinforced Composite Material," General Electric Co. Space Sciences Lab., TIS R63SD61, August 1963.
56. Flom, D. B., Mazzio, V.F., and Friedman, E. "Whisker Reinforced Resin Composites", Air Force Report, AFML/TR-66-362, 1967.
57. Hedgepeth, J. M. and Van Dyke, P. "Local Stress Concentrations in Imperfect Filamentary Composite Materials," J. Comp. Materials, Vol. 1, pp. 294-309, 1967.
58. Van Dyke, P. and Hedgepeth, J. M., "Stress Concentrations from Single-Filament Failures in Composite Materials", Textile Research, Vol. 39, No. 7, pp. 618-626, July 1969.
59. Fichter, W. B., "Stress Concentration Around Broken Filaments in a Filament-Stiffned Sheet, NASA TN D-5453, 1969.
60. Hedgepeth, J. M., "Stress Concentrations in Filamentary Structures", NASA TN-D-882, May 1961.
61. Zweben, C., and Rosen, B. W., "A Statistical Theory of Material Strength with Application to Composite Materials", J. Mech. Phys. Solids, Vol. 18, pp. 180-206, 1970.
62. Zweben, C., "A Bounding Approach to the Strength of Composite Materials", Engineering Fracture Mechanics, Vol. 4, No. 1, pp. 1-8, 1972.
63. Kreider, K. G. & Leverant, G. R., "Boron Fiber Metal Matrix Composites by Plasma Spraying," AFML-TR-66-219, AFML, July 1966.
64. Cooper, G. A. and Kelly, A., "Role of the Interface in the Fracture of Fiber-Composite Materials", ASTM Spec.Tech. Pub. 452, 1969.
65. Davis, John G., Jr., "Compressive Instability and Strength of Uniaxial Filament-Reinforced Epoxy Tubes, NASA TN D-5697, March 1970.
66. Biot, M., Mechanics of Incremental Deformations, John Wiley and Sons, Inc., N. Y. 1965.
67. Drucker, D. C., Greenberg, H. J., and Prager, W., "The Safety Factor of an Elastic-Plastic Body in Plane Strain", J. Applied Mech., Vol. 18, p. 371, 1951.
68. Koiter, W. T., "General Theorems for Elastic-Plastic Solids", Chapter IV in Progress in Solid Mechanics, Sneddon and Hill, Eds., North Holland, 1960.

Bibliography

1. Fiber Composite Materials, American Soc. Metals, 1965.
2. Holliday, L. (Ed.) Composite Materials, Elsevier Publishing Co., 1966.
3. Fiber-Strengthened Metallic Composites, Am. Soc. Test. Mats., STP 427, 1967.
4. Broutman, L. J., and R. H. Krock, Eds., Modern Composite Materials, Addison-Wesley,1967.
5. Schwartz, R. T. and Schwartz, F. S., Eds., Fundamental Aspects of Fiber Reinforced Plastic Composites, John Wiley, 1968.
6. Metal Matrix Composites, American Soc. Test. Mats., STP 438, 1968.
7. Tsai, S. W., Halpin, J. C. and Pagano, N. J. (Eds.) Composite Materials Workshop, Technomic Pub. Co., Stamford, Conn. 1968.
8. Interfaces in Composites, American Soc. Test. Mats., STP 452, 1969.
9. Dietz, A. G. H., (Ed.) Composites Engineering Laminates, MIT Press, Mass. 1969.
10. Lubin, G., (Ed.) Handbook of Fiber-glass and Advanced Plastic Composites, Van Nostrand and Reinhold, N. Y. 1969.
11. Design and Testing of Composite Materials, American Soc. Test. Mats., STP 460, 1970.
12. Levitt, A. (Ed.) Whisker Technology, Wiley, N. Y. 1970.
13. Wendt, F. W., Liebowitz, H. and Perrone, N. Eds., Mechanics of Composite Materials. Pergamon Press, 1970.
14. Proceedings, Annual Conferences, Reinforced Plastics/Composites Division, Society of the Plastics Industry, N. Y. ; Annual AIAA/ASME Structures, Structural Dynamics and Materials Conferences; Annual National SAMPE Symposium.

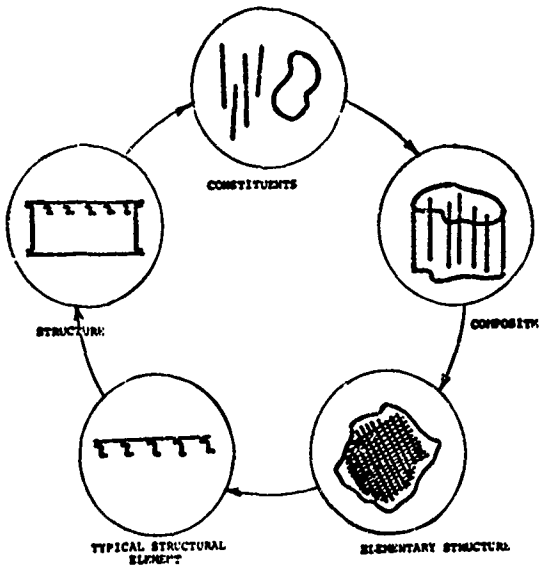

Fig. 1. Composite Structural Design and Analysis Cycle

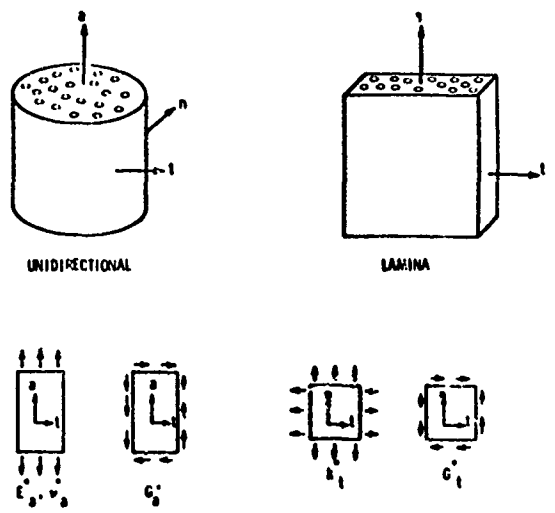

Fig. 2 Unidirectional Fiber Composite Material Properties

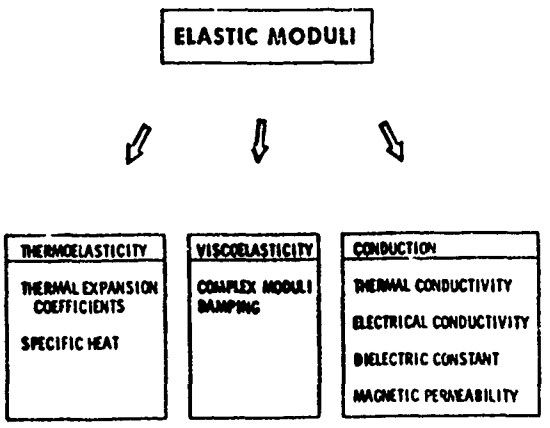

Fig. 3 Inter-relationship of Composite Physical Properties

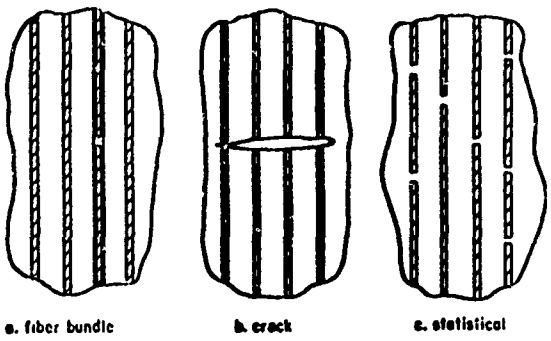

Fig. 4 Possible Failure Modes for a Fiber Composite Material

CROSS-SECTION GEOMETRY

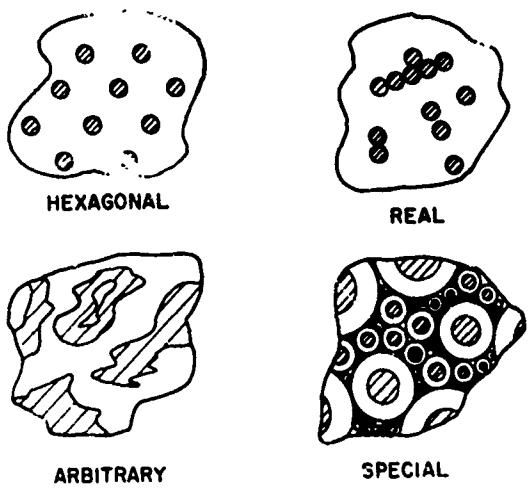

Fig. 5 Cross-sections of unidirectional fibrous composites transverse to the fiber axes.

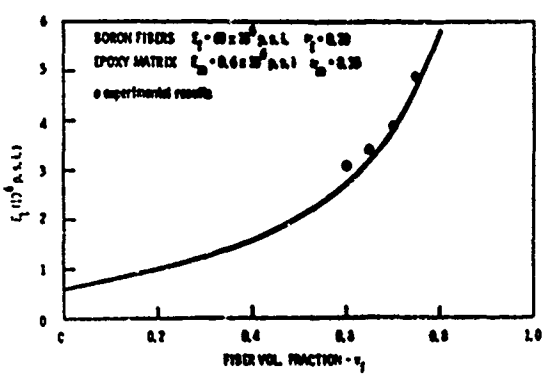

Fig. 6 Transverse Young's modulus of boron/epoxy composite cylinder assemblage and comparison with experimental data.

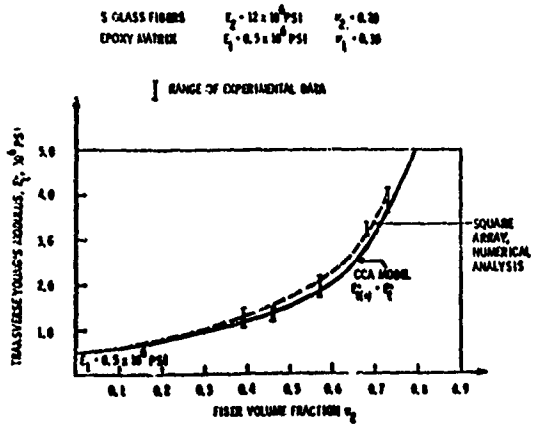

Fig. 7 Comparison of Theory and Experiment for Transverse Young's Modulus (from ref. 3)

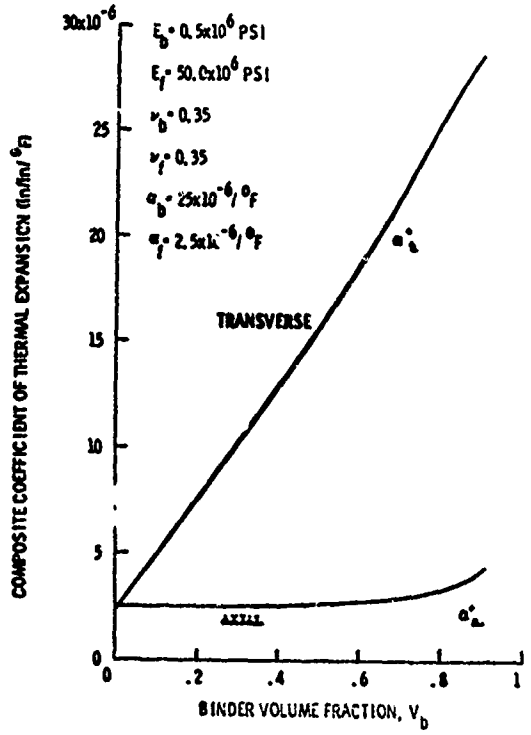

Fig. 8 Effective Composite Thermal Expansion Coefficients.

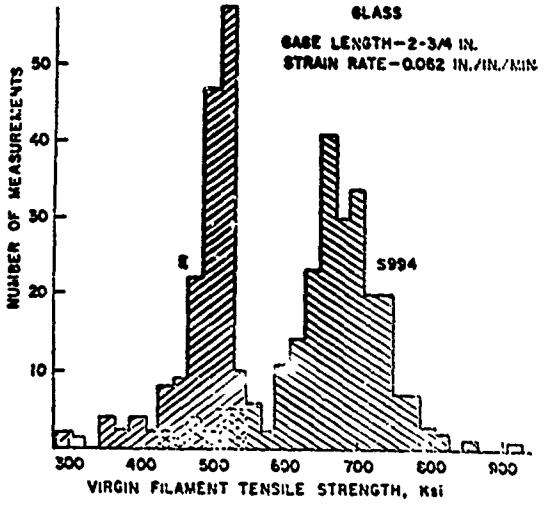

Fig. 9 Typical Histograms for Tensile Strength of Individual Glass Fibers.

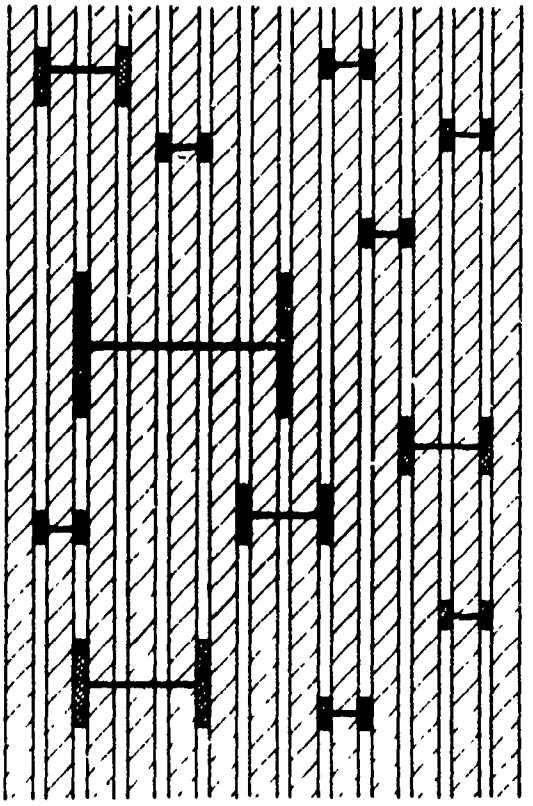

Fig. 10 Distribution of Damage in a Fiber Composite Material Resulting from an Applied Tensile Load.

STATISTICAL TENSILE FAILURE MODEL

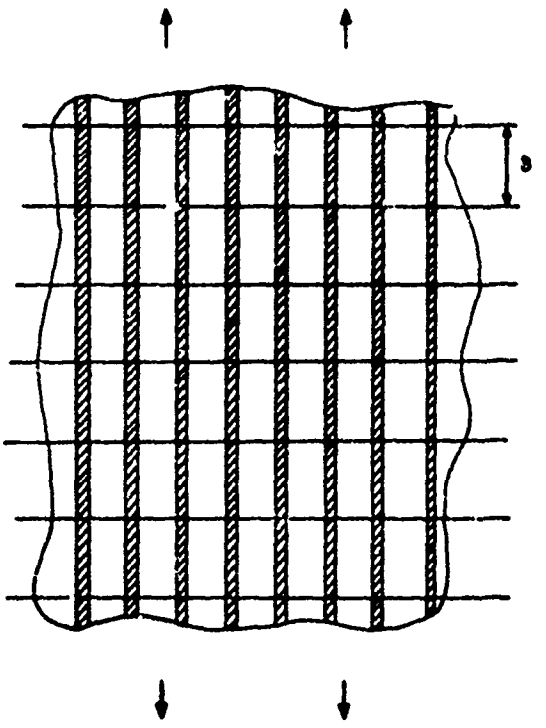

Fig. 11 Geometry of Composite for Statistical Tensile Failure Model.

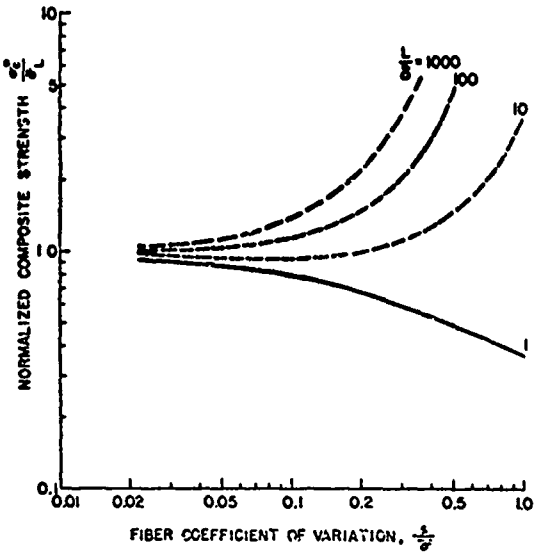

Fig. 12 Effect of Fiber Strength Properties upon Composite Tensile Strength for Cumulative Weakening Failure Model.

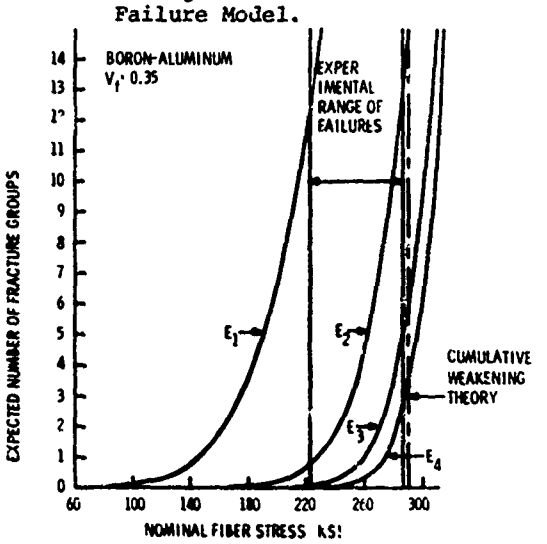

Fig. 13 Expected Number of Fracture Groups For Boron/Aluminum Composites.

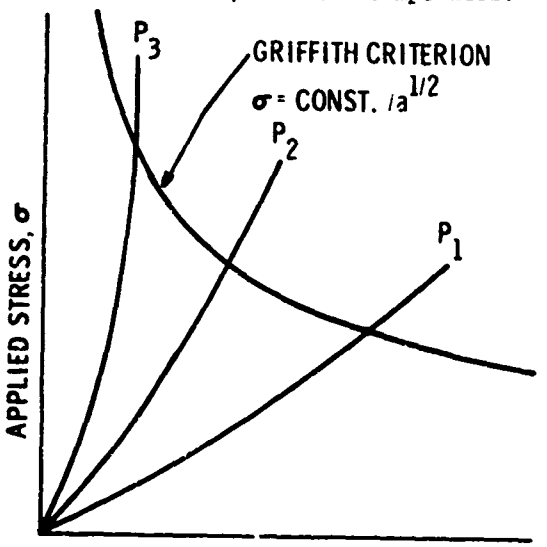

Fig. 14 Criterion for Probability of Failure by Crack Propagation

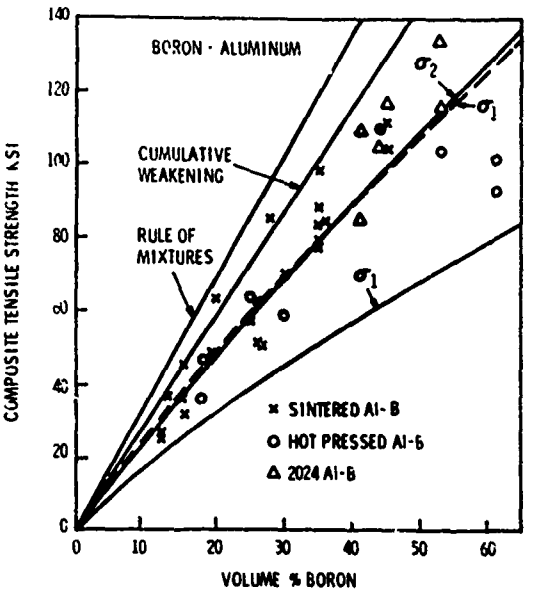

Fig. 15 Comparison of Bounding Theories of Tensile Strength with Experimental Data for Boron/Aluminum Composites.

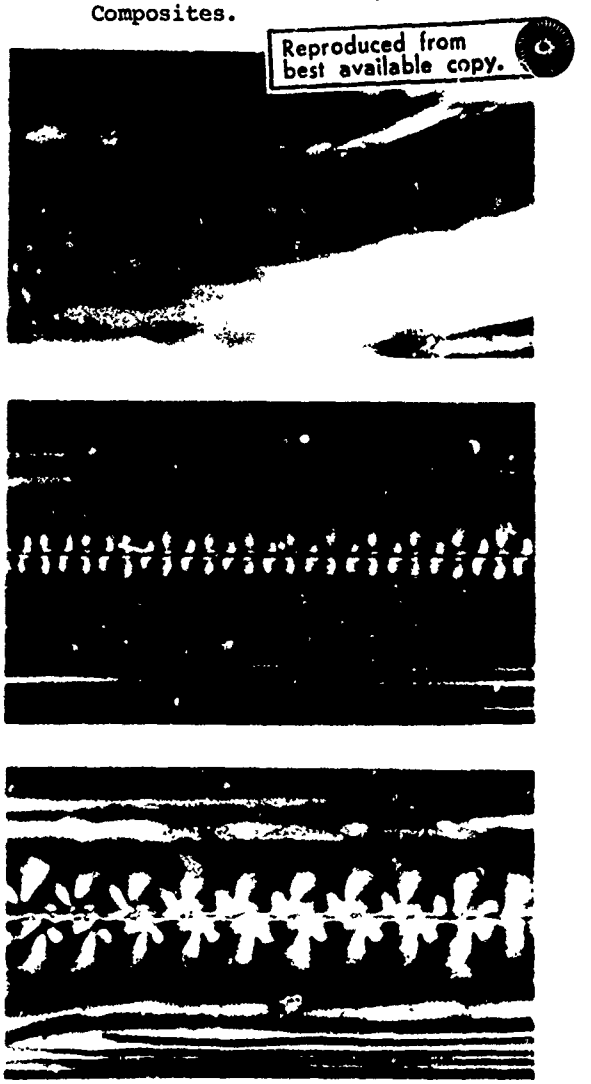

Fig. 16 Photoelastic Stress Pattern for Three Individual E-glass Fibers Imbedded in an Epoxy Matrix.

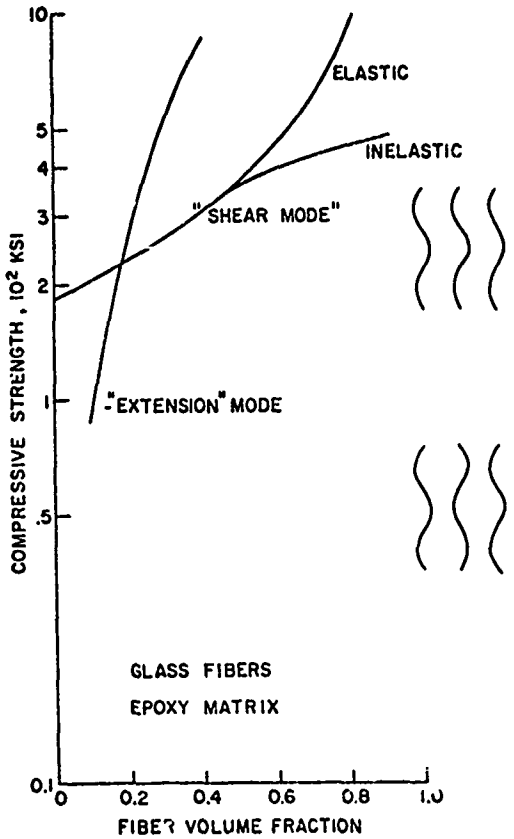

Fig. 17 Compressive Strength of Glass-Reinforced Epoxy Composites.

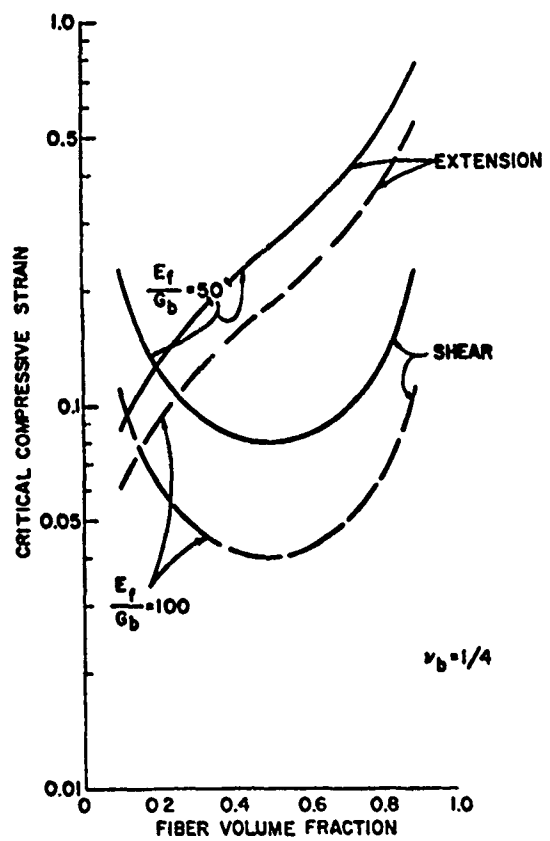

Fig. 18 Critical Compressive Strain for Fibrous Composites.

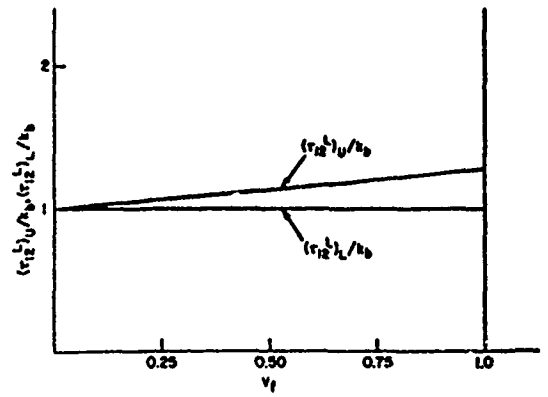

Fig. 19 Bounds on the Limit Load τ_{12}^L, for a Shear Stress Applied in a Plane Parallel to the Fibers of a Uniaxial Fibrous Composite.

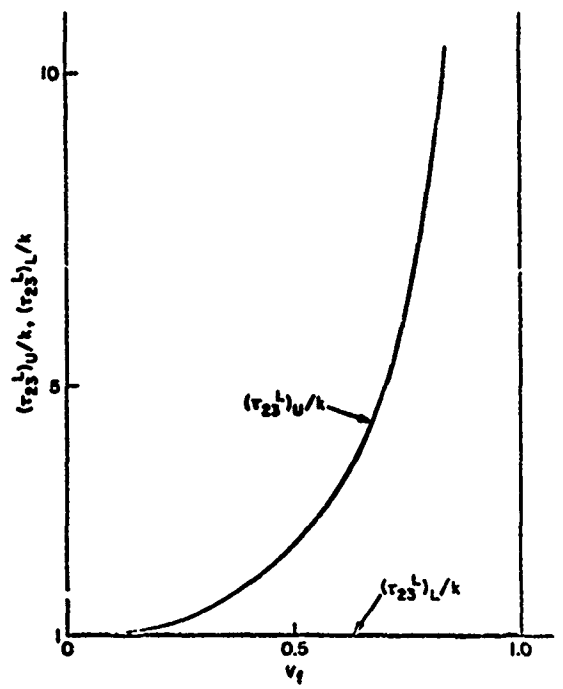

Fig. 20 Bounds on the Limit Load τ_{23}^L for a Shear Stress Applied in a Plane Normal to the Fibers of a Uniaxial Fibrous Composite.

FIBER AND MATRIX MATERIALS FOR ADVANCED COMPOSITES

R. J. Diefendorf
Materials Division
Rensselaer Polytechnic Institute
Troy, New York 12181, U.S.A.

SUMMARY

Composite materials provide a solution for the engineering use of high specific strength-high specific modulus, but brittle materials. These brittle materials are used as fibrous reinforcement to provide strength and stiffness in the composite. The fundamental principles for selecting the reinforcements are described, as well as the concepts used to form these materials into high strength filament. Detailed information on the preparation, structure and properties of boron, carbon and organic filament are presented. Matrix materials, which are used to transfer stress to the fiber and also prevent brittle failure, are discussed in less detail. The techniques for combining filaments and matrix into prepreg or other preforms, and the fabrication into structure are considered. Finally, the mechanical properties of composites based on boron, carbon, and organic fibers are presented.

Technological demands for materials with improved properties has led to the recent increase in research and development of composite materials. The idea of taking dissimilar materials and assembling them together for improved properties dates as far back as at least biblical times. The reason for the recent increased interest has been the development of high performance fibers which make it technically feasible to produce composite materials with vastly improved mechanical properties.

I. Materials Requirements

In order to appreciate the value of high performance composite materials, one must ask: "What is really limiting in design?"

Modulus Limited Designs - Let us look over the shoulder of an automotive engineer whose job it is to specify materials for fenders. Does he pick the gauge of the sheet metal from a stress calculation for the loading caused by the headlight? No! His design is stiffness and fabrication limited. Similarly, let us look over the shoulder of an aircraft designer who is designing a stabilizer. Does he worry about loads? Yes, but the air loads are quite low. What he really worries about is stiffness (flutter). For designs where flutter is limiting, a higher specific modulus (modulus/density) material would allow a more efficient design to be made.

Many designs are limited by strain considerations. For example, a Boeing 707 wing with 1.6% and 3.2% strain would appear as in Fig. 1[1]. Or imagine a floor of a Boeing 747 which deflected 20 cm, and was sound from an engineering standpoint, but not psychologically. In many cases, the inherent high strength of a material cannot be used because the deflection is too high at the breaking load. More efficient designs could be made with higher modulus materials whereby higher stresses would be attained at lower strains.

Strength Limited Designs - These examples shouldn't imply that there are no structures which are strength limited. For example, a pressure vessel is almost purely limited by strength. A rubber balloon doesn't need much stiffness. However, the increase in dimensions may be a difficulty. A good example where specific strength (strength/density) is important is the suspension cables of a suspension bridge or electric power transmission cable. At the present time, suspension bridges can't be made much longer than the Verazano Narrows bridge, because increased bridge length requires a non-proportionate increase in cable and associated structure weight. The cables are approaching a length, that they can just support their own weight. Obviously, lighter or stronger materials would be required to build longer suspension bridges.

In summary, lighter, stronger, and stiffer materials give improved design efficiencies.

Materials Approaches

Now let us leave the designer and look at what the materials person did to try to develop better materials. The materials scientist refined grain size, dispersion hardened, etc., but he only tried to improve strength. The reason is simple: the modulus of a

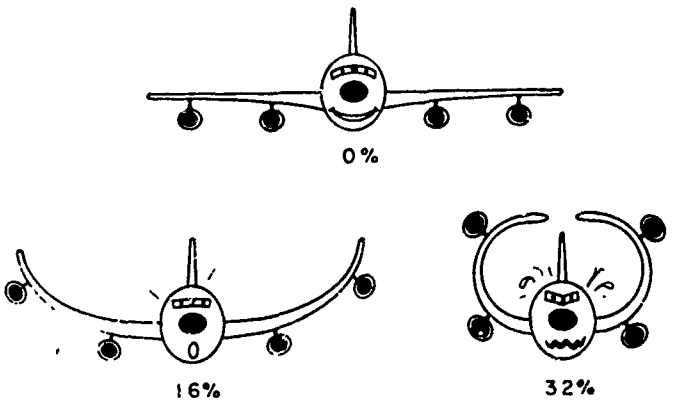

Figure 1. Strain Limitations in a Typical Wing Structure (after Gordon).

material cannot be increased, but the strength can. Also, if the materials scientist was in the aircraft industry, where specific modulus is important, all the common engineering materials have the same specific modulus[2]. In other words, there is no advantage in using Sitka spruce instead of balsa, or magnesium, aluminum, titanium, steel, molybdenum or tungsten for volume limited designs. These materials have a density range from .06 to 19.3, yet the specific modulus is almost the same (Table 1a). For some applications, the lighter material does have an advantage since its dimensions are larger per pound, and the section modulus is correspondingly higher. However, for properly designed structures, there would be little difference.

High Specific Modulus Materials

The question arises: Are there any materials which have higher specific moduli than conventional engineering materials? An incomplete answer is shown in Table 1b. The chemical elements, berylium, boron, and particularly carbon, have much higher specific moduli than conventional engineering materials. Also, the compounds between these elements plus aluminum, silicon, nitrogen and oxygen often have high specific moduli. These materials would certainly offer drastic improvements in structures if these materials were also strong.

Table 1a. The Moduli, Density and Specific Moduli of Selected Materials

Material	Modulus	Density	Specific
Spruce	13.	0.5	26.2
Magnesium	41.4	1.7	25.6
Glass	69.	2.5	27.6
Aluminum	69.5	2.7	27.
Titanium	117.8	4.5	27.
Iron	207.	7.8	26.2
Molybdenum	276.	10.5	27.

Table 1b.

Berylium	304.	1.8	166.
Boron	442.	2.3	193.
Carbon	1010.	2.3	442.
Organic Fiber	152.	1.5	101.
Silicon Carbide	497.	3.2	159.
Aluminum Nitride	345.	3.3	117.
Aluminum Oxide	345.	4.	90.
Silicon Nitride	380.	3.2	119.

Theoretical Strengths of Materials

When a material is tested mechanically and found to fail at a low stress, it is not known whether the material is inherently weak, or whether the specimen was improperly made. Therefore, a theoretical calculation to determine the strength of a flaw-free material is of great value. The derivation of the equations for theoretical strengths of covalently bonded materials from quantum mechanics has not been accomplished. Theoretical strengths are usually determined by assuming the modulus of the material, that the force-extension relationship follows a sine, Morse, or similar function, and that a separation parameter is related to the interatomic spacing[3]. Kelly has calculated both the cleavage and shear strengths for the most widely spaced planes in the crystals (Table 2)[4]. Failure would occur at the lower theoretical strength. For metals which fail in shear,

an approximate theoretical strength is given by:

$$\sigma_{th} = 0.02E$$

Table 2. Theoretical Strengths of Materials (after Kelly)

	$E \frac{GN}{m^2}$	$G \frac{GN}{m^2}$	ν	$\alpha_{max} \frac{GN}{m^2}$	$\tau_{max} \frac{GN}{m^2}$	$\frac{\alpha_{max}}{\tau_{max}}$
Au	67	2.0	0.46	2.7	0.08	34
Cu	110	3.5	0.42	3.9	0.14	28
Ni	220	6.9	0.37	6.1	0.28	22
Fe	210	6.2	0.36	4.8	0.69	6.8
NaCl	84	2.5	0.16	0.38	0.41	0.95
Al_2O_3	670	14.5	0.17	4.6	1.7	2.7
C_α	1750	51.	0.1	13.8	12.1	1.2

Although different authors give slightly different numerical factors for cleavage failure of covalently bonded materials, a good expression is:

$$\sigma_{th} = 0.1E$$

Hence, the same covalent materials which have high specific moduli will also have high theoretical strengths. While graphite and ceramic materials have traditionally had very low strengths in commercially produced materials, they have also given the highest known strengths in nominally flaw-free whisker or fiber form. These observed strengths still fall far below that expected from calculation, but it also appears realistic that elongations at least as high as 2% are possible for materials in fiber or whisker form.

Impact Strength

If high specific modulus materials appear attractive from a high strength standpoint also, why not use them in a monolithic form? Why not make a horizontal stabilizer skin out of a monolithic sheet of chemically vapor deposited boron? Let us assume adequate properties could be attained. Then, let the plane taxi down the runway getting ready for take-off, and a rock gets thrown up off the runway, hits the boron stabilizer, and the impact initiates a crack. From then on, the crash analysis would simply be a study of crack propagation in brittle materials. Engineering materials must have some impact strength.

Even in cases where impact is not a problem, designers stay away from brittle materials. There is a good reason; improper machining or assembly of a part can often raise local stresses to very high values. Stress analysis is very good with large dimensions, but apt to be poor in localized areas. Obviously, difficulty can occur if structural integrity depends on local stresses. Ductile metals will yield and redistribute the load if high local stresses exist, but brittle materials will fracture. The problem can be solved, if the ceramic material can be given some pseudo-ductility. The whole purpose of composites is how to take a brittle material and give it some pseudo-ductility to minimize local stress concentrations, and a non-catastrophic failure mode.

An example is illustrative. Suppose we decide to make a composite horizontal stabilizer out of boron and epoxy. The boron will be made in small diameter filament, such that we can get very high strength. Also, many filaments will be placed in the structure to get a redundancy in design. The boron filament will be laid parallel to the principle stress axes to minimize deflection. These filaments will be separated and retained in a high strain epoxy resin. Again, the plane taxis along the runway, a rock gets thrown up off the runway, and breaks a few of the thousands of boron filaments in the structure. Debonding at the fiber-matrix interface and fracture in the epoxy absorb the filament fracture energy and arrest crack propagation. The epoxy transfers the stress to neighboring fibers and the plane takes off safely.

Composite Potential

The whole basis for filamentary composites is that strength and modulus of brittle materials are traded off for a measure of impact strength. The strength and modulus of a fiber can only be used unidirectionally. For triaxially stressed states where fibers must be oriented in at least three directions, the improved performance that could be obtained with composites is not great. Fortunately, structural elements are usually stressed in one direction (beams), or two directions (plates and thin walled shapes) and not in three directions. For biaxially and uniaxially stressed elements, the performance

increase possible with high modulus-high strength fiber reinforced composites cannot be approached with any other materials concept.

II. High Strength Fiber Processes

While the last sections described the potential advantages of high modulus filaments, these advantages cannot be used unless processes exist or can be developed to make these high modulus materials into high strength filament (or fiber). The development of these processes has probably been the most important factor in the present history of high modulus composites. The processes can be divided into two major categories which depend on the type of microstructure. In the first, single crystal whiskers or filaments are grown which usually have exceedingly fine diameters and very high strengths. The strength of these whiskers comes from the structural perfection of the single crystal and the fine dimensions. Whiskers are discontinuous and considered to be hard to handle, so the question arises: can continuous fine diameter filament be made? While a good measure of success has been made by Tyco Laboratories in drawing single crystal filament from the melt, most conceivable processes for continuous filament would result in a polycrystalline microstructure. Ceramic materials, with their highly directed covalent bonds, are apt to have weak grain boundaries; this is accentuated by the fine diameter of the filament. Ceramic type fibers with grain sizes of the order of the filament diameter are very weak. Either very fine grained (or elongated grain) materials, or else no grain boundary (single crystal) materials are desired. The grain sizes that are necessary are several hundred angstroms or less, and in the limit zero, e.g. glass. In other words, although the nature of the material may be important, processing techniques are needed to make the desired single crystal or very fine grain size filament. The following sections describe the methods for making the present leading types of high modulus fiber and their properties.

Continuous Filament Processes

There are three major filament processes. Chemical vapor deposition is used to make boron and silicon carbide. The pyrolysis and orientation of carbonaceous materials is used to form oriented high modulus carbon fibers. Finally, aromatic organic polymers can be spun to give a highly oriented, relatively high specific modulus fiber. In the following sections, the leading example of each type of process is described in detail.

A. Boron Filament

Boron filament is made by depositing "amorphous" boron on a heated tungsten wire by the hydrogen reduction of boron trichloride. Fig. 2 details a typical "single stage" reactor.

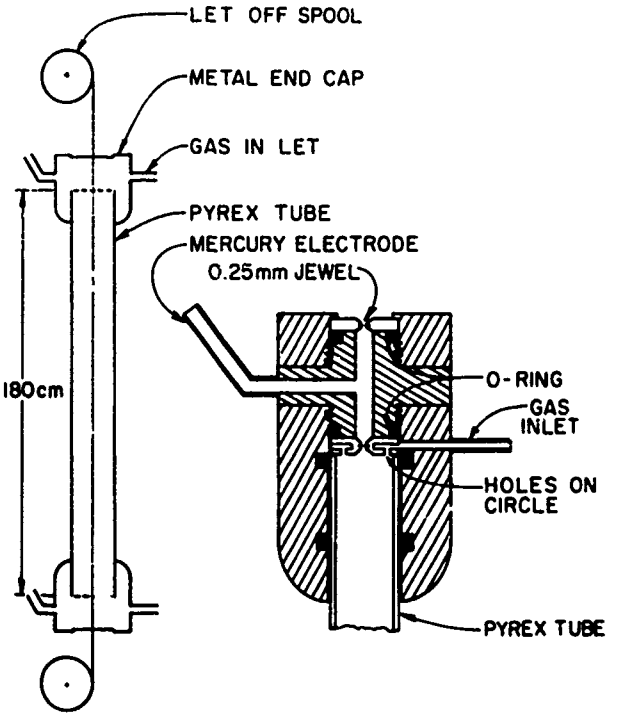

Figure 2. Typical Chemical Vapor Deposition Apparatus for Boron Filament.

Tungsten wire about 12μm (0.005 in.) in diameter is drawn off a spool, transported through a borosilicate glass tube reactor with mercury end seals, and then wound up on a take-up spool as 100μm (0.004 in.) diameter boron filament. The diameters of the initial tungsten wire and the final boron filament are selected by the specific modulus of the filament, the cost per meter and handleability of the tungsten substrate, and the curvature that the boron filament may have in a structure. The specific modulus as a function of final diameter/substrate diameter is shown in Fig. 3. Because of the high density of

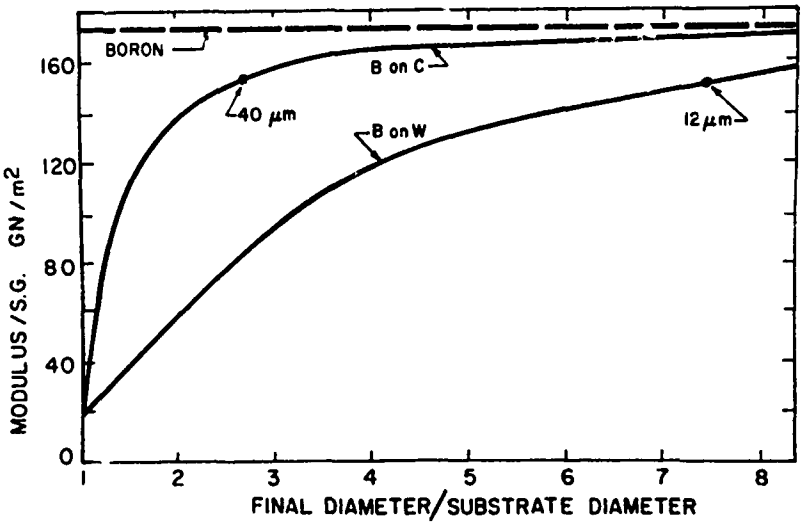

Figure 3. Specific Modulus of Boron Filament as a Function of the Ratio of the Final Filament Diameter to Substrate Diameter.

the tungsten substrate, there is a high penality in specific modulus for any ratio of initial to final filament diameter ratio of less than eight. The tungsten substrate diameter, at 12μm, is slightly more expensive than the minimum cost/meter wire at 25μm, but this is more than balanced by the flexibility in making smaller diameter boron filament. Smaller diameter tungsten wire, which is much more expensive per meter is not obtainable in long lengths (due to breakage in manufacture), and becomes more difficult to handle in making boron (due to breakage during deposition). Practically, a tungsten substrate limits boron filament to a minimum final diameter of 100μm. Larger filament diameters are particularly attractive since the substrate cost remains the same per meter, and capital and labor costs are lower. Mechanical properties for 140μm diameter boron filament (twice the amount of boron per meter) are identical to 100μm diameter material.

The mercury end seals on the reactor serve to keep air from entering the reaction tube and to make electrical contact. The filament is heated generally by high voltage direct current. Since the resistance of the filament decreases and the thermal conductive losses increase as boron deposits, the temperature of the filament decreases as it traverses the reactor. A slight decrease in temperature is beneficial, but multistage reactors have been used to provide a flatter temperature profile. However, the decreases in strength caused by interfaces forming in the boron between each stage have often overbalanced the improved processing speeds.

The maximum filament temperature must be less than 1400°C to produce amorphous boron. Higher temperatures produce coarse grained and weak β-rhombohedral boron. Occasionally, crystals of β-rhombohedral boron or other crystal structures nucleate randomly at temperatures well below 1400°C, but this is usually caused by insufficient gas flow, or catalytic impurities on the substrate.

The chemical equation for the overall reaction that is occurring is:

$$2BCl_3 + 3H_2 \rightarrow 2B + 6HCl$$

The free energy for this reaction at amorphous deposition temperatures is positive, which means that the amount of boron that can be removed from the gas per pass is quite low. Depending on the conditions and species assumed to be present, the amount of boron that can be deposited per pass varies from 6 to 18%. The amount that can be stripped from a stoichiometric gas mixture if only amorphous material is to be deposited is lower, being approximately 1½%. The low stripping efficiency requires that rather effi ent (and expensive) recycle systems be used to keep boron trichloride costs to a minimum.

The deposition rate of the boron is very high compared to that observed in many chemical vapor deposition systems, but a 100μm diameter boron filament still requires a contact time of 15 to 30 seconds for preparation. This contact time, together with power supply and start-up problems, has led to the design of production plants where many reactors are run in parallel to provide high output.

Microstructure of Boron Filament

The outer surface of boron filament has the appearance of an ear of maize. This structure originates when the boron nucleates in the die mark grooves of the tungsten substrate. In cross-section, the micro-structure consists of parabolic cones with the apex at the substrate. Although the structure may be amorphous, the growth cones are a source of weakness, probably because of the stress concentration where two cones meet. The effect of this growth cone stress concentration has been minimized in recent years by more uniform nucleation which results in a smoother outer surface.

During deposition, the tungsten core is converting through a sequency of borides to WB_4. A dimensional increase of about 30% is associated with the boriding, and early boron filaments often split because the boriding occurred too late in the deposition process. Although this boriding places the core in residual compression, there are dimensional changes occurring in the boron sheath which give a net residual stress pattern as shown in Fig. 4. The outer compressive residual stress, combined with the inherent hardness of boron, makes boron filament relatively insensitive to surface flaws.

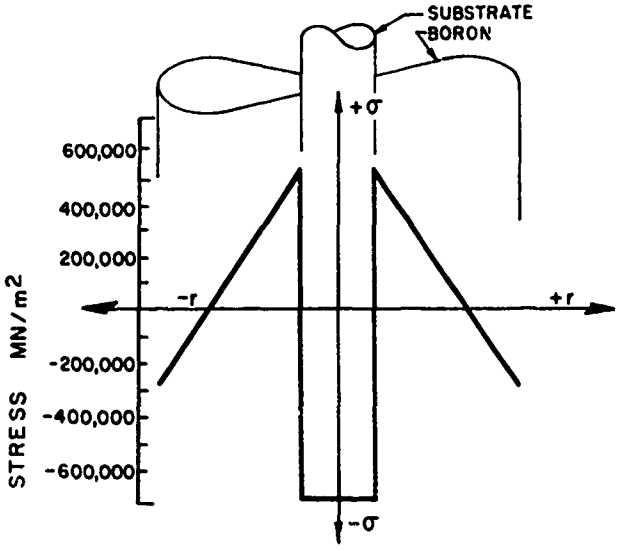

Figure 4. The Residual Stress Pattern in Boron Filament.

B. Carbon Fibers

Graphite is strong and stiff in the two directions of the basal plane, and weak and compliant in the third perpendicular to the basal plane. The problem is how to build a structure which makes use of the strong directions without suffering from the poor properties of the third. Obviously, the graphite basal planes must be aligned parallel to the fiber axis if high modulus and high strength is to be achieved, but high alignment will accentuate the poor shear and tensile strength between the planes. A strong fiber microstructure must consist of small elongated grains.

There are two different conceptual ways to get high modulus graphite fibers:

1) Start with a highly oriented polymer fiber which upon decomposition gives an oriented graphite structure.

2) Strain anneal an unoriented carbon fiber at high temperature. The stress field orients the basal planes parallel to the fiber axis.

Polyacrylonitrile (PAN) is the most prominent fiber in the first class, while rayon and pitch fibers are typical of the second. Because of the commercial importance of carbon fiber produced from PAN, a more complete description will be presented (Fig. 5).

In addition to satisfying the general prerequisites of a precursor material, namely, that it be a large volume-commercially available fiber which produces a good carbon yield

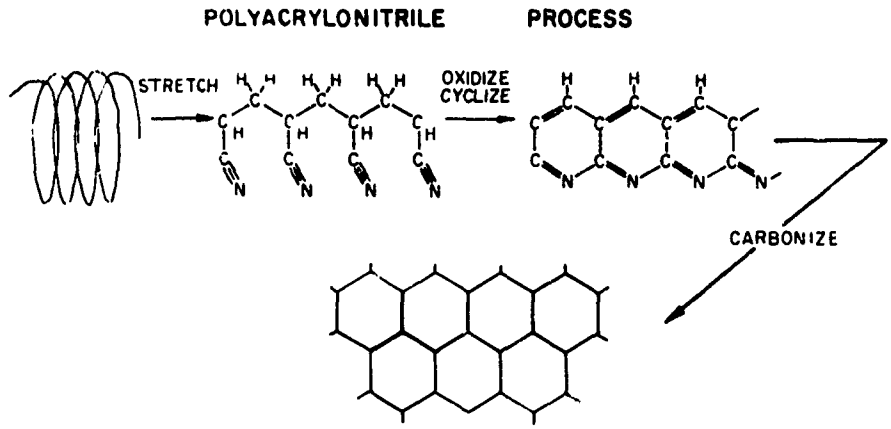

Figure 5. The Generalized Schematic of the Chemistry for Production of Carbon Fiber From Polyacrylonitrile.

upon pyrolysis, PAN has the added advantage that high modulus carbon fibers can be made by simple heat treatment of the prestretched (oriented) PAN fiber. The manufacturing processes vary but, in general, it consists of stretching the precursor prior to, or during, oxidation at about 220°C or slightly higher[5]. After oxidation, the fibers are converted to carbon (carbonized) by heating in an inert atmosphere to 1000°C, followed by a heat treatment ("graphitization") to a temperature in the range of 1000°C to 2500°C.

The high degree of axial alignment of graphite basal planes necessary for high modulus carbon fibers is related to the original alignment of the linear PAN polymer parallel to the fiber axis. The initial stretching of the PAN helps to increase the axial alignment of the polymer molecules. During the stretching of the linear molecules, some rotation of the cyanide units occurs about the linear backbone. While the resulting structure is not syndiotactic, the stretching of PAN places the cyanide units in close proximity, where they can more readily participate in the cyclization or formation of a ladder polymer that develops during the subsequent stabilization stage. During stabilization the fibers must be kept under tension to maintain the alignment of the PAN polymer while it transforms to ladder polymer, otherwise relaxation occurs and the resulting ladder polymer is disoriented with respect to the fiber axis.

If PAN is heated in the range from 25°C to 300°C, an exothermic reaction (associated with ladder polymer formation) is known to occur at approximately 280°C (depending on polymer composition) with the evolution of sufficient heat to cause complete fusion of the polymer with loss of orientation. The fusion caused by this exothermic reaction can be minimized by employing a very slow rate of heating through this critical temperature range to form oriented ladder polymer. High modulus carbon fibers have been successfully produced in this manner[6]. However, stabilization can be achieved quickly by oxidation at 220°C or slightly above. Stabilization at this temperature has been shown to permit the formation of oriented ladder polymer while reducing the intensity of the exothermic peak.

After stabilization, the precursor has an oriented cyclic or ladder structure with a high enough glass transition temperature that it is not necessary to maintain tension in the remaining processing. Considerable nitrogen and hydrogen are still present in the naphthyridene type rings that form the basic units of the polymer, and these elements are eliminated from the structure during the carbonization stage (heating to 1000°C). The carbon atoms which remain are principally in the form of extended hexagonal ribbon networks. Although these ribbon networks tend towards alignment with the fiber axis, their degree of ordering relative to each other and the fiber axis is relatively low. The effect of this is to produce fibers of low strength and modulus. As heat treatment temperature is increased, the structure is found to exist of highly tangled undulating long ribbons of graphite, perhaps 30Å wide and thick. With further heat treatment, the tangling and amplitude of undulation decrease and the ribbon size increases to a width and depth of several hundred angstroms and with a length microns long (Fig. 6). The change in preferred orientation of the basal planes is most simply measured by the "half-angle" which is one-half the angular spread parallel to the fiber axis for which the x-ray diffraction intensity drops to one-half the on-axis value. A plot of half-angle versus modulus is shown in Fig. 7.

Associated with the increase in axial alignment is a corresponding increase in radial alignment with the basal planes parallel to the outer fiber surface. Typical representations for radial preferred orientations are shown in Fig. 8 for fully stabilized fibers[7]. Commercially produced fibers are usually not completely stabilized

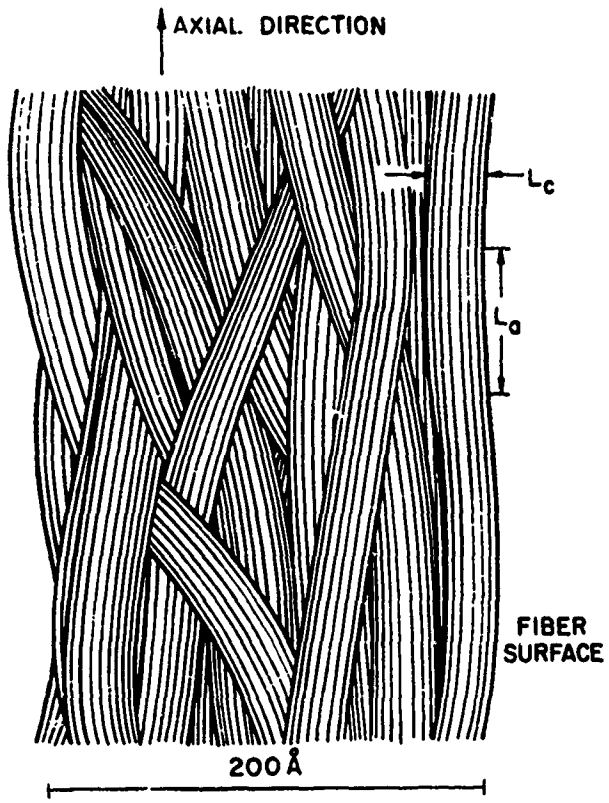

Figure 6. Schematic Diagram of Ribbon Structure Model for Carbon Fibers.

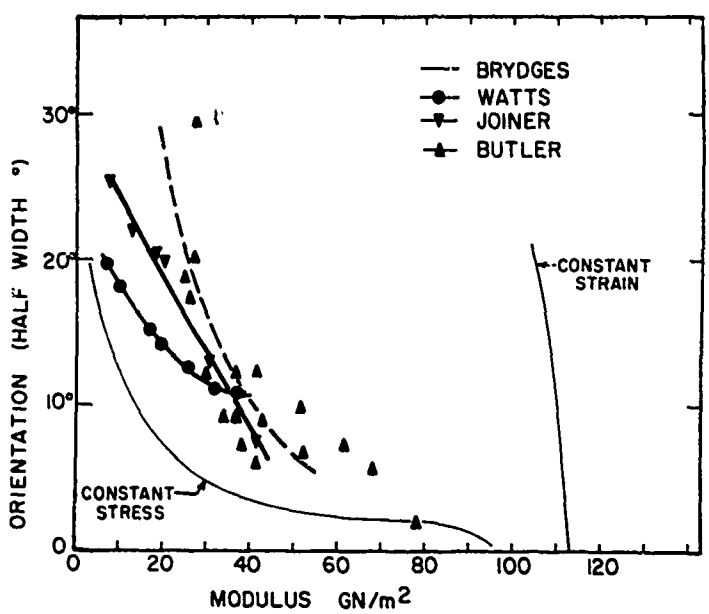

Figure 7. The Modulus of Carbon Fibers as a Function of Preferred Orientation of Graphite Basal Planes.

and show a more complex microstructure, but the outer surface always shows the "onion-skin" structure. There are two main consequences of the radial structure. Firstly, the shear strengths of high modulus carbon fiber composites is directly related to the portion of low energy basal planes at the fiber surface. Since axial and radial preferred orientations are related, the higher the fiber modulus is, the lower the composite shear strength. Secondly, the onion-skin structure results in a high residual stress upon cool-down, which decreases the coupling between ribbons and causes lower tensile strengths.

Rayon and pitch fibers are processed to carbon fibers which again appear to consist of intertwinned ribbons. In these cases, there is no preferred orientation, such that

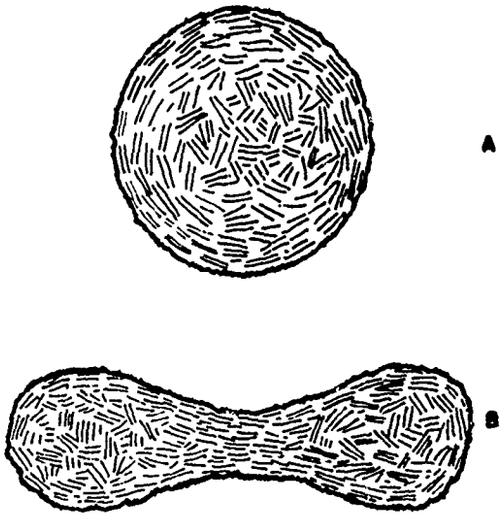

Figure 8. Schematic Representations For the Radial Preferred Orientation of Fully Stabilized PAN Based Carbon Fibers.

simple heat treatment will not yield a texture. The preferred orientation is introduced by loading the filament at a temperature that is high enough such that diffusion of carbon is rapid. The carbon fiber is deformed (stretched) to strains as high as 60% to 100% to obtain high modulus fibers. Although the process can be applied to any carbon fiber with sufficient strength, the high temperature required for the strain anneal is a disadvantage.

In summary, carbon fibers can be made from a variety of organic materials. Although the general structural feature of intertwinned ribbons is common to all forms, the details of the orientation of these ribbons is important. With the present commercial fibers, an increase in modulus is associated with a decrease in tensile strain and shear strength. These properties are not necessarily related, but improved fibers will require careful control of the radial as well as the axial preferred orientation.

C. Organic Fibers

The ultrahigh modulus of graphite results from the tight Sp^2 bonding of the basal plane. The structure is similar to that of a multi-fused ring aromatic chemical. High modulus organic fibers are possible if a portion of the ring system can be incorporated into a polymer. Highly oriented ladder or para-polyphenylene type polymers would give attractive specific moduli. The major problem is how to get these intractable polymers into a highly oriented fiber form. The first organic fiber produced with a moderately high modulus was DuPont's wholly aromatic nylon, Nomex. The modulus is low when compared to present high modulus organic fibers, but Nomex was developed primarily for thermal stability. Nomex is produced by solution polycondensation of n-phenylene diamine and isophthaloyl chloride in cold dimethylacetamide (Fig. 9). The polymer is soluble in

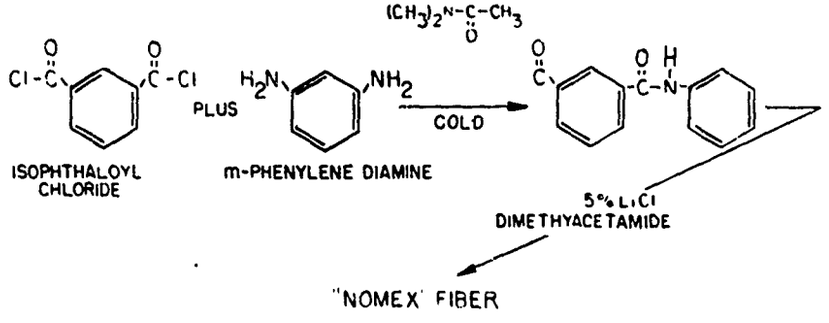

Figure 9. The Chemistry For Spinning Nomex Fiber.

solution of 5% LiCl in dimethylacetamide and is relatively easy to spin. Substitution of para-oriented phenylene groups increases the ease of crystallizing and orienting the polymer and gives a higher modulus, but it makes preparation and spinning more difficult, as well as lowering the solubility in solvents. Although the composition and process for DuPont's PRD-49 is not completely known, several DuPont patents, which produce high modulus fibers, appear pertinent[8,9]. In these patents, para-aminobenzoyl chloride is polycondensed in any of several solvents such as N, N', N dimethylphosphon-triamide and combined with a mixture of 6.5% lithium chloride in N, N' dimethylurea or other suitable solvents (Fig. 10). The resulting swollen mixture is heated to 130°C and is spun into water at 70°C. The fiber is dried and then given a brief heat treatment at approximately 500°C to improve orientation and crystallinity. A second approach useful for producing high modulus organic fiber is to spin a more soluble meta polyamic acid fiber, and then imidize. Obviously, variations are possible such as polyamide-imides and ordered copolyamides.

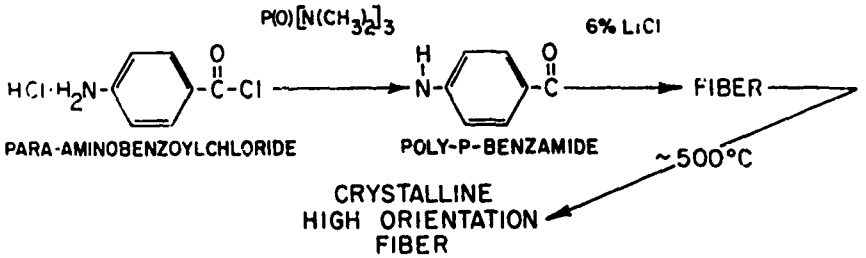

Figure 10. The Chemistry for Spinning a High Modulus Organic Fiber.

In order to obtain high specific modulus, the orientation of the polymer in the fiber must be extremely high. DuPont's PRD-49 has a very highly oriented and crystallized microstructure. In fact, it is the most structured high modulus organic fiber presently available. While this is desirable for good tensile properties, the fiber deforms at rather low loads in compression.

III. Commercially Available Fiber and Matrices

Although there are many fibers and matrices that are potentially attractive, very few have reached "commercial" production. In the case of fibers, boron, one organic, and carbon fibers from polyacrylonitrile, dominate the market. For matrix materials, there appears to be a much greater number, particularly of epoxy resins. In the case of epoxy resins, each prepregger and fabricator has his own "formulation", but it is usually based on the same basic resin system. Differences in resin systems are often of more value to the marketing man than to the engineer. The description of resin matrices will be limited to those systems made by major manufacturers rather than on specific formulations. Similarly, the metal matrices will be limited to those actually used.

A. Fibers: Boron, PRD-49, Carbon

1. Properties of Boron Filament

Boron was the first high modulus fiber to be developed, and the greater maturity of the product shows in the consistant composites that can be made from boron. Some of the reproducibility that is associated with boron is inherent to the system. For example, the modulus and surface properties of boron are not dependent on preferred orientations as are the organics and carbon. The number of variables which need to be controlled, (and can be controlled in boron), is also fewer. The major limitation to widespread use of boron filament is its cost and in the very long term the availability of the raw materials.

The mechanical strength of boron filament in early material was often quite variable. Dirt on the substrate, and inclusions picked up going through the mercury contacts gave weak filament. Improper boriding of the tungsten core caused the filament to split. However, selected production runs and, in particular, laboratory runs could average 3.8 GN/m^2 as compared to normal strengths of 2.5 GN/m^2. There has been a gradual improvement in the strength of boron during the past years, mainly by eliminating conditions that produce bad material. Average strengths are now 3.3 GN/m^2 or slightly higher (Table 3)[10]. Few individual tensile breaks exceed 4.1 GN/m^2, and future increases in strength of boron filament will probably be limited to 3.8 GN/m^2 with the present process. The strength of boron filament now appears to depend on the surface roughness of the substrate. The present tungsten substrate is quite rough (as well as being dense and expensive). In one experimental program funded by the U.S. Air Force Materials Laboratory, relatively smooth

carbon monofilament was used for a substrate[11]. In spite of several difficult processing problems, boron strength in individual boron filaments breaks were as high as 8.3 GN/m^2, and the breaks were still observed to occur at points where defects were present on the original substrate. Future improvements in boron filament strength will depend on the development of uniform substrates, but it appears that strengths of at least 10 GN/m^2 should be possible.

Table 3. Properties of Boron and Boron Filament (Diameter: 100μm)

	Boron	Boron Filament[10]
Density	23.4 Kg/m^3	25.6 Kg/m^3
Tensile Modulus	420 GN/m^2	400 GN/m^2
Hardness (KPH)	3.6×10^9 Kg/m^2	3.6×10^9 Kg/m^2
Shear Modulus		165 GN/m^2
Tensile Strength 1 inch gauge		3.3 GN/m^2
Standard Deviation		0.2 GN/m^2
Strain to Failure		0.8%
Poisson Ratio		0.21
Thermal Expansion Coefficient to 325°C		4.9×10^{-6}/°C

The response of boron to temperature is mainly related to transformation of amorphous boron to polycrystalline β-rhombohedral boron, and the reactivity of boron with its environment. Both short time tensile tests at elevated temperatures and room temperature tests after short high temperature exposures give similar results. As long as the exposure time and temperature is short and low enough, the measured strength is found to be close to the room temperature value. Increased exposure results in an increase in the number of low strength breaks although there remains an appreciable number of high strength breaks. The low strength breaks are usually associated with a recrystallized spot on the filament. A temperature of 800°C in vacuum may be maintained for a period of hours, while a temperature of 900°C or above may be held for only minutes before recrystallization starts, and strengths are decreased.

The strength retention of boron filament in air as a function of temperature is very much worse as might be expected. At only several hundred degrees centigrade, a boric oxide film forms and the strength remains on a plateau at about 0.6 of its initial strength. Above 500°C, particularly with water vapor present, the boric oxide film becomes fluid, the oxidation rates increases, and the strength drops drastically to essentially zero by 600 to 700°C[12].

Boron, like carbon, is a very reactive element. Boron will react with almost all metal matrix materials to form a boride, as well as quite often forming a low melting eutectic. This requires that metal matrix processing be performed at relatively low temperatures for short times as for magnesium and aluminum, or a protective coating be placed on the boron. Silicon carbide coatings about 2.5μm thick and nitrided (boron nitride film) filament have both proved effective in inhibiting attack by aluminum matrices. For higher melting matrices, such as titanium, the silicon carbide coating provides marginal long-time protection.

The tensile modulus of boron filament is maintained close to the room temperature value of 400 GN/m^2 to about 250°C. At higher temperatures, the modulus decreases at an increasing rate, being about 240 GN/m^2 at 650°C and 220 GN/m^2 at 800°C[13]. Creep appears to be negligible up to 800°C, and thereafter is low, but complex, due to residual stress relief and recrystallization. Although the overall structure of a boron filament is not isotropic, the filament is dominated by the large amount of boron present and behaves isotropically. Hence, the Poisson ratio of 0.21 is typical of brittle isotropic materials.

2. Cost of Boron Filament

The present price for boron filament is approximately $290/lb. for 100μm filament and $205/lb. for 140μm filament. Approximately one-third of the cost, or $100/lb., is due to raw materials cost for 100μm filament. The remaining $200/lb. is added by direct labor, amortization, quality control, packaging, marketing, and profit. Both the materials and labor cost should decrease with increased volume of produce. The raw materials cost is high for two reasons: 1) a highly uniform, high strength, small diameter,

substrate in very long lengths is not cheap; 2) boron trichloride is used mainly for boron filament and, therefore, is only made in pilot plant quantities. The 12μm diameter tungsten wire, which is used as substrate, was originally used for filaments in Christmas tree lights and in instrument lamps. The price was $3.85/1000 meters, and it was often not available in long lengths, (greater than 10,000 meters). Price projections for large quantities were not encouraging as labor and die costs were major items and did not significantly change with volume. However, the price of tungsten has decreased to $2.00/1000 meters and in moderate quantities, quotations to values as low as $1.00/1000 meters have been made, perhaps resulting from a threat of using an alternate substrate and also due to a relatively stable boron demand. The substrate lengths have also increased to 30,000 meters and more, which decreases labor required for reactor threading. Based on these quotations, the cost of substrate for one pound of 100μm and 140μm boron filament is $25 and $12.50 respectively. Boron trichloride accounts for about $33 of the cost in one pound of boron. The basic costs for the boron trichloride process and raw materials are low. Large production could reduce the cost of boron trichloride to $3-5/lb. boron filament, although for the quantities of boron filament projected out for the next several years, the price is not apt to fall below $16-17/lb. boron filament. The total materials cost for the next few years will not be less than $30/lb., or $42/lb. for 140μm and 100μm filament. Should a low cost substrate become available, raw materials costs for very large quantities could conceivably fall to $10/lb. For quantities of boron filament as large as required to have materials costs in the $30-42/lb. range, selling prices as low as $70-100/lb. have been quoted by manufacturers. Any lower prices for boron filament would depend on larger volume, new low cost substrate, and improved processing to lower capital equipment costs or labor [14].

3. Properties of Carbon Fibers

There is a profusion of commercially produced high modulus carbon fibers. The fibers are available in a bewildering array of yarns and tows with differing moduli, strengths, cross-sectional areas and shapes, twists, plies and number of fiber ends. They may be purchased in meter lengths or in "continuous" lengths. Availability with such a diversity of physical properties is one of the benefits of carbon fibers as each use tends to require different sets of optimum properties. One major problem is the cost required to evaluate this large number of fibers since complete evaluation requires actual composite tests as well as individual fiber characterization.

Certain general comments can be made about the types of fibers. First, twist in yarns or tows, (even "false twist" in tows), is undesirable as it gives lower strengths, particularly in compression, as well as lower moduli. Part of the reason for the decrease in properties can be directly attributed to the increase in misorientation that the twist introduces, but part is also due to the resin rich and poor areas that occur because of less perfect packing associated with twisted yarns and tows. Second, the number of fibers in a yarn and particularly in a tow affect its cost and prepregging handleability. While the cost of a heavy tow is significantly cheaper than a light one, the processability into high quality prepreg has generally been more difficult. Third, the strain to failure decreases with increasing modulus in the modulus range of interest, for all fibers produced to date. This makes high modulus carbon composites sensitive to impact and brittle failure. Finally, as film modulus increases the surface of the fiber becomes more highly covered with graphite basal planes oriented with their "c"-axis perpendicular to the fiber axis. This lowers the wettability of the fiber surface, and also decreases shear strength in composites.

The fiber properties can be classified into three main types: 1) rayon base carbon fiber with a crenulated irregular cross-section whose tensile strength is observed to increase with modulus, ("Thornel" by U.C.C.; Hitco); 2) polyacrylonitrile base (Courtelle) carbon fiber with a circular cross-section whose tensile strength decreases with modulus in the range of interest, (Morganite-Whittaker, Courtaulds-Hercules and Rolls-Royce); 3) polyacrylonitrile base with a dog-bone cross-section whose tensile strength increases with modulus in the range of interest, (Celanese, Great Lakes Carbon). The properties of these types of fiber are shown in Table 4. Early quoted values of strength were often those obtained in good pilot plant runs. Present values from production runs, are very similar to the earlier good pilot plant values.

Lower modulus PAN base carbon fibers are flaw sensitive and therefore are affected by abrasion [18]. More careful handling should increase fiber tensile strength in the future. The effect of surface abrasion on higher modulus fibers is not so well known, but it appears to be much less important. Internal flaws may be more significant if the work at Harwell [19] and Rensselaer Polytechnic Institute is correct [7]. Assuming this to be the case, improved precursor fibers or processing would be required for higher strength. The author has analysed the ratio of strengths at two gauge lengths for a group of runs, to obtain an estimate of the inherent flaw-free strength of a 380 GN/m^2 modulus Courtelle base carbon fiber the ratio was extrapolated to unity and the inherent

Table 4. Properties of Carbon Fibers (Au Surface Treated)

	Rayon Base			Pan Base Circular Cross-Section			Pan Base Dog-bone Cross-Section			
	Thornel (15)			Courtaulds-Hercules (16)			Great Lakes (17)			
	25	50	75	A	HTS	HMS	3T	4T	5T	6T
Modulus (GN/m^2)	170	390	520	207	262	379	210	260	330	400
Tensile Strength (GN/m^2)	1.2	2.7	3.6	2.7	2.5	2.2	2.1	2.4	2.7	2.8
Density	1.43	1.67	1.82	1.75	1.77	1.92	1.80	1.78	1.85	1.90
Diameter	≈ 6.6 μm			≈ 8 μm			≈ 5 x 13 μm			

strength of the fiber was found to be 12 GN/m^2. While this value is well above present strengths of carbon fibers, the strain to failure is similar (or lower) to fracture strains in virgin fiber glass. This value probably gives an upper limit on the strength that can be obtained from present processes in the future.

The present range of fiber moduli is from 200 GN/m^2 to 550 GN/m^2, well below the theoretical value of 1020 GN/m^2. Experimental fibers have been made with moduli as high as 800 GN/m^2, but the poor shear strength between the aligned basal planes in the fiber is very noticeable when observing the fracture surfaces.

Present production techniques for obtaining high modulus graphite fibers require high temperatures ($T \geq 2400°C$), which result in a low shear modulus and necessitates very high alignment of basal planes for high modulus. While this provides high tensile modulus, the structure will give much lower effective compressive moduli because of buckling. Improved fibers will require a lower temperature process to be developed to retain higher shear moduli.

The modulus and strength of all the present carbon fibers is constant at least to 1000°C. Since some of the fibers (PAN base) have only been heat treated to slightly higher temperatures, irreversible property changes occur at temperatures near the processing heat treatment temperature or higher. This uncertainty in modulus and strength would not be a problem with carbon-metal matrix composites, since the reaction of the fine diameter carbon fibers with a metal matrix would limit use of carbon fiber composites to temperatures well below 1000°C.

The onset of oxidation as measured by thermogravimetric analysis varies for the different fibers (20). For low modulus PAN base and rayon base fibers, oxidation starts slightly below 400°C. High modulus PAN base fibers begin to oxidize between 600 and 700°C. These results are for short times; long time applications would require an operating temperature 100°C lower. Oxidation can be inhibited or stopped by metal matrices, but any machining which exposed the fibers would allow oxidation to begin.

Only two metals appear suitable for metal matrix composites of carbon fibers. Aluminum is non-wetting, but can be made to wet carbon fibers by applying a suitable coating. Nickel is also satisfactory as it has a low solubility of carbon. However, if high temperature processing is used, nickel is found to recrystallize the fiber and degrade the strength. For other metal matrices, including nickel base alloys, diffusion barrier coatings on the fibers will be required. Larger diameter carbon fiber will be necessary such that the thickness of the layer which prevents diffusion does not decrease the specific strength and modulus too greatly.

The thermal expansion coefficients of carbon fibers are unusual as they are negative for high modulus fibers parallel to their axis at room temperature. This negative expansion can be combined with the positive expansion perpendicular to the fiber to make zero expansion coefficient structures. Although the small values of coefficient of thermal expansion mean that there will be high thermal stresses, it should be pointed out that all high modulus fibers have low thermal expansion coefficients. This is a general problem in high performance composites.

The properties of carbon fibers perpendicular to their fiber axis cannot be measured directly because of their small size and must be derived from composite data. This behavior will be described in composite properties.

4. Cost of Carbon Fibers

The present price varies from $60/lb. to $300/lb. for continuous fiber products in small quantity to a low of $45/lb. or less for meter lengths in large quantity. The present market is very small and the above prices do not necessarily reflect the total costs or manufacturing costs. However, future estimates of selling price can be made rather accurately. If special precursors are necessary, the price for several hundred thousand pounds of fiber would be from $40 to $100/lb. depending on desired modulus. Prices for similar quantities of a heavy tow using a commercially available precursor fiber are in the range of $10 to $20/lb. depending on modulus. These values appear to be about as low as present processes will yield. Although pitch base fibers have a substantially lower raw materials and, possibly, a lower processing cost, these processes have yet to be reduced to commercial practice. Never-the-less, this process has the possibility of producing fiber in the $1 to $3/lb. range which makes it competitive with glass and other structural materials.

5. Properties of PRD-49

Organic fibers are the newest high modulus fibers on the market, and the properties described are those for DuPont's PRD-49-3 as shown in Table 5. The product is available as continuous length yarns or rovings of a golden yellow fiber.

Table 5. Properties of DuPont's PRD-49-3 Organic Fiber[27]

Modulus	140 GN/m^2
Tensile Strength 10 inch	2.8 GN/m^2
Strain to Failure	2.0 %
Density	1.47 gm/c.c.

The specific modulus and strength are very competitive with carbon fibers at present. Future trends are more difficult to predict. The modulus of PRD is probably as high as can be obtained with the present polymer as the orientation and crystallinity are extremely high. However, the boundary between an organic and carbon fiber is indistinct, and future organic fibers could have substantially higher moduli if desired. The present value of 140 GN/m^2 for modulus is a good compromise as it is very compatible with the moduli of metals, and the low density of the fiber still provides a high specific modulus. The compression characteristics of PRD or other highly aligned crystalline structures are not good, as the structure buckles at low stresses, deformation bands appear which are very similar to those in metals. Future improvements in compression would appear to require some major changes in polymer chemistry.

PRD is likely to be limited to temperatures not exceeding 150°C, as its modulus drops rapidly above this temperature. It is thermally stable below this temperature, and resistant to environmental effects, although moisture pickup may be a problem. PRD is very abrasion resistant and easy to handle although this toughness presents some difficulty in machining. Finally, the PRD is a good dielectric and shows promise for radomes and similar applications.

6. Cost of PRD-49

PRD is priced at $50/lb. at present, which makes it competitive with carbon. Considering the processing and materials costs of PRD as compared to conventional textile fibers, it should be relatively expensive for a textile fiber. An estimate of its price at the several hundred thousand pounds per year level would be $10/lb. or less. This is based on the present price of Fiber B of $2.65/lb., an apparently similar product, and the relative prices of the competitive fibers at that time.

B. Matrices: Epoxies, Polyimides, Aluminum

The proprietary nature and the large number of epoxy resins make complete coverage impossible. However, most epoxy systems are based on either; 1) DGEBA: diglycidyl ether of bisphenol A, or 2) cycloaliphatics; bis (2, 3 epoxycyclopentyl) ether of ethylene glycol. The choice depends on trade-offs of shelf life and performance. Several examples are shown in Table 6. DGEBA resins such as Epon 828 have good shelf life and are cheap (less than one dollar a pound). However, the properties in the neat form or in composite performance do not match the cycloaliphatics such as ERL 4617. These improved properties in ERL 4617 are obtained at a much higher cost (about $10/lb.), short prepreg shelf life, and long postcure. The high elongation of ERL 4617 with MDA cure is

Table 6. Properties of Epoxy Resins[21,22]

	Epon 828/ MDA/BF_3	ERLA 4617/PDA	ERLA 4617/MDA	Epoxy Novalak
Heat Distortion Temperature	145°C	175	170	220
Tensile Modulus (GN/m^2)	3.5	5.4	4.8	3.4
Tensile Strength (GN/m^2)	.062	.13	.13	.043
Percent Elongation	3.0	2.8	6.0	1.6
Compressive Modulus (GN/m^2)	3.6	6.1	5.2	
Compressive Yield Strength (GN/m^2)	.15	.22	.19	

MDA - methylene dianiline
PDA - metaphenyldiamine

especially beneficial in giving toughness to uniaxial and cross plied composites. Higher temperature capability can be obtained with epoxy-novalaks, but with a large sacrifice in strength and toughness.

Although a large number of polymer systems have been and are being worked on for temperatures as high as 300°C, only the polyimides have reached a limited commercial usage. The major problem with polyimides is the elimination of water of condensation and solvents during the processing cycle. Processing must be done properly and slowly to prevent void formation in the composite. One technique to minimize void formation is the use of an addition polymerization cure of the polyimide so that no additional volatile matter is produced. The penalty for this advantage is a somewhat lower maximum, continuous use temperature of 250°C. A typical example of this type of system is Geigy's P-13N (Table 7). Price of P-13N is $75 a gallon for 85% solids.

Table 7. Properties of Geigy P-13N Resin[22]

Heat distortion temperature	> 300°C
Tensile modulus (GN/m^2)	3.8
Tensile strength (GN/m^2)	.075
Percent elongation	2.5
Density (gm/ml)	1.33

e only metal matrix to be used in substantial quantity is the aluminum alloy 6061. ly contains magnesium and silicon in approximate proportions to form magnesium e thus making it heat treatable. It is used both for plasma sprayed and diffusion ded boron/aluminum. The room temperature properties are shown in Table 8.

Table 8. Properties of 6061 Aluminum Alloy[23]

(0.6% Silicon, 0.27% Copper, 1.0 Magnesium, 0.20 Chromium)

	Annealed	Fully Aged
Ultimate tensile strength (GN/m^2	0.127	0.316
Yield (GN/m^2)	.056	.281
Elongation (%)		
Shear strength (GN/m^2)	.084	.211
Modulus (GN/m^2)		
Density (gm/c.c.)	2.71	

C. Fabrication

There have been numerous occasions when fiber from the same production run and resin from the same batch have been fabricated by different groups into simple test bars which gave quite different mechanical test results. The importance of great care and good fabrication procedures cannot be overemphasized. This is particularly true with the more brittle systems.

1. Organic Resin Prepreg Fabrication

Although test specimens and some small parts are made using wet resin and matched metal molds, most resin matrix composites go through the intermediate step of forming "prepreg". The prepreg can be in the form of continuous tape (1.2 cm to 15 cm wide, commonly 7.5 cm) or in the form of broadgoods. In the case of tape, a large number of filaments are unwound from a creel, collimated into a uniaxial ribbon, impregnated with resin, and partially cured into tacky tape. Broadgoods are made by a circumferential winding on a drum, which is later split axially to form the sheet.

Boron filament is laid up as a single layer about 0.13mm thick with a fine type 104 "E" glass scrim cloth for support. The whole tape is carried on a low-stick, plastic-coated paper. The relatively large diameter boron fibers allow very careful collimation and control of spacing to be obtained. The consequences of this perfection will be shown later in the mechanical test results.

The large number of fibers in carbon and PRD tows cause additional problems in pre-pregging, particularly the heavy tows. At best, central portions of the tows are resin poor; at worst, especially with high viscosity or polyimide resins, the central portions may be non-impregnated or voidy. Collimation is also more difficult, particularly when catenary is present (one side of the tow longer than the other). Crossovers are common, and the degree of alignment is usually no better than $\pm$ 5° locally. Because of the more flexible nature of carbon and organic fibers, scrim cloth backings are generally not used. A good prepreg tape will have enough tack and drape to be able to form shapes with gentle curvature. Epoxy resins generally give acceptable tack and drape, but the high performance cycloaliphatics have a short shelf life. Polyimides and other high temperature resins tend to be stiff and hard to work with.

Prepreg tapes can be used with numerically controlled tape laying machines for large surfaces such as aircraft skin covers. More complicated shapes such as fan blades are usually more economical to hand lay up. Curing is generally performed by compression molding in matched metal dies, or by vacuum bag and autoclave molding. In either case, the curing recommendations of the prepregger should be used as a guide. Prepreg prices have generally followed the rule that one kilogram of prepreg is equal to the cost of one kilogram of fiber.

2. Metal Matrix Composite Fabrication

Three processes have been used to make metal matrix composites:

1) Liquid melt infiltration
2) Diffusion bond
3) Plasma spray.

Liquid metal infiltration has been used to make boron/magnesium and coated boron/aluminum composites. The excellent filament-matrix compatibility of boron/magnesium allows cheaper uncoated boron filament to be used in this low cost process. For the case of aluminum matrices, the boron filament must be coated with either a protective coating of boron nitride or silicon carbide. Shapes such as I beams, tubes, and rods have been continuously cast, and the specific strength and modulus are good.

The major activity in metal matrix composites has been the work performed by several companies to provide boron reinforced aluminum tape or sheet. In the technique used by Hamilton-Standard, a 6061 metal foil 25μm thick is wrapped on a drum, overwound with a single layer of coated boron filament, and then metal is plasma sprayed over the fibers to form a foil. The foils can be plied and then diffusion bonded by the customer at 520°C for one hour under compression of 0.035 GN/m^2 to form a multilayer composite [24].

Harvey Aluminum and Amercom produce boron/aluminum sheet by diffusion bonding the boron filament in a 6061 aluminum alloy matrix. Monolayer and multilayer sheets can be made up to 46 cm wide by 4½ meters long. There is essentially no limit on thickness and the composites are available with fiber volume fractions from 40 to 50 volume percent. The composite sheet can be diffusion bonded, brazed, spot welded or adhesive bonded into more complex parts. Diffusion bonding is preformed under similar conditions to plasma sprayed tapes. For braze bonding, 718 aluminum alloy can be specified. Prices are now about $330/lb. for small quantities. Future selling prices are strongly coupled to fiber cost, and the present producers estimate that the cost of one kilogram of boron/aluminum composite should be equal to one kilogram of boron fiber for large quantities [25].

IV. Properties of High Performance Composites

The properties of composites depend not only on fiber and matrix properties and the interfacial bond between them, but on the fabrication and test techniques as well.

Furthermore, mechanical test data are usually obtained from relatively small well made test specimens. For composites that are not flaw sensitive, the test results from small specimens may be used to adequately describe larger scale hardware. However, for brittle composites, such as surface-treated, high modulus graphite/epoxy, the application of small specimen test data to a large structure will over-estimate the strength of the structure, for the structure is more apt to have strength reducing flaws. The property data to be presented is from small test specimens and only for uniaxial layups. The data is for the four most highly developed systems: boron/epoxy, graphite/epoxy, PRD/epoxy and boron/aluminum. Pertinent information on higher temperature resin matrix composites is also presented.

The mechanical properties of boron/epoxy composites are shown in Table 8. The good fiber alignment and the fracture characteristics are such that composite properties are well predicted by the law of mixtures from fiber moduli and the average fiber strength measured at a 2.5 cm. gauge length. In addition to the good tensile strength, compressive and interlaminar shear strength are also high.

Table 8. Properties of Boron/Epoxy Composites[26]

(Uniaxial Layup, 50 v/o AVCO-5505 Resin)

	22°	190°C
0° Tensile Strength (GN/m^2)	1.73	1.38
0° Tensile Modulus (GN/m^2)	210	197
0° Flexural Strength (GN/m^2)	2.07	1.65
0° Flexural Modulus (GN/m^2)	200	165
90° Flexural Strength (GN/m^2)	.13	.079
90° Flexural Modulus (GN/m^2)	21-27	9.0
0° Compressive Strength (GN/m^2)	3.10	1.45
0° Compressive Modulus (GN/m^2)	228	217
0° Short Beam Shear Strength (GN/m^2)	.103	.038

Table 9 presents composite values for some better carbon fiber/resin composites. The poorer fiber alignment and differing fracture modes make prediction of composite properties from available data difficult. In general, moduli parallel to the fiber axis are about 15% lower than that calculated from the rule of mixtures. Lower preferred orientations in chopped fiber mat results in still lower 0° moduli, but higher 90° moduli. Accurate predictions of tensile strength cannot be made from fiber tensile test data collected at 2.5 cm. gauge length, and data at short gauge lengths is generally not available. Low modulus fibers are more sensitive to surface flaws, and the strengths of these fibers show a greater gauge length effect than high modulus fibers, that is, the shorter the gauge length, the higher the tensile strength is. Consequently, composites reinforced with low modulus fibers may have observed strengths that are higher than the rule of mixtures fiber strength value based on a 2.5 cm. gauge length. For a 200 GN/m^2 modulus fiber, the average experimental strengths are commonly 10-15% high. As the fiber modulus is increased, fracture becomes more brittle such that, for the present surface treated fibers of 400 GN/m^2, the fracture surface has a typical mirror-hackle appearance. Fracture is initiated at gross flaws in the composites and composite strengths fall below that calculated by the rule of mixtures. Strength values are typically about 25% low. Tensile, and compressive strengths are well balanced with intermediate modulus carbon fiber composites, and interlaminar shear strengths are high. Higher modulus carbon fiber composites are often more limited by the poorer compressive and shear strengths than their tensile strengths. However, the high modulus carbon fiber composites have a unique characteristic in that cross plied structures can be made with zero expansion coefficient. This allows extremely light stiff, strong, dimensionally stable structures to be made.

The properties of PRD-49-3/epoxy composites are shown in Table 10. While the tensile strength of the composites is good, compression and bend properties only match aluminum. This limits the usage areas to pure tension applications such as pressure vessels if maximum performance is to be achieved. However, combinations of PRD (for tension) and a surprisingly small amount of boron (for compression) are attractive for hybrid composites.

Boron/aluminum composites can be fabricated by either plasma spraying or diffusion bonding (Table 11). In general, diffusion bonding gives superior properties. Early diffusion bonded samples often failed in 90° tensile tests by fiber fracture or interfacial debonding. The higher 90° tensile values shown in the table correspond to recent results with newer fibers and improved processing. As can be seen, the compressive strength is extremely high and essentially never limiting in design. The tensile

strength is somewhat lower than the corresponding values for epoxy matrices, but room temperature strength is maintained to 200°C with useful strength to 325°C.

Table 9. Properties of Graphite/Resin Composites[16,17,22]

	HMS, I Cycloaliphatic Epoxy		HTS, II Cycloaliphatic Epoxy		5T	6T*	HMS Polyimide	HTS Polyimide
	Mat	Continuous	Mat	Continuous	—	—	—	—
Fiber Volume	55	54	55	60	60	60	61	57
0° Tensile Strength (GN/m^2)		.70		1.38	1.17	1.03		
0° Tensile Modulus (GN/m^2)		179		131	172	207		
90° Flexural Strength (GN/m^2)	.055	.037	.083	.041				
90° Flexural Modulus (GN/m^2)	9.65	8.2	8.96	6.9				
0° Flexural Strength (GN/m^2)	.61	.95	1.08	1.65	1.45	1.38	1.07	1.56
0° Flexural Modulus (GN/m^2)	165	186	103	124	172	207	193	159
0° Compressive Strength (GN/m^2)		.81		1.43	.96	.83		
Interlaminar Shear Strength (GN/m^2)	.055	.072	.103	.131	.090	.076	.065	.098
0° Thermal Conductivity (cal/cm·sec.°C) ($\times 10^{-4}$)		400						
90° Thermal Conductivity (cal/cm·sec.°C) ($\times 10^{-4}$)		15						
0° Thermal Expansion Coef. ($\times 10^{-6}$)		-0.6						
90° Thermal Expansion Coef. ($\times 10^{-6}$)		+29						

* HMS, HTS: Hercules-Courtaulds high modulus and high strength fibers, respectively.
I, II: Morgan-Whittaker high modulus and high strength fibers, respectively.
5T, 6T: Great Lakes Carbon 50 and 60 million modulus fibers, respectively.

Table 10. Properties of PRD-49-III/Epoxy Resin Composites[27]

(Uniaxial Layup, 60 v/o Fiber, BP 907 Resin)

	0°	90°
Tensile Strength (GN/m^2)	1.45	.019
Tensile Modulus (GN/m^2)	87	8.0
Flexural Strength (GN/m^2) (Yield)	.34	
(Ultimate)	0.7	
Compressive Strength (GN/m^2)	.25	.082
In-Plane Shear Strength (GN/m^2) (55 v/o)	.039	
In-Plane Shear Modulus (GN/m^2) (55 v/o)	2.8	
Short Beam Shear Strength (GN/m^2)	.069	
Poisson's Ratio	0.32	
Coef. of Thermal Expansion (°C x 10^6)	-6	+
Thermal Conductivity (54 v/o) (cal/sec/cm/°C)	40 x 10^{-4}	3.4 x 10^{-4}
Moisture Regain (Fiber only)	1.5%	
Density (g/cm^3)	1.37	

Table 11. Properties of Boron/Aluminum Composites[24,25]

(Uniaxial Layup, 48 v/o Fiber, 6061-T6 Matrix)

	Plasma Spray	100μm dia. Filament Diffusion	140μm Bond
0° Tensile Strength (GN/m^2)	1.2	1.4	1.5
0° Tensile Modulus (GN/m^2)	207	234	228
90° Tensile Strength (GN/m^2)	.10	.28(.11)	.28(.15)
90° Tensile Modulus (GN/m^2)	83	165	186
0° Compressive Strength (GN/m^2)		> 4.3	> 3.2
0° Compressive Modulus (GN/m^2)		234	228
Interlaminar Shear Strength (GN/m^2)	.089		
Shear Modulus (GN/m^2)	48		
Poisson's Ratio	.22	.22	

V. Conclusions

The development of high strength-high modulus fibers provides significant potential increases in hardware performance. Furthermore, the continued development of these fibers can be expected to further improve properties and also to reduce cost. The incorporation of these fibers into structural materials has been successfully accomplished with good translation of the fiber strength to the composite strength. At present, the improvements in performance are not being exploited because of the high material and fabrication costs at the current low volume production and lack of confidence. It is believed that costs will decrease with increased volume and development of new low cost fibers. Lack of confidence, however, must be overcome with experience and a much broader data base than is now available.

Acknowledgment

The author would like to thank his graduate students for their help in preparing this manuscript. Special thanks are extended to J. Weiss for reading the manuscript and to J. Nelson for the drawings.

References

1. Gordon, J. E., "Some Considerations in the Design of Engineering Materials Based on Brittle Solids", Proc. Royal Soc., A282, 16, (1964).

2. Gilman, J. J., "Ultrahigh Strength Materials of the Future", Mechanical Engineering, 83(9), 55-59, (1961).

3. Cottrell, A. H., "Strong Solids", Proc. Royal Soc., A282, 2-9, (1964).

4. Kelly, A., "High Strength Materials, Contemp. Phys. 8, No.4, 313-329, (1967).

5. Johnston, W., Phillips, L., and Watt, W., "Carbon Fibers from Acrylonitrile Polymer Fibers", British Patent 1,110,791, Appl. April 24, and Dec. 29, 1964.

6. Standege, A. E., and Prescott, R., "High Strength and High Modulus Carbonaceous Fibers", British Appl. No. 49850/65, Nov. 24, 1965.

7. LeMaistre, C. W., "Origin of Structure in Carbon Fibers", Ph.D. Thesis, Rensselaer Polytechnic Institute, Troy, New York (1971).

8. Kwolek, S. L., "Aromatic Polyamides for Fiber Production", French 1,526,745, May 24, 1968.

9. Antal, P. S., DeDominicus, A. J., and Szucs, D. L., "Poly-p-benzamide Spinning Compositions", German, 1,924,736, Dec. 11, 1969.

10. Krukonis, V., AVCO Corporation, Personal communication.

11. Mehalso, R., and Diefendorf, R. J., "Carbon Monofilament, A Substrate for Boron Deposition", Presented at 10th Biennial Conference on Carbon, Lehigh, Pa., June 1971. Abstracts available from American Carbon Committee, Penn State, Pa.

12. Veltri, R., and Galasso, F., "Tensile Strength of Boron Filament at Elevated Temperatures", Nature 220, 781, (1968).

13. Ellison, E. G., and Boone, D. H., "The Modulus of Boron Filament at Elevated Temperatures", J. Less Common Metals 13, 103, (1967).

14. Hoffman, P., AVCO Corporation, Personal communication.

15. Union Carbide Technical Information Bulletins Nos. 465-200 ca(Thornel 25), 465-205 ca(Thornel 505), 465-221 ca(Thornel 755), available from Union Carbide Corporation 270 Park Avenue, New York, New York 10017.

16. Hercules Advanced Composites Product Data, "Hercules Continuous Filament Graphite Fiber", No. 815-2. Also Jordon, C., Personal communication for most recent data. Hercules Incorporated, 910 Market St., Wilmington, Delaware 19899.

17. "Fortafil" High Performance Graphite Fiber Products Folder. Also, Prescott, R., Personal communication. Great Lakes Carbon Corporation, 299 Park Avenue, New York, New York 10017.

18. Johnson, J., "Factors Affecting the Tensile Strength of Carbon Fibers", Amer. Chem. Soc. Polymer Preprints, 9, (2), 1316-1323 (1968).

19. Sharpe, J. V., and Burnay, S. G., "High Voltage Electron Microscopy of Internal Defects in Carbon Fibers. Presented at the International Conference on Carbon Fibers, their Composites and Applications, London, 1971. Available from: The Plastics Institute, 11 Hobart Place, London S.W. 1, England.

20. Shapiro, I., "Thermogravimetric Studies of the Oxidation of Carbon Fibers", Presented at the American Ceramic Society, Chicago, Illinois, April 1971.

21. Soldatos, A. C., Burhans, A. S., Cole, L. F., and Mulvaney, W. P., "High Performance Cycloaliphatic Epoxy Resins for Reinforced Structures with Improved Dynamic Flexural Properties", Advances in Chemistry No. 92, "Epoxy Resins", pg. 86-95. American Chemical Society, Washington, D.C. 1970.

22. Fothergill and Harvey, "Designing with Carboform Carbon Fibre Reinforced Plastic", Publication No. 35, (1971). Fothergill and Harvey, Littleborough, Lancashire, England.

23. "Aluminum Standards and Data 1971". The Aluminum Association, 750 Third Avenue, New York, New York 10017.

24. Hamilton Standard Release No. HSCM-4-C. "Borsic Aluminum Tape", Hamilton-Standard Windsor Locks, Connecticut 06096.

25. Dolowy, J., "Properties of Boron/Aluminum Composites", presented at American Ceramic Society West Coast Meeting, Anaheim, California. Nov, 1971.

26. Krukonis, V., AVCO Corporation, Personal communication.

27. Moore, J. W., "PRD-49, A New Organic High Modulus Reinforcing Fiber", E. I. duPont De Nemour and Co., Inc., Textile Fibers Department, Wilmington, Delaware.

COMPOSITES IN THE STRUCTURAL DESIGN PROCESS

by

M. E. Waddoups
Project Structures Engineer
General Dynamics Corporation
P.O. Box 748
Fort Worth, Texas 76101
USA

SUMMARY

The use of advanced composites as a primary structural material for aircraft structures has required alteration of the characterization and design process. Specific departures from conventional lightweight metal design practices have resulted because of the fabrication and process control characteristics, the failure characteristics of the material, and the additional structural design variables. Each of these subject areas with the attendant impact of composite materials on design practice will be reviewed. Case examples from actual prototype hardware are presented.

INTRODUCTION

The conversion of advanced filaments and matrices into aircraft structures has been guided by a single overwhelming requirement--reproducibility. The successful use of aluminum alloys in aircraft structures has been primarily a consequence of in-process control and reproducibility of vital components. This parallel in composite materials is the antithesis of the material design problem. While it may be theoretically possible to construct an ideal material for every given application it then becomes necessary to characterize a wide variety of structural materials within a single filament matrix combination. When one considers the testing, the data development, and the process control standards development required to produce consistent aircraft structural components it is soon determined that utilizing the ultimate advantage of composite materials is, at least for the short-term problem, impractical. This has led to the conception of material systems. In material systems, the components are optimized for a broad class of applications within aircraft structures. The constituent properties, filament volume/matrix volume relationships, and process control parameters for producing the final form of the material are standardized. This standardization has led to a set of reproducible materials for which characterization processes and standard design data presentation techniques allow the material to be confidently designed for a wide variety of aircraft structural components. Implementation of the material systems into the structural design process is dependent upon the characterization data, criteria postulation, and design data presentation to the product designers. Each of the cited steps are mutually dependent upon understanding the structural characteristics of the materials.

CHARACTERIZATION STRATEGIES

The basic material unit for an advanced composite system is the lamina or monoply. This lamina consists of filaments bound in a partially cured matrix and temporarily bonded to some suitable carrier form so that the material can be handled. Boron-epoxy production tape is shown in Figure 1. The monoply can usually be characterized as a transversely isotropic material. The stiffness characterization for membrane stress applications necessitates measurement, as a minimum,of the elastic modulus parallel to the filaments, the elastic modulus perpendicular to the filaments, the Poisson's ratio, and the in-plane shear modulus of the basic lamina unit. The lamination theory can be used to compute the basic stiffnesses of laminates constructed from the lamina. The stiffness characterization process is complicated by the fact that the matrix dependent properties, i.e. the transverse moduli and shear moduli, are time-dependent and nonlinear in stress and time. This may seem to be an insurmountable complication; however, in practical laminates, the design objective is to provide maximum strength for the actual load demands of the structure. Consequently, the laminate properties are generally filament property dominated. The nonlinear extensional deformations are controlled by matrix properties. For the practical structure, the problems of characterization of the matrix dependent responses become second order. An exception is glass-epoxy for which filament viscoelasticity is important.

Two alternate strategies have been developed for the fracture process. The first approach considers that structural collapse will occur when any stress at a point in the structure reaches a limiting value as defined through lamina and laminate test. This strategy implies that by characterizing the structural capacity in the principal directions for the laminae, performing the lamination analysis, conducting an elastic structural analysis, and subsequent application of a failure theory a sufficient characterization of

the structure will be obtained. This has been found to be applicable for the design of composites in the areas of continuous material. In the design of major attachments, cut-outs, and examination of the damage tolerance of the material, an alternate concept has been explored. This concept treats structural breakdown as dominated by local performance of the material and is closely related to the fracture process of a brittle solid. This behavior has been demonstrated in several experiments. The introduction of a sharp flaw into a composite material results in a size dependence which is suggestive of a fracture toughness controlled failure mechanism. A consequence of the behavior is pronounced scaling dependence of the composite structural properties.

Fatigue characterization has been pursued using two alternate strategies--use of simple history (constant amplitude) characterizations to produce a data base for damage rule analysis and use of random history characterizations for the examination of history effects on fatigue life.

CHARACTERIZED SYSTEMS - BORON/EPOXY

Boron-epoxy was the first advanced filament-based material system developed in the United States. About six months were required to develop this material system after stabilization of filament production. A variety of filament spacings, constituent properties for the matrix, and basic forms for the material tape system were explored. In some of these initial systems, matrix properties were found to be of primary importance in successful conversion of the bundle strengths of the filaments into laminate strengths for the engineering laminate. The first sandwich beam tests were tests to indicate the ultimate potential of boron-epoxy. Development of a reproducible tensile coupon actually trailed the development of the materials system by approximately one year. The early development of boron-epoxy was guided by observations made with the sandwich beam tests as shown in Figure 2 (Reference 1). The key to the sandwich beam test is the method used to introduce the load into the test specimen facing sheet. This specimen design translates to the entire structure where attaining a high structural efficiency in the composite structure is also dependent upon a carefully designed load introduction scheme.

The stiffness of a boron-epoxy laminate can be adequately characterized, at least for the initial portion of the stress-strain curve, by first characterizing the laminae properties and following this with a lamination theory based analysis. The failure mechanisms of complex laminates in boron-epoxy have been studied; however, one of the objectives in developing the material system was to extend the transverse ply failure strains to levels equal to the strain failure for the properties parallel to the filaments. This resulted in a material which could operate at stress levels in the neighborhood of 2/3 of the capacity of the filament controlled failure modes without substantial degradation in matrix dependent properties. The breakdown of the transverse lamina can be discerned within the stress-strain curve of the laminate (Reference 1). Calculations based upon sequential breakdown of lamina can be made to estimate the ultimate strength capacity of boron-epoxy laminates (Reference 2).

The coefficient of variation in strength for boron-epoxy has been shown to translate from lamina to laminates (Figure 3) and from unnotched specimens to specimens with small round holes (Figure 4) (Reference 3). For a round hole, the strength capacity of an infinitely wide sheet is strongly dependent upon hole radius (Reference 4).

For flaws, the load capacity of a composite structure has been found to be fracture toughness controlled. The effective fracture toughness of boron-epoxy may be deduced from either hole radius experiments or sharp flaw experiments. It has also been found that standard characterization techniques, (sandwich beam test, a simple coupon test, and quality control level flexure tests) can be statistically correlated (Reference 5).

Boron-epoxy, in production tape forms, is a brittle material with a coefficient of variation in strength comparable to aircraft metal alloys. For a sheet of material to be used in membrane applications, the material variability is preserved with and without discontinuities. At a discontinuity, such as a round hole, the fracture process is statistically independent; hence, structural strength is a function of complexity (number of holes and fastening techniques). The endurance of laminates with unloaded discontinuities is remarkably high (Reference 4). The material has reached a point of production application.

CHARACTERIZED SYSTEMS - GRAPHITE-EPOXY

Graphite-epoxy has not evolved into a single family of specified tape systems such as boron-epoxy. This development has been initiated; however, it has been impeded by the wide variety of filament/matrix forms available. The potential application of a graphite-based composite system offers attractive properties at what appears to be a substantially lower price. Certain candidate graphite-epoxy tape systems have received preliminary

characterization. These systems have been formulated to meet requirements similar to the requirements specified by boron-epoxy for reproducibility and for structural properties. The reproducibility has not been met in the tape system; however, this appears to be a consequence of the state of development rather than a serious impediment to the future development of graphite-epoxy. Proceeding again as with the previous characterizations of boron-epoxy the stiffness characterization can be adequately completed by characterizing the basic unit, the monoply, and utilizing monoply properties and laminate analysis to give preliminary predictions for the stiffness of engineering laminates. The fracture process for graphite-epoxy appears to be identical to that of boron-epoxy. The fracture sensitivity to flaw size and flaw shape is as important as it is in boron-epoxy. The fatigue characteristics of graphite-epoxy appear to be superior to other available engineering materials. In fact, in one set of experiments a sharp flaw was implanted into the material and resulting fatigue experiments showed an actual increase in residual strength (Reference 4). The hole size dependence problem for the case of a round hole is as important in graphite-epoxy as it is in boron-epoxy. In fact, most of the initial observations of the fracture characteristics of the advanced composite systems were made in graphite-epoxy. The cost trends for graphite-epoxy are very encouraging. A material form structurally equivalent to boron-epoxy can be obtained at prices which may bottom out in the $30 to $40 per pound range at projected material usage requirements over the next five years. This means that a substantial proportion of the development of advanced comp in the United States is focused on the optimization and the development of a materi. system that can be reproduced and used to fabricate major parts.

JOINTS

As discussed earlier in the presentation of test techniques, load introduction into a composite structure is a key feature of the design of the structure. Thus it seems appropriate to present the development of major attachment systems within the same context as the development of the material system. When a bolted joint or a bonded joint is introduced into a composite structure, the character of the mechanical breakdown of the structure is vastly altered. In this case, matrix properties become very important and many of the structural failure modes observed appear to be closely related to the mechanical breakdown of the laminate as observed in matrix dependent failure modes. The system used to fasten the composite structure must be developed independently and the treatment of the fatigue characterization and the static characterization of the major attachments must be treated independently since the failure characteristics differ from those of the basic material. Two techniques have been developed to characterize bonded joints. The first of these techniques is the classification of the static fracture characteristics of the material with respect to available strengths, available efficiencies, and the fracture process. The second technique is the characterization of the fatigue properties of bonded joints. In bonded joints, development has been concentrated on three basic configurations: the step-lap joint, the tapered scarf joint, and the multiple step joint configuration. Preliminary design data is available for each of these configurations and limited data is available on the scaling of a design as different load intensities are incurred in the basic joining area. Fatigue problems associated with joining appear to be of the same magnitude as those encountered in designing splices for metal structures. The slope of fatigue S-N curves appear similar to the slope of the S-N curves achieved for a metal-to-metal joint either with comparable adhesives or under a comparable K_T (Reference 6). The load history effects on the anticipated life of the joint must be treated carefully (Reference 7). The design of bolted joint systems has also received parallel development through the bonded joint. Initially, a bonded joint was thought to be the most efficient joint configuration; however, bolted joints have been shown to be equally feasible; in some instances bolted joints have been shown to be competitive from a weight standpoint. The static fracture capacity of bolted joints has been determined to be scale dependent. In fact, in developing bolted joint data careful attention must be paid to the absolute dimensions of the system as well as the nondimensional parameters of the joint. The fatigue in a bolted joint has been reported only for a constant amplitude characterization. In these characterizations; however, the bolted joint fatigue response is comparable to the fatigue response of a bonded joint. Attachment systems paralleling the basic material system development have been developed for the development of advanced composite structures.

CRITERIA

Boron-epoxy was developed as a direct substitute for metal in aircraft structure. Initially, the criteria postulated for designing metal structure was utilized in designing composites. For the substitution designs examined, the strength/lifetime characteristics observed have been equivalent to those for metals. For the first stage in the development of advanced composites, this has been a feasible and useful approach. The original design criteria was postulated under three major assumptions--(1) no changes to current Air Force structural design criteria with respect to loads and overall safety factors, (2) special criteria applied to expected operational stresses to prevent mechanical breakdown of the composite matrix and (3) allowables philosophy similar to current metals

practice. The criteria for structural characterization was developed to allow freedom in laminate optimization. Current design criteria may be stated as follows: (1) Design ultimate load results in a stress that does not exceed the design ultimate stress for the laminate used (Figure 5), where design ultimate stress is the maximum stress obtainable without rupture of any lamina. (2) Design limit loads are defined by vehicle specification and shall result in a stress that does not exceed the design limit stress for the laminate used, where the design limit stress is the stress beyond which the laminate suffers damage or degradation of stiffness.

For the characterized systems previously cited, the material properties perpendicular to the fiber direction dominate the limit load failure of the laminate, Figure 6. This results from failure of the matrix. Although the linear properties dominate the design, secondary failures such as matrix crazing, loss of environmental resistance, and loss of capacity to maintain fuel and other fluids can be avoided completely if the previously mentioned criteria are followed. The resulting designs will provide superior fatigue life. Even with the conservative criteria, a substantial advantage in mechanical properties can be observed for advanced composites over typical aircraft structural materials. An example of the impact of this type of criteria and the selected design stress levels for boron-epoxy is shown in Figure 7, and an example of the presentation of the stress allowables information prepared within the characterized material properties presented and the criteria statement is shown in Figure 8.

The postulated criteria is effective only in predicting the strength capability available in the material for the case of the pristine material and limiting size of discontinuities. Current research in fracture mechanics of composite materials is determined the relationship of fracture statistics to design allowables for the material and rational technologies for predicting damage accumulation rates for the materials. As the number of members constructed from composite materials increase, the criteria statements will probably be re-examined and explored further.

FABRICATION METHODS

Composite material systems were developed with future fabrication methods as a dominating factor in selection of material form. The material appears as a collinated set of unidirectional filaments carried in a semi-jelled epoxy resin with a backing scrim material and a paper or other easily removable carrier which renders the material handleable (Figure 1). This composite tape system can be applied lamina by lamina to form plies and plies can be laminated to form a part. Two methods are generally used to fabricate advanced composites parts. These include hand lay-up of a lamina on Mylar templates which give the shape to be used in the construction of a part. These Mylar templates are then transferred to a master bond form, and the tape materials are stripped from the template and laminated ply by ply outward in the direction of the master template.

A scheme for the lay-up of the tape has been developed in the form of tape laying machines (Figure 9) which fully automate the process including delivery of tape in the proper direction on the master bond form. The machine laminates the tape side by side and shears the material at the boundaries of the parts. Typical components fabricated from the advanced composite materials are shown in Figure 10. Woven materials have not been developed from the advanced composites. The degradation in strength caused by weaving plus the difficulties in maintaining resin content control in such materials have precluded their use for high-performance parts. Drilling and machining of graphite-epoxy parts can be accomplished with standard tools. Because of the hardness of the boron filaments, diamond tools or ultrasonic machining techniques must be used to provide attachment holes.

In general, it is most cost effective to construct the parts to the correct size, leaving only the minimum amount of trim. The material scrap factors described in the preceding paragraphs are exceedingly low. While the material costs are high, the low scrap is an offsetting factor when compared to the cost of construction, and when compared also against machining aluminum parts, for which in the case of integrally machined parts, in access of 90% of the material is not used.

MATERIAL IMPACT UPON STRUCTURAL DESIGN

The full impact of composite materials in the design of structures has not been realized. Some reflection of the physical properties of the material indicate that substantial alterations will be made in the design process as use progresses. Initial observations indicate that because the material does not yield there is a necessity that a more detailed analysis be made earlier in the design process to avoid stress concentrations and to formally define major load paths in the structure. Because of this demand teams of specialists, including designers and stress analysts, have resorted to the application of large scale structural analysis techniques such as the finite element method

for determining the distribution of load within a structure, even early in the preliminary design process. Because of the difficulty and number of computations involved in even the simple strength analysis of composite materials, digital computers are employed even for determining design allowables and checking safety margins of the design. Many portions of the design process have been fully automated, and the methods have been utilized for fully automated redesign of structure. Beyond the impact that composite material has on the simple calculation efforts required for the design of a structure are the fundamental impacts on the allowables philosophy, criteria and characterization strategy.

Advanced composite materials are brittle, but they possess a low coefficient of variation in filament-dominated fracture processes. The materials also do not have a propensity for through-crack nucleation or propagation during cyclic loading processes. It has been demonstrated that the fracture statistics for advanced composite materials translate from straight unnotched specimens to specimens with uniformly sized flaws, without distortion of the coefficient of variation of the material. This indicates that the failure process is relatively independent of surface area in a laminate since a 1 x 9 inch coupon will give approximately the same variability in fracture as an area a quarter of an inch square, as in the case of focusing the stress concentration near a small round hole. However, individual flaw sites must be assumed to be statistically independent. A penalty in mean capacity of the structure must be paid for increasing design complexity. This is in contrast to the response of metal where the effects of plasticity in at least the static case negate much of the penalty which would be a result of increasing the complexity of the structure. Thus, there are quantitative arguments which reinforce the designers intuition that the most reliable structure is the simplest structure that can be made to do the job. With respect to fatigue performance, the major portions of the structure which are fatigue critical have been found to be so history dependent that the most acceptable characterization strategy is a real-time, flight-by-flight random simulation of the expected service environment for both design development tests and for major structural component qualification tests. Because of the uncertainties involved in scaling from laboratory structures to full-scale structures, careful attention is being paid to the quality of the data which can be scaled and to the quality of the data which cannot be scaled. Even with the use of the best analytical techniques, the probability of a designer achieving a safe design without first going through a development test program is sufficiently small that any attempts to achieve quantitative reliability must be coupled with full-scale testing. The material impact on structural design has not been rapid; in fact, the first stage has been to develop materials systems which exhibit characteristics that allow them to directly replace a metallic structure. Where the comparable metal component exists, direct one-for-one weight savings comparisons have been made at the extreme of minimum efficiency. This is a direct one-to-one substitution of a composite component for a metal component. This stage is being outgrown as the weight savings available with advanced composite materials have been established. Thus, the full impact of the physical properties of the material will be realized as the technology is scaled up to the conceptual design stage.

ANALYSIS OF COMPOSITE STRUCTURES

The availability in the aircraft companies of large-scale digital computation has been a key feature in the rapid introduction of composite materials from the state of the simple material system to full-scale working flight hardware. The necessity of digital computation is easy to realize. First, consider the computation required for the simple determination of the state of stress in a laminate at a point. Using the assumptions of lamination theory, it is found that the lamina stiffnesses must be transformed from the lamina reference axes to the particular axis for a global reference in a laminate. Following this operation, the individual stiffnesses of the layers must be summed in scalar operations involving thickness for the determination of both inplane extensional stiffness, coupling stiffness, and bending stiffness for a laminated structure. Following the determination of the distribution of strain in the structure, the system must then be decomposed from the basic membrane strains and curvatures applied to the element to the strains in the lamina for either stresses or strains for comparison with failure surfaces (Reference 9). Conducting these operations with slide rule computation simply impedes the capability of the design organization to consider either sufficient lamination patterns to optimize the structure or sufficient points within the structure to allow full confidence in the integrity of the component. Thus, the role of the digital computer has been an integral part of the growing composite design capability.

ANALYSIS OF LAMINATES

Most major design organizations in the United States have the above-mentioned operations involved in determining the constituent properties for laminates and the decomposition of strains and curvatures into information for design allowables fully automated and directly accessible to the design engineer. These laminate analyses proceed from a variety of assumptions from the first, simple application of yield theory, and appropriate failure

surfaces for estimates of damage threshold or linear projections of the ultimate capacity of the material. The same processes have been developed to account for additional problems such as change in stiffness of the laminate due to progressive breakdown of the lamina and extensions for prediction of ultimate strength when, for instance, the breakdown (Reference 2) of the non-load-bearing direction material in a 90 ± 45° laminate controls the basic fracture of the laminate system. These analysis procedures appear in the form of computer codes and the development of a capable design organization requires training engineers in the use and interpretation of the data from the codes.

ANALYSIS OF ELEMENTS

The next level of analysis has been to code the behavioral response of generalized composite elements such as flat plates, (References 10 & 11), stiffened panels (Reference 12), cylindrical shells (Reference 13), and other basic building block elements for aircraft structure. The analysis required to determine the state of inplane strains and curvatures in these types of building block elements have required a generalized implementation of numerical methods for solving the boundary value problems. This is principally due to the anisotropic behavior of the material which renders close-form solutions available for only the simplest of elements. In the library of already catalogued techniques, are included methods for the analysis of anisotropic plates for lateral loads, dynamic response, and stability (Figure 11) for the cases of both uniform and nonuniform boundary tractions, and for distribution of material properties in the element. In fact, a library of analysis procedures is available for most of the elements commonly encountered in the design process.

ANALYSIS OF COMPLEX STRUCTURES

The finite element method has been almost universally used (References 14, 15 and 16) in making further analyses of major structures for determining load path stiffnesses for elastic computations and normal modes for failure computations. Finite element methods reduce the problem of elastic or nonlinear analysis of a complex structure to a problem of almost elementary bookkeeping; therefore, it is particularly amenable for use by design engineers and people not completely familiar with the theoretical bases of the methods. This has made the finite element method particularly amenable to the analysis of the complex advanced composite structure. While the task in finite element analysis has been reduced to a description of the geometry, appropriate selection of element locations, and coding the appropriate data for final solution of displacements and internal strains in the structure to a problem of bookkeeping, the data management problem, nevertheless, is quite difficult.

The need to obtain relatively precise information on the distribution of internal forces and strains on the structure even earlier in the preliminary design process has caused considerable emphasis to be placed upon development of methods to automate the development of the finite-element representation of a complex structure. One of the most highly developed areas is the utilization of the digital computer for numerical description of lines and subsequent division of the structure into a finite element simulation for wings and empennage-type structure (Reference 17). This coding of the appropriate software for immediate evaluation of the structures was deemed necessary because of the first-order importance of the participation of the structural stiffness in such failure modes as static aeroelastic divergence and flutter stability of the aircraft. Specific procedures have been developed which allow the development of a complete simulation from a first-order description of the structure such as basic airplane geometry and desired surface network to a grid for the finite-element simulation. The need for this type of analysis can be seen when one realizes that for a single planform and within a single weight it can be shown that varying material orientation in the composite structure can cause a fluctuation in flutter speed of approximately 40 percent for equal weight structures. All of the structures are not acceptable from the standpoint of strength, and this latitude in an interaction between strength and flutter speed for composite lifting surfaces forms a formidable design problem which is being investigated. Generally, if careful simulation techniques are used and care is taken to ensure that the fabrication processes are represented correctly, an accuracy in the neighborhood of 5 percent on such gross responses as vibration and normal modes can be achieved for large-scale complex structures. It is also noted that the displacement related phenomenon such as stability and vibration response are found with first-order accuracy. Distribution of the stresses within the structure are not as accurately represented, and the failure mechanics knowledge is not sufficient to precisely detail the strength of the structure. A distribution of strength in composite structures as tested in the United States has shown the accuracy of the design process is, however, equivalent to the accuracy which can be obtained in the design of metallic structure. The availability of the methods for the analysis of complex structures has been a key element in the rapid advancement of composite design technology.

REFERENCES

1) M. E. Waddoups, "Characterization and Design of Composite Structures," Composite Materials Workshop, Technomic Publishing Co., 1968, p. 309.

2) M. E. Waddoups and P. H. Petit, "A Method of Predicting the Nonlinear Behavior of Laminated Composites," Journal of Composite Materials, Volume 3, No. 1, January 1969.

3) J. C. Halpin, J. R. Kopf and W. Goldberg, "Time Dependent Static Strength and Reliability for Composites," Journal of Composite Materials, Volume 4, October 1970.

4) M. E. Waddoups, J. R. Eisenmann and B. E. Kaminski, "Macroscopic Fracture Mechanics of Advanced Composite Materials," Journal of Composite Materials, Volume 5, October 1971.

5) B. E. Kaminski, "Effects of Specimen Geometry on the Strength of Composite Materials," ASTM Symposium on Analysis of Test Methods for High Modulus Fiber and Composites, April 12, 1972.

6) D. Y. Knoishi and T. T. Matoi, "Design Guidelines for Advanced Composites Joints," Fifth St. Louis Symposium on Advanced Composites, April 6-7, 1971.

7) M. E. Waddoups and R. V. Wolff, "Assessment of Reliability Analysis for Adhesive Joints," ASTM Symposium on Analysis of Test Methods for High Modulus Fibers and Composites, April 13, 1972.

8) M. S. Howeth and B. E. Chitwood, Patent Number 3,574,040, "Apparatus for making Laminated Structural Shapes by the Controlled Detrusive Placement and Polymerization of Tectonic Filamentous Tapes," Fort Worth Operation, Convair Aerospace Division of General Dynamics Corporation.

9) S. W. Tsai and E. M. Wu, "A General Theory of Strength for Anisotropic Materials," Journal of Composite Materials, Volume 5, January 1971.

10) J. E. Ashton and M. E. Waddoups, "Analysis of Anisotropic Plates," Journal of Composite Materials, Volume 3, January 1969.

11) J. E. Ashton, "Analysis of Anisotropic Plates - II," Journal of Composite Materials, Volume 3, July 1969.

12) L. M. Lackman and R. M. Ault, "Minimum-Weight Analysis of Filamentary Composite Wide Columns," Journal of Aircraft, Volume 5, No. 2, April 1968.

13) S. Cherry and B. P. C. Ho, "Stability of Heterogeneous Aeolotropic Cylindrical Shells under Combined Loading," AIAA Journal, Vol. 1, No. 4, April 1963.

14) M. E. Waddoups and J. R. Blacklock, "The Application of Finite Element Stiffness Matrix Analysis for Composite Structure," Proceeding of the International Conference on the Mechanics of Composite Materials, Pergamon Press, 1970.

15) W. Lansing, W. Dwyer, R. Emerton and E. Ronall, "Application of Fully Stressed Design Procedures to Wing Empennage Structures," AIAA/ASME 11th Structures, Structural Dynamics and Materials Conferences, April, 1970.

16) E. J. McQuillen and S. L. Huang, "Graphite Epoxy Wing for BQM-34E Supersonic Aerial Target," Journal of Aircraft, Volume 8, No. 6, June 1971.

17) A. D. Mayfield, "Structural Design Optimization of Wing-Type Structure," AIAA/ASME 11th Structures, Structural Dynamics and Materials Conference, April 1970.

18) M. E. Waddoups, L. A. McCullers and J. D. Naberhaus, "The Relationship of High Speed Digital Computation to the Design of Advanced Composite Lifting Surfaces," AIAA/ASME 12th Structures, Structural Dynamics and Materials Conference, April 1971.

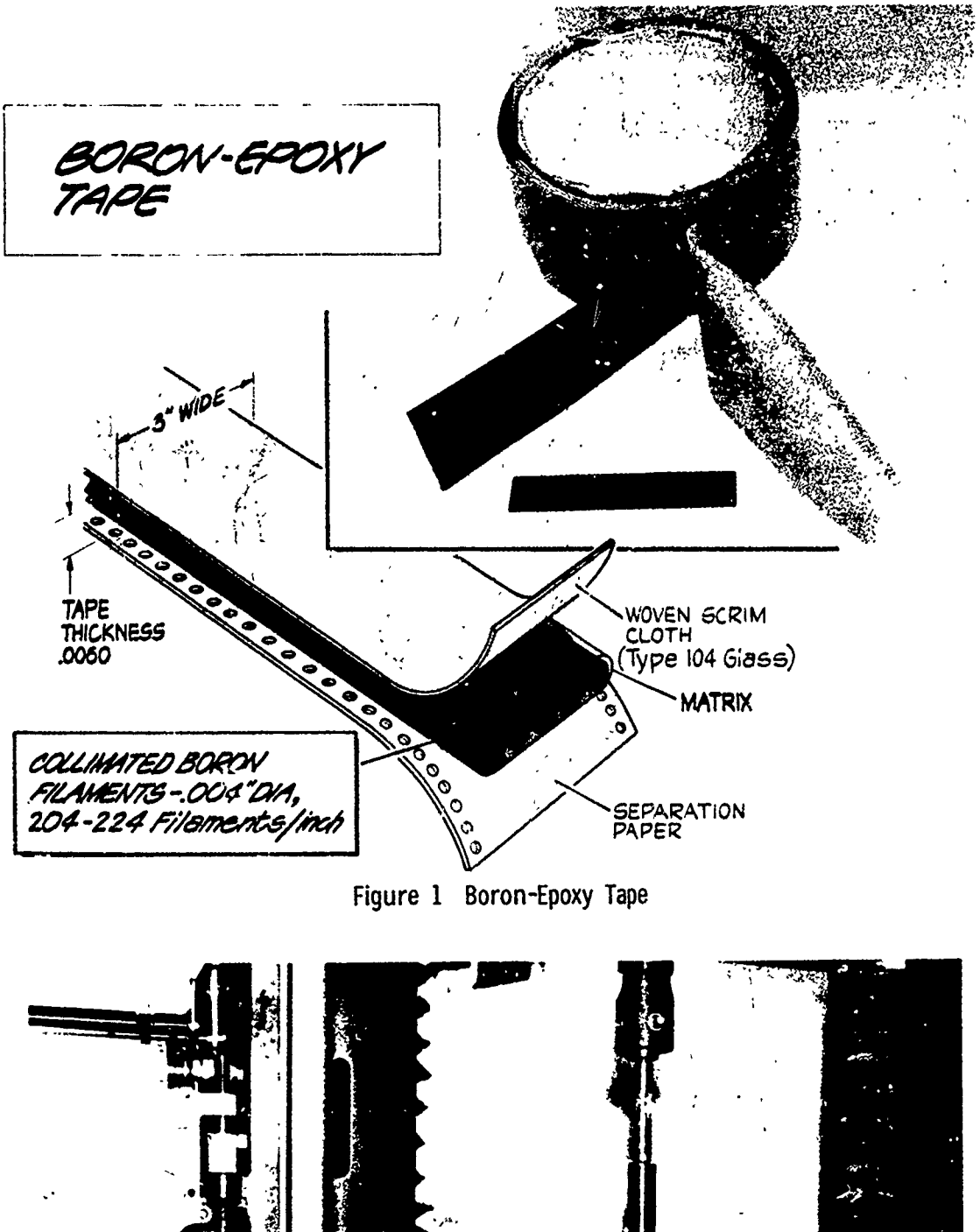

Figure 1 Boron-Epoxy Tape

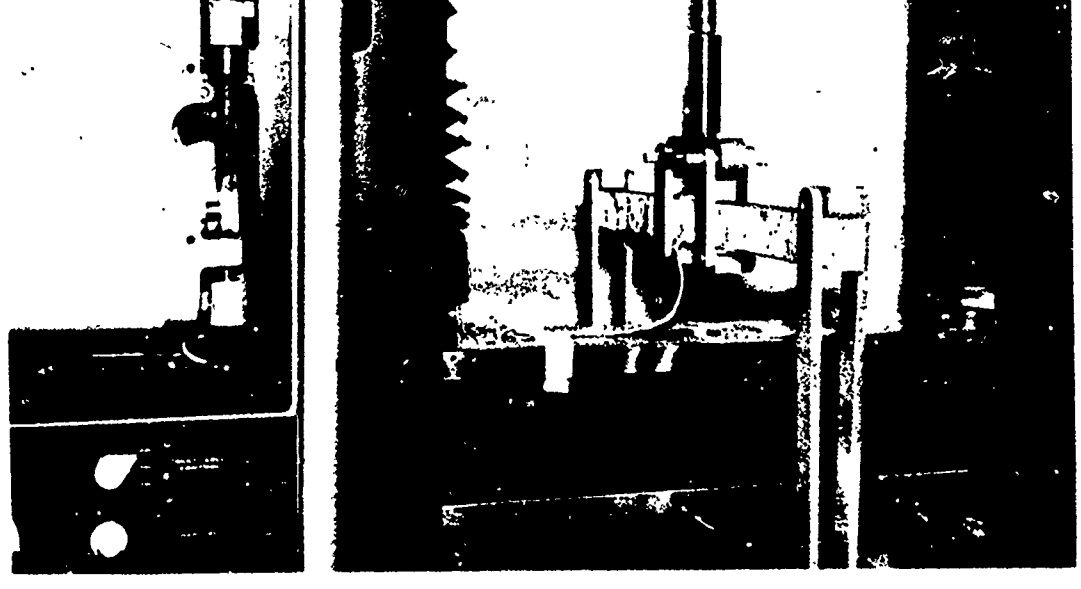

Figure 2 Tension - Sandwich Beam

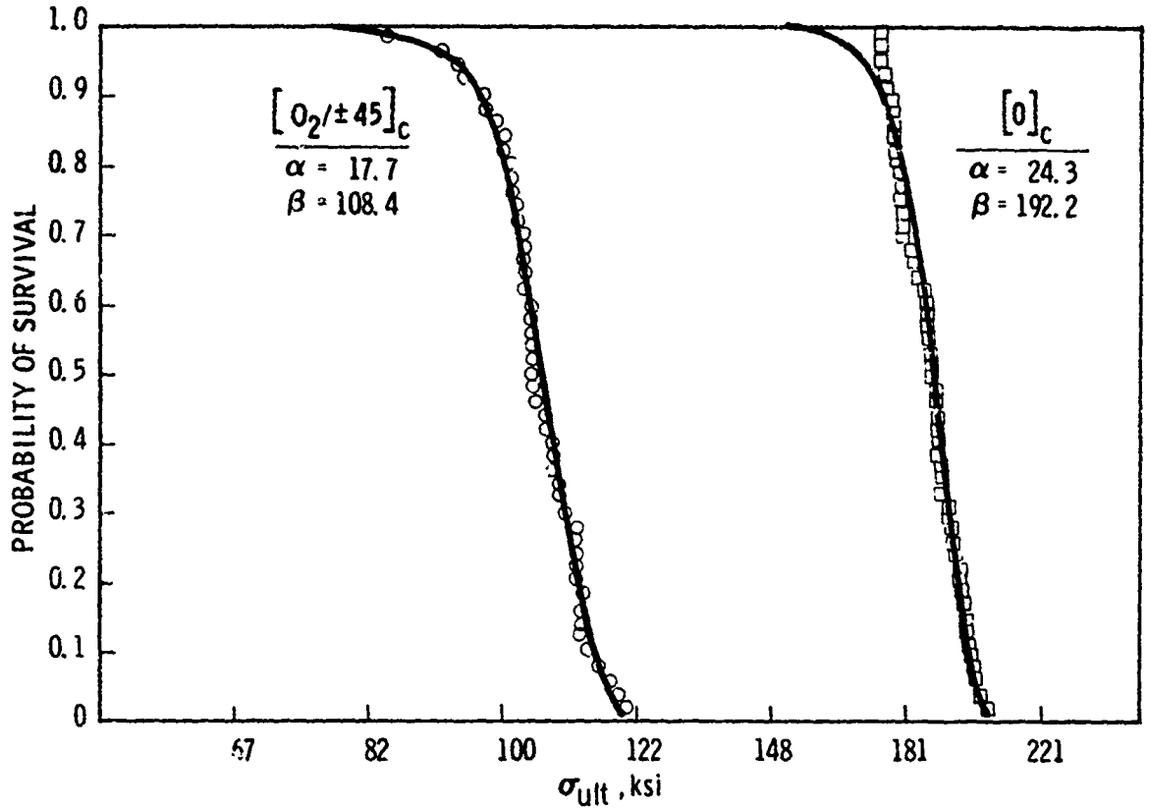

Figure 3 Boron-Epoxy Lamina vs. Laminate

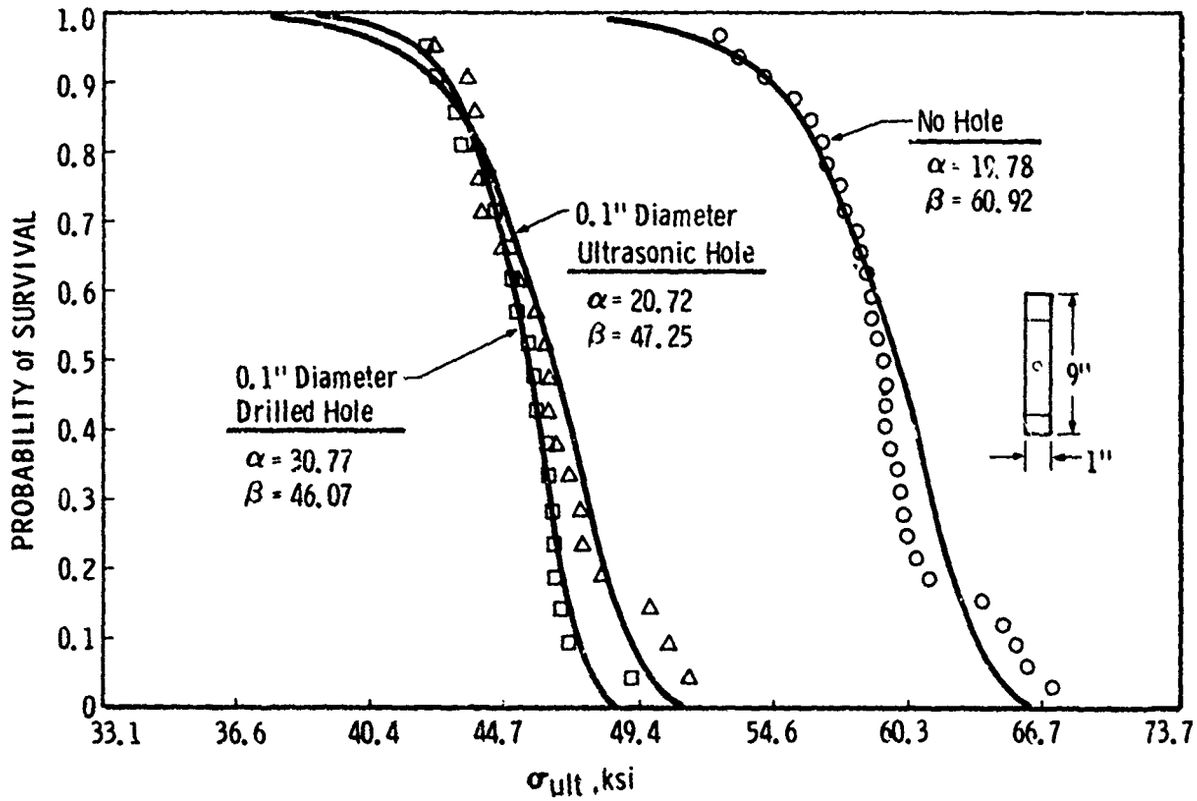

Figure 4 Survival Curves for [0/±45/90]S Boron-Epoxy

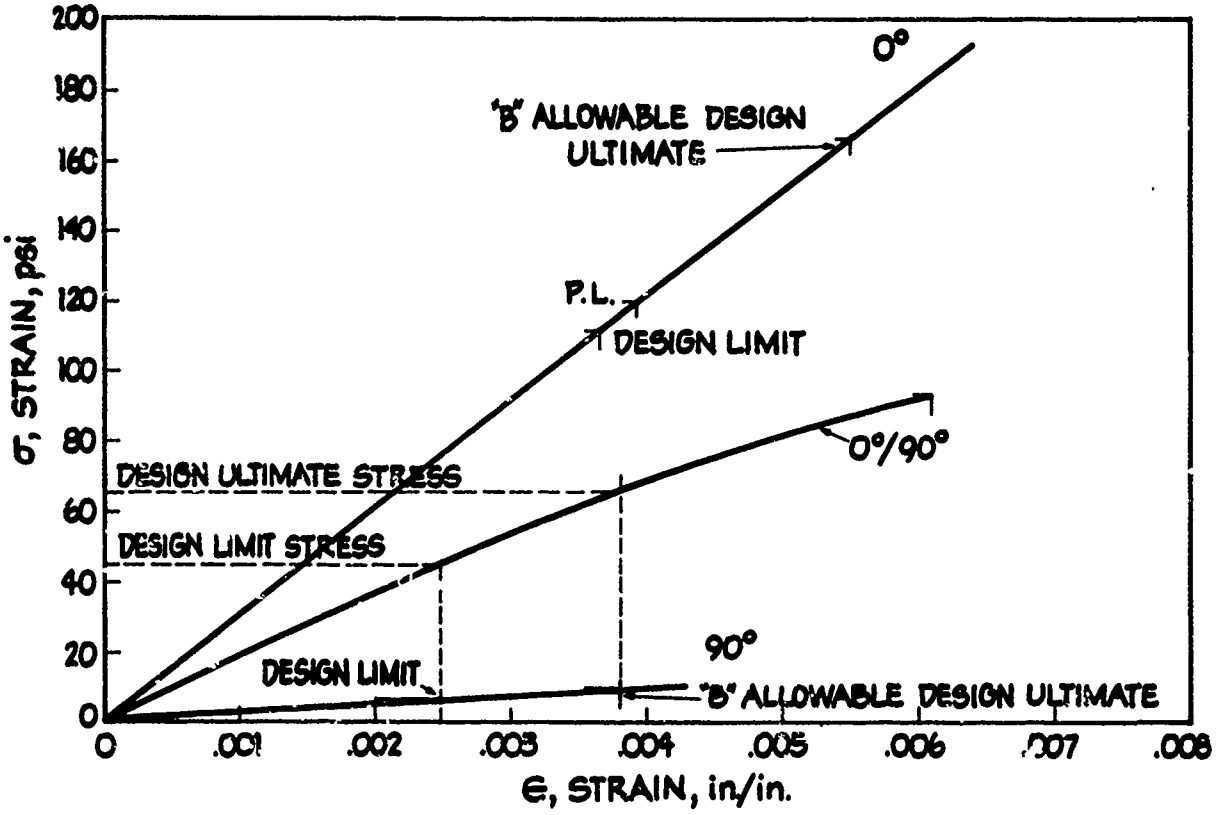

Figure 5 Criteria Example 0/90-Degree Laminate

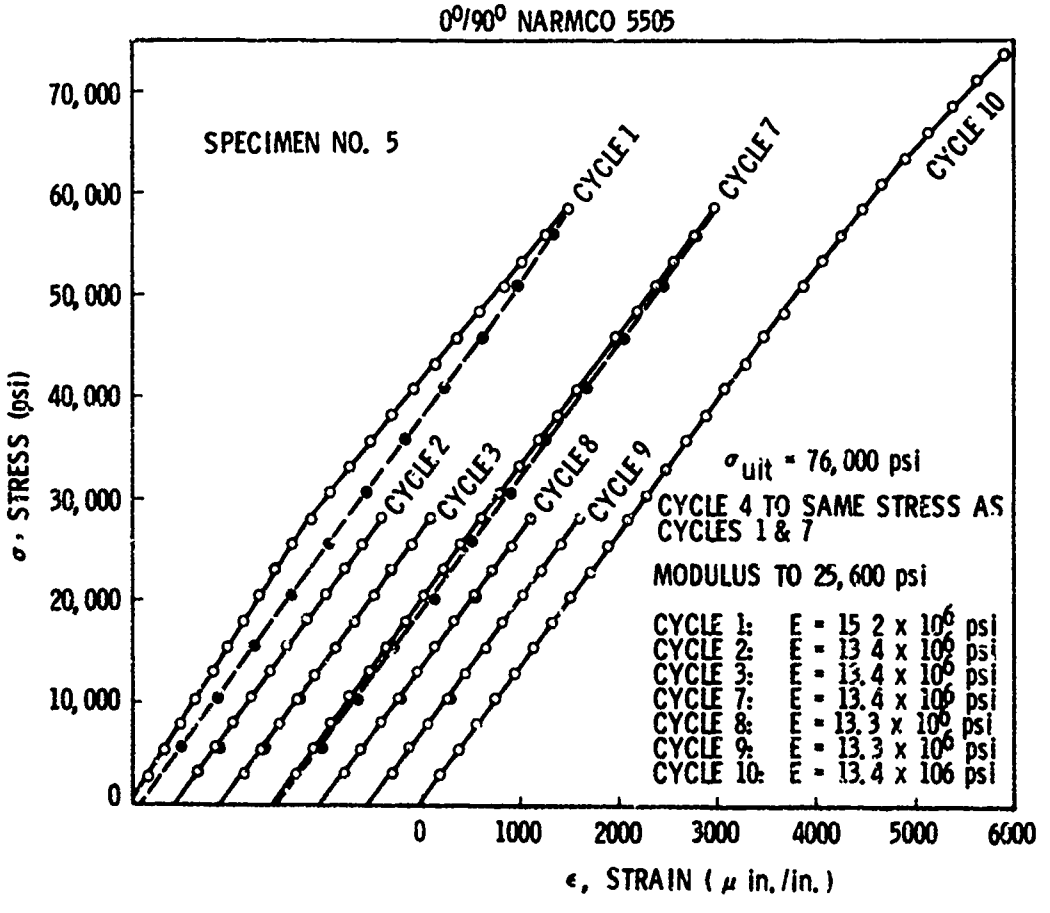

Figure 6 Low Cycle Fatigue

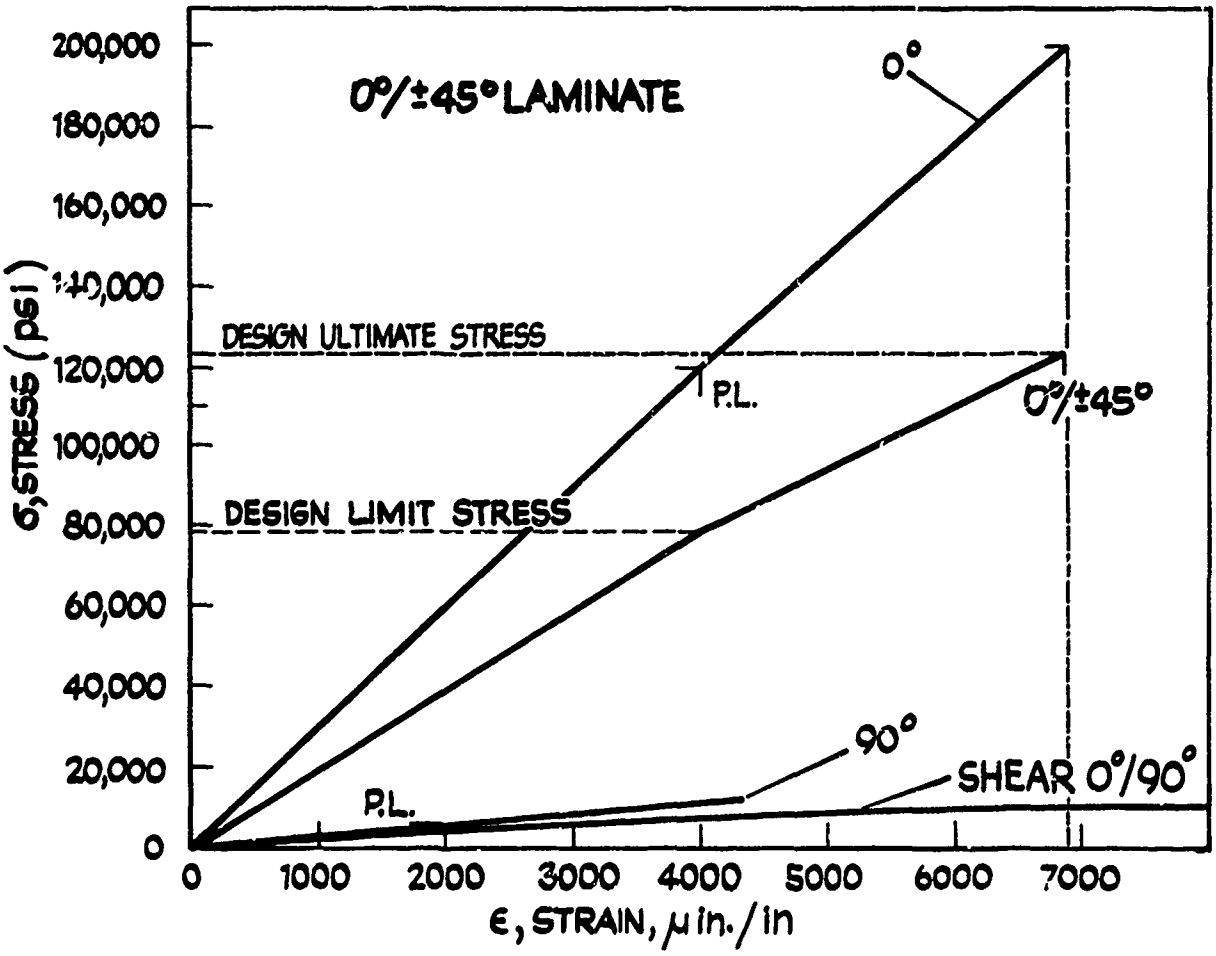

Figure 7 Criteria Example

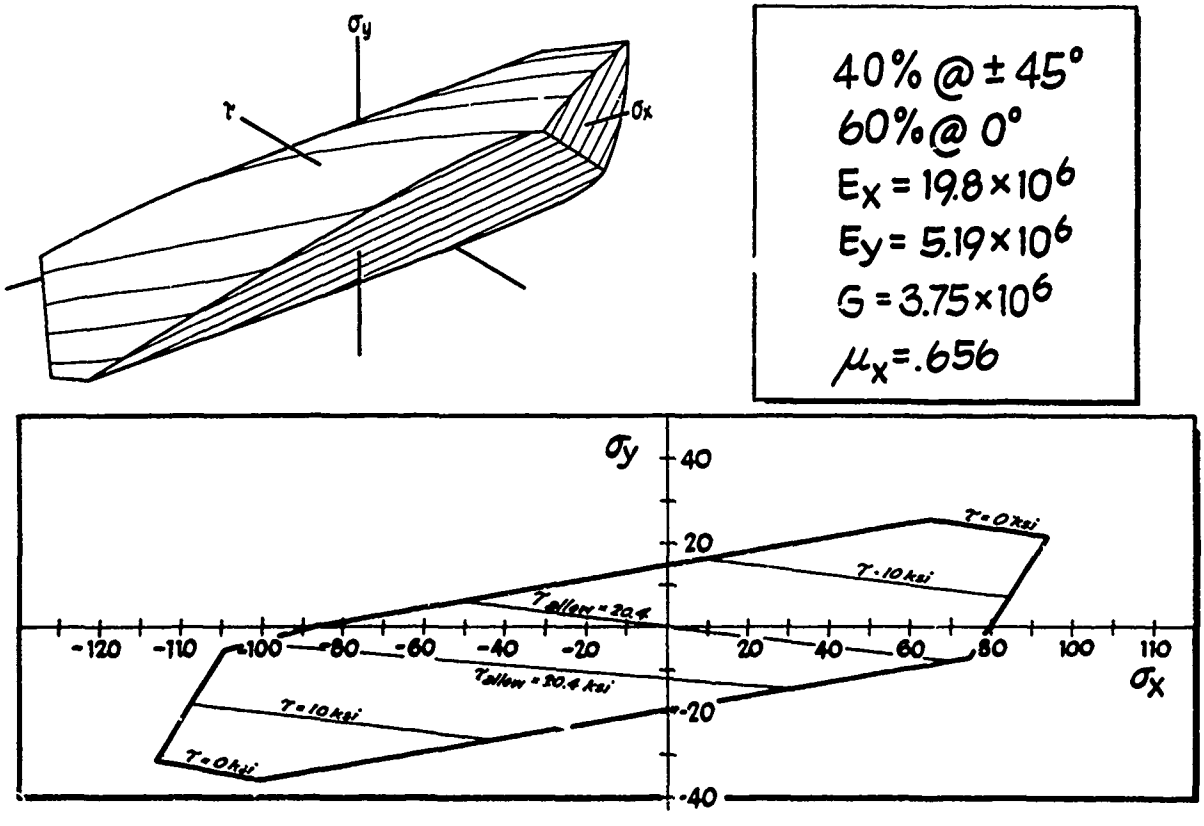

Figure 8 Limit-Interaction Curve

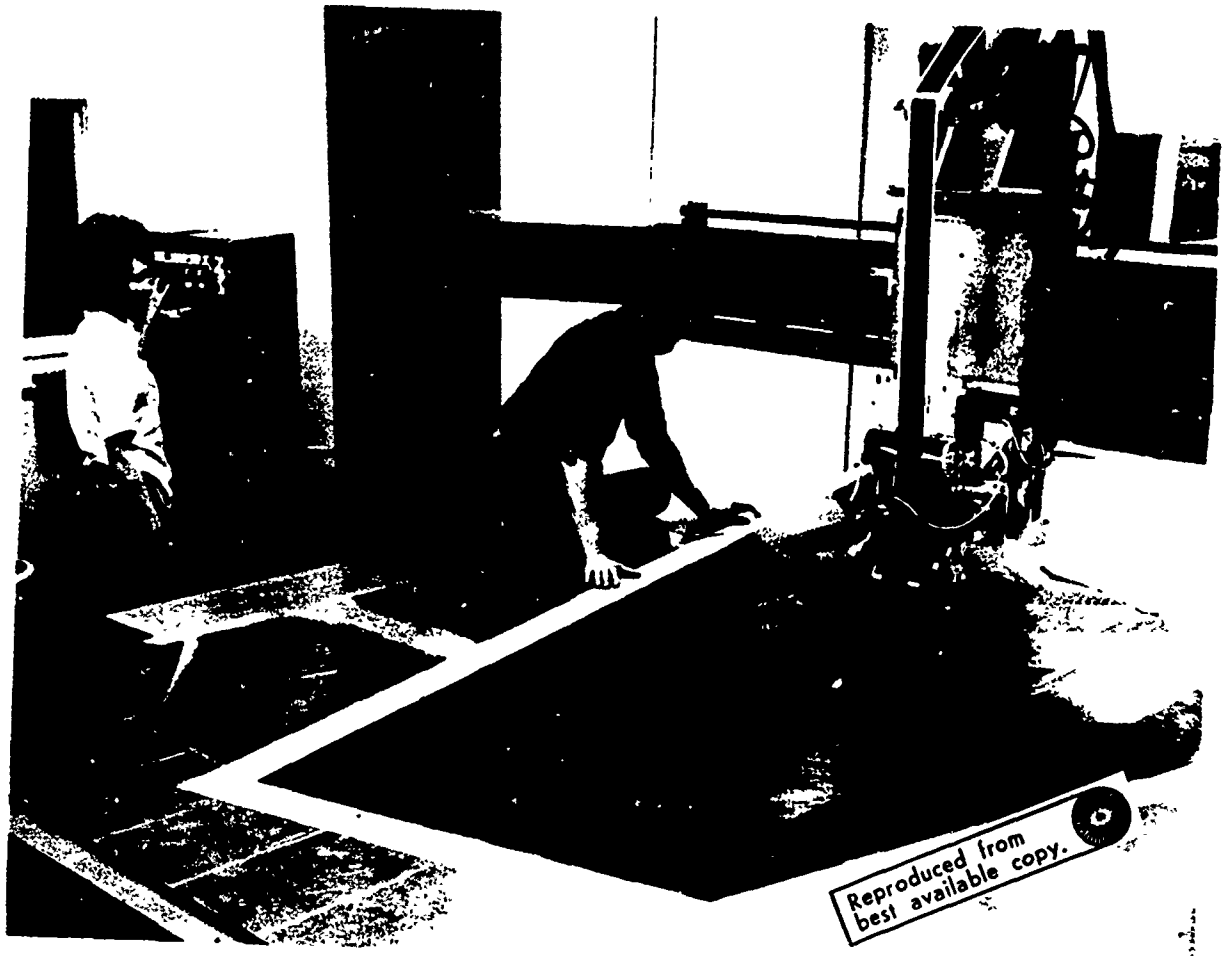

Figure 9 Tape Laying Machine - Ply on Ply

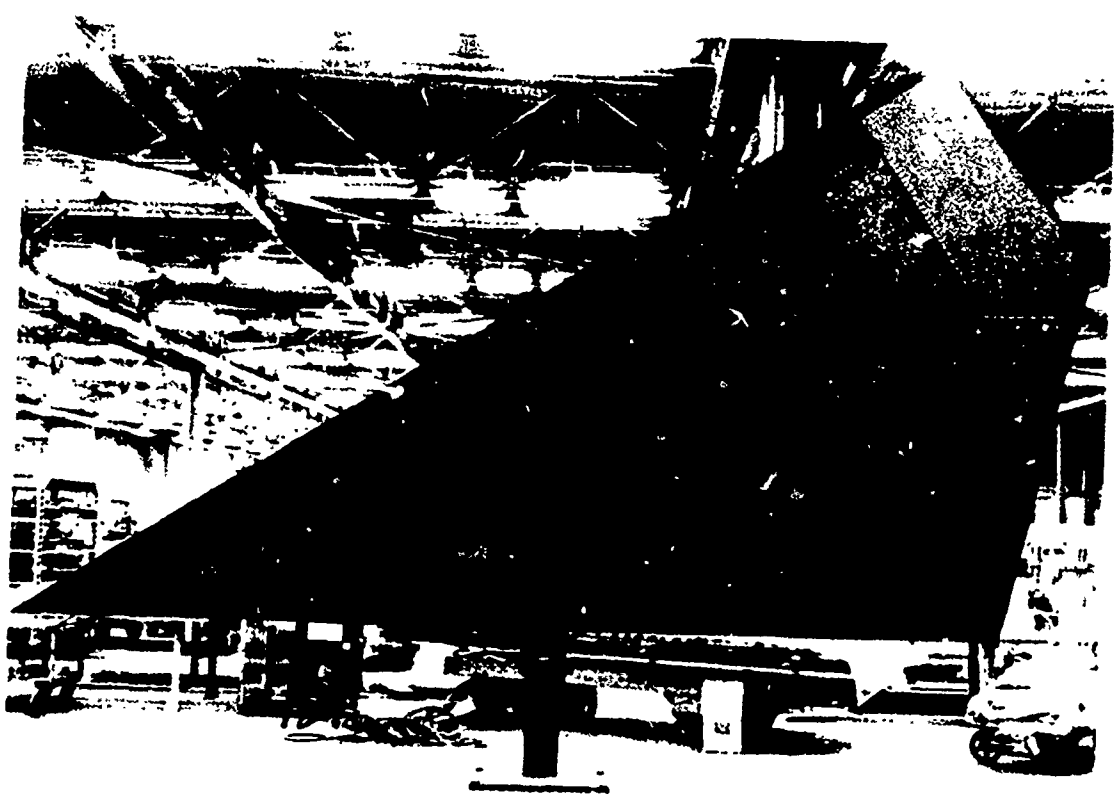

Figure 10 Complete Tail Assembly

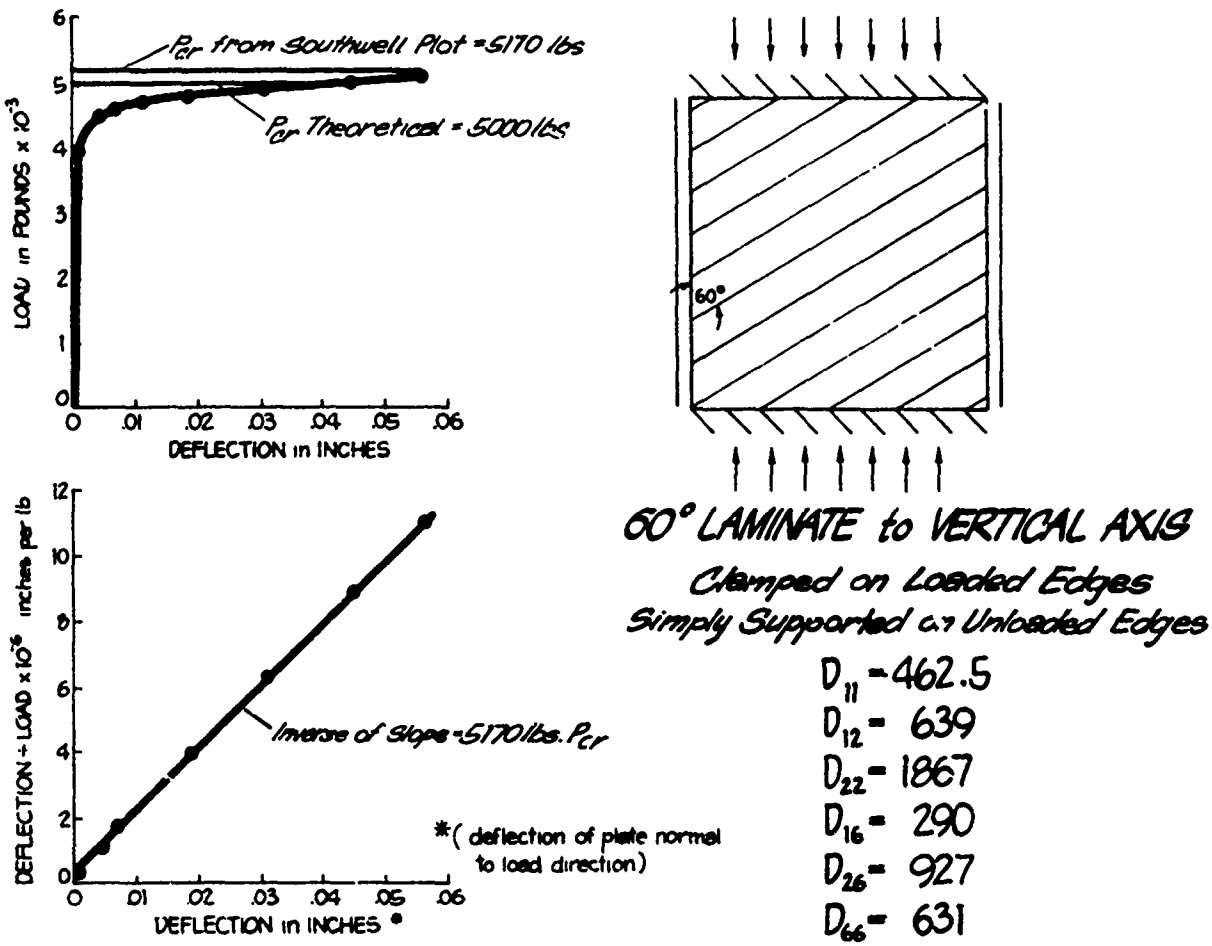

Figure 11 Anisotropic Plate Buckling Test Results

EXPERIMENTAL METHODS FOR COMPOSITE MATERIALS

by

B.E. Read and G.D. Dean
Division of Materials Applications, National Physical Laboratory,
Teddington, Middlesex, TW11 OLW, England.

SUMMARY

A wide range of techniques is discussed for measuring the elastic, viscoelastic, ultimate strength, thermal and electrical properties of fibre reinforced composites. Main emphasis is given to the determination of the basic properties of unidirectionally reinforced composites and, for this purpose, the mechanical test samples considered are mainly in the form of rectangular bars. However, some consideration is given to methods involving honeycomb sandwich structures, circular rods, plates, rings and cylinders. For determining the static Youngs moduli and Poissons ratios, tensile and compressive tests are considered in addition to flexure methods (cantilever, 3-point and 4-point) and also the honeycomb sandwich technique. Methods for measuring the shear moduli include both torsion and off-axis tensile tests. Comparative elastic data obtained by these methods are collected and discussed for unidirectional silica fibre-epoxy, carbon fibre-epoxy, boron fibre-epoxy and boron fibre-aluminium composites. Creep and stress relaxation methods are outlined for studying time-dependent viscoelastic behaviour and results illustrated for nylon-rubber and boron-epoxy composites. Several dynamic tests are described including the low frequency forced non-resonance, torsion pendulum, audiofrequency resonance and ultrasonic pulse techniques. Dynamic elastic constants and damping factors are illustrated for carbon fibre-epoxy composites as a function of frequency and fibre volume fraction. Methods are assessed for determining the tensile, compressive, flexural and shear strength, fracture energy and fatigue life, and selected data are illustrated for some carbon fibre, boron fibre and glass fibre composites. Techniques for measuring the thermal expansion coefficient, thermal conductivity, heat capacity, electrical resistivity, dielectric constant and loss are outlined, and some results presented for unidirectional carbon fibre composites. Brief mention is made of magnetoresistive and thermomagnetic data obtained on a composite formed by the unidirectional solidification of a eutectic InSb-NiSb mixture.

1. INTRODUCTION

Owing to the structural complexities of fibre reinforced composites, an adequate characterization of their properties frequently requires the combined application of several experimental techniques. The purpose of this paper is to survey the range of available methods for determining the elastic, viscoelastic, ultimate strength, thermal and electrical properties and to present and discuss comparative data for a number of composites. Major emphasis will be given to the determination of the basic properties of unidirectionally reinforced composites and, consequently, many of the selected methods apply to specimens in the form of narrow rectangular bars. However several of the tests are applicable, either directly or with some adaptation, to plates, and some consideration is also given to methods based specifically on circular rods, honeycomb sandwich structures, plates, rings or cylinders.

The most obvious feature of unidirectionally reinforced composites is the extreme directional dependence, or anisotropy, of their mechanical properties, and this fact can have an important bearing on the selection of experimental methods and on the interpretation of data. In the case of composites containing polymeric matrix materials, the viscoelastic behaviour must also be considered. This behaviour manifests itself, for example, in a dependence of the apparent elastic constants on the rate of loading in a stress-strain measurement or on time for specimens subjected to a constant load or deformation. Certain of the strength, thermal and electrical properties will also be directionally dependent and may depend on the experimental time scale. For determining the elastic, viscoelastic and strength characteristics, the same basic method can often be employed. However, since this is not generally the case, and since a given method usually requires modification depending on the property under investigation, the determination of elastic, viscoelastic and strength properties will be considered separately in Sections 2, 3 and 4 and a brief outline of thermal and electrical measurements given in Section 5. This subdivision is also convenient for purposes of data comparison.

2. MEASUREMENT OF STATIC ELASTIC PROPERTIES

Most studies of the elastic properties of fibrous composites have involved pseudo static tests in which the stress-strain measurements are made at low rates of loading or after sufficient periods of elapsed time. Besides the possibility of rate dependencies, the stress-strain curves may also be non-linear. In specifying the elastic constants of a material it is therefore necessary to verify, or assume, that the stress becomes linearly dependent on strain when the latter is small. For quasi-homogeneous anisotropic materials, the elastic properties may then be defined in terms of the generalized Hookes law (1). Using contracted subscripts i and j each having values 1, 2, 3, 4, 5 or 6, equivalent in tensor notation to 11, 22, 33, 23, 13 and 12 respectively, Hookes law may be written as,

$$\sigma_i = c_{ij}\,\epsilon_j \qquad \ldots (1)$$

$$\text{or} \quad \epsilon_i = s_{ij}\,\sigma_j \qquad \ldots (2)$$

where the σ_i and ϵ_i are stress and strain components, respectively, being normal components for $i = 1, 2$ or 3 and shear components for $i = 4, 5$ or 6. The c_{ij} and s_{ij} are modulus and compliance components, respectively, related by the matrix inversion $[c_{ij}] = [s_{ij}]^{-1}$, and we note that the repeated subscript j in equations (1) and (2) indicates summation from 1 to 6.

Under conditions of static equilibrium, strain energy considerations ensure that $c_{ij} = c_{ji}$ and $s_{ij} = s_{ji}$, and sample symmetry may cause a further reduction in the number of independent elastic constants. For a unidirectionally reinforced composite it is customary to take direction 1 parallel to the fibre direction and directions 2 and 3 perpendicular to the fibres and in the width and thickness directions, respectively, where appropriate. If these directions correspond also to the orthogonal reference axes parallel to the sample faces, and the fibres are randomly packed in the transverse plane, then the specimen becomes hexagonally symmetric and is characterized by five independent moduli or compliances (1),

$$\begin{aligned} c_{11} &\qquad\qquad s_{11} = 1/E_1 \\ c_{22} &= c_{33} \qquad\qquad s_{22} = s_{33} = 1/E_2 \\ c_{12} &= c_{13} \qquad\qquad s_{12} = s_{13} = -\nu_{12}/E_1 \\ c_{23} &\qquad\qquad s_{23} = -\nu_{23}/E_2 \\ c_{44} &= \tfrac{1}{2}(c_{22} - c_{23}) = G_{23} \qquad\qquad s_{44} = 2(s_{22} - s_{23}) = \frac{2}{E_2}(1 + \nu_{23}) = 1/G_{23} \\ c_{55} &= c_{66} = G_{12} \qquad\qquad s_{55} = s_{66} = 1/G_{12} \end{aligned} \qquad \ldots (3)$$

and the remaining c_{ij}'s and s_{ij}'s are zero. Here we have adopted the usual terminology, according to which E_1 and E_2 are the respective Youngs moduli measured in directions parallel and perpendicular to the fibres, G_{12} and G_{23} are shear moduli for shear forces in directions 2 and 3 and on planes perpendicular to 1 and 2 respectively, and $\nu_{12}(= -\varepsilon_2/\varepsilon_1)$ and $\nu_{23}(= -\varepsilon_3/\varepsilon_2)$ are Poissons ratios obtained from appropriate strain measurements during successive loading in the 1 and 2 directions. It follows that the five independent compliances, and hence moduli, can be determined from a combination of two tensile (or compressive) and one shear (G_{12}) experiment. In practice the measurement of G_{23} may serve as an alternative to the determination of ν_{23}.

For very thin specimens, such as composite plates, subjected to stresses in the 12 plane, the plane stress condition $\sigma_3 = \sigma_4 = \sigma_5 = 0$ is frequently assumed. When referred to the principal directions 1 and 2, the specimen is termed orthotropic and is characterized by four independent compliances s_{11}, s_{12}, s_{22} and s_{66} where the s_{ij}'s are given by Eq. (3). Alternatively, four reduced stiffness components Q_{11}, Q_{12}, Q_{22} and Q_{66} may be invoked where $Q_{ij} = c_{ij} - c_{i3}c_{j3}/c_{33}$ for i, j = 1, 2, and $Q_{66} = c_{66}$.

In cases where the fibres are oriented at some angle other than 0° or 90° to the sample faces, then the sample symmetry is reduced and the number of non-zero constants increases. With reference to the sample axes, we denote these transformed constants by c'_{ij}, s'_{ij} or Q'_{ij}, and note that the evaluation of the material constants c_{ij}, s_{ij} and Q_{ij} from the measured values of c'_{ij}, s'_{ij} and Q'_{ij}, respectively, can be effected by standard transformation procedures (1, 2). The basic elastic stiffnesses Q_{ij} can also be used to predict the elastic properties of certain multidirectional laminates formed from consecutive layers of differently oriented orthotropic sheets (2). As shown in Section 2b, the results of laminated plate theory can be used to estimate G_{12} from tensile tests on bidirectional (cross-ply) specimens.

2a. Measurement of Youngs Moduli and Poissons Ratios

Axial Tensile and Compressive Tests

According to Eq. (3), the compliances s_{11}, s_{22}, s_{12}, s_{23} and s_{44} can be determined from measurements of the Youngs moduli E_1 and E_2 and the Poissons ratios ν_{12} and ν_{23}. These quantities are conveniently determined by uniaxial loading as in Fig. 1, using a tensile testing machine equipped with calibrated load cell, and employing either strain gauges or extensometers to measure both longitudinal and lateral sample deformations. The specimen shape and dimensions are not critical for tensile modulus determinations, providing that a reasonably long gauge length of uniform cross section is available. The use of end tabs on the specimen is desirable for purposes of gripping, and self-aligning grips serve to avoid the application of bending moments. Reference 3 illustrates an experimental set-up which utilizes extensometers for determining the Youngs moduli and Poissons ratios of AGARD silica-epoxy and silica-phenolic composites. For an applied load W parallel to the fibre direction,

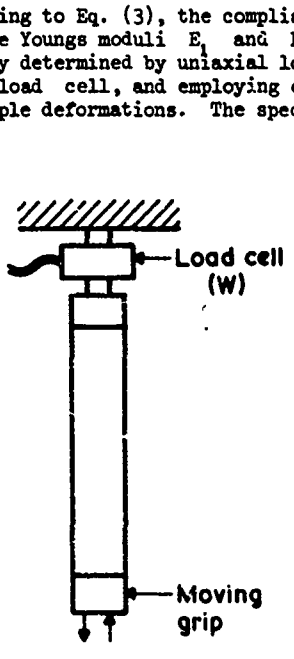

FIG.1 TENSION OR COMPRESSION

$$E_1 = \left(\frac{W\ L}{\Delta L\ ab}\right)_1 \qquad \ldots (4)$$

and $$\nu_{12} = \left(\frac{\Delta a\ L}{\Delta L\ a}\right)_1 = \left(\frac{\Delta b\ L}{\Delta L\ b}\right)_1 \qquad \ldots (5)$$

whereas for loading perpendicular to the fibre direction,

$$E_2 = \left(\frac{W\ L}{\Delta L\ ab}\right)_2 \qquad \ldots (6)$$

and $$\nu_{23} = \left(\frac{\Delta b\ L}{\Delta L\ b}\right)_2 \qquad \ldots (7)$$

In these equations a, b and L are the initial specimen widths, thicknesses and gauge lengths, respectively, and ΔL, Δa and Δb are the measured changes in L, a and b, respectively. The subscripts 1 and 2 are included to indicate the loading direction, and for loading in direction 2 the fibres are taken to be parallel to the width dimension a.

Equations (4) to (7) can also be used to determine the Youngs moduli and Poissons ratios for specimens subjected to compressive loading. For compression measurements, shorter specimens of relatively large cross-sectional areas are desirable to avoid buckling. The technique is particularly useful for determining

the transverse properties E_2 and ν_{23} since, in the transverse direction, samples are relatively weak in tension. If both modulus and ultimate strength values are required (i.e. the complete stress-strain curve) then the sample dimensions and alignment techniques become more critical in order to avoid failure in the clamping regions. References 4 to 7 give a number of specimen dimensions which have been used, and Park (8) has recently reported clamping methods and a "dog bone" shaped specimen which yield higher values for both modulus and strength.

Flexure Methods

The moduli E_1 and E_2 of unidirectional composites can also be determined from various flexure tests on beams having fibres oriented along the length and width directions, respectively. The cantilever, 3-point and 4-point bending methods are most familiar. In the cantilever method, the sample is clamped at one end, as shown in Fig. 2, and the displacement at the opposite end is measured as a function of the applied load W. An inherent problem associated with this technique arises from the occurrence of both longitudinal and shear deformations, and this problem is particularly severe for fibrous composites owing to the large E/G ratios typically encountered. For isotropic beams, Timoshenko and Goodier (9) have discussed the distribution of normal and shear stresses. On each cross section, normal (or bending) stresses are distributed across the thickness, increasing from zero at the mid-plane to maximum tensile and compressive values on the upper and lower surfaces respectively. Along the length of the beam the normal stresses increase from zero at the loaded end to a maximum at the clamped end. The shear stresses are uniform along the beam length but are distributed across both the depth and width. For narrow beams the shear stresses are a maximum on the neutral plane and decrease to zero on the upper and lower surfaces. For sufficiently long beams the displacement δ at the loaded end becomes,

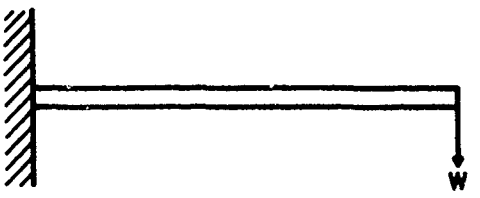

FIG.2 CANTILEVER BENDING

$$\delta = \frac{WL^3}{3EI} \qquad \ldots (8)$$

where $I (= ab^3/12)$ is the moment of inertia of the cross section about the transverse axis. Assuming that Eq. (8) may be applied to anisotropic beams, then measurements of δ as a function of W can thus yield either E_1 or E_2 depending on whether the fibres are oriented along the length or width of the beam. Corrections for shear deformation may either be obtained theoretically (9) or investigated experimentally by varying the length to thickness ratio of the beam. The experimental method also serves to eliminate the effects of localized stress concentration in the clamping region. Rothman and Molter (10) have employed the static cantilever method, analysed according to Eq. (8), to determine E_1 for unidirectional carbon fibre-epoxy specimens. The values obtained were about 6% lower than values derived from the 4-point bending method (Table 2), possibly due to the neglect of shear deformations.

The effects of shear deformation also influence the determination of E_1 and E_2 using the 3-point bending technique. In this method the beam is supported near to each end, and is loaded centrally from above (Fig. 3). Each side of the loading point, the distribution of normal and shear stresses is similar to that existing in the cantilever beam and for long beams the vertical displacement δ under the applied load W is given by,

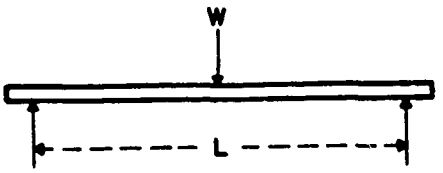

FIG.3 3-POINT BENDING

$$\delta = \frac{WL^3}{48EI} \qquad \ldots (9)$$

This equation neglects the contribution from shear deformation and also the effects due to localized stress concentrations and deformation around the loading and support points. Both theoretical (9, 11, 12) and experimental (13) correction procedures have been proposed to account for these effects, and Ogorkiewicz and Mucci (14) have made a systematic investigation of various types of support using a glass fibre-epoxy specimen. In the latter study shear deformations were estimated to be negligible on account of the large span to thickness ratio (=63), and small diameter rollers located in semicircular grooves were found to provide the most suitable method of support.

Problems associated with shear deformations are eliminated in the 4-point bending method in which a pure bending moment is produced over the central gauge length (Fig. 4). With this technique the Youngs modulus can be determined from the equations,

$$E = \frac{WcL^2}{16I\delta} = \frac{Wcb}{4\varepsilon I} \qquad \ldots (10)$$

where W is the total applied load, L the central gauge length, c the distance between inner and outer pivots on each side, δ the vertical deflection of the beam mid-point relative to the inner pivots and ε the longitudinal surface strain in the central region. In practice either δ or ε may be determined using, for example, a displacement transducer or strain gauge respectively. As in the case of the three-point bending method, this technique is subject to errors arising from local stress concentrations, frictional effects and indentations at the supports. The use of roller pivots would seem to offer the best chance of minimizing these problems (14).

The stress distributions and equations considered above, relevant to the analysis of the different bending tests, are based on considerations for isotropic materials. A recent analysis at the NPL by Johnson (15) of the bending and twisting of anisotropic beams, has established the validity of Eq. (10) for sufficiently long beams (L>20b) having 0° and 90° fibre orientations and subject to a pure bending moment (as in a 4-point test). Equations were also derived appropriate to the 4-point bending of "off-axis" unidirectional composites. Such measurements, in combination with the bending and torsion of 0° and 90° oriented specimens, can yield all five independent elastic constants.

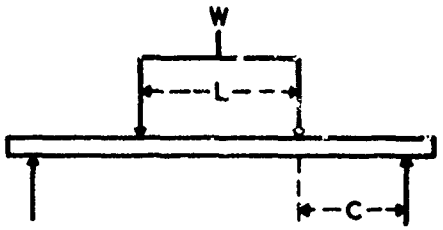

FIG.4 4-POINT BENDING

Honeycomb Sandwich Tests

Many of the experimental difficulties encountered with the tensile, compressive and flexure tests can be eliminated by the use of a honeycomb sandwich structure (4, 5), in which a thin composite strip or plate forms one of the surface layers (Fig. 5). Although more difficult and costly to construct, such structures enable a more uniform application of load

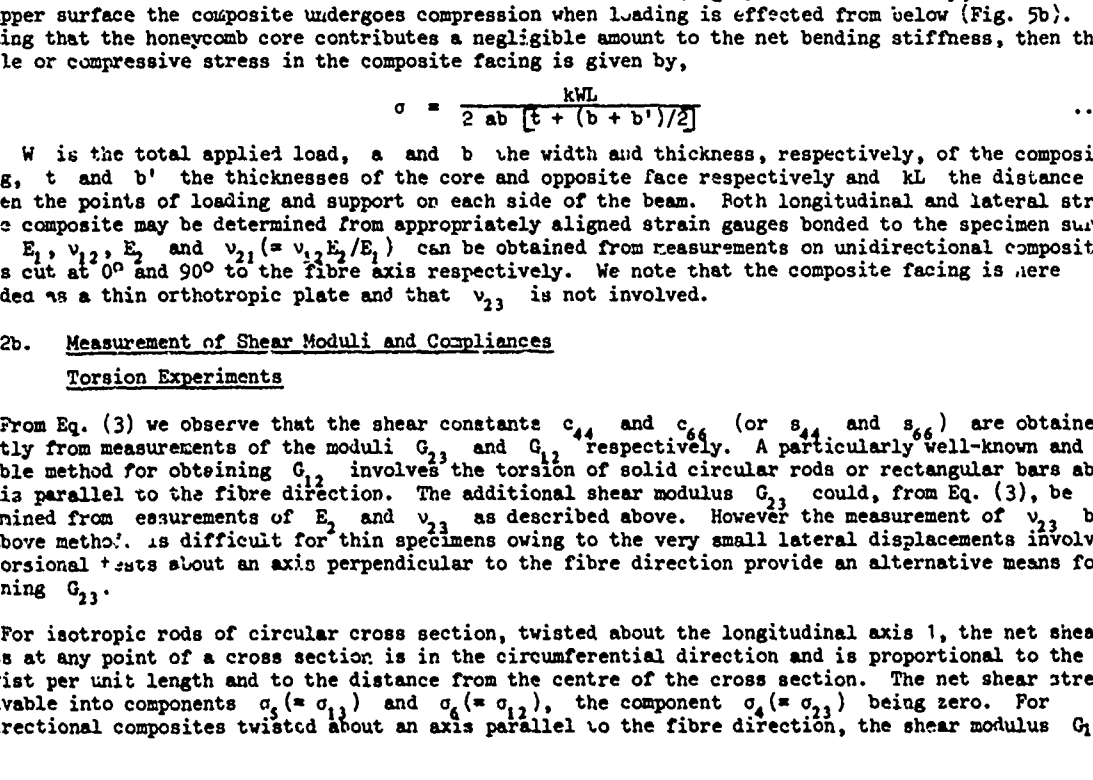

FIG.5 HONEYCOMB SANDWICH

to the composite, thus eliminating clamping and support problems, and also provide support against buckling under compression. If the composite specimen is bonded to the lower surface of the honeycomb, it is subjected to tension when the sandwich beam is loaded from above (Fig. 5a). Alternatively, if bonded to the upper surface the composite undergoes compression when loading is effected from below (Fig. 5b). Assuming that the honeycomb core contributes a negligible amount to the net bending stiffness, then the tensile or compressive stress in the composite facing is given by,

$$\sigma = \frac{kWL}{2\,ab\,[t + (b + b')/2]} \qquad \ldots (11)$$

where W is the total applied load, a and b the width and thickness, respectively, of the composite facing, t and b' the thicknesses of the core and opposite face respectively and kL the distance between the points of loading and support on each side of the beam. Both longitudinal and lateral strains in the composite may be determined from appropriately aligned strain gauges bonded to the specimen surface. Hence E_1, ν_{12}, E_2 and $\nu_{21}(=\nu_{12}E_2/E_1)$ can be obtained from measurements on unidirectional composite strips cut at 0° and 90° to the fibre axis respectively. We note that the composite facing is here regarded as a thin orthotropic plate and that ν_{23} is not involved.

2b. Measurement of Shear Moduli and Compliances

Torsion Experiments

From Eq. (3) we observe that the shear constants c_{44} and c_{66} (or s_{44} and s_{66}) are obtained directly from measurements of the moduli G_{23} and G_{12} respectively. A particularly well-known and suitable method for obtaining G_{12} involves the torsion of solid circular rods or rectangular bars about an axis parallel to the fibre direction. The additional shear modulus G_{23} could, from Eq. (3), be determined from measurements of E_2 and ν_{23} as described above. However the measurement of ν_{23} by the above method is difficult for thin specimens owing to the very small lateral displacements involved, and torsional tests about an axis perpendicular to the fibre direction provide an alternative means for obtaining G_{23}.

For isotropic rods of circular cross section, twisted about the longitudinal axis 1, the net shear stress at any point of a cross section is in the circumferential direction and is proportional to the angle of twist per unit length and to the distance from the centre of the cross section. The net shear stress is resolvable into components $\sigma_5(=\sigma_{13})$ and $\sigma_6(=\sigma_{12})$, the component $\sigma_4(=\sigma_{23})$ being zero. For unidirectional composites twisted about an axis parallel to the fibre direction, the shear modulus G_{12}

may be obtained from,

$$G_{12} = G_{13} = \frac{2M_t L}{\pi r^4 \phi}, \quad \ldots (12)$$

assuming the material to be transversely isotropic. Here M_t is the twisting moment applied to each end surface, ϕ the angle of twist over a gauge length L and r the specimen radius.

In the case of bars of rectangular cross section, the stress distribution in torsion is somewhat more complicated, and for thin isotropic samples the maximum shear stress occurs at the centres of the wider lateral surfaces. The following approximation, taken from Ref. 9, has been used (13, 16) to determine G_{12} for unidirectional composites twisted about the fibre axis,

$$G_{12} \simeq \frac{3M_t L}{\phi\, ab^3 (1-0.63\, b/a)} \quad \ldots (13)$$

where, as usual, a and b are the sample width and thickness respectively. This equation is valid to a good approximation for small values of b/a such that $\tanh(\pi\, a/2b) \simeq 1$. An alternative approximation, valid for $1 \geq b/a > 0.25$ and for $L > 20b$, has recently been derived by Johnson (15),

$$G_{12} \simeq \frac{3M_t L(1+\lambda^2)\left[45(1+\lambda^4) + 464\lambda^2\right]}{56\, I\, \phi\, (9+82\lambda^2+9\lambda^4)} \quad \ldots (14)$$

where $\lambda = b/a$ and $I = ab^3/12$. Eq. (13) has been employed by two sets of workers (13, 16) to determine G_{12} for unidirectional AGARD silica-epoxy composites. In each investigation an Instron tensile test machine was employed, together with a suitable loading device, in order to produce the required torque M_t through loads $W = M_t/a$ applied to each corner of a rectangular specimen as in Fig. 6. The angle ϕ was measured with the aid of offset displacement transducers over a central gauge length of 50mm. Closely related tests, in which loads are applied to four corners of a square plate, are described in references 5 and 10.

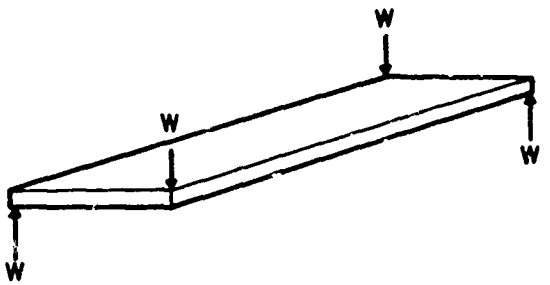

FIG.6 TORSION

The determination of G_{23} from torsional tests about an axis 90° to the fibre direction follows, for small b/a such that $\tanh(\pi\, a\, G_{23}^{\frac{1}{2}}/2b\, G_{12}^{\frac{1}{2}}) \simeq 1$, from a modified form of Eq. (13),

$$M_t = \frac{ab^3}{3L}\, \phi\, G_{12} \left[1 - 0.63\, \frac{b}{a} \left(\frac{G_{12}}{G_{23}}\right)^{\frac{1}{2}}\right] \quad \ldots (15)$$

in which the width direction a is taken to be parallel to the fibres. An alternative equation, similar in form to Eq. (14), has been given by Johnson (15).

Off-Axis Tensile Tests on Unidirectional and Bidirectional Laminates

Two simple methods for determining G_{12} for unidirectional orthotropic specimens are of particular interest. These involve the tensile loading of (a) unidirectional specimens having fibres oriented at different angles to the loading direction (Fig. 7a), and (b) bidirectional laminates having individual layers with +45° and -45° fibre orientations, respectively (Fig. 7b). Regarding method (a), the modulus E_x, determined at an angle θ to the fibre direction, is related to G_{12} through the coordinate transformation of compliances,

$$\frac{1}{E_x} = \frac{1}{E_1}\cos^4\theta + \frac{1}{E_2}\sin^4\theta + \left(\frac{1}{G_{12}} - \frac{2\nu_{12}}{E_1}\right)\sin^2\theta\cos^2\theta \quad \ldots (16)$$

Hence G_{12} (and also ν_{12}) may be obtained from measurements of E_x at four known angles θ. Pabiot (17) has employed this method, based on Eq. (16), to determine E_1, E_2, G_{12} and ν_{12} for the AGARD silica-epoxy composite. Measurements of the tensile stress σ_x at a single angle θ can also yield G_{12} if the shear strain is also determined. In this case the shear stress component equals $(\sigma_x/2)\sin 2\theta$ and the shear modulus can be written,

$$G_{12} = \frac{(\sigma_x/2)\sin 2\theta}{(90-\gamma)\pi/180} \quad \ldots (17)$$

where $90-\gamma$ is the angular change, in degrees, of the initial right angle between directions parallel and perpendicular to the fibres. This method has been employed by Halpin and Pagano (18) for a rubber/nylon fibre composite, the angle γ being measured with the aid of an appropriate grid system drawn on the sample surface. Greszczuk (19), on the other hand, employed a strain gauge rosette to measure the shear strain for an S-glass-epoxy composite. For the particular case $\theta = 45°$ the latter method is based on the equation,

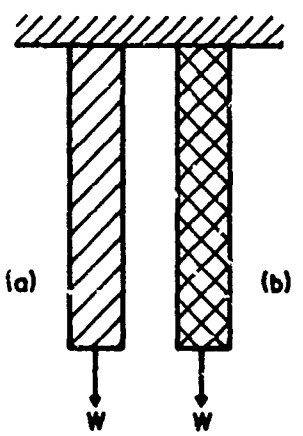

FIG.7 OFF-AXIS AND ±45° TENSION

$$G_{12} = \frac{\sigma_x}{2(\varepsilon_x - \varepsilon_y)} \qquad \ldots (18)$$

where ε_x and ε_y are strain components measured along and perpendicular to the loading direction respectively. The off-axis loading experiments are relatively simple and inexpensive to perform. However, the clamping method must be designed to allow the free rotation of the upper and lower edges of the sample, so that a uniform state of stress exists (18).

The determination of G_{12} from tensile tests on $\pm 45^\circ$ laminates has been discussed by Petit (20). With this technique, the shear modulus determination is based on the following relationship, derived from laminated plate theory,

$$G_{12} = \frac{2U_1 E_x}{8U_1 - E_x} \qquad \ldots (19)$$

where E_x is the measured Youngs modulus in the direction x (at $+45^\circ$ and -45° to the respective laminae orientations) and U_1 is given by,

$$U_1 = \frac{E_1 + E_2 + 2\nu_{21} E_1}{8(1 - \nu_{12}\nu_{21})} \qquad \ldots (20)$$

Hence if E_1, E_2 and ν_{12} are known from longitudinal and lateral loading tests (above) then G_{12} may be obtained from measurements of E_x. Using straight sided coupons and also axial sandwich beam constructions, Petit derived apparent G_{12} values as a function of the calculated shear strain $\varepsilon_{12} = (1 + \nu_{xy})\varepsilon_x$ for both graphite-epoxy and boron-epoxy composites. The measured values of ν_{xy} averaged about 0.85, illustrating slight deviations from pure shear conditions (for which $\nu_{xy} = 1$). Also the G_{12} values decreased continuously with increasing shear strain showing that the behaviour in shear is appreciably non-linear. Quoted values of G_{12} (as in Table 1) should therefore refer to the limit of very small strains. At shear strains below about 0.01 the results were in excellent agreement with those obtained from a cross sandwich beam technique (4, 20). The latter method requires a relatively elaborate construction but yields accurately a state of pure shear in the central region of the cross sandwich.

Several other methods have been investigated for determining the shear properties of composites. The so-called "picture-frame" method for square plates (7) yields an undesirable stress non-uniformity, whilst the "rail shear" test has received favourable comment (7). A method involving the use of split rings (19) has given shear moduli which agree well with those obtained from other techniques for an S-glass-epoxy composite. Tension and torsion tests on thin-walled cylinders have been recommended for the determination of both longitudinal and shear constants of orthotropic composites (21), although few results seem yet available. Despite the somewhat specialized processing and test facilities required, this method deserves future study owing to the relatively uniform and well-defined stress-strain fields involved.

2c. Results of Static Elastic Measurements

One method of assessing the relative merits of the above techniques is to compare values obtained for the various elastic constants on given materials. However, this is by no means a simple task, owing to the variations encountered in fibre and matrix type, processing conditions, fibre fraction and void content. In order to minimize these variations, results obtained by a given author, or by different workers on nominally the same material, should be compared. Examples of such comparisons are exhibited in Tables 1 to 3 for three types of composite.

In Table 1 we have collected together recent data reported for a unidirectional silica-epoxy composite by different laboratories. The results were obtained as part of an AGARD cooperative programme on composite materials. The samples investigated ranged in specific weight from about 1.65 to about 1.89 and a dependence of the results (particularly G_{12}) on specific weight was generally observed. The values in Table 1 correspond to the average specific weight value of 1.80. The average E_1 value is 46.1 GN/m^2 with a spread of about ±6%. The value of 41.2 GN/m^2 obtained from 3-point bending seems rather low, suggesting that the experimental corrections for shear and sample deformation at the supports may be slightly inadequate. Considerably larger scatter is observed for the E_2 values (average E_2 = 14.7 GN/m^2 ± 20%) possibly due to clamping errors for the short specimen lengths and the observation of transverse creep effects. The most pronounced observation concerns the wide range reported for G_{12}. This undoubtedly arises from the non-linear behaviour in shear, a typical result for unidirectional composites.

Regarding the E_1 values for carbon fibre-epoxy specimens in Table 2, the most notable result is the considerable increase observed by Park (8) using a clamping method which ensures good specimen alignment. The variation of E_1 with carbon fibre type is also evident. The results for boron-epoxy composites in Table 3 illustrate the relatively large value of E_1 in compression using the sandwich beam technique. We also note that the stress-strain behaviour in shear, obtained from the $\pm 45^\circ$ laminated specimen, was continuously non-linear, and that the value of G_{12} given corresponds to the smallest strains analysed. Table 3 also illustrates the relatively low anisotropy of the boron-aluminium composite, as represented by the E_1/E_2 ratio, arising from the relatively high modulus of the aluminium as compared with the epoxy matrix. Although the different methods illustrated in Tables 1 to 3 appear to give overall agreement in elastic constant values, the rather wide scatter emphasizes the scope for further improvement in standardising methods and, in particular, the need for selecting identical and well characterized samples for purposes of data comparison.

3. MEASUREMENT OF VISCOELASTIC PROPERTIES

A typical feature of polymeric materials is the observed dependence of the apparent elastic moduli or compliances on the experimental time-scale. Such behaviour is frequently termed viscoelastic since, at small strains, it can be described phenomenologically by models comprising both linear elastic elements (Hookes Law springs) and Newtonian viscous elements (dashpots). The terms "anelastic" or "relaxation" are

Table 1

Comparative Values of Elastic Constants for AGARD Silica-Epoxy Composite[a]

E_1 (GN/m^2)	E_2 (GN/m^2)	ν_{12}	ν_{21}	ν_{23}	G_{12} (GN/m^2)	Method	Equations	Ref (Year)
47.1		0.25				Tension	(4),(5)	16 (1971)
					5.88[b]	Torsion	(13)	
46.4	13.7	0.22	∿0.07			Tension	(4)→(6)	22 (1971)
48.1	11.7					Compression	(4),(6)	
45.0	15.1[c]	0.26	0.09	0.44		Tension	(4)→(7)	3 (1971)
49.4	18.0	0.22	0.08		7.80	Off-Axis Tension	(16)	17 (1971)
44.1	13.7	0.24				Tension	(4)→(6)	13 (1971)
41.2						3-point Bending	(9)	
					Range 3.69→7.51	Torsion	(13)	
47.7		0.26				Tension	(4),(5)	23 (1971)
	15.9		0.09			Compression	(4)→(6)	
					6.80	In-Plane shear		

a. 66% by volume Silica Fibres. Standard Unidirectional Sample 150mm × 40mm × 4mm. Where possible values given for specific weight of 1.80. Otherwise averages given over range of specific weight.

b. Value corresponds to $\tau_{max} = 9.81\ MN/m^2$.

c. Due to creep in transverse tension, strain measured 1 min. after load application.

Table 2

Some Comparative Values of E_1 for Carbon Fibre-Epoxy Composites by Different Methods

Fibre Type	Matrix	Vol % Fibres	E_1 (GN/m^2)	Method	Equation	Ref (Year)
Celanese Graphite Fibres	Epi-Rez 508 Epoxy	60	297	Conventional Tension (Dog Bone)	(4)	8 (1971)
			324	Tension (Straight Bar) Modified Grips		
			365	Tension (Dog Bone) Modified Grips		
Thornel 50	ERL 2256 Epoxy	58	165	Tension	(4)	10 (1969)
			170	4-Point Bending	(10)	
			157	Cantilever Bending	(8)	
Morganite Type I (Treated)	ERL 2256 Epoxy	62.6	223	Tension	(4)	12 (1969)
			239	3-Point Bending	(9) Shear Corrected	

also used to describe this behaviour. From a structural point of view, the observed time dependencies result from the relatively weak forces of interaction between neighbouring chain molecules or between localized side-chain groups. Subsequent to the application of a given force, the molecules rearrange to new equilibrium conformations at a rate dependent on their thermal mobility, and these processes give rise to an observed increase in the material deformation with time. The covalent three-dimensional structures of most reinforcing fibres preclude the longer range movements required for significant viscoelastic response, and the fibre behaviour tends to be purely elastic. Consequently, for unidirectional composites comprising polymeric matrices, modes of deformation most influenced by the matrix would be expected to give rise to the largest viscoelastic effects. We have already noted in Table 1 the observation

Table 3

Elastic Constants of Boron-Epoxy and Boron-Aluminium Composites By Different Methods

Composite Type	E_1 (GN/m^2)	E_2 (GN/m^2)	ν_{12}	G_{12} (GN/m^2)	Method	Equation	Ref (Year)
3M-SP-272 Boron Fibre-Epoxy	204				Tension	(4)	24 (1971)
	245				Compression Sandwich	(11)	
	203				3-Point Bending	(9) Shear Corrected	
	212	26.2	0.36		Uniaxial Sandwich	(11)	20 (1969)
				7.7[a]	Sandwich $\pm 45^\circ$ Fibre Orientations	(19),(20)	
Boron Fibre-6061 Al 50% Fibre Vol. Fract.	239	162			Axial Compression	(4)	25

a. Value obtained at shear strain $\varepsilon_{12} = 0.00183$ and stress $\tau_{12} = 14\ MN/m^2$.

of time dependencies in the elongation of the transversely loaded silica-epoxy composite, and similar effects might also be expected in shear.

3a. Creep and Stress Relaxation

Probably the simplest technique for studying viscoelastic phenomena is the well-known creep test in which the increase in strain with time is recorded for samples subjected to a constant load or stress. The creep behaviour of anisotropic materials may be studied by measuring the time dependence of a given strain component $\varepsilon_i(t)$ resulting from an applied constant stress component σ_j. If $\varepsilon_i(t)$ is proportional to σ_j at all times t after the stress application, then a creep compliance component $s_{ij}(t)$ can be evaluated as the ratio $\varepsilon_i(t)/\sigma_j$, providing that σ_j is the only non-zero stress component. For an arbitrary stress history, the strain component $\varepsilon_i(t)$ can then be represented, for a linear anisotropic viscoelastic material, by (18),

$$\varepsilon_i(t) = \int_{-\infty}^{t} s_{ij}(t-\tau)\frac{d\sigma_j(\tau)}{d\tau}\,d\tau \qquad \ldots (21)$$

where τ is used to represent times prior to t and the repeated subscript j again indicates summation. Closely related to the creep test is the so-called stress relaxation experiment in which the specimen is subjected to a fixed strain and the decrease in stress with time is observed. For linear response, if a single strain component ε_j is held constant, and all other strain components are zero, then stress relaxation modulus components $c_{ij}(t)$ are obtained as the ratio $\sigma_i(t)/\varepsilon_j$, where $\sigma_i(t)$ is the time dependent stress component. For an arbitrary strain history, stress-strain relations are of the form,

$$\sigma_i(t) = \int_{-\infty}^{t} c_{ij}(t-\tau)\frac{d\varepsilon_j(\tau)}{d\tau}\,d\tau \qquad \ldots (22)$$

In tensile stress relaxation tests, the decrease in tensile stress is measured for a fixed tensile strain, and relaxation moduli such as $E_1(t)$ and $E_2(t)$ are obtained. Components such as $c_{11}(t)$ and $c_{22}(t)$ are not determined since lateral strains are also applied. For stress relaxation in shear, however, relations such as $c_{66}(t) = G_{12}(t)$ are valid. It should also be emphasized that reciprocal relations such as $s_{11} = 1/E_1$, which apply in static tests, are not generally valid for time dependent phenomena (e.g. $s_{11}(t) \neq 1/E_1(t)$). Experimentally, each of the methods discussed in Section 2 can be adapted to the measurement of creep compliances or stress relaxation moduli, providing that facilities are available for recording time dependencies of the deformation or load. The Instron testing machine is suitable for this purpose, and equipment specifically designed for tensile creep measurements on plastics and composites has been described (26).

Few results are yet available on the creep or stress relaxation of fibrous composites, but two recent studies are of interest. Halpin and Pagano (18) measured the creep of orthotropic sheets of nylon fibre reinforced rubber using longitudinal, transverse and off-axis tensile loading. Tensor components of the creep compliance were determined with reference to axes defined by both the fibre and loading directions. Fig. 8 shows the results for the shear coupling compliance $s'_{16}(t)$ referred to the loading axes, and the recovery of strain following the removal of load is also shown. The linearity of response, as represented by the superposition equations (21) and (22), is verified by the successful prediction of the creep from the recovery data. Good agreement was also obtained between the respective compliance components measured with reference to the sample and loading axes, using standard transformation equations based on symmetric compliance matrices. This result is also indicated in Fig. 8 and provides accurate confirmation of the symmetry relations $s_{ij}(t) = s_{ji}(t)$ which cannot be assumed from equilibrium strain energy considerations.

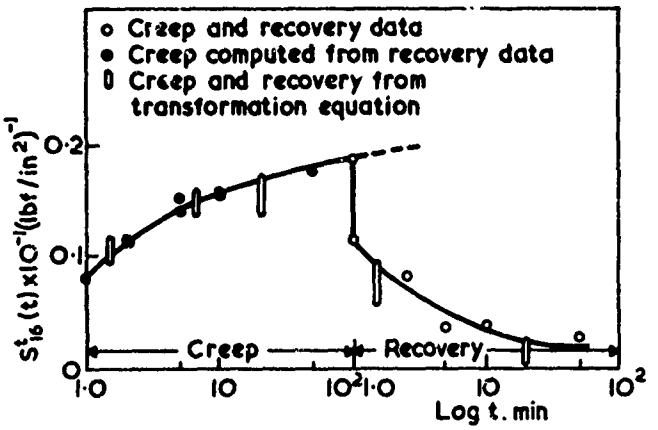

FIG.8 CREEP AND RECOVERY FOR NYLON IN RUBBER

For the relatively rigid boron-epoxy system, Ashton (27) has obtained stress relaxation results for a laminate with ±45° fibre orientations using 4-point flexure of a honeycomb sandwich beam. It follows from Eq. (19) that $E_x(t) \approx G_{12}(t)$ so that the relaxation is dominated by the shear component. The failure of the relaxation curves to superpose at different strain levels, as illustrated in Fig. 9, shows that the viscoelastic behaviour for this polymer in shear is non-linear and that equations (21) and (22) require modification. This behaviour, which contrasts with that exhibited by the softer nylon-rubber composite, was qualitatively ascribed to stress concentrations within the epoxy matrix which cause the linearity limits to be exceeded locally.

3b. Dynamic Methods

Viscoelastic phenomena in composites may also be investigated by a range of dynamic tests in which both the moduli and damping properties are measured as a function of frequency. At low frequencies, where inertial forces are negligible, it follows from Eq. (21) that the linear strain response to prescribed sinusoidal stresses can be expressed by $\varepsilon_i^* = s_{ij}^* \sigma_j^*$ where the complex stress and compliance components are of the form

$\sigma_i^* = \sigma_{0,i} \exp(i\omega t)$ and

$s_{ij}^* = (\varepsilon_{0,i}/\sigma_{0,i}) \exp(-i\delta_{ij})$

respectively. Here $\sigma_{0,j}$ and $\varepsilon_{0,i}$ are the amplitudes of the stress and strain cycles, respectively, ω is the frequency in radians per sec., $i = \sqrt{-1}$ and δ_{ij} is the phase angle by which the strain cycle is found to lag the stress cycle (see Fig. 10). If the prescribed stress is parallel to the fibre axis, and other stress components are absent, then it follows that,

$$\sigma_1^* = (1/s_{11}^*)\varepsilon_1^* = E_1^* \varepsilon_1^* = (E_1' + i E_1'')\varepsilon_1^* \quad \ldots (23)$$

from which,

$$E_1' = (\sigma_{0,1}/\varepsilon_{0,1}) \cos \delta_1, \quad E_1'' = (\sigma_{0,1}/\varepsilon_{0,1}) \sin \delta_1, \quad \ldots (24)$$
$$E_1''/E_1' = \tan \delta_1$$

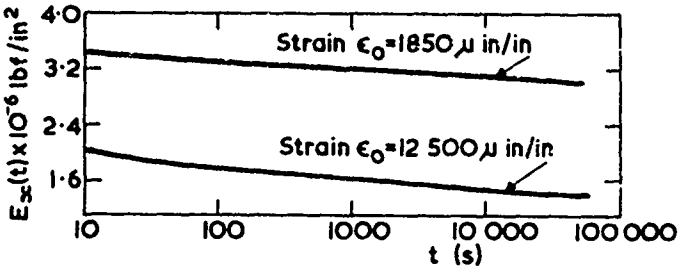

FIG.9 STRESS RELAXATION OF BORON-EPOXY

where δ_1 is used as a contracted form for δ_{11}. E_1' and E_1'' are real and imaginary components, respectively, of the complex modulus E_1^*, and are proportional to the maximum energy stored and the energy loss per cycle, respectively. The so-called loss tangent $\tan \delta_1$ is also proportional to the ratio of energy loss to maximum energy stored per cycle. Equations similar to (23) and (24) also hold for low frequency experiments in tension perpendicular to the fibre direction and for torsion about the fibre axis. In these cases, the real and imaginary components of E_2^* and G_{12}^* are respectively involved, as well as the appropriate loss tangents. The variation of E', E'' and $\tan \delta$ with frequency is shown schematically in Fig. 11. So-called "relaxation regions" are generally observed in which E' increases with frequency and both E'' and $\tan \delta$ exhibit peaks. Outside of these frequency regions, the loss factors become small and E' becomes essentially frequency independent. Similar frequency dependencies should be observed for the components of other complex moduli such as G^*. For polymeric solids, the significance of these effects in terms of molecular motional frequencies is discussed by McCrum, Read and Williams (28), and this reference also contains a survey of dynamic mechanical test procedures.

Low Frequency Non-Resonance Method

In the low frequency forced non-resonance technique, the real and imaginary components of the relevant moduli are determined from direct measurements of stress and strain amplitudes and the loss angle according to equations (24). This method is most suited to high loss materials, having $\tan \delta$ values above about 0.1 and has the advantage that the frequency may be continuously varied, not being determined by sample resonance. Fig. 12 illustrates equipment developed at the NPL with which a sinusoidal deformation of fixed amplitude may be applied by means of a mechanical eccentric device in the frequency range 0.1 Hz to 20 Hz. Specimens are deformed either in tension, 3-point or 4-point bending, the strain being monitored by displacement transducers and the force measured with calibrated load cells. Outputs of the displacement

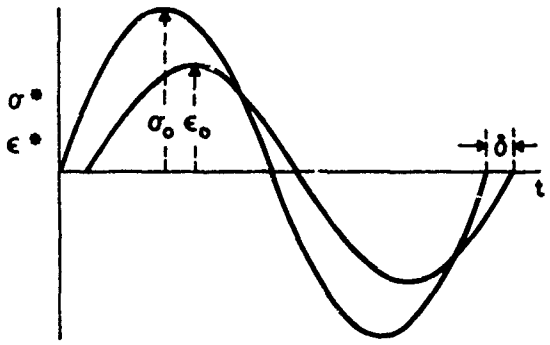

FIG.10 LOW FREQUENCY METHOD

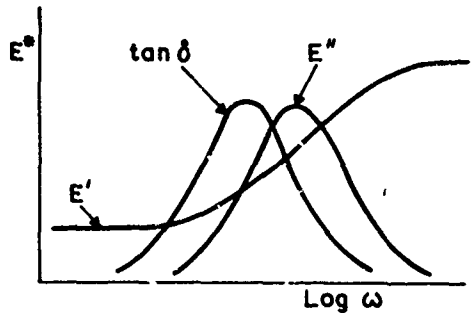

FIG.11 E*-FREQUENCY PLOTS

transducer and load cell are analysed for amplitude with a digital voltmeter, and the loss angle is derived from the time interval between the zero points of the sinusoidal outputs, using an electronic counter. An extension of the frequency range to 10^{4} Hz is being effected by the incorporation of an electromagnetic vibration generator and piezoelectric transducers for monitoring the stress and strain cycles.

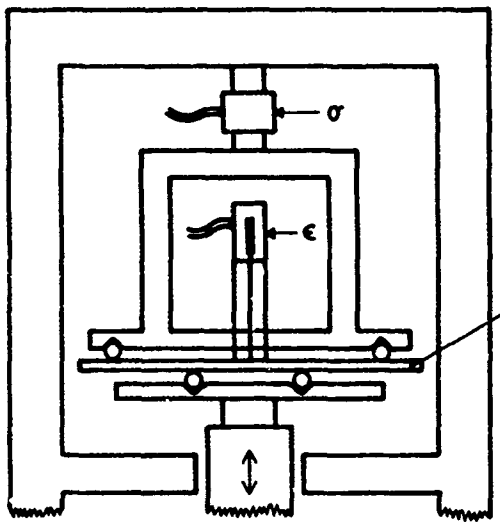

FIG.12 LOW FREQUENCY NON-RESONANCE METHOD

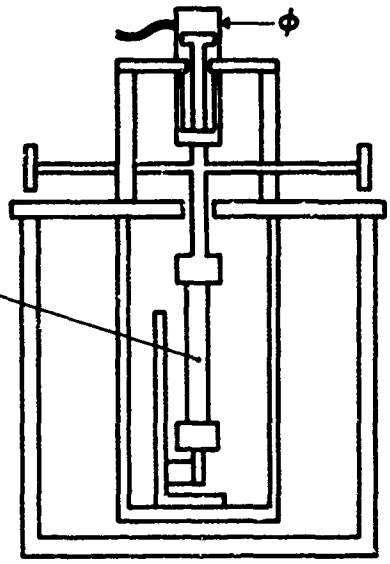

FIG.13 TORSION PENDULUM

Torsion Pendulum

Low frequency dynamic properties in shear are most often determined by means of the well-known torsion pendulum technique. In this method one end of the specimen is clamped to a freely suspended inertia arm (Fig. 13) which is pulsed electromagnetically, and the free decay of torsional oscillations observed. As indicated schematically in Fig. 14, the angular motion may be described by a sine curve whose amplitude decreases exponentially with time. This decay is characterized by the logarithmic decrement Λ given by,

$$\Lambda = (1/m)\ln(\phi_n/\phi_{m+n}) \qquad \ldots (25)$$

where ϕ_n is the amplitude of the n'th cycle and m is the number of swings over which the decay is measured. For low damping the loss tangent may be calculated from $\Lambda \approx \pi \tan\delta$ and the real part of the shear modulus G' may be evaluated from the period of oscillation P,

$$P^2 = \frac{4\pi^2 I}{(M_t/\phi)}\left(1 + \frac{\Lambda^2}{4\pi^2}\right) \qquad \ldots (26)$$

where I is the moment of inertia of the pendulum and (M_t/ϕ), the twisting moment per unit deflection, is theoretically related to the shear modulus through equations such as (12) to (15). The term containing Λ in Eq. (26) is usually negligible. For unidirectional composites, it will be observed from equations

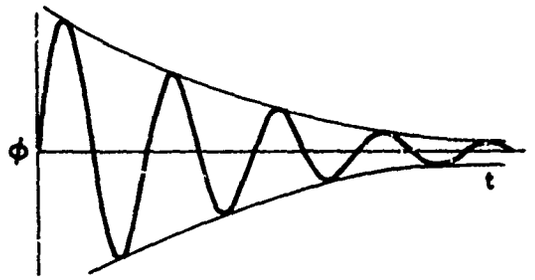

FIG.14 FREE DECAY METHOD

(12) to (14) that twisting about the fibre axis yields the components of G_{12}^* whereas from Eq. (15) torsion about a perpendicular axis involves a combination of G_{12}^* and G_{23}^*.

The torsion pendulum is best suited to the study of low loss materials ($0.001 < \tan\delta < 0.3$), and its frequency may be varied over about a decade by altering the moment of inertia and the sample dimensions. In practice, the frequency is usually fixed at about 1 Hz and variations in G' and $\tan\delta$ are determined over a wide temperature range. Temperature variation provides a powerful means of exploring multiple loss peaks in polymers (28). Since the torsional rigidity of a specimen may depend significantly on tensile loads, the inertia arm is preferably suspended from above the sample than from below. Some designs employ a low loss bearing for the suspension, but with this method frictional effects in the bearing can yield serious errors in Λ, particularly for less rigid specimens. Other designs use for the suspension a torsion wire which may be passed over a pulley for purposes of counterbalancing the weight of the inertia arm. The pendulum designed at the NPL, and illustrated in Fig. 13 uses a suspension comprising three thin steel strips mounted symmetrically about the neutral axis. This method eliminates frictional losses and maintains a degree of lateral rigidity in the system. The added stiffness also enables higher loss samples to be studied by eliminating or minimizing the effects of critical damping. Measurements of Λ and P are made with and without the specimen, and the material properties are determined from appropriate equations which take into account the effects of added stiffness. With the NPL equipment, the torsional oscillations are detected with a rotary differential transformer, the output of which is analysed with a digital voltmeter and electronic counter. Data is recorded on punched tape and analysed by computer, and the temperature is automatically controlled in the range -200°C to +200°C.

Audiofrequency Forced Resonance Methods

In the audiofrequency range, typically 20 Hz to 10^5 Hz, dynamic mechanical properties are usually determined by resonance methods in which the specimen is driven by a sinusoidal force of constant amplitude and the resulting deformation amplitude measured as a function of frequency. Peaks are observed in the amplitude versus frequency plots, as illustrated in Fig. 15, corresponding to the different resonance modes of sample vibration. For low losses, the loss tangent is approximately obtained from the width of a peak, Δf_n (Hz) at an amplitude $1/\sqrt{2}$ of the maximum amplitude (i.e. when the amplitude level is 3dB below the maximum),

$$\tan\delta = \Delta f_n / f_n \qquad \ldots (27)$$

where f_n is the resonance frequency in Hz corresponding to the peak maximum of the n'th mode, the fundamental mode corresponding to $n = 1$ and $n = 2, 3$, etc. representing the harmonics. Alternatively, the loss tangent may be determined after tuning the frequency to resonance and recording the free decay of the vibration amplitude when the driving force is removed. This method is analogous to that described for the torsion pendulum, and is useful for low losses and low resonance frequencies when the peaks become too narrow for a precise bandwidth determination. In general the modulus is proportional to f_n^2, the proportionality constant being determined by the sample dimensions and density, and the resonance mode.

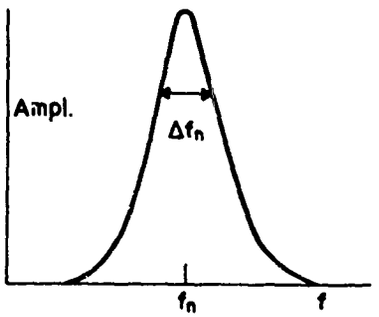

FIG.15 RESONANCE PEAK

Three different types of resonance method may be employed, depending on whether flexural, torsional or longitudinal vibrations are excited. In detail, each of these methods may be designed in a variety of ways by employing different methods of excitation, clamping or support. By way of example, the three techniques currently employed at the NPL will be briefly described. For studying the transverse resonance modes, the B & K Complex Modulus Apparatus is employed, in which the sample is clamped either at one or both ends. The former (cantilever) method, illustrated in Fig. 16, is more often used, the sample being driven at the free end by an electromagnetic transducer in combination with a small magnetic mass bonded to the specimen tip. A similar transducer, or alternatively a capacitive transducer, is used to detect the vibration amplitude at some optimized position near to the top of the specimen. The amplitudes are recorded on a B & K level recorder which also serves to advance the frequency of the driving oscillator synchronously with the recorder chart. An electronic counter is employed for the accurate determination of resonance frequencies. Using specimens with 0° and 90° fibre orientations, the respective moduli E_1' or E_2' are evaluated from,

$$E' = 48\pi^2 \rho \left(\frac{L^2 f_n}{b k_n} \right)^2 \qquad \ldots (28)$$

where ρ is the sample density and k_n has values of 3.52, 22.0 and 61.7 for $n = 1$, 2 and 3 respectively. With this method, it is necessary to ensure that the attached masses are sufficiently small not to significantly influence the results. In the case of composites, resonance frequencies of the higher modes

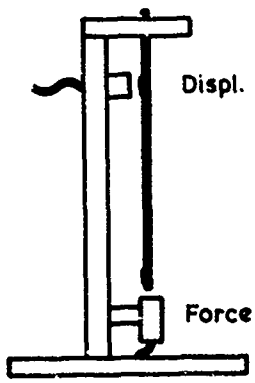

FIG.16 TRANSVERSE RESONANCE

may be appreciably influenced by contributions from shear deformations, owing to the high E/G ratios. This affect has been explored by Dudek (29) and other types of flexural resonance equipment have been employed with composites (30, 31, 32).

The torsional and longitudinal resonance devices developed at the NPL are illustrated in Figs. 17 and 18 respectively. In the torsional method, the bar is oscillated in a free-free mode by means of a magnetostrictive wire looped under one end of the specimen. Coils surround magnetically polarized parts of the wire near to each end, and generate oppositely phased mechanical waves which act to excite torsional vibrations in the sample. The vibration amplitude is detected by a similar wire looped under the opposite end of the sample. The appropriate shear modulus is calculated from,

$$\frac{M_t L}{\phi} = \frac{4 L^2 f_n^2 I_s}{n^2} \qquad \ldots (29)$$

where I_s, the torsional moment of inertia per unit length of sample, is equal to $\rho ab(a^2 + b^2)/12$ for rectangular bars. $M_t L/\phi$ is the twisting moment per unit deflection and is related to the appropriate shear moduli by equations such as (12) to (15). We thus note that torsional resonance tests about axes parallel and perpendicular to the fibre axis, respectively, can yield both G_{12}' and G_{23}', as in the case of the torsion pendulum.

In the longitudinal resonance method, flat polarized metal plates are placed close to and parallel with each end of the specimen. An alternating voltage applied to one of the plates produces the driving force and the resonance amplitude is detected electrostatically at the opposite end. The specimen is supported by two sets of needles located one third the length of the bar from each end. For bars of rectangular cross section E_1' or E_2' may be evaluated from,

$$E' = 4 \rho L^2 f_n^2 / C_\ell n^2 \qquad \ldots (30)$$

using samples with 0° and 90° fibre orientations respectively. The correction factors C_ℓ, which depend on the beam dimensions and Poissons ratio, are tabulated in an NPL publication (33).

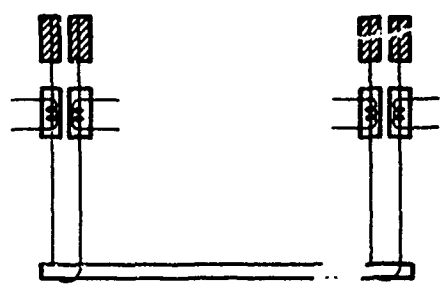

FIG.17 TORSIONAL RESONANCE

Ultrasonic Pulse Technique

This test offers a rapid and reliable method for determining all the dynamic elastic stiffness components of a composite specimen of small size and requiring relatively little preparation. The technique utilises the dependence of the velocities of elastic waves propagating in an anisotropic medium upon the density and one or more dynamic stiffness components. In principle, therefore, a knowledge of the density and velocity along a sufficient number of directions allows all the elastic moduli of a material of arbitrary symmetry to be defined.

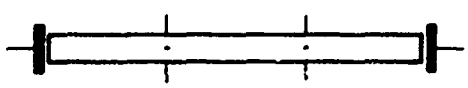

FIG.18 LONGITUDINAL RESONANCE

For purely elastic materials, Musgrave (34) has shown that three bulk waves may be propagated in any direction and that the solution to the equation,

$$\det M_{ik} = 0$$

where $$M_{ik} = c_{ijkl} n_j n_l - \rho V^2 \delta_{ik}$$

gives the velocities, V, of the waves for any wave normal, (n_1, n_2, n_3). One condition of Musgraves analysis is that the solution applies to plane waves travelling in an infinite medium which requires that velocities are related to stiffness components, c_{ij}, see equation (1). In practice, this condition is satisfied for the propagation of waves of wavelength less than specimen dimensions. If this equation is solved for a unidirectional composite possessing hexagonal symmetry, see equation (3), the velocities of waves travelling along principal axes are simply related to the density and a single component by expressions of the form $V = \sqrt{c_{ij}/\rho}$. Thus longitudinal and shear moduli may be calculated from measurements of the velocities of longitudinal and transverse waves, respectively, travelling along, and normal to, the fibre axis. The remaining components $c_{13} = c_{12}$, necessary to define fully the elastic behaviour, must be deduced from a measurement of the velocity of a wave propagating at an angle to the fibre axis. For low loss viscoelastic materials, $V = \sqrt{c_{ij}'/\rho}$. Although, in principle, both real and imaginary components of stiffness may be determined from the velocity and attenuation of a wave, attenuation by scattering in composite systems usually makes loss measurements impossible.

In an experimental arrangement (35) designed at the NPL to measure dynamic elastic moduli, ultrasonic pulses of frequency around 5 MHz (wavelength ≈ 1mm) are introduced into a specimen by immersing it in a tank of water in which longitudinal pulses may be propagated between a transmitting and a receiving transducer. The time differences between the arrival of a pulse through water and through water plus the specimen is measured by an accurate electronic delay circuit and is related to the wave velocity by the specimen thickness. The specimen is mounted on a turntable so that waves may be incident at any angle. Since transverse waves cannot be generated along principal axes of the specimen in this way, a shear wave transducer may be glued directly to the specimen. This, however, can produce inaccuracies owing to the effect of the layer of glue, and possibly a more reliable method involves measurements of the velocities of quasi-transverse waves at angles to the fibre axis. Fig. 19 shows the refraction of a longitudinal wave incident at an acute angle to a plane of the composite containing the fibre axis. The refracted quasi-transverse wave has velocity V_T and a displacement vector which is not precisely perpendicular to the wave direction, the deviations being dependent upon material anisotropy. A plot of V_T^2 against $\cos 2r_T$ is linear near $\cos 2r_T = -1$ and may be extrapolated to give the velocity of the pure shear wave along the fibre axis. The component $c'_{12} = c'_{13}$ may be calculated from the quasi-transverse wave velocity at some angle r_T, usually 45°, once all the other components are known, although reliably accurate values may only be deduced from very accurate measurements of velocity and values for the other components. This is inevitable as no bulk wave velocity is particularly sensitive to the magnitude of this component.

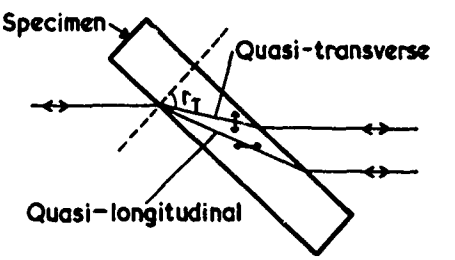

FIG.19 REFRACTION BY A SPECIMEN

Specimen dimensions, typically, 5cm × 1cm × 1cm are ideal, where the long dimension contains the fibre axis, and adjacent faces should be machined accurately perpendicular. Although smaller dimensions are satisfactory, an uncertain inaccuracy is introduced if these are comparable with or smaller than a wavelength. The accuracy of this technique is usually limited by factors that influence the quality of the composite specimen studied. Parameters such as the void content and variations in fibre fraction and packing arrangement with position in the specimen affect wave velocities and, in addition, voids reduce pulse amplitude by scattering the wave. The technique, therefore, contributes information on specimen quality and is valuable for characterizing material symmetry and homogeneity by means of measurements made along a range of directions and in the same direction but at various positions of the specimen.

Results of Dynamic Measurements

The majority of dynamic moduli and loss factors for fibrous composites have been obtained using audiofrequency resonance and ultrasonic methods, and details of the results can be found in references (10) and (29) to (32). Some dynamic moduli and loss tangents obtained with the NPL equipment on a low modulus carbon fibre-epoxy material are also shown in Fig. 20. A fair measure of agreement is found between the dynamic moduli obtained by the different methods and $E_1' \gg E_2' > G_{12}' > G_{23}'$ at all frequencies. The loss tangents observed in shear and transverse tension are greater than those in longitudinal tension and rise with frequency in the low audio-frequency range. Further work is required to minimize the observed scatter (due partly to density variations between samples cut from the same sheet) and obtain more precise results on the frequency dependence of the dynamic parameters.

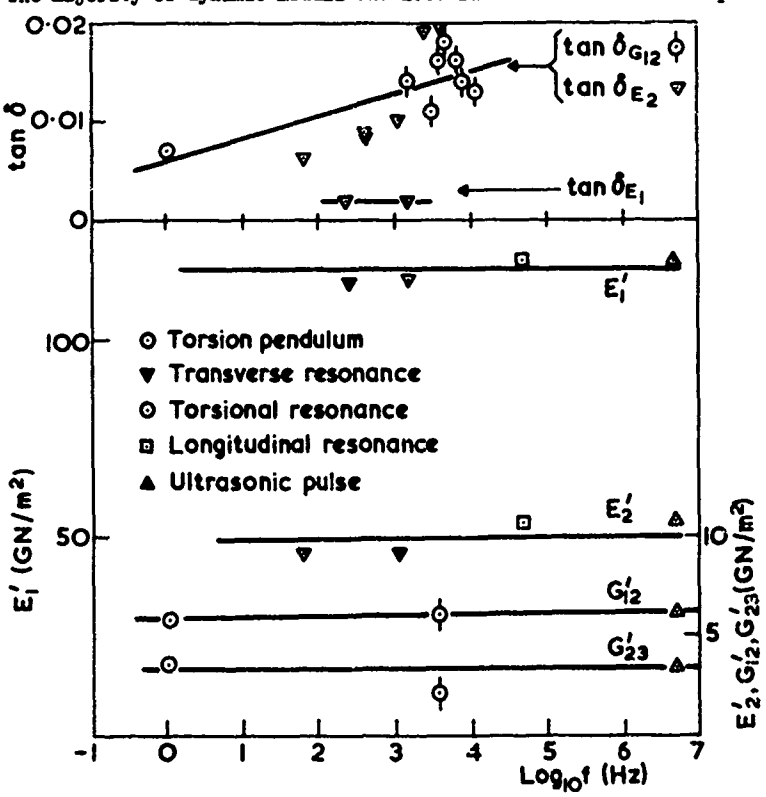

FIG. 20 DYNAMIC MODULI AND LOSS TANGENTS FOR LOW MODULUS CARBON FIBRE-EPOXY (60% FIBRE VOLUME FRACTION)

Results of ultrasonic measurements are illustrated in Fig. 21 which shows the variation of four dynamic stiffness components with fibre volume fraction for a unidirectional type II carbon fibre-epoxy composite. The scatter in values for the c_{13}' component was too great to allow any trend with fibre fraction to be observed.

The value for c_{13}' for a 60% fibre fraction, together with values for the other stiffness components at this fibre fraction (obtained from Fig. 21) are shown in Table 4. The values for Youngs moduli, Poissons ratios, and shear moduli were derived from these assuming transverse isotropy.

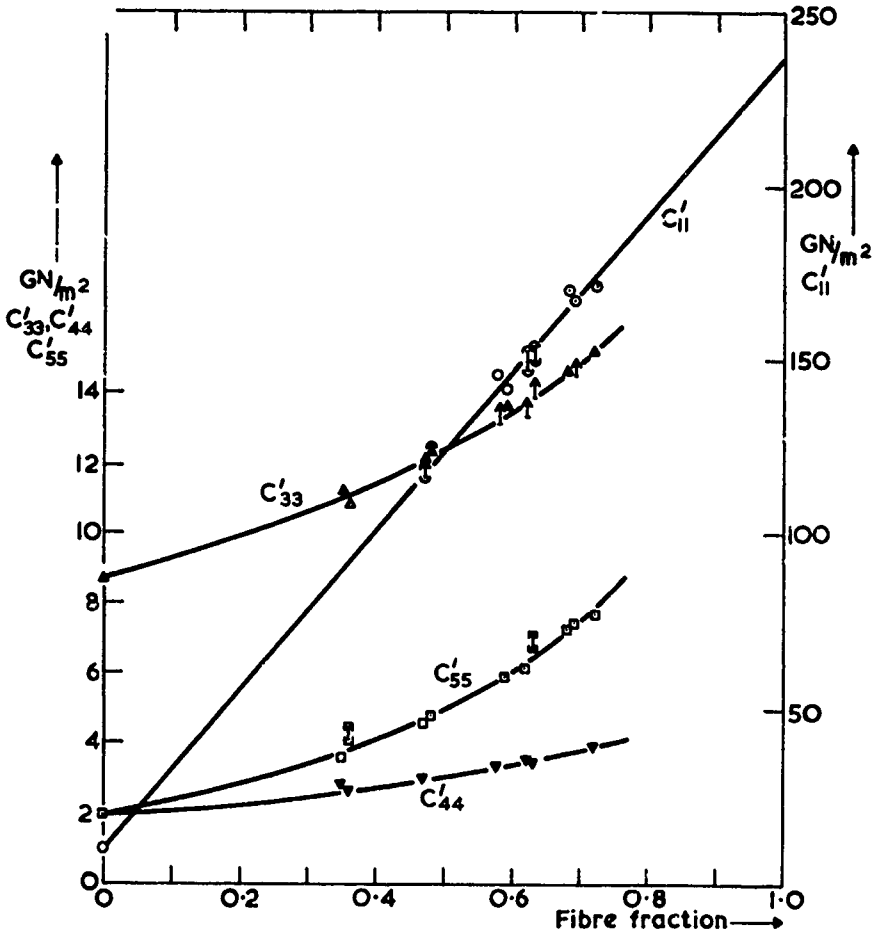

FIG. 21 VARIATION OF ELASTIC STIFFNESS COMPONENTS OF TYPE II CARBON FIBRE REINFORCED EPOXY WITH FIBRE FRACTION

Table 4

Dynamic Elastic Constants for Transversely Isotropic Type II Carbon-Epoxy at 60% Fibre Volume Fraction (GN/m^2). Frequency = 5MHz

c_{11}'	$c_{22}'=c_{33}'$	c_{23}'	$c_{12}'=c_{13}'$	c_{44}'	$c_{55}'=c_{66}'$	$E_1' \simeq \frac{1}{s_{11}'}$	$E_2' \simeq \frac{1}{s_{22}'}$	$\nu_{12}'=\nu_{13}' \simeq \frac{-s_{12}'}{s_{11}'}$	$\nu_{21}'=\nu_{31}' \simeq \frac{-s_{12}'}{s_{22}'}$	$\nu_{23}'=\nu_{32}' \simeq \frac{-s_{23}'}{s_{22}'}$	G_{23}'	G_{12}'
146	13.5	6.7	7.0	3.4	6.05	141	11.0	0.35	0.025	0.49	3.4	6.05

4. STRENGTH OF COMPOSITE MATERIALS

The ability of many composite materials to sustain high loads is a reflection of the properties of the fibres and so test procedures designed to measure ultimate properties of composites usually concentrate on unidirectional material. The fracture behaviour of composite systems is, however, generally complex and an understanding of the processes of crack propagation under a variety of stress conditions requires consideration of the anisotropic and inhomogeneous nature of the composite microstructure. The design of composite components to utilise efficiently the load bearing capacity and crack resisting properties of the fibres therefore involves a knowledge of matrix properties and the character of the fibre-matrix interface. A comprehensive account of the principles of fibre reinforcement in a range of composite systems is given by Kelly and Davies (36).

In this section, test methods are considered for studying failure in composite materials. A test that is designed to determine 'static' strength involves an applied strain rate of around 0.01/minute. Under certain conditions, failure may result for applied stress levels different from the static value. These conditions include repeated cyclic loading, fatigue; sustained loading at a constant stress level, creep; and impact loading. In addition to the maximum stress, further information is required on the number of cycles to failure, the time elapsed before failure and the energy required to cause failure, respectively, from each test.

The purpose of performing failure tests on composite materials is, ultimately, to improve the efficient design of components and structures utilising these materials. This may be achieved by producing fundamental material properties that may be used confidently by the designer. However, the stringent requirements of such techniques are not always necessary to yield valuable data. For example, qualitative results may be used to compare the relative merits of a range of materials to assist the choice of the optimum material for a specific application. Also, the material scientist requires test methods for means of indicating property control or trends in material improvement brought about by revised processing or fabrication techniques. Some of the test methods to be described are capable of producing values which are constants for the material under test and hence independent of specimen dimensions and the test arrangement. In these tests it is necessary to establish a macroscopically pure state of stress in the volume of the specimen through which fracture occurs. In other tests, the stress condition is not pure but is a combination of shear, tensile and compressive components. These tests are designed so that one component predominates but the mode of failure, and hence measured values, usually depends upon test variables. The results cannot, therefore, be used confidently as design data but are valuable for material comparison where only qualitative data is required related to a material property.

Test methods used for determining the energy necessary to fracture a material commonly involve a measurement of either the work done in loading a test specimen to failure or the energy lost by an impacting device in breaking the specimen. Results from these techniques generally contain contributions from the energy required to initiate failure and the energy dissipated in propagating a crack across the specimen. The relative magnitudes of these contributions depends upon material and test parameters. In a test where the strain energy stored in the specimen and released on failure is more than sufficient to propagate the crack, the measured energy is solely that to initiate failure and will depend upon ultimate material properties and specimen dimensions. Alternatively, a stress concentrating feature, such as a notch, may localise the failure resulting in a controlled crack growth so that all the energy is consumed by processes associated with the mechanism of crack propagation and, in the limit, no energy would be stored or lost in the bulk of the specimen. In this case, a lower limit to the fracture energy of the material is obtained. The effect of a notch in many composite materials is, however, reduced by their ability to relieve the stress concentration associated with the notch tip by debonding or splitting, and thus a greater volume of the specimen is unavoidably involved in the fracture process.

The reliability of test data on any composite system is determined by the reproducibility in results obtained for a number of specimens or a range of test variables. Where measurements of ultimate strength and work of fracture are found to depend upon factors such as rate and method of loading or specimen and notch geometry, this dependence should be investigated fully to obtain a comprehensive understanding of the material's failure behaviour. Scatter in individual results may arise from imperfect reproducibility of test conditions, from variations in fibre properties from batch to batch or changes in specimen character brought about by slight differences in processing conditions. For these reasons, an estimate of the value of various test methods for measuring fracture properties by a comparison of results on a certain composite system is valid only if the character of the specimens studied is identical. Where possible, therefore, test methods will be illustrated by reference to results quoted in the literature for a single source of material.

The methods to be discussed are generally applicable to fibre reinforced plastic, metal and ceramic matrices. Most of these methods are described in the ASTM standards so the details are not presented, but emphasis is placed on considerations important to the testing of composites, particularly those containing very strong or stiff fibres. Emphasis will also be placed on unidirectional systems but, owing to the anisotropy of ultimate properties and failure modes, mention will be made on the testing of off-axis and angle-ply specimens.

4a. Measurement of Tensile and Compressive Strength

Tensile Test

The arrangement used for testing a material under tension has been described in Section 2 and is illustrated schematically in Fig. 1. If failure occurs in the specimen gauge length, the tensile strength may be calculated from the ratio of the maximum sustained load to the initial cross-sectional area.

The problems associated with establishing a uniform state of pure tensile stress in the specimen are enhanced when the material studied contains fibres of high modulus aligned in the direction of applied load. Accordingly, specimen dimensions and alignment and the design of the grips are critical features of this test if premature failure, from the introduction of bending moments and stress concentrations, is to be avoided. Bending forces are reduced by using self-aligning grips and a system whereby the specimen is allowed to rotate to align itself in the direction of a small applied load before the grips are finally tightened. A design similar to that shown in Fig. 22 from reference (8) will achieve this situation. The function of the grips is to transfer a tensile stress to the gauge length of the specimen by means of a shear stress applied at the specimen-grip interface such that,

$$\tau_g A_g = \sigma_T A_s \qquad \ldots (3)$$

where τ_g is the frictional stress at the interface of total area A_g and σ_T is the tensile stress in the specimen at a cross-sectional area A_s. Self tightening grips raise τ_g as σ_T is increased but reinforcement tabs, glued to the specimen in the area between the grips, may be necessary to prevent crushing of the specimen. The specimen should be designed so that when the ultimate tensile stress of the specimen is reached, τ_g is below the limiting frictional stress and the shear strength of the composite. This requirement may be assisted by waisting the centre of the specimen and this also promotes failure away from the grips where the stress condition is more uniform. A variety of shapes for the reduction of specimen width are discussed by Dastin et al (6). Table 5 illustrates an increase in measured tensile strength for a specimen of carbon fibre reinforced plastic with reduced gauge section.

When symmetrical angle-ply laminates are tested for tensile strength, a marked dependence upon specimen width is observed (37, 38) which varies with the angle between the laminate fibre axes. The tensile testing of unidirectional material at an angle to the fibre axis introduces shear deformations in the plane of the specimen which are constrained by the grips. This effect may be reduced by increasing the length to width ratio of the specimen which diminishes the influence of the grips in the centre of the specimen (39).

A split disc method (ASTM 2291) has been designed to measure the tensile strength of specimens in the shape of a ring. The loading arrangement reduces the shear stresses associated with grips but introduces a small bending moment into the specimen. The method has produced reproducibly high values for the strength of composite materials.

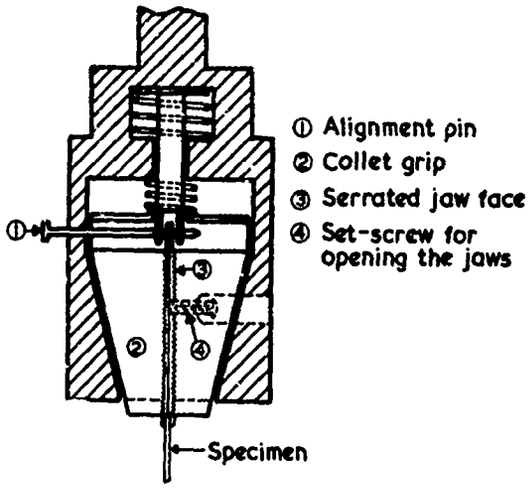

FIG.22 SPECIMEN ALIGNMENT (8)

Compression Test

The compressive and tensile strengths of composites are usually not equal, so both properties need to be evaluated. Conventional methods for the measurement of compressive strength involve mounting a free standing specimen, of suitable cross-sectional area to prevent buckling, between parallel, hardened steel plattens of a testing machine. This procedure is not suitable for many composite materials possessing high anisotropy in strength as the lateral stresses produced at the specimen ends can give rise to end failure by splitting parallel to the fibre axis. The design of clamps and sockets to supply support to the specimen ends has been described (40, 41) and buckling has been prevented in the testing of flat specimens by using a honeycomb core (42) to give lateral support to the specimen whilst contributing a negligible restraint to the compressive load. The care required in specimen preparation and alignment between the plattens of the test machine is, again, particularly important when testing high modulus composites to ensure that the compressive load is distributed evenly across the specimen cross-section. A successful support design has been employed at the Royal Aircraft Establishment for the testing of cylindrical specimens of type I carbon fibre reinforced plastic (43). The specimen ends are glued into holes prepared in mild steel end fittings whose faces are then machined accurately perpendicular to the specimen axis. The sample is waisted and reproducible results have been quoted for failure away from the end fittings. The use of self-tightening grip assemblies to transfer a compressive load to a specimen of rectangular cross-section has been described by Park (8) and Broutman (44). Grip alignment is achieved by means of a sleeve which fits closely over both assemblies. Broutman (44) presents results for a variety of shapes of waisted specimens. Table 6 shows compressive strengths for some composite systems and illustrates the low values that can be obtained on

Table 5

Comparative Tensile Strength Values (MN/m^2)

Fibre	Matrix	Volume % Fibres	σ_T^u	Method	Reference
Celanese Type I	Epi-Rez 508 Epoxy	~60	1117	Grips. Waisted Specimen	8
			889	Grips. Straight Specimen	
Harwell Type I	Epoxy	60	863	Grips. Straight Specimen	54
			1069	Flexure. L/b = 40	
Morganite II	Epi-Rez 508	50-55	1020	Grips. Waisted Specimen	8
Morganite Type II	Epoxy	~64	1240	Grips	24
			1500	Flexure	
Boron	Epoxy	~50	1200	Grips. Straight Specimen	38
Boron	3M SP-272 Epoxy	>50	1280	Grips	24
			1770	Flexure	
Boron	SP-272 Epoxy		1450	Grips. Straight Specimen	42
			1470	Honeycomb Beam	

high modulus material if the precautions outlined are not taken.

Table 6

Comparative Compressive Strength Values (MN/m^2)

Fibre	Matrix	Volume % Fibres	σ_c^u	Method	Reference
Morganite Type II	Epi-Rez 508 Epoxy	∿50	986	Grips	8
			772	Free Standing	
Morganite II	Epoxy	∿64	993	End support	24
Celanese Type I	Epi-Rez 508 Epoxy	60	786	Grips	8
			398	Free Standing	
Harwell I	Epoxy	56	727	End Fittings	43
Morganite I	Epoxy	63	460	End supports	24
Boron	SP-272 Epoxy	>51	3060	Honeycomb Beam	24
			3170	Honeycomb Beam	42
E-Glass	Epoxy		980	Grips	44

Flexural Test

If only a qualitative assessment of tensile strength is required for comparison or control purposes, the three or four point bend tests offer methods that overcome the gripping problems associated with tensile testing and require relatively little specimen preparation. However, owing to the presence of a shear stress distribution in the specimen and the high ratio of tensile to shear strength of many composite systems, results and failure modes are often dependent upon specimen dimensions.

The test arrangements have been discussed previously and are shown schematically in Figs. 3 and 4. If failure is initiated at a point of loading, reaction pads or larger diameter rollers should be used to relieve stress concentrations. A maximum tensile stress arises on the surface of the beam opposite the centre roller in 3-point loading and, for a material that has equal tensile and compressive stiffnesses and is linearly elastic to failure, this maximum stress has magnitude,

$$\sigma_{max} = \frac{3}{2}\frac{WL}{ab^2} . \qquad \ldots (32)$$

σ_{max} is equal to the tensile stress component σ_1 in the testing of longitudinal specimens and to σ_2 or σ_3 for transverse samples. Eq. (32) is used to calculate flexural strength for tensile failures in the region of maximum stress.

The mode of failure under 3-point flexure depends upon the span-to-depth ratio, L/b, of the beam and the relative magnitudes of the tensile, compressive and interlaminar shear strengths of the composite. A maximum shear stress of magnitude $3W/4ab$ occurs on the neutral plane and so a rough criterion for expecting a tensile failure is,

$$\frac{2L}{b} > \frac{\sigma^u_{max}}{\tau^u_{min}} \qquad \ldots (33)$$

where σ^u_{max} and τ^u_{min} are, respectively, the maximum tensile and minimum shear strengths for the composite. τ^u is equal to the ultimate value for the stress component σ_5 or σ_6 in the measurement of longitudinal tensile strength and to σ_4 for transverse tensile strength. This expression is readily satisfied in measurements of transverse strength but forms only a broad criterion (11) for expecting a certain type of failure in longitudinal specimens owing to uncertainties in σ^u_{max} and τ^u_{min} arising from the presence of defects in the matrix and from scatter in fibre strength, fibre distribution and fibre orientation (assuming variations with fibre fraction and surface treatment are known). Even when predominantly tensile failures have been observed in longitudinal samples, some composite systems exhibit a dependence of calculated flexural strength upon span-to-depth ratio and upon interlaminar shear strength as reflected by fibre treatment, see Table 7. It can be concluded that the mode of failure, and hence calculated flexural strength, of a specimen in 3-point bending may be influenced by shear interactions which are made negligible only by working at large span-to-depth ratios. For this reason, ratios in excess of 40 are necessary for some composite systems. Although 4-point loading has the advantage of introducing a pure bending moment in the volume of the beam between the inner loading points, the criterion for no shear failure in the volume between the inner and outer rollers is then,

$$\frac{4c}{b} > \frac{\sigma^u_{max}}{\tau^u_{min}} \qquad \ldots (34)$$

which requires a longer beam than the 3-point method.

Table 7

Variation of Flexural Strength (MN/m^2) with Span-to-Depth Ratio and Interlaminar Shear Strength (MN/m^2) for Type I and Type II Carbon Fibre-Epoxy Composites

FIBRE	VOL %	ILSS	SPAN-TO-DEPTH RATIO				Ref.
			10	16	20	40	
Type I Untreated	60	~25	365	483	621	676	54
Type I Treated	60	~70	910	965	1041	1069	54
Type II Untreated	60	~65	986	1172	1262	1165	54
Type II Treated	60	~90	1207	1379	1434	1386	54

Results from flexure tests on off-axis specimens show a significant dependence of strength upon specimen width which varies with the angle between the fibre axis and the applied bending moment (39). This arises from a twisting moment induced in the beam by coupling between tensile and shear deformations. The magnitude of this effect can be reduced by using samples of large length to width ratio and removed altogether with balanced angle-ply systems since the twisting moments induced by each layer cancel.

Tensile and flexural strengths are compared in Table 5. The general lack of agreement between tensile and flexural strength values is probably attributable to differences in failure mode and the validity of the assumptions involved in deriving Eq. (32).

The testing of a honeycomb sandwich beam in flexure offers the advantage of separating tensile and compressive failure modes. Fig. 5 shows how a specimen may be loaded in tension or compression and how clamping and support problems are eliminated. The beam design and properties of the honeycomb core are given in references (4) and (5). The maximum tensile or compressive stress occurs in the area of the outer face of the specimen between the centre supports and is of magnitude:

$$\sigma_{max} = \frac{kWL}{2ab[t + (b + b')/2]} \qquad \ldots (35)$$

cf. Eq. (13). If the specimen fails by tension or compression before failure of the core or the opposite face, then this equation may be used to calculate the specimen strength. The function of the honeycomb core is to transmit a tensile or compressive load to the specimen by means of a shear stress established at the specimen-honeycomb interface. The magnitude of this shear stress is,

$$\tau_{max} = \frac{W}{2a[t + (b + b')/2]} \qquad \ldots (36)$$

and so the bond shear strength must be greater than $\sigma^u b/kL$ to produce a tensile failure in the specimen. σ^u is dependent upon specimen character as described in the previous test. A comprehensive set of data comparing the sandwich beam test with other methods for determining flexural and compressive strengths is not available in the literature. However, Tables 5 and 6 illustrate some measurements on boron-epoxy which indicate that this technique shows promise as a reliable test for compressive and flexural strength measurements.

b. Measurement of Shear Strength

Short Beam Shear Test

The relative magnitudes of the maximum shear and tensile stresses in a beam under 3-point flexure depends upon the span-to-depth ratio of the specimen. If a sufficiently small ratio is chosen, a shear mode of failure is favoured in the neutral plane of longitudinal specimens corresponding to an ultimate interlaminar shear stress of magnitude,

$$\tau^u = \frac{3W}{4ab} \qquad \ldots (37)$$

Although, in general, it is found that the calculated shear strength is dependent upon specimen dimensions, results are influenced by the quality of the fibre matrix bond. The test is, therefore, valuable for indicating the deterioration of bond strength under different environments and for assessing improvements in composite shear strength resulting from various treatments of the fibre surface.

The validity of Eq. (37) is limited to beams of small width-to-depth ratio, a/b. Sattar and Kellog (45) calculate that the shear stress in the neutral plane varies along the width reaching a maximum value at the sides which is higher than the value given in Eq. (37) by a factor which depends upon a/b and the composite system studied. For this reason, width-to-depth ratios below 2 are recommended. The span-to-depth should be chosen to produce a shear failure and an approximate criterion for predicting this is given, as discussed previously, by $2L/b < \sigma^u/\tau^u$. Span-to-depth ratios between four and six are commonly used, but values as high as eight have been quoted as giving shear failures in specimens of low shear strength. When testing materials of high shear strength, such as treated carbon fibre reinforced plastic, a complex failure mode can be obtained with ratios as low as four. This type of failure can be realised by reference to the load deflection curve (46), see Fig. 23. Reducing the ratio further invalidates the test by introducing compressive stresses between the top and bottom rollers and so an alternative test method, such as a torsion test, should be used to measure the shear strength. Table 8 illustrates the variation of interlaminar shear strength with fibre treatment and span-to-depth ratio. It may be concluded

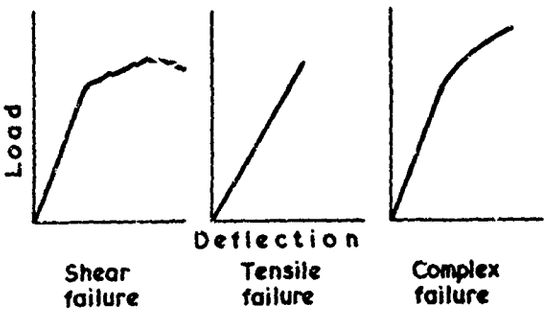

FIG.23 LOAD-DEFLECTION CURVES FROM SHORT BEAM SHEAR TEST

that interlaminar shear strength increases with fibre strength and treatment but decreases with L/b especially if a tensile failure is caused by choice of too high a ratio.

Torsion Test

The torsion test is suitable for specimens in the shape of an accurately prepared rod or tube and, owing to the pure shear stress established, is suitable for producing fundamental material data. The specimen is tested in a machine capable of applying and recording a torque. Collet type grips have proved successful and grip alignment is again an important precaution. If a shear failure results at a torque, M_t, the shear strength may be calculated from,

$$\tau^u \simeq \frac{M_t}{2\pi r^2 b} \qquad \ldots (38)$$

where r is the mean radius and b the wall thickness of the specimen. Owing to the uniform state of shear that occurs in a thin walled tube under

Table 8

Variation of Interlaminar Shear Strength (MN/m^2) with Span-to-Depth Ratio for Type I and Type II Carbon Fibre-Epoxy Composites

FIBRE	VOL %	SPAN-TO-DEPTH RATIO			REF.
		5	7.5	10	
Type I Untreated	60	21	20	17	54
Type I Treated	60	73	59	44*	54
Type II Treated	60	93	74	60*	54

*Tensile Break

torsion, the test offers a method for studying the dependence of shear strength with angle to the fibre axis for filament wound test specimens. Table 9 compares data from this test with results from the short beam test and reference (47) discusses the relative merits of a variety of methods for the determination of shear strength.

4c. Measurement of Fracture Energy

Impact Test Methods

In the Charpy and Izod impact tests, the work done to fracture a sample (fracture energy) is equated to the energy lost in breaking the specimen by the impact of a pendulum mass which strikes the specimen at the lowest point of its swing. One disadvantage of these methods is that an uncertain amount of the applied energy is irrecoverably lost as vibrational energy in the test system and as stored or dissipated energy carried away by the broken specimen. For this reason, the specimen is usually notched and loaded in flexure so as to localise the fracture and reduce the strain energy in the specimen and machine on failure. In the Charpy test, the specimen is supported horizontally at its ends and the pendulum mass strikes the centre of the beam, whereas the Izod test specimen is clamped to form a vertical cantilever and struck at its free end. Both tests have the advantage of being able to measure impact energies for a variety of test variables, but the Charpy test has the additional advantages of rapid interchangeability of samples and of avoiding errors associated with specimen clamping. These test arrangements are illustrated schematically in Fig. 24. Fracture energies are usually quoted as the ratio of energy lost to the area of cross-section of the specimen at the notch.

The height over which the pendulum weight falls determines the velocity of impact which may affect the mode of failure. The dependence of fracture energy on velocity should therefore be studied. Notch and specimen dimensions are critical features of these tests. Barker (48) has studied the effect of notch depth and radius on a range of carbon fibre reinforced resin systems and Harris et. al. (49) have observed that results on specimens where the notch has been sharpened by a razor show less scatter. Hancox (50) shows that although impact energies increase linearly with specimen breadth, they increase more rapidly with depth. This is interpreted in terms of a greater contribution to the strain energy stored in the thicker specimens from shear deformation. The modes of failure of composite specimens in these tests are generally complex. The fracture of treated fibre specimens is usually brittle but for untreated material, contributions from delamination and fibre pull-out increase the measured work of fracture considerably (51).

The drop weight and ballistic impact test methods are qualitative tests only. The ballistic impact method has been used (52) to observe the damage caused in a composite by a projectile of known energy. The mode of failure and extent of damage are assessed visually and so the test is valuable for material comparison only.

Table 9

Comparative Shear Strength Values (MN/m^2)

FIBRE	MATRIX	VOLUME % FIBRES	τ^u	METHOD	REFERENCE
Treated TI Carbon	Epoxy	50-60	59^T	Short Beam Shear, L/b = 5	55
Untreated TI Carbon	Epoxy	50-60	24^s	Short Beam Shear, L/b = 5	
Morganite Treated Type I	Epoxy	55	39^s	Torsion Rod	46
			44^T	Short Beam Shear, L/b = 4	
Morganite Treated Type I	Epoxy	58	59^s	Torsion Rod	46
			60^s	Short Beam Shear, L/b = 4	
Morganite Untreated Type I	Epoxy	61	22^s	Torsion Rod	46
			22^s	Short Beam Shear, L/b = 4	
Treated TII Carbon	Epoxy	50-60	77^T	Short Beam Shear, L/b = 5	55
Untreated TII Carbon	Epoxy	50-60	64^s	Short Beam Shear, L/b = 5	
E-Glass	Epoxy	58	90^s	Torsion Rod	46
			94^s	Short Beam Shear, L/b = 4	

τ^{uT} Observed Tensile Failure

τ^{us} Observed Shear Failure.

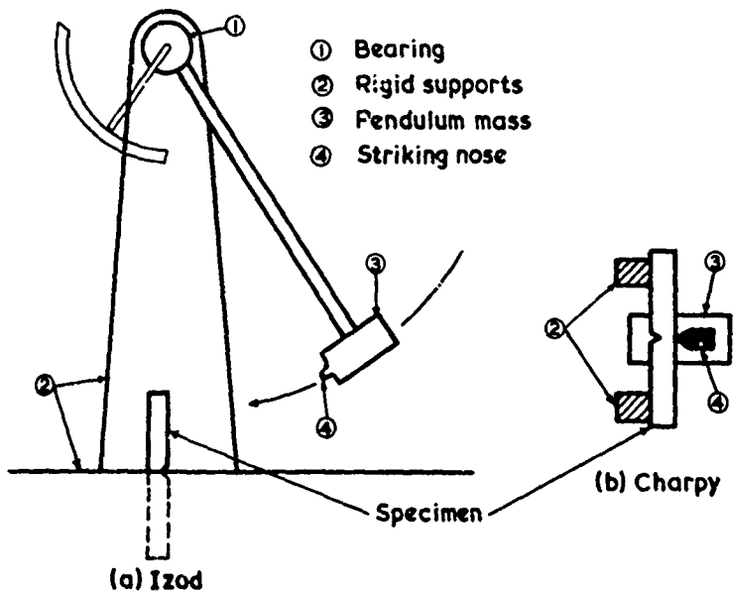

FIG.24 PENDULUM IMPACT TESTS

The Slow Bend Test

The purpose of this test is to restrict the work done to fracture a specimen to the propagation of a crack and to damaging only the material in the vicinity of the crack which results unavoidably from the crack growth. The specimen is notched and loaded in flexure as shown in Fig. 25. The usual wedge shaped notch may be used in an attempt to localise the failure but a triangular notch (53) restricts the load required to initiate failure to a small value, even for a notch insensitive material, thereby allowing controlled crack propagation and reducing the energy lost in deforming the bulk material to a negligible value. The load and deflection during the test are recorded and fracture energies calculated from the area under the curve divided by the cross-sectional area of the specimen at the notch. A schematic representation of a curve is shown in Fig. 26. Crack initiation and partial propagation is

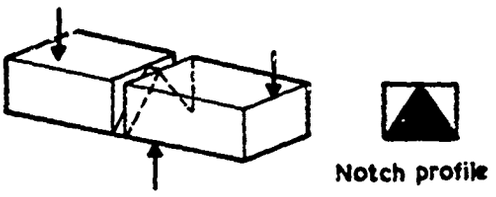

FIG.25 SLOW BEND TEST SPECIMEN

diversity in specimen and test variables for results quoted in the literature. A programme at the National Physical Laboratory has been designed to investigate the dependence of fracture energy measurements from the slow bend test upon rate of loading and notch geometry. Small but significant increases of fracture energy with cross-head speeds in the range 0.1 to 5 centimetre/minute have been observed in a woven glass reinforced epoxy system. Values from impact tests at a pendulum velocity of 5.10^4 centimetre/minute are substantially higher and, as yet, it has not been ascertained whether the discrepancy between results is due entirely to the difference in rate of loading. Further composite systems are being studied to increase confidence in measurements of fracture toughness.

associated with the sudden load drop after which the crack is arrested in the specimen. Further increase in deflection gives rise to controlled crack propagation. The use of a hard test machine and a stiff load cell is important when testing brittle materials otherwise the energy stored in the machine on crack initiation may be sufficient to propagate the crack catastrophically through the specimen. The mode of failure, being restricted to the plane of the notch, is usually different from that obtained in an impact test.

Table 10 compares results from a pendulum impact test and a slow bend test. The difference between values from the two methods is expected to be greater for treated fibre specimens where the crack propagation energy may be smaller than the crack initiation energy. A more comprehensive comparison of results on different composite systems is not available at present owing to the

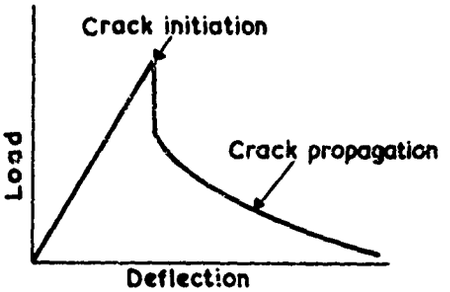

FIG.26 LOAD-DEFLECTION CURVE FOR SLOW BEND TEST

Table 10

Comparative Fracture Energy Values (KJ/m^2) for Some Carbon Fibre Reinforced Plastics

FIBRE	MATRIX	VOLUME % FIBRE	F.E.	METHOD	REFERENCE
Type II Untreated	Epikote 828 Epoxy	60	250	Notch Izod	52
Type II Treated		60	80		
Untreated Type I	Polyester	40	68	Slow Bend	49
			67	Notch Charpy	
Type I Treated	Polyester	40	18	Notch Charpy	49
Type I Untreated	Epoxy	40	42	Slow Bend	56
Type I Treated			6		

4d. Measurement of Fatigue Life

The mechanical properties of materials decrease under repeated application of a cyclic load. In composite materials, the reduction in strength is brought about by the gradual introduction of microcracks in the matrix and a deterioration of the fibre-matrix bond. A study of the fatigue behaviour of composites may be made under tensile-compressive, flexural and torsional deformations. In general, the fatigue life depends upon the mode of failure and so the precautions outlined in the various test methods in Section 4a should be taken if premature failure, from the introduction of bending moments or stress concentrations, is to be avoided. Lossy composite systems are likely to show a dependence of fatigue life upon frequency owing to the heat generated in the specimen during each cycle (57), although this dependence will be reduced if the material is reinforced with conducting fibres (56).

The rate at which the residual strength decreases under a particular loading condition depends upon the amplitude of the cyclic stress and the mean stress level (58). An illustration of fatigue behaviour is therefore given by a plot of the stress amplitude against the logarithm of the number of cycles to failure for a range of mean stress levels, (S-N curve). Examples of S-N curves, obtained from reference (56), are shown in Fig. 27 for the tensile and flexural fatigue behaviour of type I carbon fibre reinforced plastic. If a sufficiently large range of mean stress levels and amplitudes is covered, the data may, alternatively, be presented by means of constant life plots which show the relationship between stress amplitude and mean stress for constant fatigue lives. Owen and Morris (59) have obtained a constant life plot at 10^6 cycles for type I carbon fibre-epoxy composite, see Fig. 28.

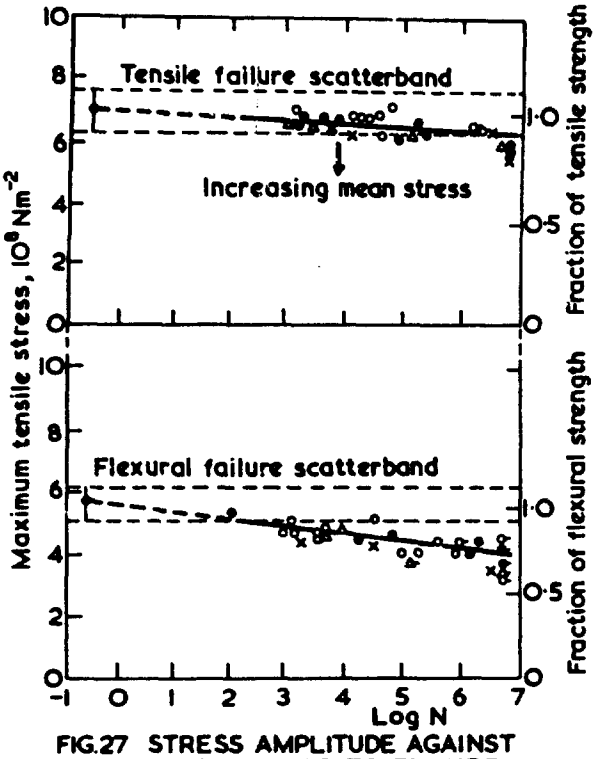

FIG.27 STRESS AMPLITUDE AGAINST NUMBER OF CYCLES TO FAILURE TYPE I CFRP (56)

The peak of the curve for each life is displaced from the zero mean stress level owing to the lower compressive strength compared with the tensile value for this system.

There are no standards for the fatigue testing of composites. The ASTM manuals STP 91 and 91A describe basic terms and definitions and references (56)→(59) recommend specimen dimensions and cycle frequencies for unidirectional and cross-ply carbon and glass reinforced plastics.

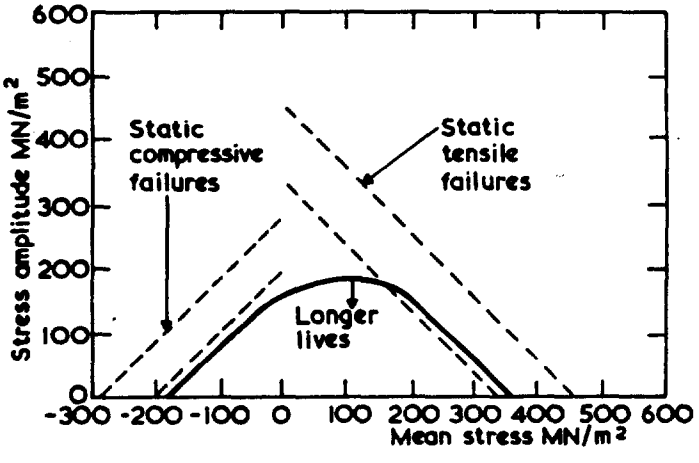

FIG.28 CONSTANT LIFE CURVE FOR TYPE I CFRP AT 10^6 CYCLES (59)

5. THERMAL AND ELECTRICAL MEASUREMENTS

Regarding the thermal properties of unidirectional composites, the linear expansion coefficient and thermal conductivity are of particular interest owing to the predicted anisotropy of these quantities. The linear expansion coefficient, $\alpha_l = \Delta L/L\,\Delta T$, is determined from measurements of the change in length ΔL resulting from a temperature change ΔT. For plastic specimens of length between 50 mm and 125 mm, a standard method (ASTM D696-70) employs a dial gauge, or equivalent device accurate to ±10 μm, in contact with a vitreous silica tube which rests on the top surface of the sample. For smaller specimens, or in cases where α_l or ΔT is small, then more sensitive methods may be required. One such method (60) has been developed at the NPL and includes a tilting mirror and autocollimator to measure the length change of samples relative to that of fused silica slip gauges. With this technique, which is illustrated in Fig. 29, length changes accurate to 0.01 μm can be measured. Table 11 includes values of the linear expansion coefficients α_1 and α_2, measured along and perpendicular to the fibre axis, respectively, for some unidirectional carbon fibre composites.

Several methods have been developed for the determination of thermal conductivity. Absolute measurements can be made by means of the guarded hot plate method (ASTM C177-3) in which the sample is sandwiched between a heated and a cooled plate, and a guard plate surrounding the hot plate (and maintained at the same temperature) ensures that the heat flow is normal to the sample surface (Fig. 30).

At steady state, the thermal conductivity, $k = qL/A(T_1-T_2)$, is evaluated from the measured rate of heat flow q, temperature difference T_1-T_2 and distance L between the two sample surfaces, and area A of a selected isothermal surface. Various comparative methods have been used, and these are simpler and less time consuming than the absolute technique. In the Northrup method (61), the sample is placed in series contact with a standard material of known conductivity and the heat flow determined from the temperature drop across the standard. Bishop and Rogers (62) have developed a method of this kind in which the steady state thickness of a layer of melting wax in contact with the sample is measured. Rapid determinations on small samples are possible with the NPL thermal comparator (63), which measures the differential temperature decrease of two initially heated phosphor bronze spheres, one of which is in contact with the specimen (Fig. 31). With this technique the thermal conductivity is obtained by comparing graphically the differential cooling rate with the cooling rates observed for a range of conductivity standards. In the so-called "flash method" (64), a short duration light pulse is absorbed on the front surface of the sample and the temperature of the rear surface is recorded as a function of time. From this record, the thermal diffusivity and heat capacity are obtained, and the conductivity is evaluated as the product of diffusivity, heat capacity and density. Table 11 illustrates the anisotropy of thermal conductivity for some undirectional carbon fibre composites.

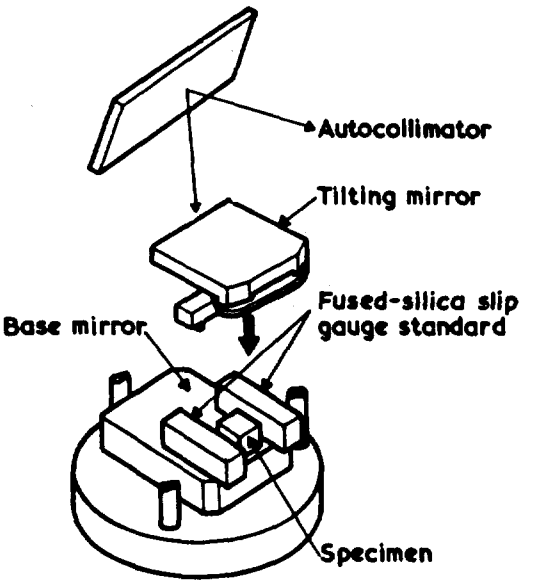

FIG.29 TILTING MIRROR DEVICE FOR THERMAL EXPANSION MEASUREMENT

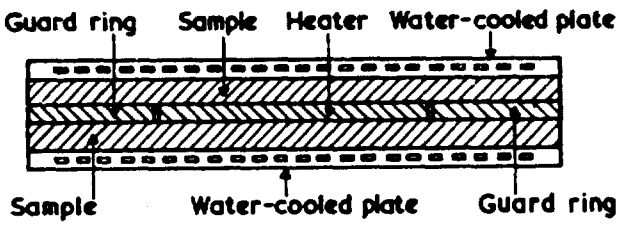

FIG.30 THERMAL CONDUCTIVITY. GUARDED PLATE

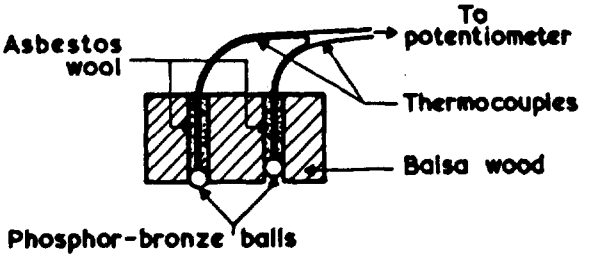

FIG.31 THERMAL COMPARATOR

For the determination of heat capacities, the method of mixtures is often adequate, but the differential scanning calorimeter, recently automated at the NPL, is particularly rapid and convenient. In the latter method, the differential power input is measured necessary to maintain the sample and a standard at the same temperature as the temperature is varied.

The electrical conductivity of a material is equal to the inverse of the resistivity, ρ, which is defined as the d.c. resistance between opposite faces of a cube of the material of unit length. Thus,

$$\rho = \frac{RA}{L} \qquad \ldots (39)$$

where A is the cross-sectional area of the sample of resistance R in the direction of the length, L. The anisotropy in resistivity of a composite material is obviously governed by the relative conductivities of its components. For example, a composite containing uniaxially aligned metal fibres in an insulator can have a resistivity varying from 10^{-6} ohm.m along the fibres to several orders of magnitude higher transverse to this direction, whereas an insulating system, such as a glass reinforced plastic, may have a resistivity greater than 10^{12} ohm.m which depends only slightly upon direction. Some values for a unidirectional carbon fibre reinforced plastic system are given in Table 11. Test methods designed to cover this range of resistivity involve the measurement of the resistance of a known length and area of a sample either by recording the current through and voltage across the sample or by comparison with a standard resistor using a bridge circuit. Owing to the dependence of the resistivity of many materials upon temperature or specimen surface condition, tests should be performed in a temperature and humidity controlled environment.

Table 11

Some Thermal and Electrical Properties of Unidirectional Carbon Fibre Composites[a]

Fibre Type	Matrix Type	Volume Percent Fibres	α_1 (10^{-6}/°C)	α_2 (10^{-6}/°C)	k_1 Jm/m² s °C	k_2 Jm/m² °C	ρ_1 μΩm	ρ_2 μΩm	Method	Ref.
RAE Type I Carbon Fibre	Polyester	40	-0.69	28.7					Auto-collimator 17°C→60°C	NPL Report M 523 ST 4837
					17	0.63			Comparative Melting Wax	68,69
							26	68,000		
	Polyimide	50 (Nominal)			27	0.70				70
							17	61,000		
Thornel 25	ERL 2256	50	0.4	41					Length Change Compared with Invar Standard	71
Thornel 40		67	-0.7	29						
Thornel 25		50			12.1	0.63			Flash Method	
Thornel 40		67			54.4	0.96				

a. α = linear expansion coefficient, k = thermal conductivity, ρ = electrical resistivity. Subscripts 1 and 2 denote directions along and perpendicular to the fibre direction respectively.

Resistivities below 1 ohm.m are commonly measured by the method described in BS 3239 and shown in Fig. 32. The probes X and Y have an accurately known separation and contact the specimen at points separated from the neighbouring current contact by a least 1.5 times the cross-sectional perimeter of the specimen. Measurement of the voltages across XY and across the standard resistor, r_s, enables the specimen resistance to be deduced. Alternatively, comparison of the resistance of the specimen with the standard may be made using a Kelvin double bridge. This bridge eliminates the contribution of the resistance of the connecting leads to the required resistance values. When a constant voltage is applied across a dipolar insulating material, polarisation of the medium results in a current flow that decreases with time to an equilibrium value, i_e, see Fig. 33. The resistance may be quoted as the ratio of applied voltage to the equilibrium current or to the current after a known time. For the measurement of insulation resistance, see for example reference (28) and BS 903. C2, the specimen commonly takes the form of a thin disc sandwiched between electrodes. The three terminal cell, illustrated in Fig. 34a, employs a guard ring which is connected into the circuit so that fringing fields and conduction across the surface of the specimen do not contribute to the measured current. Fig. 34b shows a circuit for the measurement of surface resistance, R_s, as described in BS 903 C1. The surface resistivity is then calculated from the equation,

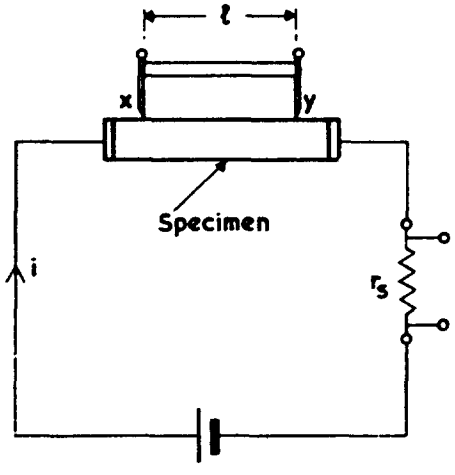

FIG.32 MEASUREMENT OF LOW RESISTIVITIES

$$\rho_s = \frac{2\pi R_s}{\log_e (d_2/d_1)} \qquad \ldots (40)$$

where d_2 is the internal diameter of the guard ring and d_1 is the diameter of the inner electrode. Electrical screening and the reduction of thermal emf's are important precautions in the measurement of very low current.

The response of a dipolar insulating material to an alternating voltage or field ($E^* = E_0 \exp(\underline{i}\,\omega t)$) is represented by the real and imaginary components, ε' and ε'' respectively, of a complex dielectric constant ε^*,

$$\varepsilon^* = D^*/E^* = \varepsilon' - \underline{i}\,\varepsilon'' \qquad \ldots (41)$$

$$\tan \delta_\varepsilon = \varepsilon''/\varepsilon'$$

where D^* is the complex dielectric displacement (charge) and $\tan \delta_\varepsilon$ is the dielectric loss tangent, δ_ε representing

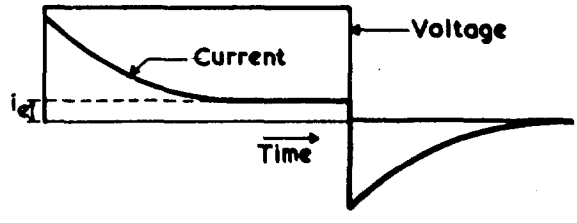

FIG.33 VARIATION OF CURRENT WITH TIME IN POLAR DIELECTRICS

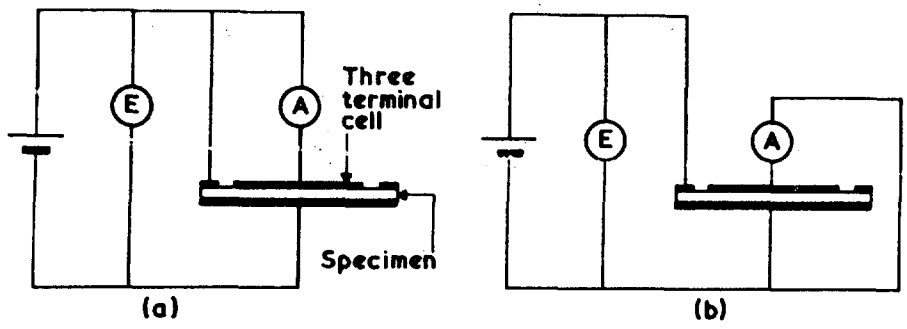

FIG.34 MEASUREMENT OF HIGH RESISTIVITIES

the phase angle by which the displacement cycle lags the applied field. This phase lag arises from the finite time required for the electric dipoles to orient in the field, and has a similar origin to the transient charging current observed in resistivity measurements. For dipolar materials, ε' decreases with increasing frequency, showing the largest drop in frequency regions (or relaxation regions) where ε'' and $\tan \delta_\varepsilon$ exhibit maxima. This behaviour is analogous to, and may be correlated with, the frequency dependence of the complex mechanical compliance, and may be interpreted structurally in terms of the dipolar mobility (28). For heterogeneous composite mixtures, the dielectric constants will depend on the dielectric constants, concentrations and shapes of the constituents and a review of this subject has been given by De Loor (65). We also note that the dielectric field and displacement are vector quantities and that, in general, the dielectric constant is a second rank tensor ($D_i^* = \varepsilon_{ij}^* E_j^*$ where $i, j = 1, 2$ or 3). For anisotropic materials, such as oriented structures or unidirectional fibrous composites, more than one component of the dielectric tensor may be required to fully characterize the material.

A feature of dielectric measurements is that they can be performed with little difficulty over a very wide range of frequency (10^{-4} to 3×10^{10} Hz), and details of available methods are given by McCrum, Read and Williams (28). For low frequency measurements ($< 10^8$ Hz) samples are conveniently studied in the form of flat circular discs within a three-terminal cell, and it is convenient to regard the sample as being electrically equivalent to a capacitance C_x in parallel with a resistance R_x. The dielectric parameters are then determined from,

$$\varepsilon' = \frac{C_x}{C_o}, \quad \varepsilon'' = \frac{1}{R_x \omega C_o}, \quad \tan \delta_\varepsilon = \frac{1}{R_x C_x \omega} \qquad \ldots (42)$$

where $C_o = A\varepsilon_o/d$ is the capacitance of the dielectric cell of area A and electrode separation d in the absence of the specimen. ε_o is the permittivity of free space. In the frequency range 10^{-4} to 10^{-1} Hz the d.c. transient current method outlined above can, with suitable transform analyses, be used to measure the components of ε^*. At frequencies between 10^{-2} and 10^7 Hz, various bridge circuits are used to determine C_x and R_x and hence the components of ε^* (Eq. (42)). The equipment employed at the NPL includes an ultra-low frequency Scheiber bridge (10^{-2} to 10^2 Hz) and a transformer ratio-arm bridge (10 to 10^6 Hz) which is commercially available from the General Radio Co. The latter method is capable of high accuracy and has the added advantage that impedances between the guard circuit and electrodes do not enter the balance condition. In the range 10^5 to 10^8 Hz a resonance circuit is employed, together with a two-terminal dielectric cell, and C_x is determined by means of a variable precision capacitor which is used to tune the circuit to resonance with and without the sample. The dielectric loss tangent is determined from the difference in half width of the resonance peak with and without the specimen. In the microwave region, typically 10^9 to 3×10^{10} Hz, slotted lines or cavity resonators are employed and the dielectric parameters determined from the effect of the sample on the standing waves. Although a wide range of methods is thus available for the measurement of dielectric properties, few systematic studies seem to have yet been made on fibre reinforced composites. Dielectric measurements have been employed, however, to monitor the degree of cure of thermosetting polymers (66).

A noteworthy example of results obtained from electrical and thermal measurements on composites is afforded by some work recently reviewed by Weiss (67) on composites formed by the unidirectional solidification of metallic eutectic mixtures. One interesting result concerns an effect known as magnetoresistance, which is particularly significant in a eutectic containing aligned needles of NiSb (1.6 weight percent) in a matrix of InSb semi-conductor. If an electrical current flows in the longitudinal direction of a bar of this composite, and the NiSb needles are oriented in the transverse direction, then the measured resistance in the longitudinal direction exhibits a marked increase if a magnetic field is applied in the transverse direction perpendicular to the fibres. For a magnetic induction of 10k Gauss the resistance is found to increase by a factor of about 16. Weiss has interpreted this result in terms of the Hall effect by means of which the magnetic field induces a voltage in the fibre direction. This voltage is short-circuited by the conducting fibres and the Hall current flowing through the fibres produces a further Hall voltage parallel to the primary current. The secondary Hall voltage adds to the primary voltage, thus producing an additional resistance due to the magnetic field. Magnetoresistive devices made from the InSb - NiSb eutectic have found several applications including the measurement of magnetic fields and as non-contacting variable resistances. Apart from the resistance increase in a magnetic field, a temperature difference is also observed between the two lateral surfaces of the composite containing the fibre ends. This observation results from the Peltier effect of the Hall current at the fibre extremities, as a result of which heat is absorbed at one surface and emitted at the other. The inverse effect corresponds to the creation of a Hall voltage in the longitudinal direction if the lateral surfaces containing the fibre ends are subjected to a temperature difference. We then obtain an Ettingshausen-Nernst voltage increased by the Hall effect, and at room temperature about 1 mV/°C temperature difference is observed for a magnetic field

of 7k Gauss. As a result of this thermomagnetic effect, the InSb - NiSb eutectic composite has been used for the production of a room temperature far infrared detector.

ACKNOWLEDGEMENTS

We wish to thank many of the staff members of the National Physical Laboratory for their helpful advice and comments. Thanks are also due to Drs. K.F. Rogers and J.K. Lancaster of the Royal Aircraft Establishment, Farnborough, for discussions concerning the measurement of thermal properties.

REFERENCES

1. HEARMON, R.F.S. An Introduction to Applied Anisotropic Elasticity, Oxford Univ. Press, 1961.

2. TSAI, S.W. and PAGANO, N.J. Composite Materials Workshop. Technomic Publishing Co., Stamford, Conn., 1968, p.233.

3. GUYOT, H. and HEDIARD, M. Mesures de Modules Elastiques Sur Composite Fils - Resine, AGARD Conference Proceedings No. 63, September 1971, Paper No. 5.

4. WADDOUPS, M.E. Composite Materials Workshop, Technomic Publishing Co., Stamford, Conn., 1968, p.254.

5. GRIMES, G.C. and BRONSTAD, M.E. Test Methods for Composites, Handbook of Fiberglass and Advanced Plastics Composites, Edited by G. Lubin, Van Nostrand Rheinhold Company, New York, 1969, p.708.

6. DASTIN, S., LUBIN, G., MUNYAK, J. and SLOBODZINSKI, A. Composite Materials: Testing and Design, ASTM Special Technical Publication 460, 1969, p.13.

7. HADCOCK, R.N. and WHITESIDE, J.B. Composite Materials: Testing and Design, ASTM Special Technical Publication 460, 1969, p.27.

8. PARK, I.K. International Conference on Carbon Fibres, their Composites and Applications, The Plastics Institute, London, 1971, Paper No. 23.

9. TIMOSHENKO, S. and GOODIER, J.N. Theory of Elasticity, 2nd Edition, McGraw Hill Book Co. 1951.

10. ROTHMAN, E.A. and MOLTER, G.E. Composite Materials: Testing and Design, ASTM Special Technical Publication 460, 1969, p.72.

11. MULLIN, J.V. and KNOELL, A.C. Materials Research and Standards, Vol. 10, December 1970, p.16.

12. DAUKSYS, R.J. and RAY, J.D. J. Composite Materials, Vol. 3, October 1969, p.684.

13. BRACCO, A., MANNONE, G. and SATTIN, M. Elastic Constants Evaluation of a Reinforced Plastic Material, AGARD Conference Proceedings No. 63, September 1971, Paper No. 7.

14. OGORKIEWICZ, R.M. and MUCCI, P.E.R. Composites, Vol. 2, September 1971, p.139.

15. JOHNSON, A.F. Bending and Torsion of Anisotropic Beams, Maths Report No. 96, NPL, Teddington, Middx., March 1971.

16. SPIES, G.J. and Th. de JONG. Determination of Elastic Constants of a Unidirectionally Reinforced Plastic, AGARD Conference Proceedings No. 63, September 1971, Paper No. 2.

17. PABIOT, J. Caracteristiques Lineaires et Non - Lineaires D'un Composite a Renforcement Unidirectionnel Epoxy - Silice, AGARD Conference Proceedings No. 63, September 1971, Paper No. 6.

18. HALPIN, J.C. and PAGANO, N.J. J. Composite Materials, Vol. 2, January 1968, p.68.

19. GRESZCZUK, L.B. Composite Materials, Testing and Design, ASTM Special Technical Publication 460, 1969, p. 140.

20. PETIT, P.H. Composite Materials, Testing and Design, ASTM Special Technical Publication 460, 1969, p.83.

21. HALPIN, J.C., PAGANO, N.J., WHITNEY, J.M. and WU, E.M. Composite Materials, Testing and Design, ASTM Special Technical Publication 460, 1969, p.37.

22. de MEESTER, P., DAMBRE, P. and DERUYTTERE, A. Mechanical Properties of Epoxy - Silica Composite Materials, AGARD Conference Proceedings No. 63, September 1971, Paper No. 3.

23. SLEPETZ, J.M. Elastic Characterization of Fiber Reinforced Composites, AGARD Conference Proceedings No. 63, September 1971, Paper No. 8.

24. RAY, J.D. International Conference on Carbon Fibres, their Composites and Applications, London 1971, Paper No. 29.

25. ADSIT, N.R. and FOREST, J.D. Composite Materials, Testing and Design, ASTM Special Technical Publication 460, 1969, p.108.

26. DIMMOCK, J. and SPEDDING, C.E. Composites, Vol. 1, December 1970, p.356.

27. ASHTON, J.E. J. Composite Materials, Vol. 2, January 1968, p.116.

28. McCRUM, N.G., READ, B.E. and WILLIAMS, G. Anelastic and Dielectric Effects in Polymeric Solids, Published by John Wiley and Sons, 1967.

29. DUDEK, T.J. J. Polymer Sci., Part A-2, Vol. 8, 1970, p.1575.

30. ADAMS, R.D., FOX, M.A.O., FLOOD, R.J.L., FRIEND, R.J. and HEWITT, R.L. J. Composite Materials, Vol. 3, October 1969, p.594.

31. VINH, N.P. AGARD Conference Proceedings No. 63, Sep[illegible]

32. SCHULTZ, A.B. and TSAI, S.W. J. Composite Materials, Vol. 2, July 1968, p. 368.

33. BRADFIELD, G. NPL Notes on Applied Science No. 30, Her Majesty's Stationery Office, London, 1964.

34. MUSGRAVE, M.J.P. Proceedings of the Royal Society A, Vol. 226, 1954, p.339.

35. MARKHAM, M.F. Composites, Vol. 1 1970, p.145.

36. KELLY, A. and DAVIES, G.J. Metallurgical Reviews, Vol. 10, 1965, p.1.

37. LANTZ, R.B. and BALDRIDGE, K.G. Composite Materials, Testing and Design. ASTM STP 460, 1969, p.94.

38. LEMOE, E.M., KNIGHT, M. and SCHOENE, C. Composite Materials, Testing and Design. ASTM, STP 460, 1969, p.122.

39. ISHAI, O. and LAVENGOOD, R.E. Composite Materials, Testing and Design. ASTM STP, 460, 1969, p.271.

40. GRIMES, G.C. and BRONSTAD, M.E. Handbook of Fiberglass and Advanced Plastics Composites. Ed. G. Lubin, Van Nostrand Rheinhold Company, New York, 1969, p.727.

41. STURGEON, J.B. Specimens and Test Methods for Carbon Fibre Reinforced Plastics. RAE Technical Report No. 71026, February 1971.

42. LANTZ, R.B. J. Composite Materials, Vol. 3, 1969, p.642.

43. EWINS, P.D. A Compressive Test Specimen for Unidirectional Carbon Fibre Reinforced Plastics. Aeronautical Research Council, C.P. No. 1132. 1970.

44. BROUTMAN, L.J. Modern Plastics, April 1965.

45. SATTAR, S.A. and KELLOG, D.H. Composite Materials. Testing and Design, ASTM STP 460, 1969, p.62.

46. HANNA, G.L. and STEINGISER, S. Composite Materials. Testing and Design, ASTM STP 460, 1969, p.182.

47. ADAMS, D.F. and THOMAS, R.L. Advances in Structural Composites, SAMPE, Vol. 12, 1967, AC-5.

48. BARKER, A.J. International Conference on Carbon Fibres, their Composites and Applications. Plastics Institute, London, 1971, paper 20.

49. HARRIS, B., BEAUMONT, P.W. and de FERRAN, E.M. J. Materials Science Vol. 6., 1971, p.238.

50. HANCOX, N.L. Composites Vol. 2, 1971, p.41.

51. KELLY, A. Proceedings of the Royal Society A, Vol. 319, 1970, p.95.

52. SIDEY, G.R. and BRADSHAW, F.J. International Conference on Carbon Fibres, their Composites and Applications. The Plastics Institute, London, 1971, paper 25.

53. TATTERSALL, H.G. and TAPPIN, G. J. Materials Science, Vol. 1, 1966, p.296.

54. WELLS, H., COLCLOUGH, W.J. and GOGGIN, P.R. Some Mechanical Properties of Carbon Fibre Composites. U.K.A.E.A. report Number AERE-R6149.

55. MERRALL, G.T. and STOLTON, R.E. International Conference on Carbon Fibres, their Composites and Applications. The Plastics Institute, London, 1971, paper 22.

56. BEAUMONT, P.W.R. and HARRIS, B. International Conference on Carbon Fibres, their Composites and Applications. The Plastics Institute, London 1971, paper 49.

57. DALLY, J.W. and BROUTMAN, L.J. J. Composite Materials, Vol. 1, 1967, p.424.

58. BROUTMAN, L.J. and SAHU, S. 24th SPI Conference on Reinforced Plastics, 1969, Section 11-D.

59. OWEN, M.J. and MORRIS, S. International Conference on Carbon Fibres, their Composites and Applications. The Plastics Institute, London 1971, paper 51.

60. NICKOLS, L.W. and ANTHONY, G.V. J. Sci. Instruments, Vol. 43, May 1966, p.303.

61. WILKES, G.B. Heat Insulation, John Wiley and Sons, 1950, p.62.

62. BISHOP, P.H.H. and ROGERS, K.F. The determination of thermal conductivity by means of melting phenomena, R.A.E. Technical Report 66328, 1966.

63. POWELL, R.W. J. Sci. Instruments, Vol. 34, 1957, p.485.

64. PARKER, W.J., JENKINS, R.J., BUTLER, C.P. and ABBOTT, G.L. J. Applied Phys., Vol. 32, September 1961, p.1679.

65. de LOOR, G.P. Dielectric Properties of Heterogeneous Mixtures, Thesis, University of Leiden, 1956.

66. EPSTEIN, G. Testing of Reinforced Plastics, Handbook of Fiberglass and Advanced Plastics Composites, Edited by G. Lubin, Van Nostrand Rheinhold Company, New York, 1969, p.683.

67. WEISS, H. Metallurgical Transactions, Vol. 2, No. 6 June 1971, p.1513.

68. PHILLIPS, L.N. Carbon Fibre reinforced plastics - an initial evaluation. RAE Technical Report 67088, 1967.

69. GILTROW, J.P. and LANCASTER, J.K. International Conference on Carbon Fibres, their Composites and Applications. The Plastics Institute, London 1971, Paper No. 31.

70. ROGERS, K.F. and KINGSTON-LEE, D.M. Proc. 3rd Conference on Industrial Carbons and Graphite, S.C.I., London, April 1970.

71. BLACKSLEE, O.L., PALLOZZI, A.A., DOIG, W.A., SPENCE, G.B. and HANLEY, D.P. 12th National SAMPE Symposium, Vol. 12, Advances in Structural Composites, Western Periodicals Co., 13000 Raymer Street, North Hollywood, Calif., 1967, Paper AC-6.

AUTOMATED DESIGN AND FUTURE DESIGN TRENDS

by

M. E. Waddoups
Project Structures Engineer
General Dynamics Corporation
P.O. Box 748
Fort Worth, Texas 76101
USA

SUMMARY

Due to the fact that composite materials must be designed as a part of the structural design process, the number of design variables and the complexity of the structural design problems have been increased. Modern optimization techniques may be employed for elements which must be repetitiously designed. A major portion of the increased structural efficiency available will result from the capability to use orientation as a design variable. A general trend of moving the design problem from simple component substitution to optimal component design links material behavior to nonstructural disciplines. Examples of the new class of key composites-related optimization problems are presented accompanied by illustrations of the application of modern optimization methods to composite design problems.

METHODS

The primary structural properties of composite material--strength and stiffness--may be controlled by a selection of lamination pattern. Consideration of the practical limits of structural efficiency for the material will readily demonstrate the need for design procedures in the configuration of the composite structure. The lower bound of the specific strength and specific stiffness (Figures 1 and 2) of the advanced composite material is furnished by the quasi-isotropic properties (Reference 1). It is possible to achieve strength and stiffnesses below the quasi-isotropic level; however, it is not necessary in a membrane structure since the maximum load complexity will simply demand equivalent strengths and stiffnesses in any direction.

Design of composite structure differs from design with metals in the addition of design variables and the difficulty in evaluating the effects of anisotropy on structural behavior. For example, consider the design of a simple constant thickness sheet. For metal construction, a single variable (the thickness) is required. For the composite, a minimum of six variables (3 lamina thicknesses and 3 orientations) are required. However, these new variables, if properly exploited, offer the potential of improved structural efficiency. The variables cited include only the parameters associated with the lamination of a single sheet of material. A list containing the design variables which control the material anisotropy are presented below in order of significance:

1) proportion of orientations

2) orientation

3) constituents

   - binder material
   - reinforcement
   - volume fraction

The design variables in item 3 above are lumped together because the designer, due to the necessity to have a consistent material, will generally work within a fixed material system which is characterized and available in volume.

The additional variables provide the opportunity for improving structural efficiency. Although the opportunity is obvious, the methodology through which these gains may be exploited is in an early stage of development. The new variables are being added to a process which has not been geared to the direct treatment of multivariable optimization problems.

The formalization of the structural design problem is necessary for one to properly understand the impact of composite materials. The quantitative structural design problem

may be put into perspective by (Reference 2) formalization as a constrained minimization/maximization problem. This general formulation allows review of specialized techniques available for probable solution plus examination of the restrictions presented by those methods.

The generalization (structural synthesis) is defined as the rational directed evolution of a structural system which in terms of the defined objective efficiently performs a set of specified functional purposes. A structural system is described by a set of quantities some of which are viewed as variables during the design process. Quantities that are fixed at the initiation of the process are called preassigned parameters. Those quantities describing the structural system which are allowed to vary are called design variables.

The environment to which a structural system is exposed should be replaced by several distinct sets (or parametric sets) of mechanical, chemical, or thermal loads. Each set is referred to as a load condition, and the total environment is called a loading system. A failure mode or constraint is defined as a structural behavior characteristic which should be subjected to limitation by the design engineer. Finally, the objective function which is defined in terms of the design variable is the basis used for choice between alternative acceptable designs.

As developed by Schmit (Reference 3) a class of structural synthesis problems may be stated as follows: "given the preassigned parameters and a distinct set of load conditions find the vector d (design variables) so that the objective function m(d) is minimized or maximized subject to a set of inequality constraints on the design variables. $g(d) \geq 0$ where each of the functions g(d) are such that unsatisfactory behavior in each failure mode in each load condition is prevented and the range of the values the design variables may assume is restricted." The general problem may be attacked through the techniques of math programming or, in some cases, sufficiency conditions (Reference 4). The most commonly used specialized technique is that of simultaneous failure modes in which the assumption is made that the optimal design is at the intersection of the active constraints.

Although this hypothesis has been disproven by a variety of counter examples (References 5 and 6), it has formed a useful basis for the development of efficient designs. In the design of composite structures, optimization forms a role which extends beyond that classically assumed for metallic structures. Optimization allows one to select a relatively optimal design, and in many cases, the constraints and design variables are interacting in a nonintuitive manner. In fact, the optimization technique simply allows the realization of an efficient design where the stepwise man/machine iterative solution to the problem is not economically feasible due to the time required to reach a design decision. Consider the design of a flat plate (Reference 7) as shown in Figure 3. The plate is subjected to a uniaxial load of 10,000 lbs/in and will be designed to fit within a 10-inch-square opening. Referring to the original definition of the design problem, it can be shown in Figure 4 that a general format for the problem is consistent with the original definitions. For the design problem cited, there are six design variables and twenty-two design constraints as shown in Figure 5. Adopting the optimization scheme proposed by Fiacco and McCormick (Reference 8) using the Fletcher and Powell (Reference 9) minimization scheme, the synthesis process is automated as shown in Figure 6. The thickness and orientation movements of the design variables through the design process are shown in Figures 7 and 8. The particular design problem illustrated can be solved in 3-1/2 minutes on the IBM 360-65 computer. The example problem was completely designed and the final analysis was tabulated in only 5 times the execution time required for a single analysis. The behavioral analysis included a search of the entire surface area of the plate for the state of strains in the plate of both inplane loads and bending loads.

Examination of the design shown in Table 1 illustrates that the final design was essentially orthotropic. The difference between the lamina angle shown in the table and a 0 ± 45 degree orientation is a consequence of the fact that the plate was considered plane anisotropic with a finite stacking sequence. A slight angle adjustment rendered the plate bending stiffness matrix essentially orthotropic which is encouraging since a symmetric panel with symmetric loads yielded an orthotropic bending stiffness matrix. The design compares favorably with the optimal design deduced from a simultaneous failure mode technique of all $\pm$ 45 degree lamina. An additional benefit from the optimization method used is that the design is created for which constraints are rendered least active.

The optimal design procedure produced a design which had buckling rigidity equivalent to the all $\pm$ 45 degree design and provided sufficient filaments in the direction of the load to allow the design to not be strength critical as is the all $\pm$ 45 degree design.

The panel design procedure illustrated may be used in the design of more complex structure. By determining the distribution of membrane load in a wing or tail structure,

the laminate design and optimum construction concept may be deduced. The results of this type of study are shown in Figure 9.

Table 1

Design Comparisons

Design	θ_1	t_1(in)	θ_2	t_2(in)	θ_3	t_3(in)	W(lbs)	u(lbs/in^2)	K_{bc}*
optimum (strength)	0.0°	0.00	0.0°	0.00	0°	0.315	2.27	180,000	32.0 x 10^6
optimum (buckling)	45°	0.139	-45°	0.139	0°	0.00	2.01	36,800	54.5 x 10^6
NLP (Ref. 7)	46°	0.095	-48°	0.088	0°	0.092	1.98	60,000	48.1 x 10^6

* $\sigma_{cr} = K_{bc}(\frac{t}{b})^2$

If procedures such as the one reviewed are utilized, laminates and panels including panels with multiple load condition and buckling constraints combined with internal pressure may be designed efficiently. Other procedures have been developed for designing structures such as stiffened cylindrical shells (Reference 10) and element geometries such as joints (Reference 11). The procedures have been useful in designing composite structure; however, the process of development has been inverted from the normal process of the design of an airplane. In composite materials, the material was characterized first and then knowledge was gained on the design of a laminate. The design of a laminate passed into simple structural elements which were subcomponents in the design of major components such as wings, tails, and fuselages. As knowledge was gained of these elements, the entire consideration of the component was begun. As reported in Reference 12, the design of a graphite-epoxy wing for a supersonic aerial target provided an additional design constraint. This design constraint resulted from strength interaction with overall surface stiffness requirements dictated by flutter speed requirements.

If a lifting surface (Reference 13) such as a wing or tail for a high transonic or supersonic speed aircraft is optimally designed for strength, the basic strength design results in orientation of most filaments parallel to the 50% chord of the structure. Only enough material to take the basic torsional loads and possibly react fuel pressure loads remain in the panels. This type of structure becomes flutter critical, and a stiffness/strength design interaction is required to develop an optimal design. The results of such a design study are presented in Table 2. The wing study (Reference 13) was designed for high subsonic and supersonic performance. The wing was a low aspect ratio for a 7.33 g fighter-type airplane. The optimal design for composite strength is shown in column 2. A substantial amount of weight is saved in the primary structural box, but the flutter speed of the design of 790 knots is deficient. The particular design was tailored to take advantage of the anisotropy of the material in producing a design which would washout under high angle of attack loadings. It was found that the box weight could be slightly reduced due to the load relief and the flutter speed could be increased due to the addition of torsional stiffness. However, perturbation of the design using all 0-degree filaments and then all $\pm$ 45-degree filaments showed that the optimal strength design was a lower bound on the available flutter speed and the flutter speed could be significantly increased by increasing the torsional rigidity of the design. Providing a better boundary spar stiffness and slightly increasing the shear rigidity of the basic covers, the final design, as shown in the last column of Table 2, was achieved. This wing had an acceptable flutter speed and retained weight fraction which was desired. It can be seen from the charts presented that in wing- or tail-type structure composite materials offer a substantial stiffness advantage. By proper design tailoring all the stiffness distributions meeting both the dynamic requirements and the strength requirements a clearly superior design may be achieved.

The research trend in design of composite structures in the United States retains emphasis on the development of more efficient component designs, but the major emphasis is on understanding the system impact of composite materials. Typical design study efforts include the optimization of components for flutter speed, strength, and aeroelastic effects as illustrated for metallic structures in Reference 6. Sufficient information is being collected on the minimum weight required to provide stiffness as a function of configuration, minimum weight required to provide strength as a function of configuration, and the detailed penalties due to attachment and other nonoptimum weights. This information will make solution of the problem of total system configuration design with composites possible.

Table 2

Wing Weight, Skin Strength and Flutter Speed
(Mach = 0.8) Comparison

	Aluminum	Strength Optimized Composite	All Filaments Spanwise	All Filaments $\pm 45^{\circ}$	Final Design
Wing Box Weight (lbs.)	1707	957	940	940	971
Relative Efficiency	1.00	1.78	1.82	1.82*	1.76
Flutter Speed (knots)	1040	790	640	1110	915
Laminate Characteristics					
σ/ρ	$.700 \times 10^6$	--**	3.22×10^6	$.278 \times 10^6$	--**
E/ρ	100×10^6	--	370×10^6	52.8×10^6	--
G/ρ	38.5×10^6	--	15.7×10^6	113×10^6	--

*Insufficient spanwise strength
**Nonuniform spanwise and chordwise distribution

Component demonstrations of most of the major structures found in aircraft as referenced in References 12 and 14 have established that the weight savings are real and that, on a component substitution basis, composite structures may be designed to save at a minimum 20 percent of the structural weight. With this knowledge, the design efforts are now moving towards optimization of the element on the basis of design strictly for the use of composite in the structure. In order to support this design trend, the data is being abstracted as shown in Figure 10 and the appropriate information for configuration design is transferred to the level of design of the basic system.

The problem of the design of the basic system was, in fact, treated in Reference 15 and recommendations were made by the Ad Hoc Committee on Structural Design with Fibrous Composites of the National Materials Advisory Board to "consider composite materials in the conceptual phase of design with the entire system conceived as one in which the geometry of the material is chosen jointly contributing to the optimum." At that time, the total technology needed to execute that recommendation was not available; however it is rapidly becoming a reality.

REFERENCES

1) S. W. Tsai and N. J. Pagano, "Invariant Properties of Composite Materials," Composite Materials Workshop, Technomic Publishing Co., 1968.

2) L. A. Schmit, "Structural Design by Systematic Synthesis," Proc. of the 2nd National Conference on Electrical Composites, Structures Division, A.S.C.E., 1960.

3) L. A. Schmit, "Structural Synthesis," Composite Materials Workshop, Technomic Publishing Co., 1968.

4) C. Y. Sheu and W. Prayer, "Recent Developments in Optimal Structural Design," Applied Mechanics Reviews, Vol. 21, No. 10, October 1968.

5) L. A. Schmit, "Comment on Completely Automatic Weight Minimization Method for High Speed Digital Computers," Journal of Aircraft, 1, p. 377, 1964.

6) G. Sued and Z. Ginos, "Structural Optimization under Multiple Loading," International Journal of Mechanical Science, Volume 10, 1968.

7) M. E. Waddoups, L. A. McCullers, F. O. Olson, and J. E. Ashton, "Structural Synthesis of Anisotropic Plates," AIAA 11th Structures, Structural Dynamics and Materials Conference, April, 1970.

8) A. Fiacco and G. P. McCormick, "The Sequential Unconstrained Minimization Technique for Nonlinear Programming A Primal-Dual Method," Management Science, 10, p. 360, 1964.

9) R. Fletcher and M. J. D. Powell, "A Rapidly Convergent Descent Method for Minimization," Computer Journal, 6, p. 163, 1963.

10) L. A. Schmit, W. M. Morrow and T. P. Kicher, "A Structural Synthesis Capability for Integrally Stiffened Cylindrical Shells," AIAA/ASME 9th Structures, Structural Dynamics and Materials Conference, April, 1968.

11) J. P. Wong, B. W. Cole and A. L. Courtney, "Development of the Shim-Joint Concept for Composite Structural Members," Journal of Aircraft, Vol. 6, No. 1, February 1969.

12) E. J. McQuillen and S. L. Huang, "Graphite-Epoxy Wing for BQM-34E Supersonic Aerial Target," Journal of Aircraft, Volume 8, Number 6, June 1971.

13) M. E. Waddoups, L. A. McCullers and J. D. Naberhaus, "The Relationship of High Speed Digital Computation to the Design of Advanced Composite Lifting Surfaces," AIAA/ASME 12th Structures, Structural Dynamics and Materials Conference, April, 1971.

14) J. E. Ashton, M. L. Burdorf and F. O. Olson, "Design, Analysis and Testing of Advanced Composite F-111 Fuselage," STP 497 Composite Materials: Testing and Design Second Conference on the Mechanics of Composite Materials, Pergamon Press, 1970.

15) R. G. Loewy, et. al., "Structural Design with Fibrous Composites," MAB Report 236, October 1968.

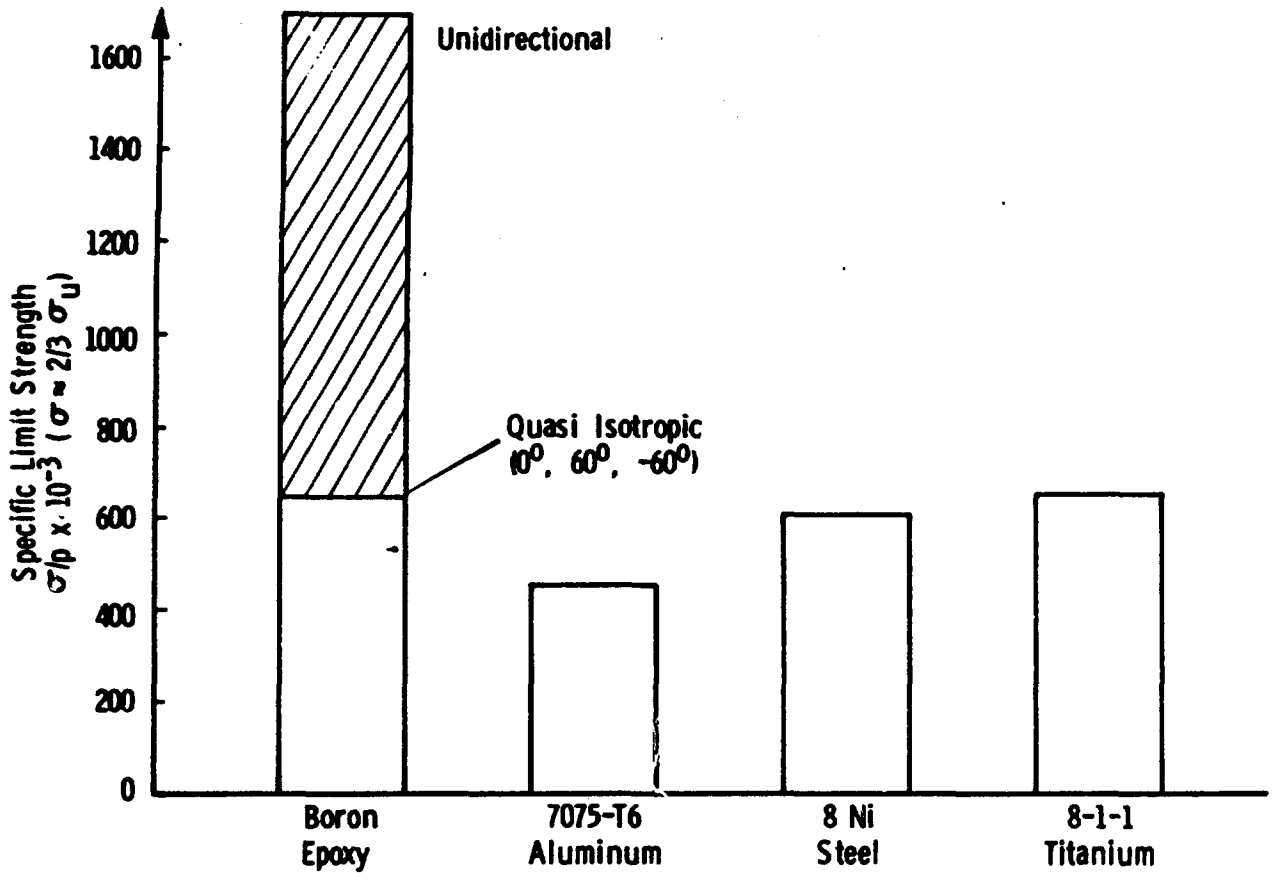

Figure 1 Specific Strength Comparison

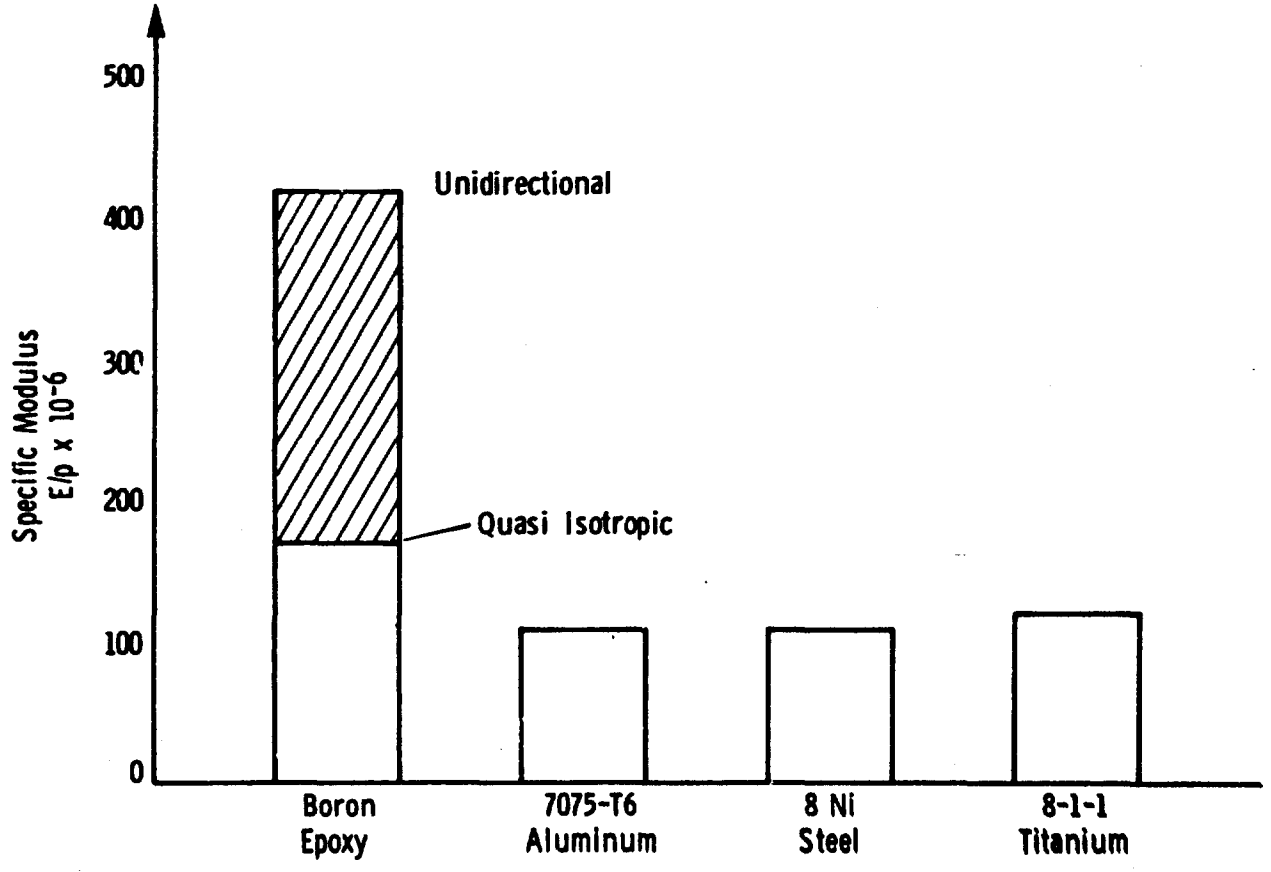

Figure 2 Specific Modulus Comparison

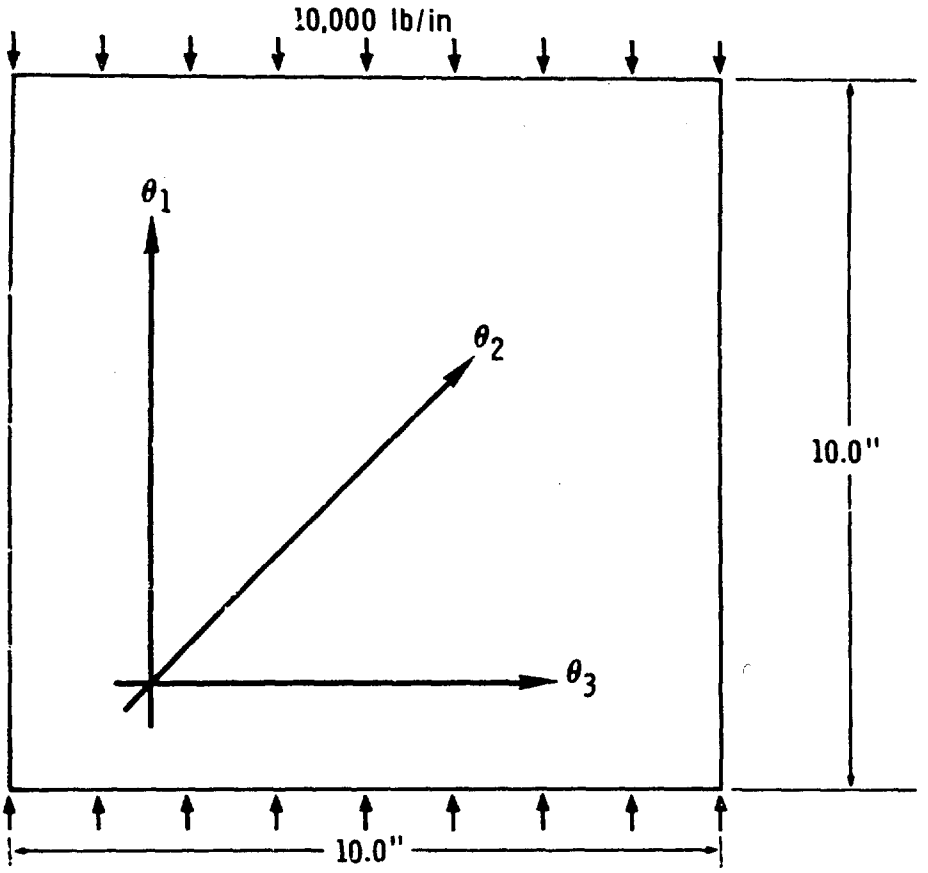

Figure 3 Flat Plate Example Problem

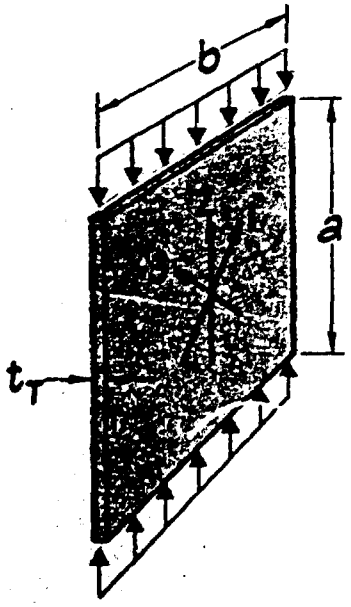

- *PREASSIGNED PARAMETERS*
  - a , b , B.C. , ρ
- *VARIABLES*
  - $\bar{d} = \{\theta_1, t_1, \theta_2, t_2; \theta_3, t_3\}$
- *OBJECTIVE*
  - $M(\bar{d}) = \rho abt_t = \rho ab(t_1+t_2+t_3)$
- *CONSTRAINTS*
  - g(1,k) = PANEL STABILITY
  - g(2,k) = STRENGTH, LAYER 1
  - g(3,k) = STRENGTH, LAYER 2
  - ———
  - ———
  - ———
  - g(n,k) = DEFLECTION

Figure 4 Problem Definition for Example Plate

DESIGN VARIABLES LIST

BEHAVIORAL CONSTRAINTS LIST

DESIGN VARIABLES

Variable	Variable Definition
VAR (1) = θ_1	Orientation 1
VAR (2) = t_1	Thickness 1
VAR (3) = θ_2	Orientation 2
VAR (4) = t_2	Thickness 2
VAR (5) = θ_3	Orientation 3
VAR (6) = t_3	Thickness 3

BEHAVIORAL CONSTRAINTS

G(1, k) = ϵ^{0° +, Lamina 1
G(2, k) = ϵ^{0° -, Lamina 1
G(3, k) = ϵ^{90° +, Lamina 1
G(4, k) = ϵ^{90° -, Lamina 1
G(5, k) = $\gamma^{0^\circ/90^\circ}$ +, Lamina 1
G(6, k) = $\gamma^{0^\circ/90^\circ}$ -, Lamina 1
G(7, k) = ϵ^{0° +, Lamina 2
G(8, k) = ϵ^{0° -, Lamina 2
G(9, k) = ϵ^{90° +, Lamina 2
G(10, k) = ϵ^{90° -, Lamina 2
G(11, k) = $\gamma^{0^\circ/90^\circ}$ +, Lamina 2
G(12, k) = $\gamma^{0^\circ/90^\circ}$ -, Lamina 2
G(13, k) = ϵ^{0° +, Lamina 3
G(14, k) = ϵ^{0° -, Lamina 3
G(15, k) = ϵ^{90° +, Lamina 3
G(16, k) = ϵ^{90° -, Lamina 3
G(17, k) = $\gamma^{0^\circ/90^\circ}$ +, Lamina 3
G(18, k) = $\gamma^{0^\circ/90^\circ}$ -, Lamina 3
G(19, k) = Deflection (stability)
G(21, k) = Plate shear V_1
G(22, k) = Plate shear V_2
G(45, k) = Approximate eigenvalue (stability)

Figure 5 Design Variables and Behavioral Constraints

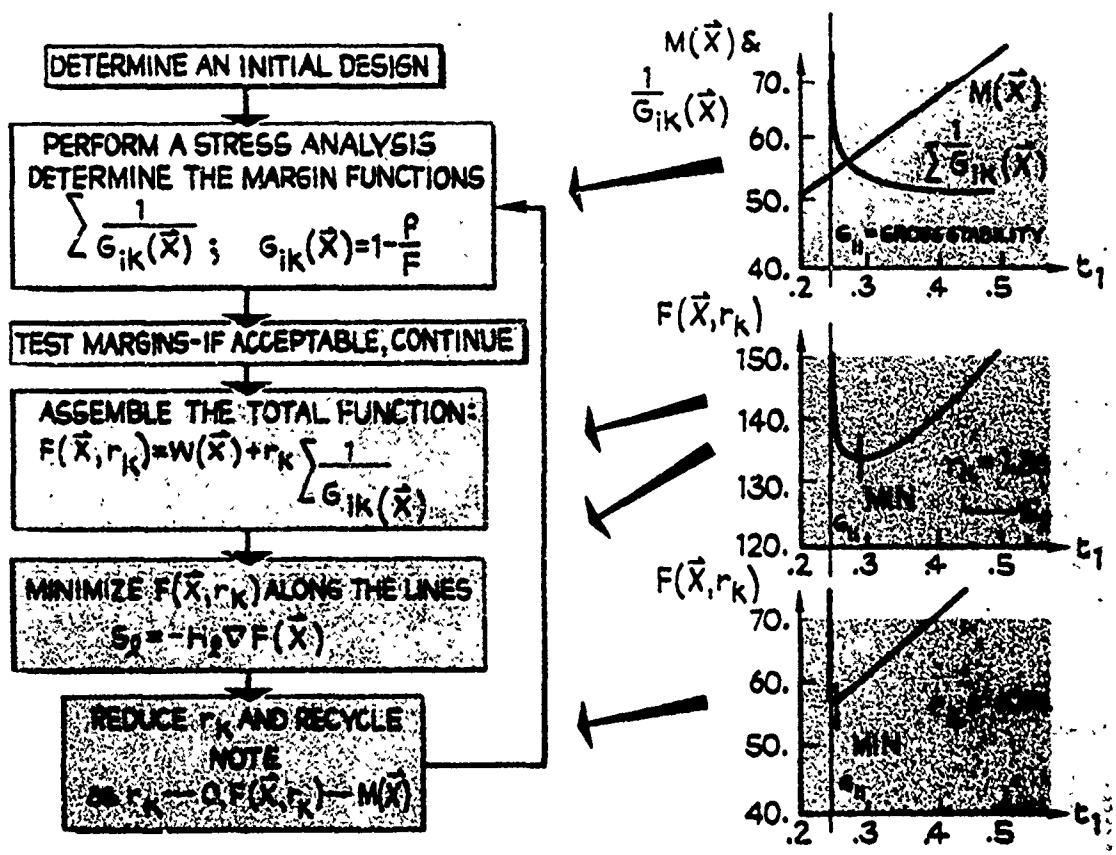

Figure 6 Synthesis Scheme

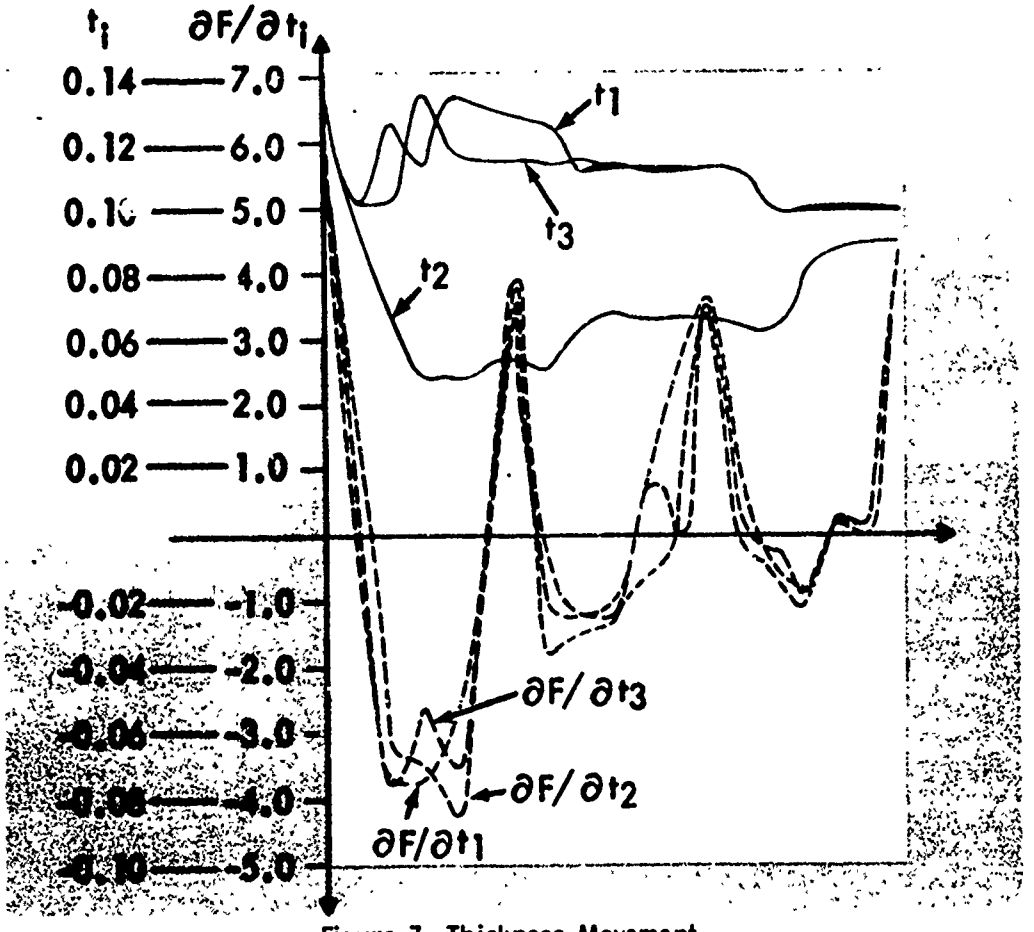

Figure 7 Thickness Movement

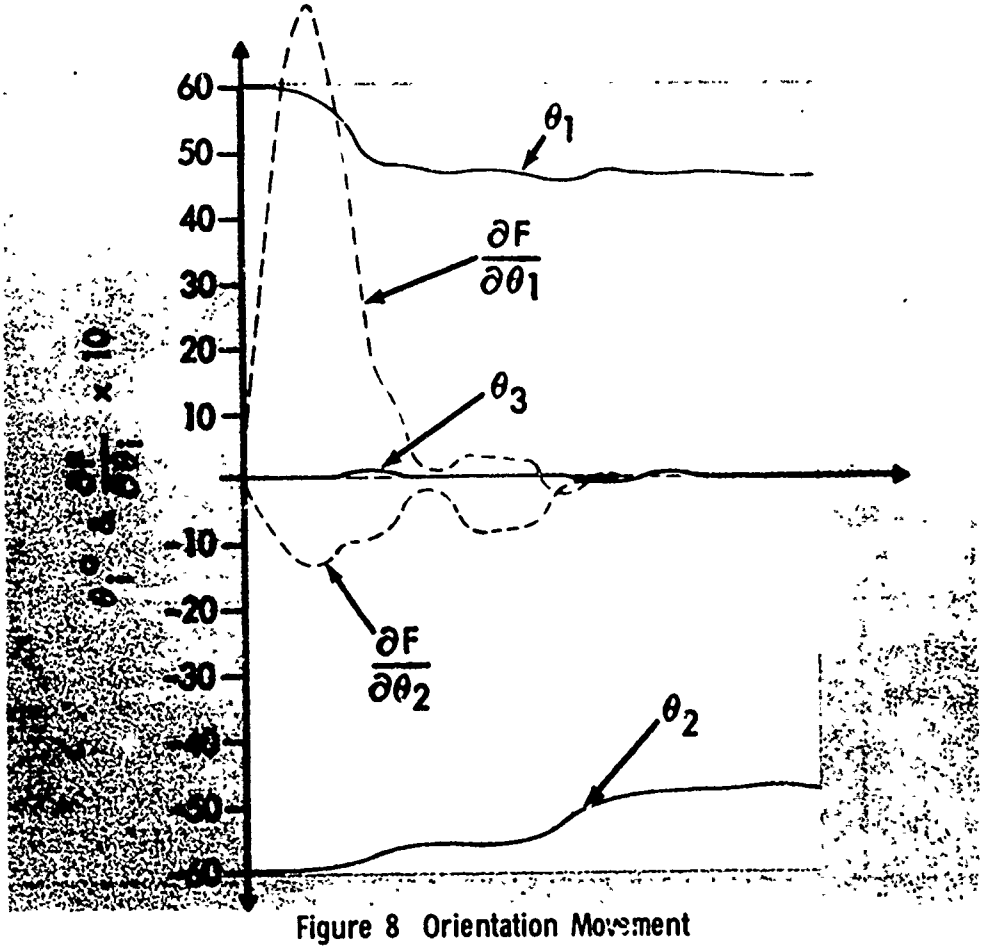

Figure 8 Orientation Movement

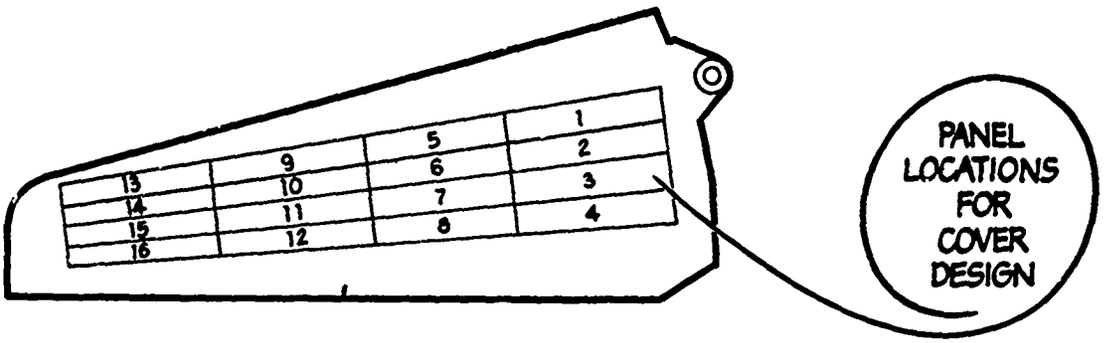

RESULTS

A = Active Variable

RUN	CONCEPT	VARIABLE STATUS								RELATIVE WEIGHT	COVER WT.-LBS
		θ_1	t_1	θ_2	t_2	θ_3	t_3	h_c	ρ_c		
1	BORON SANDWICH	A	A	A	A	A	A	A	A	1.00	557
2	BORON SANDWICH	0°	A	A	A	θ_2	t_2			1.11	618
3	BORON SANDWICH	0°	A	45°	A	-45°	t_2			1.23	685
4	BORON SANDWICH	①	A	①	A	①	A			1.30	742
5	GRAPHITE SAND.	0°	A	A	A	θ_2	t_2			.95	529
6	ALUMINUM PH.		A							3.34	1860
7	ALUMINUM SAND.		A					A	A	3.21	1788

① OPERATIONS ARE AVERAGE FROM RUN 1

Figure 9 Panel Synthesis Results

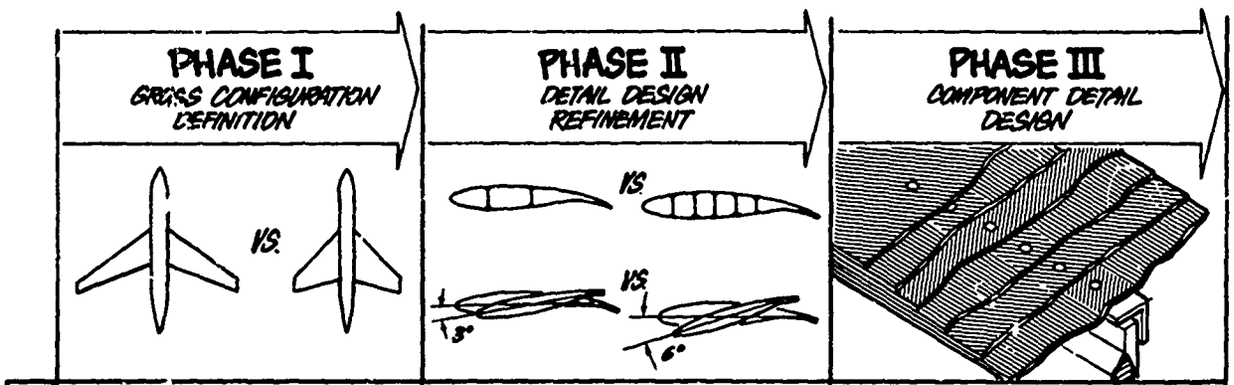

	PHASE I	PHASE II	PHASE III
INPUT	• BASIC MISSION REQMTS. • RANGE • ALTITUDE • SPEED • BASIC MATERIAL PROPERTIES $/p E/p $/LB	• AEROELASTIC REQMTS. • FATIGUE REQUIREMENTS • FLUTTER REQUIREMENTS • OVERALL STRENGTH REQMTS.	• LOCAL STRENGTH REQUIREMENTS • PRODUCIBILITY • FUNCTIONAL REQMTS.
OUTPUT	GEOMETRY • AIRFOIL TYPE • AR • t/c • λ • Λ DESIGN OBJECTIVES • DRAG LEVEL • WEIGHT GOALS • COST GOALS	• BASIC INTERNAL ARRGMT. • COMPLETE EXTERNAL CONFIG. • CAMBER, TWIST DISTRIBUTIONS • LOCAL FLOW PROBLEMS SOLVED • MAJOR LOADS, STRESSES, DEFLECTIONS	• DETAIL DESIGN • MECHANISMS • JOINTS, FITTINGS, & ATTACHMENTS • DESIGN REFINEMENTS AS RESULTS OF TEST & OPER.

Figure 10 Composites Applied at Each Level of Design

General Considerations in the Applications of Advanced Composites

I. C. Taig, Chief Structural Engineer, British Aircraft Corporation Limited,
Military Aircraft Division,
Warton Aerodrome,
Preston Lancashire.

Summary

The paper begins by comparing the characteristics of advanced composites with those of conventional airframe materials. It is shown that many considerations other than conventional mechanical properties and fabrication technology influence the selection and realisation of effective applications of composites. Particular attention is given to the assessment of cost effectiveness, to the achievement of integrity in a broad sense, including protection against adverse environmental effects and to some practical aspects of producibility. Trends in material and manufacturing costs are presented to show that in the airframe industry, most parts of the structure could benefit from the extensive use of composites in the next ten years. Expansion and redirection of the research and development effort will be needed to exploit the economic potential of the materials.

1. Material Characteristics

Advanced composite materials have attracted widespread attention amongst designers and engineers mainly because of the dramatic combination of high strength and stiffness and low weight which they exhibit. When they are considered for practical applications many more factors must be taken into account. We are dealing with a class of materials quite different from the metals which have dominated the high-performance structure field for so many years. The most obvious differences are their anisotropy, brittleness, fabrication methods and cost. A more extensive comparison of properties, taken from ref. (1), is given in the following table.

TABLE 1 Material Characteristics

Category/Property	Composite Characteristics	Metal Characteristics
Strength and Stiffness	High in fibre direction Low transversely and in shear	Approximately equal in all directions
Thermal expansion	Zero or negative longitudinally, positive transversely.	Approximately uniform, positive
Built-in stresses	Inevitable due to shrinkage in cure	Reducible and relievable
Fracture Characteristics	No inelastic ductility	Ductile
	Sensitive to 'secondary' stresses	Normally insensitive
	Susceptible to splitting and delamination	Cohesive
	Cracks often propagate in fibre direction through f bonding	Cracks influenced by load direction and grain
	Low energy absorption without multiple failures	Higher elastic/plastic energy
Environmental Characteristics	Inert to most acids and salts, Degraded by water and solvents	Corrosion risk varies
	Susceptible to erosion	Erosion resistant
	Electrolytically positive - may corrode adjacent metal	Corrosion between dissimilar metals
	Highly anisotropic electrical conductors: susceptible to lightning damage	Good conductors
Fabrication Characteristics	Finished material produced at component fabrication stage	Finished material produced and controlled before fabrication
	Wide range of layups and properties	Standard treatments, properties
	Properties vary significantly in nominally identical materials	Low variability
	Extensive non-destructive testing and inspection needed to monitor quality	Limited non-destructive inspection
Economic Factors	High basic material costs	Low-medium material costs
	Special manufacturing plant	Conventional plant
	Potentially low assembly costs	High fabrication and assembly costs

Composite materials have of course been in use for many years in such forms as plywood, reinforced concrete and glass reinforced plastics. These materials have been economically competitive with their rivals and it has been possible to exploit them without stretching their performance to the limit. With the advanced composites, the present high cost makes it essential that they should be used very efficiently if they are to make any significant impact on engineering. It is inevitable that they should first be introduced in high performance or specialised applications where these costs can be justified. Only when a substantial material utilisation is achieved will the costs reduce to a point at which widespread industrial use can be visualised.

2. Principles for Efficient Exploitation of Composites

In subsequent discussion, high structural performance is regarded as an essential prerequisite for effective composite application. This brings about an unprecedented requirement for detailed understanding of the material and the structure at all stages from material selection, through design and manufacture, to assurance and monitoring of integrity in service. The materials promise large rewards in terms of performance but the cost is high in sustained technical effort as well as in monetary terms.

Some of the principles for successful applications can be summarised in the following list:-

Select applications appropriate to the materials

(Choose suitable fibre and matrix materials)

Establish realistic design criteria.

(Analyse and design to exploit the material)

Design for integrity in detail

Design for producibility

(Control manufacturing processes)

Protect against damaging environment

(Monitor integrity in service).

In the subsequent discussion the items in brackets will not be considered since they have either been covered adequately in the previous lectures or they relate to the establishment of good practices which are outside the scope of this paper. The remaining topics will now be considered in more detail.

3. Selection of Appropriate Applications

If we consider using composite materials in a new product we must first answer two questions.

3.1. Is the application likely to be cost effective? For example, is the potential product improvement sufficient to warrant the additional cost of advanced composites? or is the composite manufacturing process so efficient that the final product cost is competitive with alternatives?

3.2. Is the application feasible, both theoretically and in terms of practical technology?

In the early days of composite application a third question may be equally vital:-

3.3. Can the composite product be developed (with a high probability of success) in the time available?

3.1. Cost Effectiveness

Examples have been quoted where the installed cost [2] and the (installation + operating) cost [3] are lower for advanced composite components than for their conventional counterparts. In such cases there is no need for a complex cost/performance trade study: cost effectiveness may be easily demonstrated. More often one must balance a performance improvement against additional component cost. A method commonly used in the aircraft industry, and, in principle, widely applicable, is based on assigning a monetary value to a unit mass saving. This value varies throughout the design and manufacture period and is highest in the early project assessment stage when the whole vehicle can be scaled down to exploit specific mass saving.

Composite material performance relative to conventional materials is subsequently quoted in terms of a structural efficiency ratio R defined as:-

$$R = \frac{\text{Mass of conventional structure replaced}}{\text{mass of composite in component}}$$

The value of this ratio varies according to the type of structural application, the loading conditions and the component design constraints. If C_1 is the in-service cost of unit mass of a component in conventional material and C_2 the corresponding cost for composites, then the application of composites is judged cost effective if

$$C_2 \geq C_1 R + V (R - 1) \quad \ldots\ldots(1)$$

or alternatively the structural efficiency required for break-even is given by

$$R = \frac{C_2 + V}{C_1 + V} \quad \ldots\ldots(2)$$

Fig. 1 shows the break-even value of R plotted against V for typical values of C_1 and C_2.

Thus at a given stage in the evolution of an aircraft an economic material efficiency ratio can be established. It remains to study any particular composite application and determine the potential structural efficiency for comparison with this break-even value.

Such an exercise has recently been carried out by the author for carbon fibre/resin composites as available commercially in the U.K. Some results are shown in fig. 2 together with the break-even efficiency for the aircraft concerned related to current material costs. On this basis it is seen that the only cost effective applications are for the reinforcement of metal flanges by unidirectional strip material (4) and for components designed wholly by stiffness. This conclusion applies, of course, only to one aircraft at a particular development stage and to the set of material properties and cost data employed.

3.2. Technical Feasibility

Before deciding to use composites for any particular application it is obvious that an adequate material must be available and it's basic properties demonstrated over the range of operating conditions.

Many of the technical factors involved have been covered by previous papers and some of the practical factors are covered later. At this stage two particular criteria which can determine feasibility will be mentioned.

Firstly, all the high performance composites known to the author are brittle materials and their resistance to impact is poor. When the composite and specimen design have been modified to improve performance in laboratory impact tests the result has usually been to increase energy absorption by creating multiple fractures - a process not conducive to the peace of mind of practical designers and users.

We therefore consider that composites should not be used in any region where high incidence impact by hard or dense objects is likely. In aircraft applications this precludes external, forward facing surfaces, such as leading edges and engine intakes and regions susceptible to ground debris impact. On the other hand, where battle damage is concerned, ballistic impact tends to produce clean holes with little loss of structural performance apart from the direct perforation effect. It has also been demonstrated that effective field repairs can be made. Furthermore, combinations of composite and conventional materials can be effective in absorbing impact and providing protection for internal equipment and crew.

Operating temperature is a second factor which may determine the feasibility of an application. In the fibre/resin composites the resin usually has an upper temperature limit between 50°C and about 200°C for epoxy and polyester systems and upto about 300°C for polyimide systems. The polyimides are both difficult and expensive to process and are inferior in general performance.

Long term exposure to high temperatures, such as the 25000 hours at 100 - 120°C. Concorde environment, has yet to be demonstrated as feasible for any system to the author's knowledge.

At low temperatures, brittleness and thermal stress cracking may be limiting factors - this aspect does not seem to have attracted sufficient attention to date.

4. Design Criteria and Structural Integrity

The efficient and safe design of composite components depends fundamentally on a suitable choice of design criteria and a philosophy of integrity demonstration appropriate to the materials.

The airworthiness authorities in the U.K. agree broadly with the following design control and demonstration procedure for the clearance of critical airframe components:-

- All raw materials released to an agreed specification
- material design properties statistically determined from large samples of test data and unifying stress analysis techniques.
- structural detail properties verified by substantial numbers of tests on fully representative details

- all fabrication processes demonstrated by NDT and cut-up tests to yield components meeting design requirements

- comprehensive structural analyses or instrumented tests relating local stresses and deformations to overall loads

- all production processes subject to batch control tests

- non-destructive examination of all finished components

- full scale tests of at least one static and one fatigue component

The 'hierarchy' of tests and the coordinating analyses are illustrated in fig 3. In the present context, the important feature of this procedure is that the nominal property values used in design are statistically derived from relevant coupon and detail specimen tests. The present advice is that design levels should be chosen to meet the following traditional criteria
a) no more than 10% of components fall below the stipulated property level.
and
b) no more than 0.1% of components fall below 90% of the stipulated level.
These criteria account specifically for variability in properties of the material as manufactured. Allowance must also be made for the influence of operating temperatures and possible degradation of material properties after exposure to the service environment for the whole aircraft life.

It should be noted that this approach does not demand that the full scale static tests should demonstrate a pre-determined strength margin or superfactor (which would penalise metal components as well as composite). It is based on the demonstration of consistent performance between full scale tests and detail tests and strength margins related to the variability of the latter.

The application of this philosophy implies the existence of a large body of consistent data in the first instance. It also implies that, for reasonable economics, consistent design practices should be followed so that new components can be designed using data accumulated from previous structures. Both these constraints are considered excellent practice for the early exploitation of advanced composites. The only reasonable alternative is the protection of structural integrity by the imposition of large safety factors unrelated to the particular component or the user's expertise. This might lead to a false impression of security and would certainly prevent the efficient use of the material.

In due course many applications of composites will appear where such stringent safety procedures are unnecessary. In such cases manufacturers will wish to reduce (perhaps to zero) the amount of special testing and also to cut costs in process control and inspection. It is likely that property levels considerably lower than those established by 'aircraft' procedures will be necessary for acceptable performance.

5. Detail Design for High Integrity

Integrity of a composite structure is not assured by demonstrating sufficient static and fatigue strength by analysis and laboratory tests. Composites are, generally speaking, imperfect materials as manufactured - containing small pores, cracks and unbonded regions at the constituent interfaces. After subjection to cycles of varying temperature and loading further damage is likely to occur. In fibre/resin composites, local resin cracking, fibre debonding and even fibre breaks are probable. It is unlikely that, for many years to come, the occurrence and influence of these effects can be accurately predicted by theory. It will be necessary to build up semi-empirically a body of information related to specific composite layups and component types to show how much degradation will occur and how much can be tolerated without danger of component failure. There is obviously a strong interaction between the physical condition of the composite and the environment in which it operates.

Again, the failure of composite components is unlikely to arise from exceeding the static strength in the fibre direction (even allowing for the effects of degradation). It is much more probable that interlaminar and normal-to-surface stresses will precipitate failure by delamination, often as a result of local stress raisers. It is theoretically possible and in time maybe economically feasible to deal with such problems entirely by calculation. At present it is usual to use theoretical calculation to design standard details - e.g. joints, splices, corner fittings, fillets and perforations - and to develop each design by testing to achieve acceptable standards.

All branches of engineering use standard components and detail designs with conventional materials. With composites this practice is likely to be even more widespread.

6. Fabrication of Components

The efficient use of composites and the nature of the materials themselves suggest that the trend will be towards the layup and curing of monolithic components rather than the sub-assembly of many prefabricated details. The principal manufacturing methods envisaged are:-

- filament winding and autoclave curing: mainly applicable to shells and frameworks.

- tape or sheet laying and autoclave or press curing: mainly applicable to sheet, strip, panel and shell components.

- matched die moulding and press curing: applicable to relatively small, accurately shaped components.

Other methods such as pultrusion, injection moulding etc are applicable to special types of component or to secondary structures using short fibre reinforcement and will not be considered further.

Each of the principal manufacturing methods imposes restrictions on the design and performance of the resulting composite - the following discussion relates to the purely physical and geometrical constraints.

The first point, which relates to the selection of material is independent of the method of layup and curing but fundamental to the overall manufacturing process. The range of fibre sizes available in present day advanced composites has an important influence on the amount of curvature along the fibre length which can be tolerated.

If the maximum permissible bending stress is taken to be 10% of the nominal fibre strength then the permissible radii of curvature for boron, glass and carbon fibres are given in the following table.

Fibre Material	Fibre diameter μm (10^{-3} ins)	Young's Modulus GN/m^2 (10^6lbf/ins^2)	Nominal Strength MN/m^2 (10^3lbf/ins^2)	Permissible Bend radius mm (ins)
Boron/tungsten	100 (4)	380 (55)	2.4 (350)	76 (3.2)
Glass	7.5 (0.3)	69 (10)	2.75 (400)	1.0 (0.04)
Carbon (	9 (0.36)	400 (58)	1.55 (225)	11.6 (0.45)
range (	6 (0.24)	210 (30)	2.25 (325)	2.8 (0.11)

This shows that components requiring rapid changes of surface direction can only be made in glass and carbon fibre composites. This effectively limits the potential applications of boron to panel structures and large diameter tubes and makes it necessary to introduce joint fittings using other materials at surface intersections.

Filament Winding

This process has been in use for many years in the production of glass reinforced plastic pressure vessels using either preimpregnated glass fibre tows or wet-layup methods. It lends itself especially to the manufacture of cylinders, tubes and bodies of revolution and with some ingenuity to the fabrication of frameworks including geodetic shell-support structures. It is essentially an automated layup process and many facilities exist, with varying degrees of automation and adaptability.

Apart from a few specific types of geometry and layup (e.g. helical windings of circular cylinders) it is not usually possible to layup individual laminae without many fibre cross-overs in a layer. In regions of double curvature, such as pressure vessel end domes, and at framework intersections this problem is particularly acute and leads to a great deal of overlapping and variation in laminate thickness. The result is that fibre damage during cure is likely and that resin rich areas or voids occur at overlaps. Furthermore the surfaces of the finished component often require machining to a final contour with the result that fibres are broken and effective material is lost. In arriving at a compromise layup to minimise some of these effects it is certain that the fibre direction will no longer be the optimum advocated by the designer. For all these reasons, filament wound components do not achieve the theoretical performance of the material and the loss in efficiency must be established experimentally and taken into account in design.

Tape and Sheet Laying

This is the most widely used technique for laying up aircraft components and it uses the materials in the very convenient form of preimpregnated tape or sheet. The process is suitable for at least partial automation and leads to a true laminated construction in which separate fibre/resin layers are superimposed without cross overs. The continuous filament process only applies to developable surfaces although a small amount of 'drape' over double-curved surfaces can be achieved.

When fabricating components other than flat panels or prismatic surfaces, the fact that tapes are produced as parallel strips with unidirectional fibres may lead to severe restrictions on fibre orientation and continuity. Fig. 4 illustrates how the fibre orientation in a single layer would vary around a tapered box so that orientation on opposite faces would be significantly different and continuous tape winding impossible.

A more general problem affecting flat panels and open sections is distortion during cooling after cure. To avoid this a balanced layup is needed - usually obtained by symmetrical disposition of laminae of equal orientation. This can place difficult constraints on the design of the laminate and in particular on the ability to vary the layup to cope with changes of loading. A final point in relation to layups made from parallel strips is that change of fibre orientation within a layer is only possible by breaking the continuity of the material and thereby losing efficiency.

Once again the theoretical efficiency of the material will be significantly reduced by the practical requirements of manufacture. All the above problems can be reduced or eliminated by the use of short fibre composite technology which is being successfully developed by E.R.D.E.(5) (6). Short fibres can be deposited from fluid suspension in virtually any concentration and orientation, producing a surface mat which can be impregnated with resin to form a tailored 'prepreg'. The penalty for use of this very flexible technique is the loss of mechanical properties which for carbon fibre/resin systems have been quoted as 70% reduction in flexural strength and 80% in stiffness. Latest developments leading to improved fibre alignment promise to reduce these penalties significantly.

Matched Die Moulding

This process, restricted by press size to relatively small components, has the same restrictions on fibre direction and, in thin sections, control of distortion. Once again short fibre composites provide a possible solution.

Attachments and Joints

All composite components are cured under pressure either on a former or mandrel or in a mould. After cure of closed surfaces and tapered open sections it must be possible to remove the curing tool. Internal pressurisation into a split external mould is a technique being successfully developed for many tubular components. However, cases arise where this is not possible and in many cases manufacture of a monolithic structure does not seem feasible. In such cases assembly of prefabricated components is necessary and this introduces the need for assembly jointing. With fibre resin composites it is usually preferable to use adhesive bonding, given that sufficiently large and robust surfaces can be provided to ensure adequate attachment. For localised attachments, mechanical fastenings are often required and most users introduce metal inserts or edge members to diffuse local loads and accommodate stresses due to geometrical offsets.

At the edges of panels and sheets normal practice is to bond a metal edge member to the composite by a tapered or stepped lap joint or a stepped splice joint as illustrated in fig. 5 and to make all mechanical attachments through the metal alone.

At the ends of compact fittings a metal shim joint is often used, interleaving thin metal shims between composite layers.

An alternative to reinforcement by metal, frequently used for local inserts and tube end fittings, is to build up a woven fibreglass/resin reinforcement. This lends itself well to incorporation in the composite process but can be very heavy if used extensively.

Joint design and performance is a complex subject which will not be discussed in detail here. It is, however, probably the most important single factor affecting the use of composites in practical structures. In some early composite fittings, the weight advantage of high strength material has been lost by excessively heavy end attachments. In all cases, component integrity will depend on joint and attachment performance.

7. Environmental Protection

The fibre/resin composites are quite different from engineering metals in their tolerance to the working environment as can be seen in table 1. Whilst corrosion is not generally a problem in the composite itself, most resins, and in the case of glass the fibre surface, are degraded by moisture and some of the fluids which are normally present. In certain instances this degradation may be small and no special precautions need be taken. This is usually at the expense of other properties: for example tolerance to heat and moisture may be achieved by complex cure cycles which yield a brittle resin and an expensive manufacturing process.

The matrix cracking and porosity referred to in section 5 make it necessary to avoid the absorption of water, fuel or other fluids into the composite which may cause physical damage by freezing or evaporation as well as chemical degradation.

Erosion is a further problem with all fibre resin composites. It is already familiar in the aircraft field where fibreglass radomes and aerial covers have been in use for many years. Surfaces exposed to rain and hail at high incidence at high speeds can be rapidly eroded. Boron/resin is slightly better but carbon/resin possibly worse than fibreglass so the same problem exists for all these materials. For these reasons surface protection of composites is likely to be necessary for many external applications. Also internally, where regular contact with or containment of fluids is required, surface sealing will be needed. Coatings must be continuous and sufficiently flexible to bridge fine resin cracks and for external purposes tough enough to withstand the local erosion conditions. Coatings of neoprene or polyurethane of up to 0.25 mm (.010 ins) have been shown to meet typical aircraft external requirements.

Lightning strike is a potentially serious hazard to composite structures, particularly those made of moderate electrical conductors such as boron/tungsten and carbon fibres. Tests conducted by the U.S.A.F. Materials and Avionics Laboratories (7) show that the problem is most acute with boron, but it has been confirmed in the U.K. that moderately high simulated lightning strikes will also damage carbon fibre composites. Non-conducting composites such as glass/resin (and equipment within them) can be adequately protected by local metal strips forming a 'Faraday cage' which preferentially conducts the lightning current. There is some controversy regarding the efficacy of strips for protecting the partially conducting materials . Whilst the first major production composite component (the F.14 taileron (8)) uses this method and U.K. tests confirm the preferential conduction of simulated lightning through adjacent metal rather than carbon fibre components, laboratory research indicates that continuous conducting coatings will be required. Some suggested

coatings are aluminium at 0.15 mm thick (either bonded foil or flame-sprayed), silver-pigmented epoxy paint, 0.1 mm thick and aluminium wire fabric using 0.1 mm diameter wires at an area density of 0.1 kg/m^2.

It would be logical to combine the requirements for erosion and lightning protection into a single protective coating either by the use of continuous metal film or the development of a specialised composite coating such as metal fabric in an elastomeric matrix. Such coatings will affect the inspection of composite components for deterioration in service and in the case of metal films might introduce their own electrolytic corrosion problems. Any development of coatings must therefore be accompanied by the parallel development of non-destructive inspection methods.

8. Economics of Airframe Applications

The assessment of cost effectiveness was discussed in general terms in section 3.1. Some current and predicted costs will now be presented and used in the cost effectiveness equation to indicate trends in the economics of applying advanced composites to airframe structures.

8.1. Material Prices

The figures quoted below relate to the price of preimpregnated boron- and carbon-epoxy tape material and are expressed as the price of that quantity of tape which yields unit mass of cured laminate with 60% fibre/volume fraction. Prices are either obtained from recently published figures or from material suppliers' quotations.

Material	Quantity ordered or rate of consumption	Price (Feb 1972) £/Kg	Price (Feb 1972) $/lb
Boron-epoxy tape (U.S. supply to U.S. customer)	10,000 lbs	(91)	107
Carbon-epoxy tape * (US/UK supply to US customer)	Small batch	(229)	270
	300 lbs	(127)	150
Carbon-epoxy tape * (U.K. supply to U.K. customer)	5 Kg batches	207-331	(244-391)
	750 Kg per week	48-76	(56-90)

* RAE Type 2 fibre (high strength) in all cases.

The marked dependence of price on quantity ordered reflects the excess production capacity currently available. Further reductions are possible by working the present plant to full capacity and again by developing new plant for larger through put and continuous processing. A reasonable forecast of the growth in my own company's consumption of carbon fibre composite leads to the price trends shown in fig. 6.

8.2. Manufacturing Costs

At present there is no experience of quantity production of advanced composite components and the definition of economical design and process details is inadequate for accurate manufacturing cost forecasting.

The following general indications of labour costs have been obtained from our own studies together with information from U.S. sources.

Item	Composite Construction	Conventional Construction	Relative labour cost
Tapered panels, simple control surfaces	Composite skins and separate edge members. honeycomb core, metal attachments.	Uniform aluminium alloy skins, honeycomb core edge members and attachments	Approx. 2:1
Fairing panels	Single-cure curved 'sculptured' panel. honeycomb core	Machined aluminium skins, honeycomb core	< 1:1
Major flying surface	Variable thickness laminate skins, varying density Al. honeycomb core, Ti edge members and fittings	Varying thickness Ti skins, Al honeycomb core, Ti fittings	Approx. 1:1

By comparison with typical airframe manufacturing costs a figure of £100/Kg is the right order to cover labour and tooling. When dealing with relatively small material quantities a substantial extra cost is required to cover process control and non destructive testing. This will be assumed to add a further £20/Kg to the present manufacturing cost but to be absorbed in the previous figure by 1975. The basis for this cost component is so uncertain that there is no justification for reducing it beyond this point.

8.3. Effect of cost trends on weight trade-off

Combining the above costs to give C_2 in equation (2) and taking C_1 to be £50/Kg, the break-even structural efficiency ratio is derived as a function of time for the following typical values of mass-saving.

Aircraft Type	Development Stage	Value V of mass saving.	Code
Strike Aircraft	Detail design	£70/Kg	A
Strike Aircraft	Project study	£150/Kg	B
Subsonic transport	Early design	£70/Kg	A
Supersonic transport	Early design	£300/Kg	C

The resulting break even efficiencies are shown in fig. 7. Referring again to fig. 2 it is seen that all the structural applications studied will become cost effective by 1980 on the basis of unit production cost alone. A survey is required of the plant development and capital re-equipment costs to complete the picture.

9. Technical Development

The rapid exploitation of the economic potential of the materials requires a vast research and development effort, both to justify structural integrity and to evolve the techniques which will enable design and production teams to produce hardware in quantity. Some highlights of the development programme are presented in table 2.

TABLE 2 Technical Development Requirements

Technology Area	Present Status	Requirement
Multidirectional laminate behaviour	Basic stress/deformation analysis well developed	Strength and integrity under realistic loading and environment
Impact and fracture properties	Fundamental theories evolving. Formalised laboratory tests.	Unifying theory and practical tests to predict full-scale performance.
Environmental resistance	Laboratory information available for humidity, temperature, fluids, erosion, lightning strike.	Long term exposure and real environment information. Tolerance of adhesive joints, mechanical joints. Protective coating performance.
Damage resistance and repair	Small amount of data on impact damage, some ad-hoc repairs.	Extensive information and field trials on in-service damage. Structural concepts with repair in mind; performance of field repairs.
Process and Quality Control.	Limited range of processes for specific applications. Cumbersome control procedures	Development of processes for wide range of applications, low product variability. Streamlined control procedures.
Structural Concepts	Limited range of applications developed.	Economically producible structural forms appropriate to the material. Standardised details.
Analysis and Design Aids.	Basic stress analysis and material layup routines available.	Automated stress analysis and strength derivation Automated optimum material and structural design. Standard practice manuals.

In many instances the development will culminate in the installation of trial structures on flying aircraft and production commitment will be delayed until satisfactory service over a substantial time period has been demonstrated. Until now, most of the pressure to develop composites has arisen from a desire for technical advancement. It now appears that potential economical advantage may become the driving force leading to expansion and redirection of development.

Acknowledgements

The author wishes to thank British Aircraft Corporation Limited and the Ministry of Defence for permission to present this paper.

References

1. Taig I.C. "Design of Airframe Components in Carbon-Fibre Composite" in Composites Jan/Feb 1972.

2. Dial D.D. and Howeth M.S. Advanced Composite Cost Comparison in SAMPE Conference Proceedings Vol. 16 Anaheim Conference Nov. 1971.

3. Anon. Cost Effectiveness of RRCM Carbon Fibre Floor Panels - privately communicated by Rolls Royce Composites Materials Limited.

4. McElhinney D.M., Kitchenside A.W. and Rowland K.A. The Use of Carbon Fibre Reinforced Plastics in Aircraft Engineering Oct. 1969.

5. Ziebland H et al in New Technology No. 46 May 1971 U.K. Department of Trade and Industry.

6. Bagg G.E.G. et al Processes for the utilisation of high strength discontinuous fibres - Proceedings of British Plastics Federation 7th International Reinforced Plastics Conference, Brighton 1970.

7. U.S.A.F. Avionics Laboratory. Proceedings of Lightning and Static Electricity Conferences Dec. 1968. Tech. report AFAL-TR-68-290 Part 2 May 1969 and Dec. 1970.

8. Lubin G. and Dastin S. First Boron Composite Structural Production Part in Proceedings of 26th Annual Technical Conference 1971 Society of the Plastics Industry Inc., Reinforced Plastics/ Composites Division.

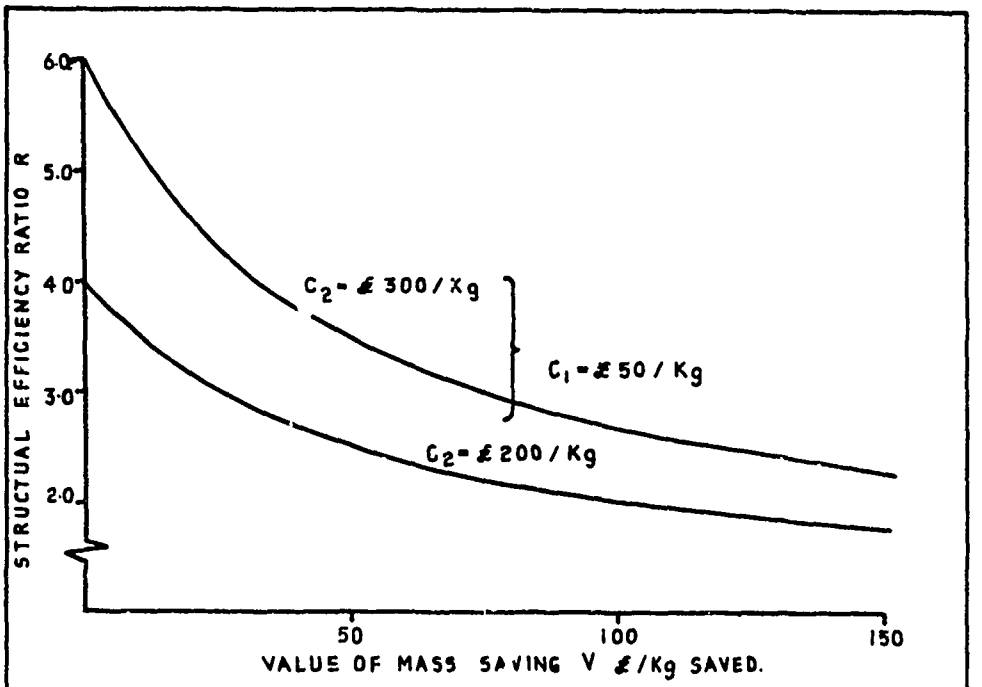

FIG. 1 BREAK-EVEN EFFICIENCY FOR COMPOSITE APPLICATIONS

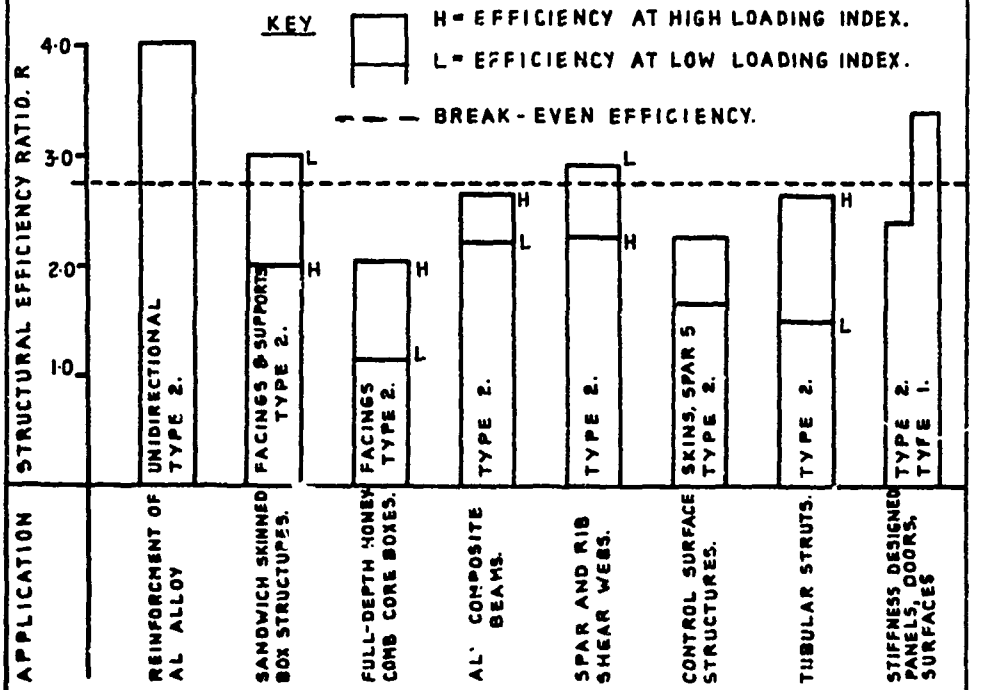

FIG.2 EFFICIENCIES OF CARBON FIBRE COMPOSITES SELECTED APPLICATIONS

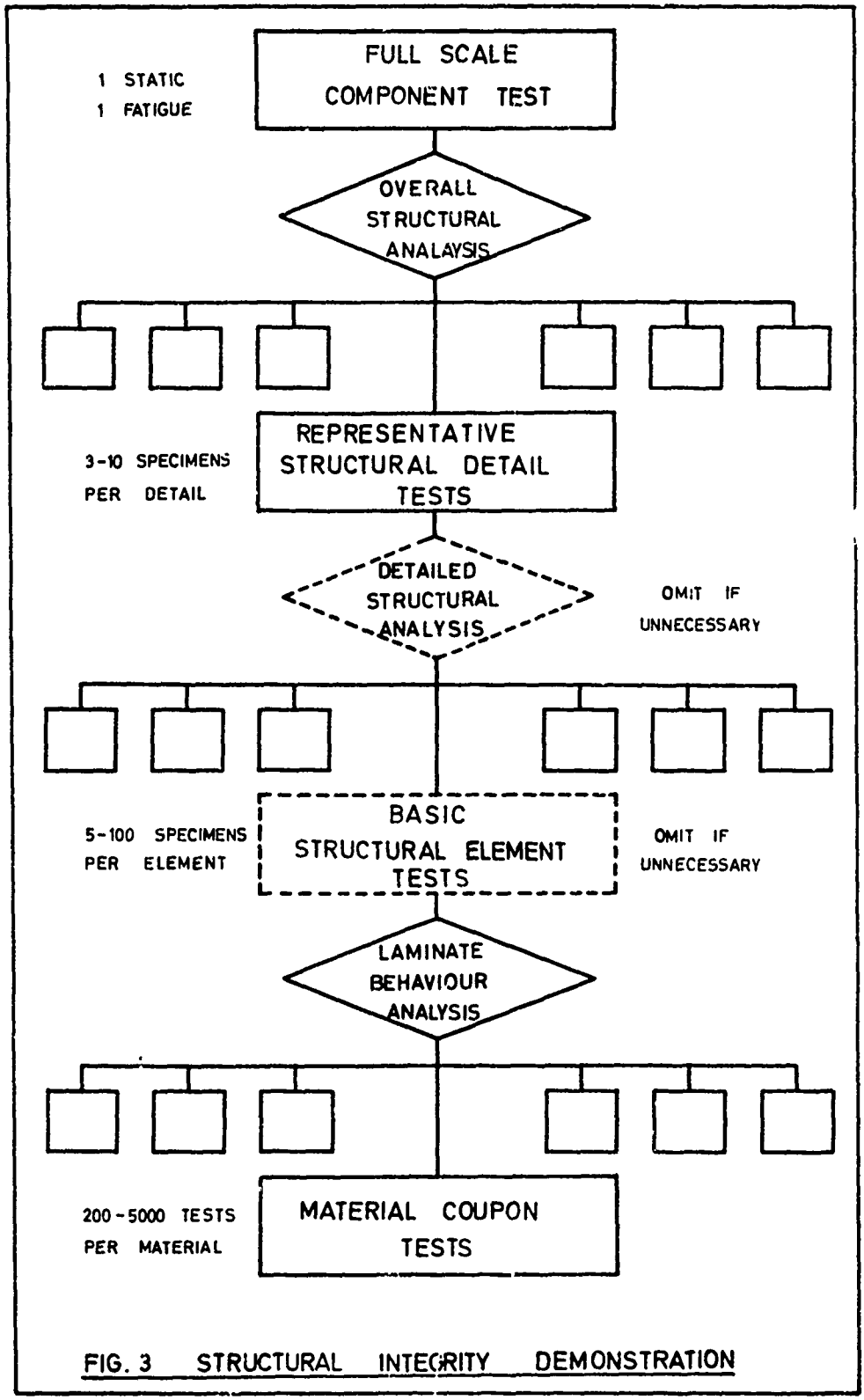

FIG. 3 STRUCTURAL INTEGRITY DEMONSTRATION

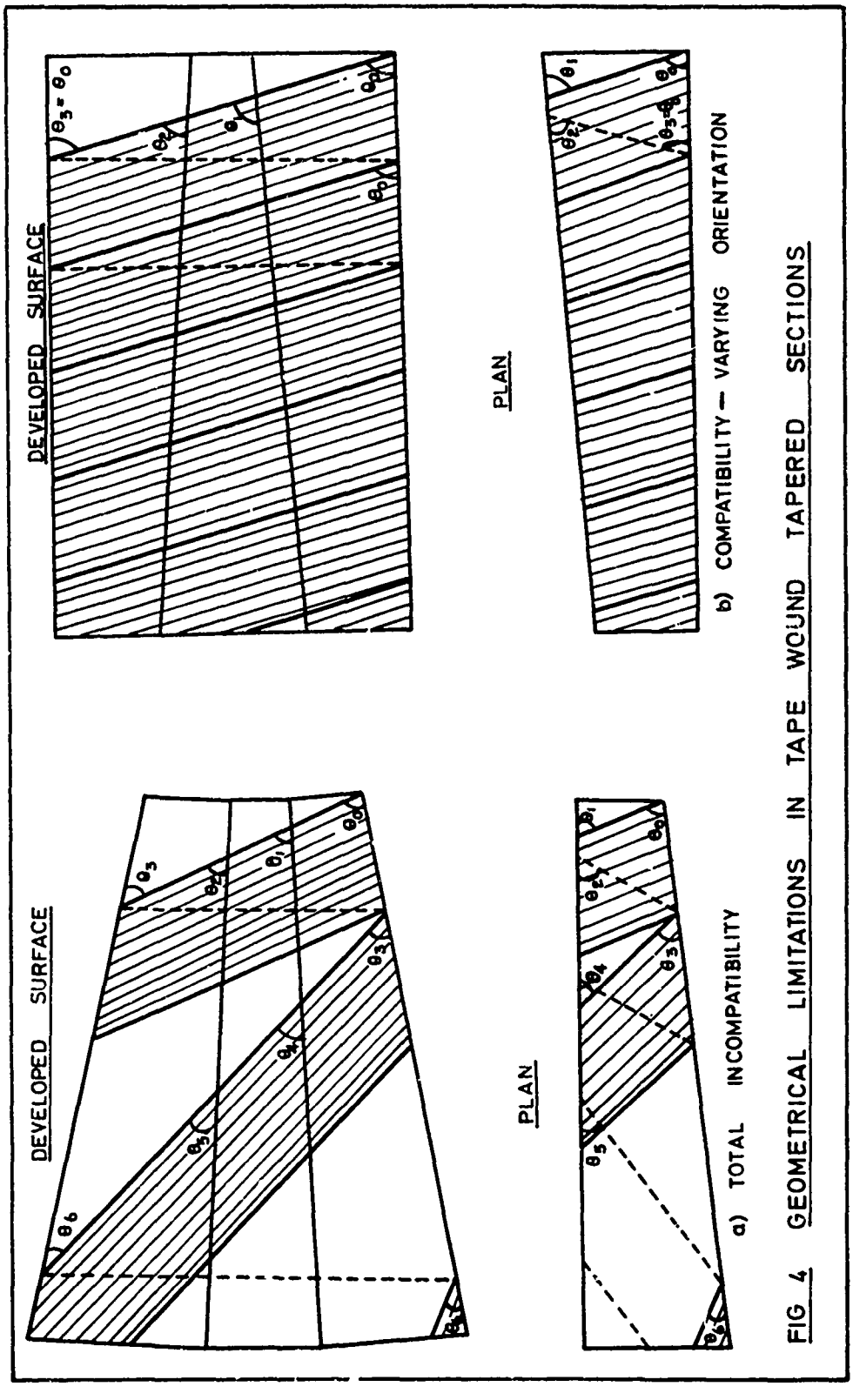

FIG 4 GEOMETRICAL LIMITATIONS IN TAPE WOUND TAPERED SECTIONS

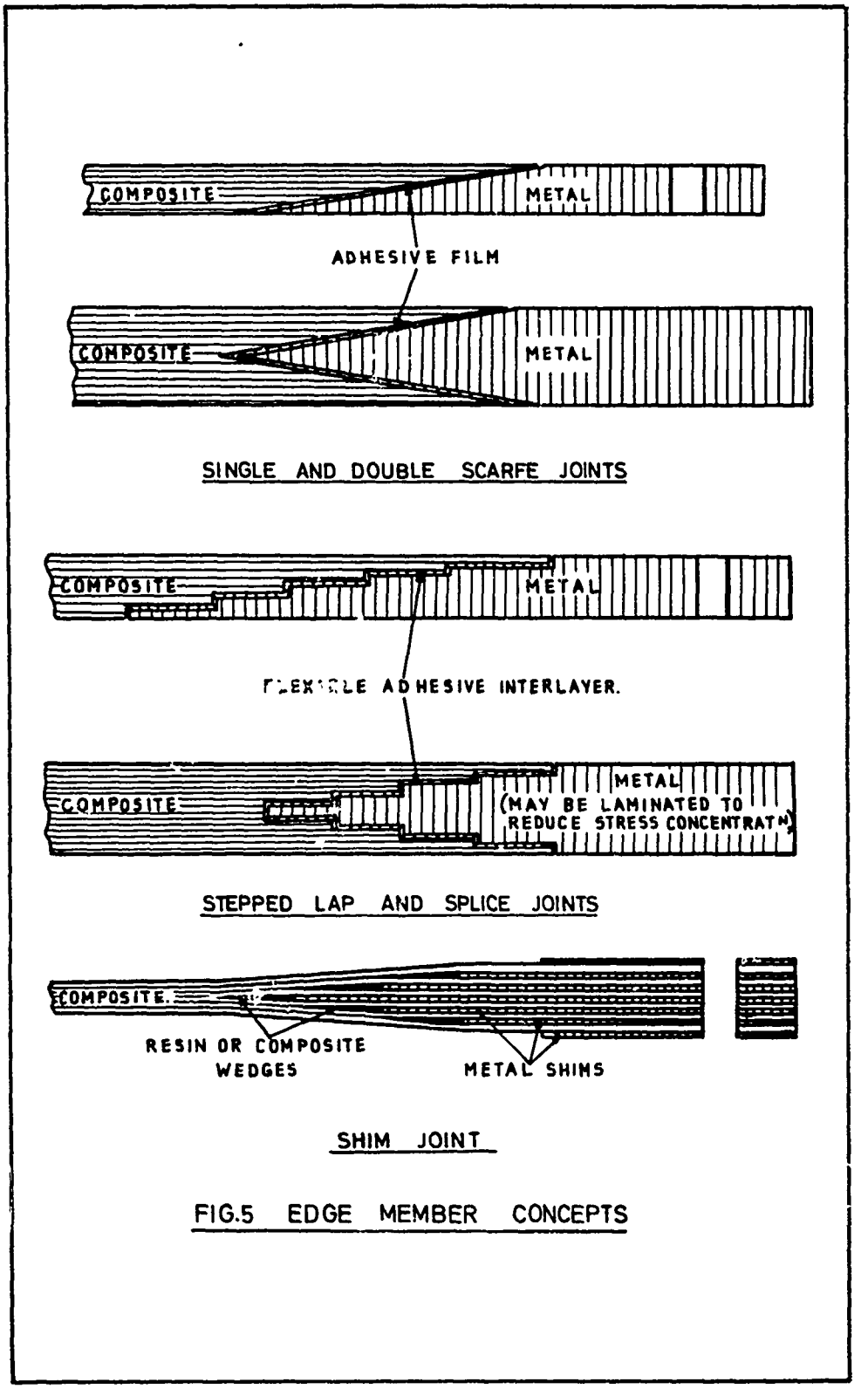

FIG.5 EDGE MEMBER CONCEPTS

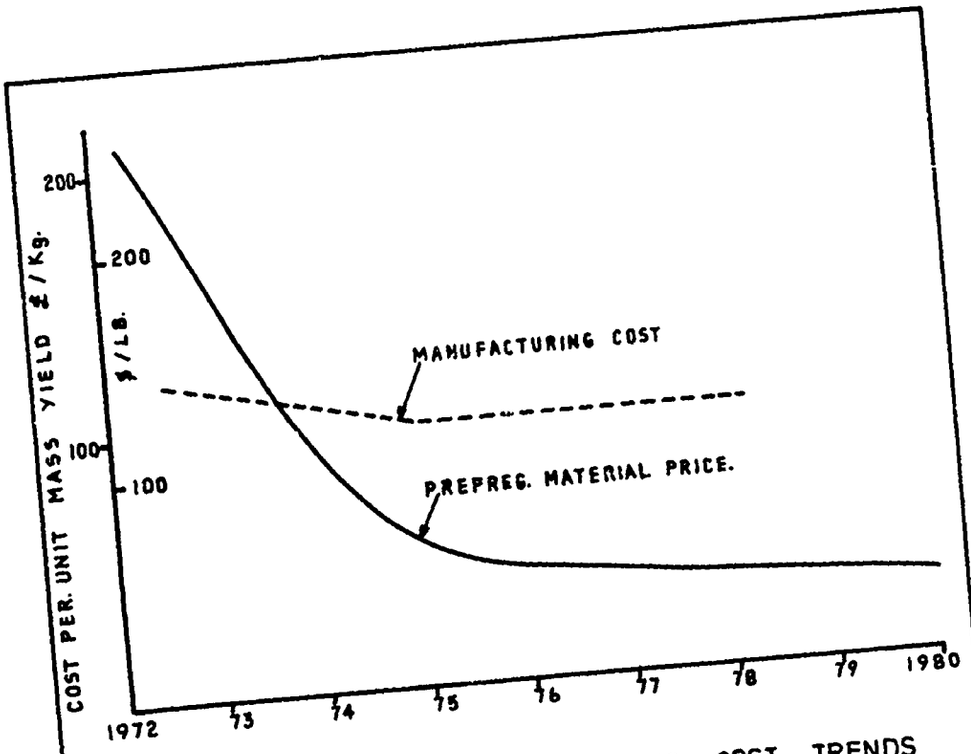

FIG. 6 MATERIAL AND MANUFACTURING COST TRENDS

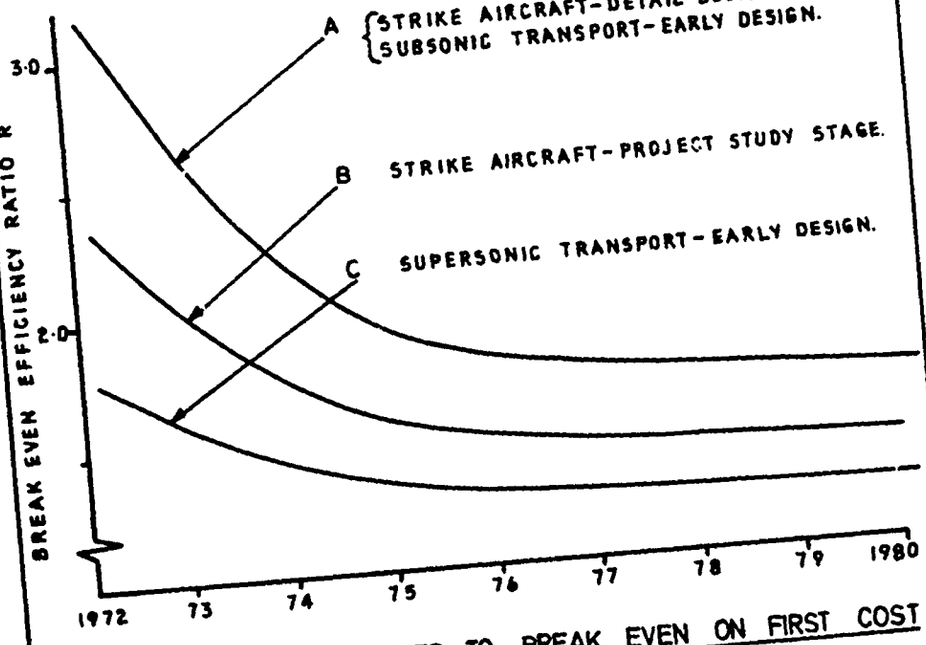

FIG. 7 EFFICIENCY REQUIRED TO BREAK EVEN ON FIRST COST

Airframe Applications of Advanced Composites.

I. C. Taig, Chief Structural Engineer, British Aircraft Corporation Limited,
Military Aircraft Division,
Warton Aerodrome,
Preston,
Lancashire.

Summary

This paper deals with a wide variety of primary and secondary structural applications of advanced composites. It illustrates, using actual or projected examples, the progressive introduction into service of components of increasing complexity and cost effectiveness. All previously unpublished information relates to carbon fibre/epoxy composites under development in the U.K. but to broaden the picture the coverage also includes boron/epoxy, carbon/epoxy and, to a lesser extent, boron/aluminium applications in the U.S.A. The range of components covered includes:- composite reinforced metal members; sandwich panel structures such as doors, floors and control surfaces; rod and tube members, box structures such as tail surfaces and wings; frames, bulkheads and fuselage shell structures. Particular emphasis is given to the design principles and practical features embodied in each application illustrating as far as possible the general considerations of the previous paper. Where information is available, mass savings and cost effectiveness data are quoted and the paper concludes with comments on the operating environment and experience in service.

Introduction

Advanced composite materials are moving rapidly from the laboratory development phase to the practical hardware stage. The driving force behind this development is the potential improvement in structural efficiency which the new materials offer. At present prices, very few applications are cost effective and most of those which will be described are intended to demonstrate the capabilities of the materials ready for their future exploitation. A reasonably broad survey of composite applications is attempted but there is no intention to make this all-inclusive. The emphasis is on applications in the military aircraft field since this is the writer's sphere of activity but occasional references are made to civil transport and helicopter applications.

The pattern which emerges is one of logical progression from relatively simple and sometimes secondary components to major structures involving totally new design concepts and exploiting the materials in sophisticated ways.

1. Composite-reinforced metal structures

The most efficient use for highly anisotropic filamentary composites is for unidirectional load transmission. This situation is very nearly achieved in the flanges of beams and frames, the stiffeners in stiffened plate structures and the spars and longerons in reinforced shell structures. By a fortunate matching of stiffness and strength, boron and some carbon fibre composites can work effectively in parallel with the conventional airframe materials: aluminium and, particularly, titanium alloys. It is natural therefore that amongst the early applications of these materials we should find the unidirectional reinforcement of metal structures. This is seen in fig. 2 of the previous paper to be the most efficient of all the applications studied to date and it also provides a measure of fail-safety since a metal load-path exists in parallel with the composite.

For these reasons floor beams with carbon fibre strip reinforcement of metal flanges (1) as shown in fig. 1, were developed for fitment in the cargo floors of the BAC 3-11 project (now cancelled). Similar structures are known to be under consideration for the Lockheed 10 11. The application is relatively straight-forward, the principal technical difficulty being the control of distortion and accommodation of thermal stresses induced during cooling after curing of the composite to the metal. Even allowing for thermal stresses and with modest design stress levels, 1 Kg of carbon fibre (RAE type 2, high strength) composite can replace 3 Kg of aluminium alloy giving an overall mass saving of 2 Kg. The cost of this application is little more than that of moulding simple tapered strips.

A similar application, this time with stiffening in mind, has been considered for a helicopter pitch control spindle (2a). Here the high stiffness (Type 1) carbon fibre was used, in spite of the fact that it's limiting strain is not particularly compatible with that of the steel substrate.

A more direct way of reinforcing a metallic structure is the incorporation of fibres into a metal matrix. This is being successfully developed with boron in aluminium and typical applications are the embodiment of prefabricated boron/aluminium strips into spars and longerons (3). This material is in some ways more versatile than a resin-matrix composite since the aluminium matrix gives greater shear and transverse tensile strength. It does not lend itself so well to easy fabrication and layup in-situ and at present is most likely to be applied in the form of standard fabricated sheets, strips and sections.

Composite reinforcement of metal is not confined to unidirectional loading situations. One of the first effective service applications of boron-epoxy composite is the local reinforcement of the

F-1 11 wing near the main pivot lug [4] as shown in fig. 2. In this case improved fatigue life is the goal and the reinforcement was introduced as a later modification for retrofit to existing wings and to avoid wholesale redesign of new wings. It is claimed that boron/epoxy doublers added 8 lbs to the aircraft weight instead of the 30 lbs penalty for redesigned metal fittings - a relative structural efficiency of 3.75. Also the cost of fitting doublers was estimated to be 60% less than that of modifying existing wings with redesigned fittings and 21% less than the redesign costs for new aircraft.

In all these applications the composite material is used to reinforce existing load paths either for strength or stiffness. An interesting possibility which may find early application on high performance aircraft, is the selective reinforcement of metal structures to control aeroelastic and flutter problems by altering the distortion modes. High stiffness composites enable the designer to have virtually independent control of flexural and torsional stiffness in relation to any axes. The first application of this type by my own company is likely to be in external store pylons but the reinforcement of fins is also being considered.

2. Panel and Control Surface Structures

Most aircraft manufacturers who are developing composites have chosen as the first flight demonstration articles simple secondary panel or control surface structures. In some cases these are relatively conventional components in which composite skins are attached to metal edge members or substructures. In others, more sophisticated concepts are employed, exploiting the special characteristics of composites. Among military aircraft alone a large number of pilot structures of this type have been evaluated. Table 1 below lists a number of these

TABLE 1. PILOT COMPOSITE COMPONENTS

Manufacturer	Aircraft	Component	Material	Remarks
General Dynamics, Convair	F-1 11	Airflow deflector door. Main landing gear door	Boron/epoxy	Evaluated on test aircraft
		Wing trailing edge panel	Boron/epoxy	Limited production evaluation
Northrop Corp.	F-5	Wing tip section	Carbon/epoxy	Service evaluation
McDonnell Douglas	A4C	Trailing edge flap	Boron/epoxy Carbon/epoxy	Components developed in both materials
McDonnell Douglas	F 4	Rudder	Boron/epoxy	Test aircraft evaluation
British Aircraft Corporation	Jet Provost Mk. 5	Rudder trim tab	Carbon/epoxy	6 tabs in service evaluation
Hawker Siddeley Aircraft	Vulcan	Airbrake	Carbon/epoxy	1 flap in service evaluation
Hawker Siddeley Aircraft	Harrier	Ferry wing tip	Carbon/epoxy	May become standard production item
Lockheed, Georgia	C5A	Leading edge slat	Boron/epoxy	11 slats in service evaluation

Whilst it is not possible to discuss all these items in detail, a number of them will be selected to show some interesting facets of composite applications. A typical component development programme is described by Fray [2b] and shows the emphasis given to full-scale evaluation of test components under a variety of loading conditions and environments prior to clearance for flight. The component itself is a simple carbon/epoxy faced sandwich structure with metal edge members and is notable for the use of rivets through bonded joints to prevent delamination. The latter principle has also been used in the Harrier wing tip under development by the same team.

A simpler item - the rudder trim tab shown in fig. 4 has been briefly described by the author [5] and embodies all-composite construction including spar members of channel and Vee-sections fabricated from $\pm 45^{\circ}$ orientated carbon fibre laminates. These provide examples of the small bend radii (about 1mm) which can easily be achieved with this material. Of all the components described here this is the only one which does not show any mass saving compared with its metal counterpart. It is over-strength and overstiff under normal service loads but is not sufficiently robust to justify the theoretically possible mass reductions.

The F-1 11 wing trailing edge panel [4] is notable as an early boron/epoxy component put into limited production so as to gain realistic manufacturing as well as service experience. Once again this is a simple composite-faced sandwich wedge with metal edge members and attachments and is almost identical in design to the metal structure which it replaces. It is typical of these 'substitution' designs that the manufacturing costs are much higher than for metal components. Dial and Howeth [4]

report a factor of about 2 in manufacturing hours alone.

The C5A slat [6] illustrated in fig. 3, is a large component which has been completely redesigned to exploit boron-epoxy skin panels and some cost economy has been achieved by reducing the number of detail parts to one tenth of those used in the metal component and the number of fasteners to one quarter. The edge members, ribs and spars of this component are mostly conventional metals and whilst more weight could have been saved by more extensive use of composites it was not considered cost effective by the makers. This again is typical of boron-epoxy composites which cannot be formed to the sharp bend angles required for detail parts and are difficult to machine for final fitting. The makers reported carbon composites much easier to work with in a parallel development exercise. This component operates in a fairly severe erosive environment and is protected on the outer surface by a polyurethane film and on the underside is sealed against moisture by a clear epoxy coating which permits visual inspection.

The available information on mass saving on these introductory components is summarised in Table 2.

TABLE 2. PIVOT COMPONENT MASS SAVINGS

Component	Material	Mass Saving %
F-1 11 Wing trailing edge panel	Boron-epoxy skins	16%
A-4C Flap	(Boron-epoxy skins	22%
	(Carbon-epoxy structure	39%
Jet Provost Rudder tab	Carbon-epoxy	0
Vulcan Airbrake	Carbon-epoxy skins	25%
C 5A Slat	(Boron-epoxy skins	22%
	(Carbon-epoxy skins	<22%

These figures are typical of conventionally designed control surfaces and panels but it is considered that further mass savings can be obtained by rather more subtle use of the materials.

In a spoiler being currently developed for Jaguar, carbon-epoxy composites are being used to transmit the external loads in a different manner from an isotropic material as illustrated in fig. 5. Air loading applied over the main surface is transmitted by chordwise bending (using mainly 90° oriented fibres) to a main tube connecting the hinges and the actuating fitting. The tube (mainly $\pm 45^{\circ}$ oriented material) transmits shear and torsion to the fittings while bending is carried by local 0° material at the deepest part of the section. This economical use of material - providing load capability only where it is necessary and effective - will save upto 50% of the mass of the corresponding metal item and will provide higher stiffness.

Whilst some of the above items maybe marginally cost effective, they have been developed and flown as demonstration articles and to obtain service experience. The next two components are the first examples of applications introduced to save cost. The first is a carbon-epoxy fairing panel for the F-1 11 wing pivot fitting for which Dial and Howeth [4] make the remarkable claim that the first cost is lower than that of a metal component by 31%. This is because the metal part required complicated sculpturing and forming to fit the inside and outside contours and provide internal clearances whilst the composite item was fabricated with local build ups for contour matching in a single stage layup. In addition to cost, a mass saving of 26% is quoted so that the composite application is doubly effective. It cannot be expected, at the current material prices that many such fortuitous applications will be found but this example points out most forcibly the potential of the composite fabrication process for economic manufacture of complex items.

The second example is the carbon-epoxy faced cabin floor panel under development by Rolls Royce (Composite Materials) for B.O.A.C. Boeing 747's. Prototype panels have been undergoing service trials in high traffic locations and are being evaluated in competition with a glass epoxy sandwich panel for replacement of the existing metal-faced panels. Floor panels have a finite life and the cost effectiveness assessment must be based on an average cost per year. Fig. 6 reproduced from ref. 7 by courtesy of Rolls Royce shows that carbon fibre panels would be cost effective by comparison with aluminium/balsa provided the life were between $1\frac{1}{2}$ and $2\frac{1}{2}$ years (compared with 5 years assumed for the conventional structure). In fact, endurance tests still in progress, indicate that the carbon fibre panels may have a significantly longer life than their metal counterparts. It appears that either carbon or glass-composite panels will be chosen to replace the metal items. Whether the higher first cost of carbon will be offset by the greater mass saving will depend on the value attributed to unit mass.

3. Tubes and Struts

In the modern aircraft tubes and struts do not constitute a large part of the airframe mass but they are often critical items from a strength and stiffness viewpoint and are usually subject to space restrictions. In helicopters they are more fundamental parts of the airframe and transmission systems. Circular cylindrical tubes are ideal components for automated composite fabrication either by the familiar filament winding/wet layup method or by pre-preg tape winding [2c]. In either case the principal problem is that of making end attachments. Westlands in common with many other firms, use glass cloth reinforcement of the tube ends with mechanical joints to the end fittings. Winny reports that a transmission shaft using Type 1 carbon-epoxy composite saves 60% of the metal component mass including the effect of glass reinforcement. Strength tests show that the composite materials work to 75% theoretical efficiency with this application.

The same principles have been applied to the manufacture of test sections of helicopter tail booms - again using glass cloth reinforcement in the region of mechanical joints. The mass saving in this application is quoted as 25%.

Composite struts are a similar, and perhaps even more effective, application. In this case there is a requirement for a large proportion of longitudinal material which makes this type of component less suitable for manufacture by winding. However, suitable manufacturing techniques have been developed by many manufacturers during the evolution of cylindrical test specimens. A typical application is the landing gear strut being developed for the Cessna YAT-37B.

4. Major Flying Surfaces

The first major impact of advanced composites on a new aircraft design is seen in the F 14 and F 15 under development for the U.S. Navy and Air Force respectively. Both aircraft feature composite-skinned tail surfaces fitted as standard from the outset. The F 14 horizontal stabiliser shown in fig. 7 is the first major production boron composite part to fly [8] and is developed from a demonstration taileron fitted to the F-1 11.

A full-depth honeycomb sandwich construction is used for the main torsion box with boron-epoxy skins and titanium alloy edge members and diffusion fittings. An interesting feature is that the edge members and fittings are laid up with interfaying adhesive, at the same time as the laminated skins and are co-cured in a single operation. The curing former is on the inside surface so that accurate matching to a machined honeycomb core is facilitated. The core itself is sub-divided into more than 20 regions of different density and these are bonded together (and to an enclosing framework of spars and ribs) using syntactic foam adhesive in a single operation.

A great deal of development has gone into the design of edge member and splice joints, and the main splice at the attachment to the mounting spigot housing has a joint efficiency of nearly 70% (i.e. the strength of the joint is 70% of that of the composite in its immediate vicinity). This is a very satisfactory performance for a stepped joint in a brittle material. The edge joint details, their representation in analysis and testing, as illustrated by Lubin and Dastin, typify the ingenuity and care which must go into the successful development of even a comparatively simple component. For this structure is relatively simple and structural efficiency has been sacrificed (by the use of full-depth core) for the sophisticated manufacturing process and the isolation of a minimum number of design and development problems. The mass saving is 19% relative to a titanium alloy structure. The static strength of the component was demonstrated on test to be 107% of the design ultimate load and the full-scale fatigue test item was unfailed, after substantially exceeding the required life, when the mounting spigot broke.

A considerably more complex (and at first sight conventional-looking) design was adopted by McDonnell Douglas [9] for a carbon epoxy horizontal stabiliser for the A-4 Skyhawk. A multi-spar/rib design was chosen, using composite faced sandwich internal webs, composite attachment angles and solid, multilayer tapered laminate skins bolted and bonded to the substructure. In spite of the large number of overlapping parts and the assembly joints, the mass saving for this item is quoted as 35%. At the time of reporting this component was still in the development stage so that actual mass savings and structural performance cannot be quoted. The programme has already demonstrated, however, that profile matching and final assembly of contoured skins onto discrete internal structure can be carried out (a proposition viewed with scepticism by some manufacturers).

A fin structure under development by my company incorporates a thin sandwich skin concept (fig. 8) in which load diffusion and face thickness variations are minimised by concentrating bending loads into unidirectional flanges, buried within the sandwich where possible and using skins for transmitting shear and local pressure. The skins are supported by spanwise members which only carry high shears at the spar locations. Ribs are used to close the box and transmit local loads from control hinges and root fittings. The basic skin concept is highly efficient because it minimises the support needed for stability as well as reducing load diffusion. The internal structure concept is based on basic beam elements incorporating back to back channel members (with or without a honeycomb core between them, according to local requirements) with the attachment flanges formed integrally with the webs. This technique has already been successfully developed with fuselage frames, as well as spars and ribs, in view. A fin mass reduction of nearly 50% compared with aluminium alloy is expected.

A similar skin design concept has been adopted by North American Rockwell [10] in a demonstration glass-epoxy filament around wing tip for the T-2B aircraft. In this case a truss-spar design was used since this lent itself better to the filament winding technique. A 40% mass saving was reported relating to the existing aluminium structure and a static strength 106% of design ultimate was achieved. Presumably the stiffness was less than the metal structure.

An early demonstration structure using boron-epoxy composites was an F-1 11B wing box extension [11] which featured honeycomb sandwich skins and spars with titanium edge members, caps and fittings. This development was significant since it incorporated a pressurised fuel tank section, established design and manufacturing confidence and provided a great deal of basic data for the F-14 horizontal stabiliser program.

A more recent and far more ambitious programme is underway to develop a mixed composite wing structure based on the F-14 main wing box. This incorporates boron/aluminium compression skin panels, mixed boron and carbon/epoxy tension panels and carbon/epoxy internal members. The use of boron and carbon in a single composite is advocated by Grumman because they have found that the effects of strain concentrations due to perforations are much lower for some carbon/epoxy systems than for boron/epoxy. A mixed composite is claimed to provide the best combination of tensile efficiency and tolerance to perforation and damage.

It can be seen from these examples that the applications technology for composites in major flying surfaces is developing very satisfactorily. However, it will be several years before the more advanced concepts, which promise mass reductions upto 50%, are fully proven and certified as airworthy components. Even the F-14 stabiliser already flying has only a limited airworthiness clearance and would not (on the evidence known to the author) satisfy the proposed U.K. airworthiness requirements as outlined in the previous lecture. The introduction of a composite wing on a production aircraft will require extensive prototype flying experience as well as rigorous adherence to all aspects of the proposed clearance procedure involving the many levels of testing and stress analysis which it implies. It is therefore unlikely that an aircraft designed to exploit such a wing will see service before the early 1980's.

5. Fuselage Structures

Apart from the floor structures already mentioned andsmall doors, fuselage structures have received far less attention than flying surfaces. This is mainly due to the greater complexity of a fuselage structure and the irregular curvature of many components which makes composite fabrication difficult. Also there are several parts of a fuselage not particularly suitable for composite application which suggests that composites will appear alongside metals in mixed structures with many joints and attachments. It is only in the case of easily removeable and replaceable items that gradual introduction on this basis can be realised rapidly.

A number of items such as pressure cabin floors, fuel tank walls, doors, airbrakes etc are governed by similar design requirements to those of the panel and control surface structures already discussed. Adaptation of similar concepts to the fuselage region should, in these cases, be straight forward.

There are many other applications, more specific to fuselages which require special consideration. In particular, curved fuselage frames and bulkheads, longerons and doubly-curved shell panels promise significant mass savings but present many practical problems.

There is little fundamental difficulty in producing curved frame flanges using mainly unidirectional material but detail design may present problems due to the anisotropy of the composites. Radial stresses are far more significant than in metals since the transverse strength maybe between 1/10th and 1/50th of the longitudinal strength. Similarly the lack of transverse stiffness may introduce support and stabilisation problems in frame flanges.

Frame webs on the other hand are difficult to produce with the desired variation in fibre orientation following the frame curvature. One solution to this problem is to build up curved webs from discrete 'tray' elements with integrally formed radial flanges. These are bonded flange to flange to produce a discretely varying fibre direction with shear continuity. An alternative is to use short fibre composites with continuously varying fibre direction. Both methods result in appreciable loss of efficiency.

To use composites efficienctly it is likely that more use will be made of sandwich skin concepts, with less reliance on discrete frames for providing circumferential and radial strength. On the other hand more emphasis maybe given to the use of discrete longerons to transmit primary bending. Fuselages are usually very inefficient structures for transmission of primary loads because in the conventional semi-monocoque structure load paths are so frequently interrupted by doors, windows, and access panels that local reinforcement of structure is the norm rather than the exception. Composite materials, due to the vast stiffness differences in different layups already being exploited in some of the structures previously discussed, lend themselves to the design of structures which although geometrically discontinuous may achieve a higher degree of structural continuity. Because of the high specific stiffness of boron and carbon composites it is possible to locate primary longerons in positions where continuity is possible rather than necessarily seeking 'extreme fibre' locations.

Double-curvature shells present a major manufacturing problem since filamentary composites only lend themselves naturally to developable surfaces. Small amounts of double curvature can be achieved by manipulating flat or singly curved laminates in the uncured state. But even when this is feasible it will often be impossible to maintain the desired fibre orientation as well as fibre continuity. A great deal of development is needed in this area - in addition to proving the structural performance of curved laminate shells - before this can be considered an established affective application.

6. Potential Applications to the next generation of aircraft

The pace of development of structural concepts, production processes, quality control techniques and approval procedures is such that extensive exploitation of composites is unlikely to appear in the next generation of civil aircraft. In this field it will be necessary to demonstrate satisfactory service performance of secondary and replaceable components - control surfaces, doors, fairing panels, floor structures etc - before embarking on composite primary structures. In the military field, on the other hand, the risks are lower and the development programmes more intensive. It is anticipated that high performance aircraft coming into service in the 80's will exploit the advanced composites extensively. Fig. 9 shows a typical light strike/trainer aircraft incorporating composites throughout the airframe.

In some areas such as the wing main box and the curved fuselage shell an all-composite basic structure may require such a long development period that an interim design exploiting composites to reinforce a metal structure may be preferred.

A study has recently been made of a typical military aircraft to determine the mass savings achievable through the use of carbon/epoxy composites on the basis of current material properties. This showed that using all-composite components throughout the airframe resulted in replacement of just over half the airframe mass by carbon/epoxy and saved over 20% of the structure mass.

Using reinforced metal for the long-development items and eliminating some of the less well-established applications approximately halved both figures.

Neither of these results will be achieved in a single step and the next decade should see the progressive introduction of more composite components, increasing in complexity and structural significance.

7. Some comments on performance of components in service

Many of the components currently being evaluated in service are being subjected to realistic environments, often without the protection recommended in laboratory studies. Some of the components, such as our own rudder tabs, are very light and 'delicate' structures and a harsh environment has been specified in order to gain practical experience rapidly. Our own experience to date is that thin carbon/epoxy skins (0.5mm) are too fragile for service handling if they are not supported by at least a backing core. Two incidents have occurred of local handling damage in unsupported areas. Apart from this, the tabs, which are being flown by the Red Pelicans aerobatic team in all-weather conditions, are giving no problems. No erosion has been detected although some flying through severe hail has taken place.

Honeycomb core undoubtedly increases robustness and the Rolls Royce floor panels which have still thinner skins are standing upwell to laboratory tests for repeated indentation and to trial service in B.O.A.C. aircraft.

It is essential in any service evaluation that regular monitoring of the components should be carried out to detect deterioration. For our rudder tabs we use visual and ultrasonic examination methods with occasional return to the factory for thorough inspection. Inspection periods were originally 50 flying hours have been extended to 100 and if continued service evaluation is agreed will probably be extended further. About 2000 hours cumulative flying has been logged to date.

U.K. experience is generally favourable. with erosion not proving as serious a hazard as expected. Also the performance of carbon/epoxy components in simulated lightning tests has been encouraging. Great difficulty has been experienced in forcing current through the composite members: the shielding effect of surrounding metal has been far more pronounced than predicted by some workers. At present we are deliberately avoiding special handling precautions for composite components but we consider that lightweight structures will, in practice, require such protection. They are brittle and therefore particularly prone to damage by heavy objects such as dropped tools.

U.S. experience also seems encouraging. Among the many items now flying no adverse reports have been encountered. It must be stated, in fairness, that no component has yet flown sufficient hours to establish complete confidence, but all the indications are that laboratory proven composite structures can operate satisfactorily in the stringent airframe environment and that the way is open for progressive advance in their exploitation.

Acknowledgements

The writer wishes to thank British Aircraft Corporation Limited and the Ministry of Defence for permission to publish this paper and Rolls Royce (Composite Materials) Limited for supplying ref. 7.

References

1. McIlhinney, D.M., Kitchenside, A.W. and Rowland, K.A. "The Use of Carbon Fibre Reinforced Plastics" in Aircraft Engineering Oct. 1969.

2. The Aeronautical Journal - supplementary papers Vol. 75/76 Nos. 732/733 Dec. 1971/Jan. 1972.
   a) Sanders, B.C. "The Effect of Carbon Fibre Composites on Design".
   b) Fray, J. "A Carbon Fibre Vulcan Airbrake Flap".
   c) Winny, H.F. "The Use of Carbon Fibre COmposites in Helicopters".

3. Forest, J.D. and Christian, J.L. "Development and Application of Aluminium-Boron Material" Journal of Aircraft Mar/April 1970.

4. Dial, D.D. and Howeth, M.S. "Advanced Composite Cost Comparison" Proceedings of SAMPE Conference Vol. 16 Nov. 1971.

5. Taig, I.C. "Design of Airframe Components in Carbon Fibre Composite" in Composites Jan/Feb 1972.

6. Aviation Week and Space Technology July 12th 1971 P. 47.

7. Anon. "Cost Effectiveness of RRCM Carbon Fibre Floor Panels" Rolls Royce (Composite Materials) Limited, Avonmouth, Bristol.

8. Lubin, G and Dastin S. "First Boron Composite Structural Production Part" in Proceedings of S.P.I. 26th Annual Conference 1971 Reinforced Plastics/Composites Division.

9. Tucci, A.T. and Palmer, R.J. "The Development and Fabrication of a Graphite Composite Horizontal Stabiliser for the A-4 Skyhawk Aircraft" Douglas Paper 5889 presented at SAMPE 16th Technical Symposium, Anaheim April 1971.

10. Whinery, D.G., Clayton, K.I. and Tanis, C. "Composite Airframe Design" in Journal of Aircraft Vol. 8 No. 11 Nov. 1971

11. Lubin, G., Ludwig, W. and August, A. "Boron Wing Extension for F-1 11B Aircraft" in proceedings of SPE 26th Annual Conference 1968.

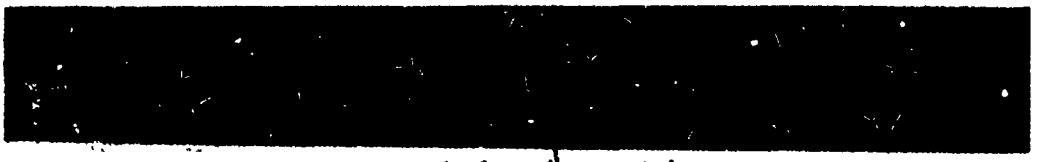

reinforcing strip

FIG 1 Metal Beam with Carbon-reinforced Flange

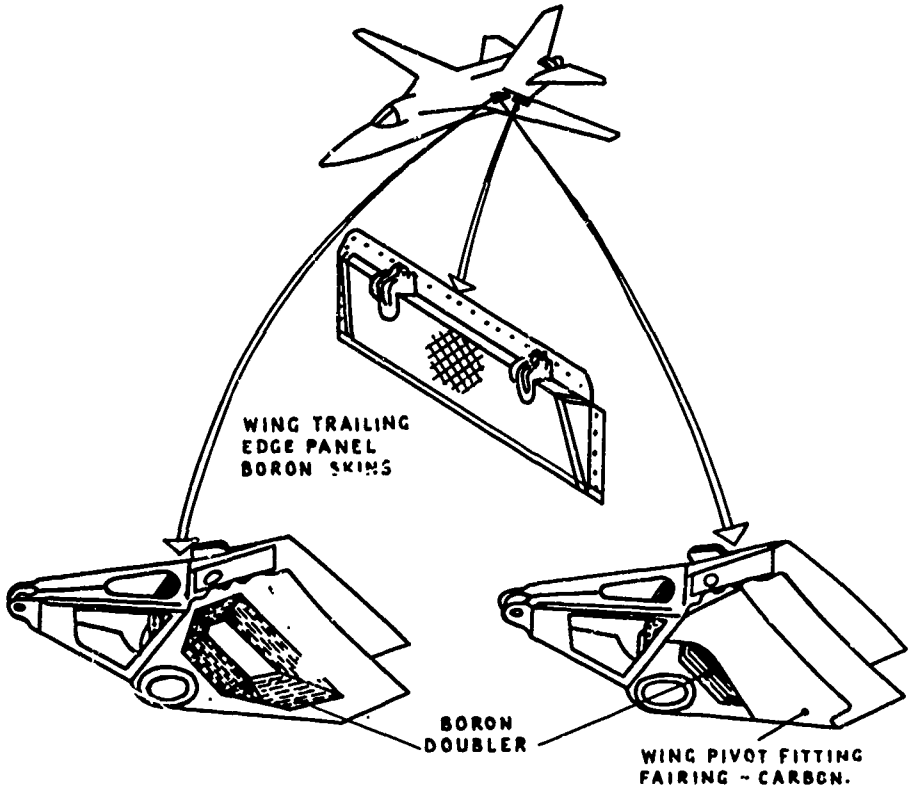

FIG. 2 F-111 PILOT APPLICATIONS OF COMPOSITES

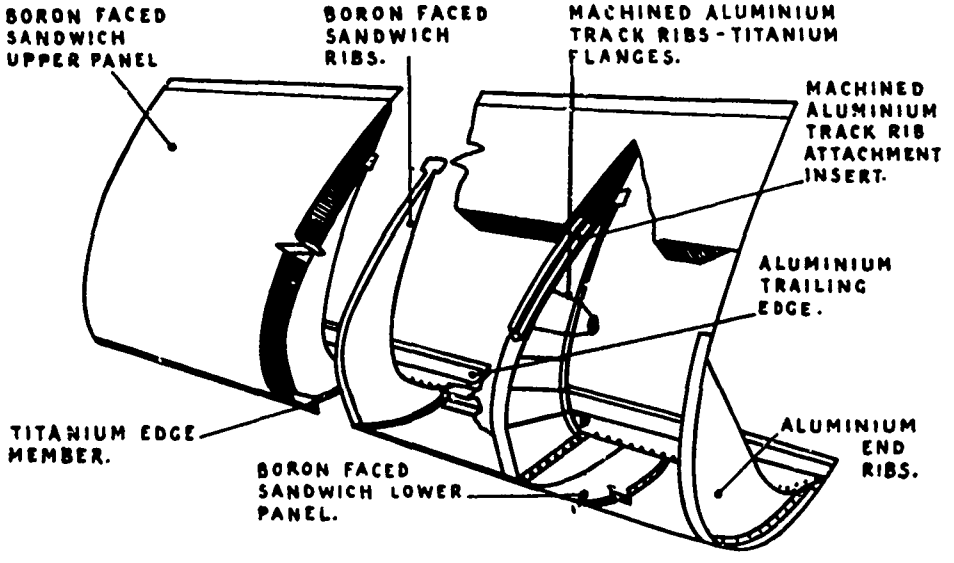

FIG. 3 C-5A SLAT CONSTRUCTION

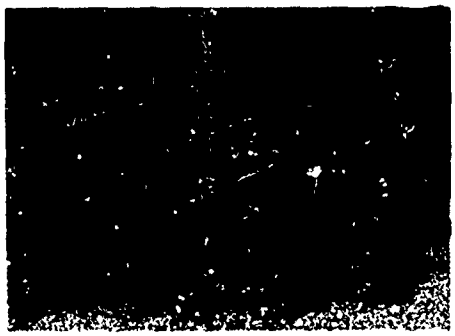

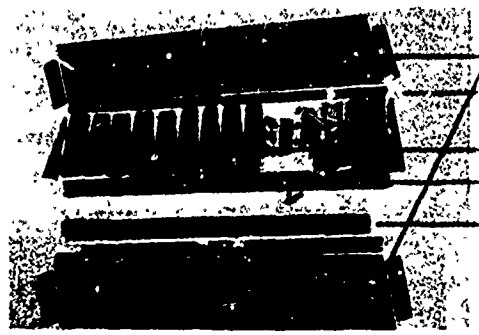

FIG 4 JET PROVOST RUDDER TABS

COMPLETE SPOILER

ADHESIVE BONDED ON FINAL ASSEMBLY.

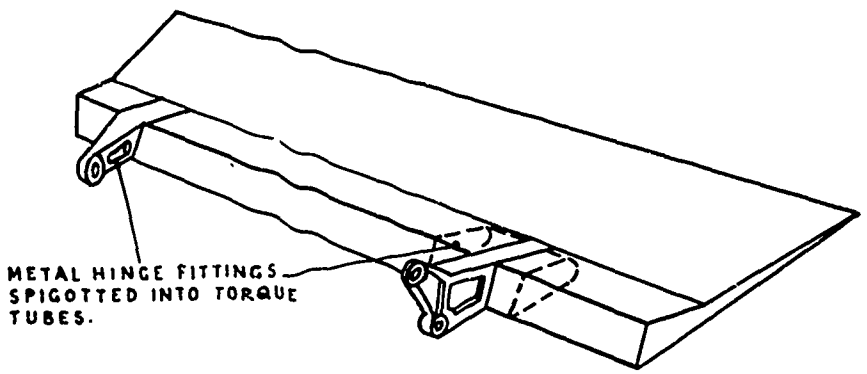

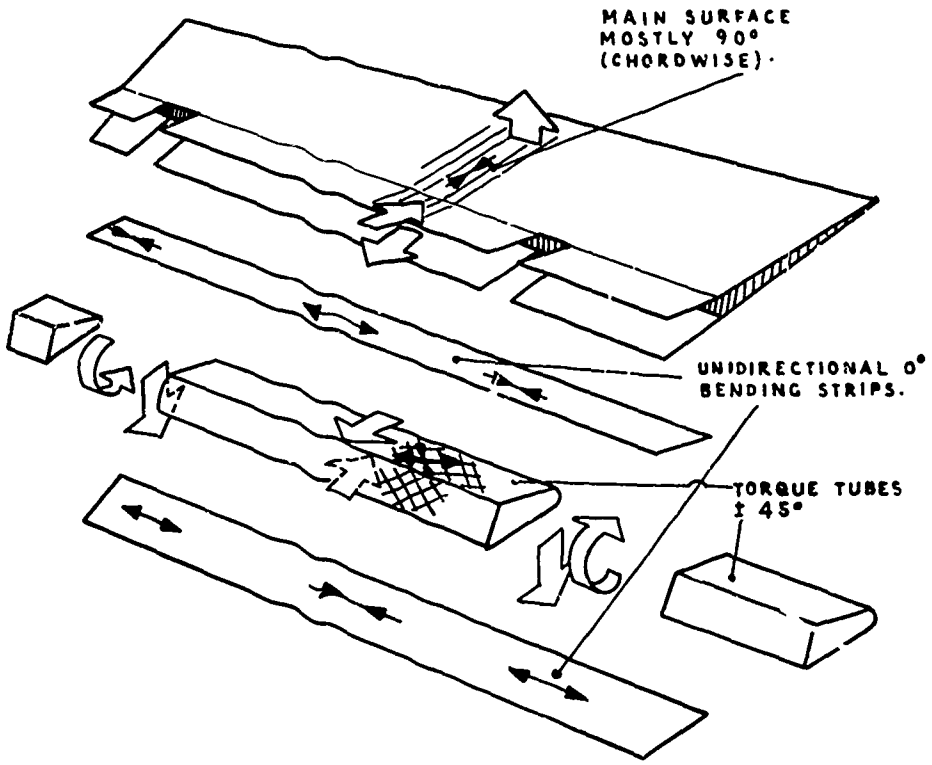

FIG. 5 JAGUAR SPOILER - COMPOSITE LAYUP

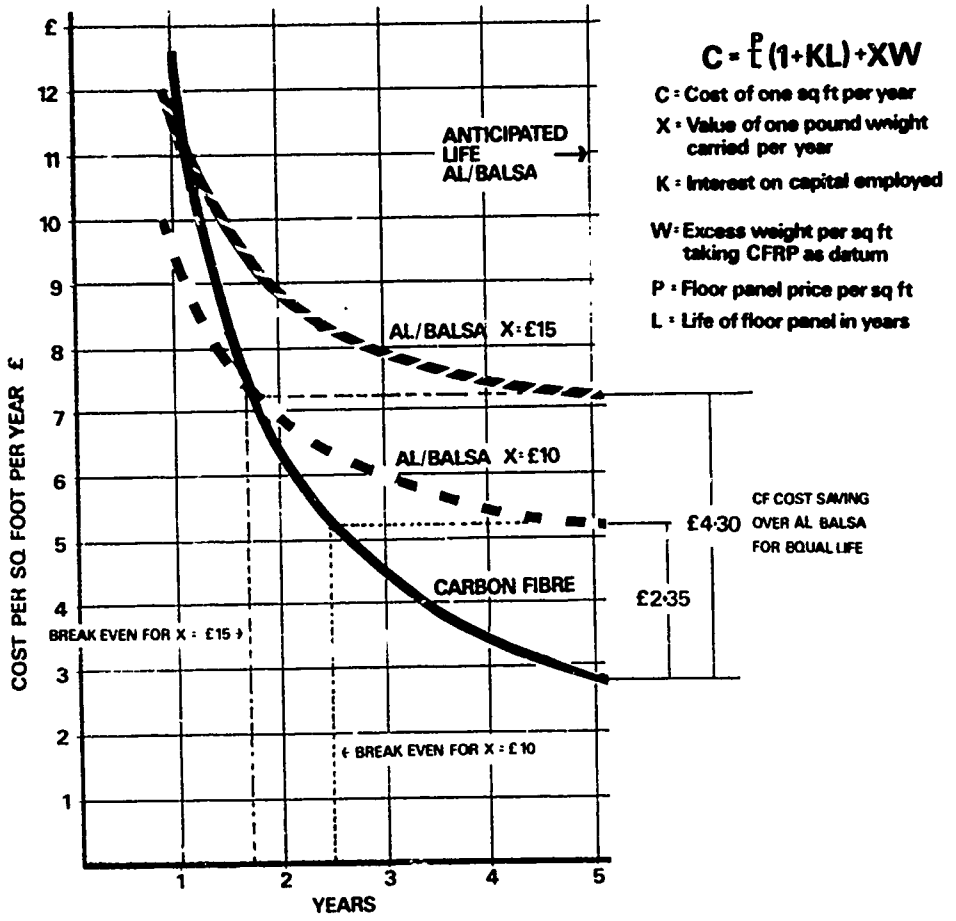

FIG 6 Cost effectiveness of RR(CM) carbon fibre floor panels

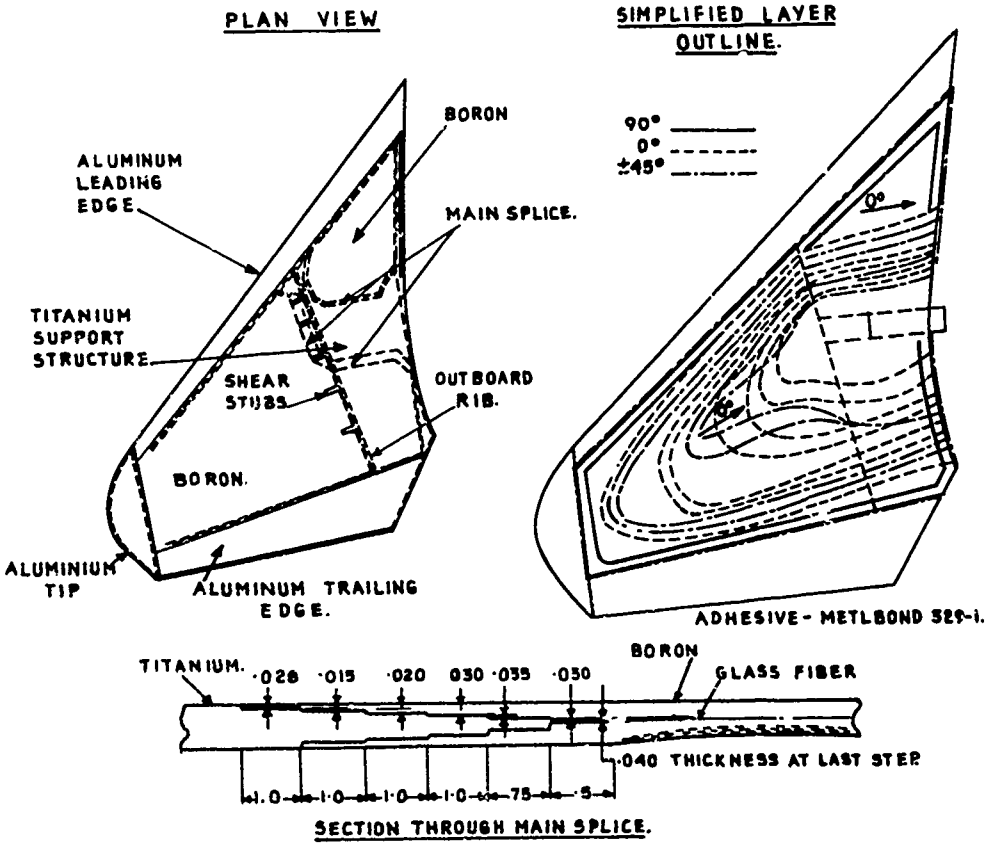

FIG 7 BORON HORIZONTAL STABILIZER

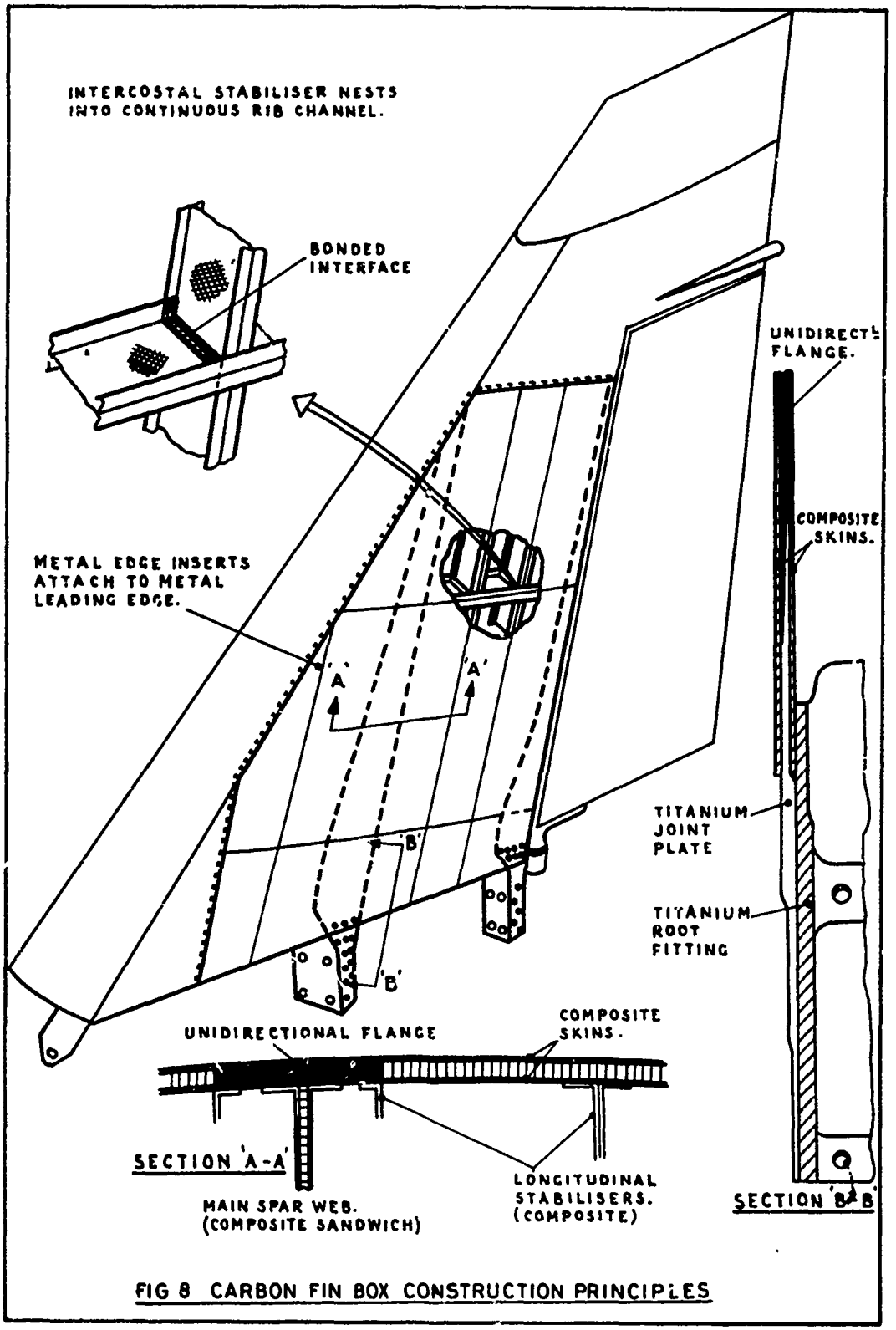

FIG 8 CARBON FIN BOX CONSTRUCTION PRINCIPLES

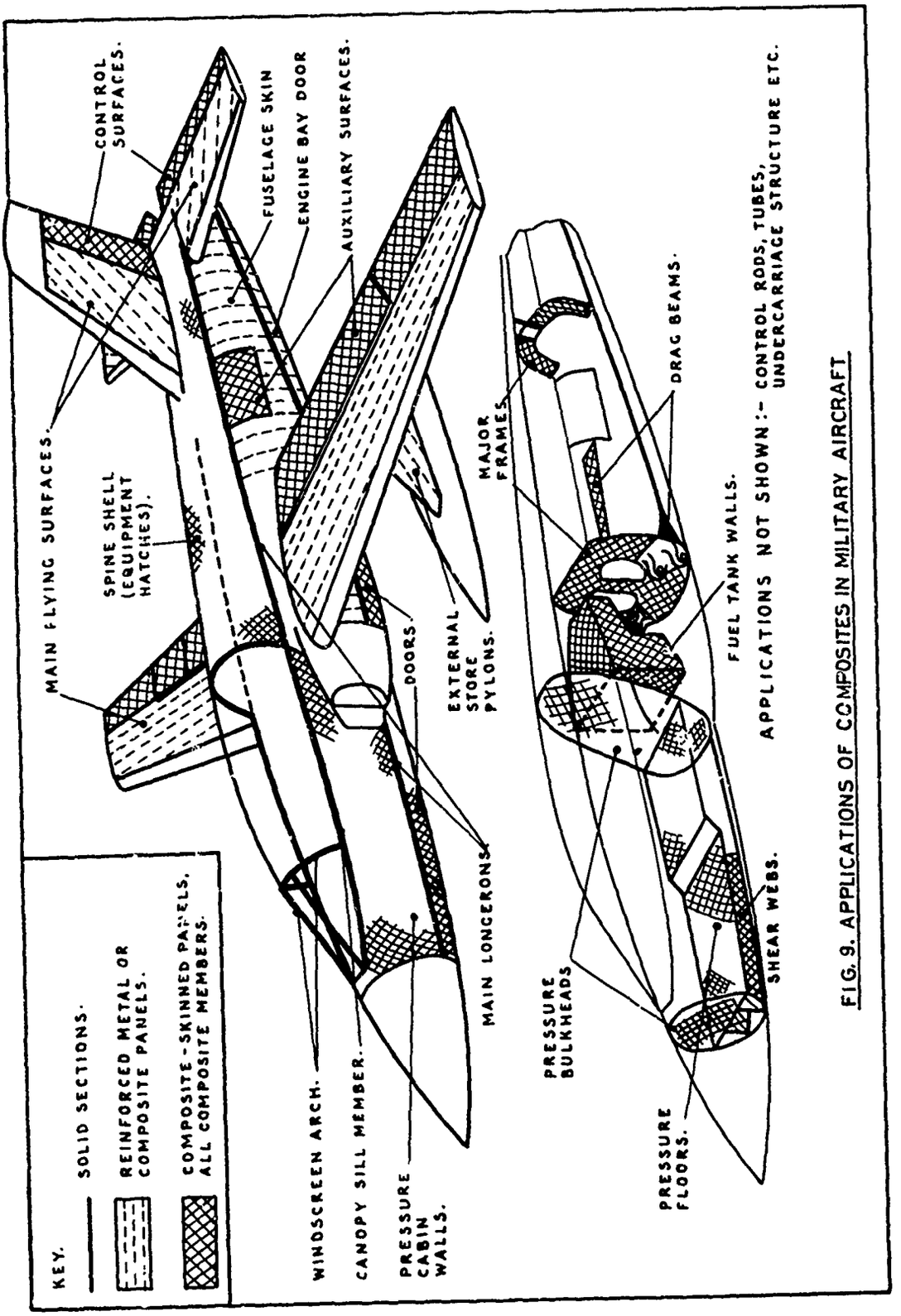

FIG. 9. APPLICATIONS OF COMPOSITES IN MILITARY AIRCRAFT